Improving Impact Properties of Novatein Through Polymer Blending and Reactive Extrusion

A thesis

submitted in fulfilment

of the requirements for the degree

of

Doctor of Philosophy in Engineering

at

The University of Waikato

by

MATTHEW J. SMITH

THE UNIVERSITY OF
WAIKATO
Te Whare Wānanga o Waikato

2018

Abstract

Novatein is a brittle thermoplastic made from protein and requires impact strength modification before it can be used in a wider variety of applications, such as in the agricultural, horticultural and meat processing industries. Polymer blending is often used for improving material properties cost effectively. This study aimed to improve the energy absorbing properties of Novatein through manipulating the morphology of blends and assessing the factors that are important during this process; these were, the choice of polymer, composition, viscosity ratio, interfacial tension and chemical interactions.

Novatein was blended with either elastomeric core-shell particles, polyethylene (PE), or biodegradable polybutylene adipate-co-terephthalate (PBAT) using twin-screw extrusion to allow for sufficient mixing and residence time for chemical interactions or reactions to form. Materials were characterized for mechanical (tensile and impact testing), thermal (dynamic mechanical analysis and differential scanning calorimetry) and morphological (microscopy and solvent extraction) properties.

The greatest increase in energy absorption occurred in blends containing core-shell particles, but only above a critical particle concentration. This was attributed to good particle dispersion, efficient stress transfer to the particles and a decrease in interparticle distance, allowing the matrix to elongate freely during fracture, forming fibrillar structures. When the particle content was high, the protein secondary structure became more ordered in these fibrils during fracture. It was suggested that the change in protein conformation contributed to the increase in energy absorption, along with matrix yielding.

In contrast, in-situ formation of morphologies required for impact strength modification through reactive extrusion of Novatein and modified polyethylene proved difficult due to the viscosity ratio and interfacial tension. In most Novatein/PE blends these factors were not favorable for PE to form stable, dispersed droplets. However, blends containing ethylene-based zinc ionomer performed well in mechanical testing, with high elongation and greatly increased impact strength attributed to strong ionic interactions at the interface. However, no changes in protein secondary structure were detected, suggesting that improvements to impact properties were as a result of morphological changes in these blends.

To preserve the biodegradability of Novatein, PBAT was used instead of PE to achieve the same goal. The compatibilization of Novatein/PBAT blends was explored using dual compatibilizer systems whereby it was found that a compatibilizer system of epoxy functionalized chain extender (Joncryl ADR4368) and imidazole catalyst brought about increased energy absorption compared to poly-2-ethyl-2-oxazoline (PEOX) with polymeric diphenyl methane diisocyanate (pMDI). Compatibilization dramatically reduced PBAT's phase size and led to a well distributed PBAT dispersion, required for improved impact properties. However, the dispersed phase coalesced at very low PBAT concentration (~ 5 wt. % PBAT) due to inappropriate viscosity ratio and interfacial tension. The onset of coalescence can typically be modified by manipulating these factors.

The viscosity ratio and interfacial tension were altered by increasing the water content in Novatein, which is included as a processing aid, leading to a reduction in blend viscosity ratio and an increase in interfacial tension. As water was removed after injection moulding, water was not considered a plasticizer at this stage.

Coalescence of PBAT was reduced when the viscosity ratio decreased and interfacial tension increased in uncompatibilized blends, with a further reduction in domain size upon compatibilization with Joncryl/imidazole. Impact strength was higher in compatibilized blends attributed to this fine domain size and improved interfacial adhesion. Increasing PBAT content to 30 wt. % showed higher impact strength, however a co-continuous morphology formed at this composition, demonstrating that composition can override the effect of viscosity ratio and interfacial tension.

Novatein thermoplastic protein can be impact strength modified through polymer blending or the incorporation of elastomeric particles, however this process is not straightforward. The unique nature of Novatein, whereby the viscosity is exceptionally high during processing and the lack of a traditional melt causes viscosity to be insensitive to temperature, make blending particularly difficult. Interfacial interaction and good particle dispersion are crucial when incorporating pre-synthesized impact modifiers into Novatein, whilst careful consideration is needed of factors such as viscosity ratio, interfacial tension and chemical interactions when blending Novatein with reactive polymers. The morphology formed during blending, along with composition and interfacial interaction, heavily influenced energy absorption. The theories presented for impact strength modification in conventional polymers can be applied here, yet additional considerations need to be made when aiming to modify impact strength in unconventional polymers such as Novatein.

Acknowledgments

There are many people who I need to thank that have made a long and lasting impression on me throughout the course of my studies, and have had considerable impact on the last four years. Firstly, I must thank my good friend and chief supervisor Assoc. Prof. Johan Verbeek. Thank you for your endless guidance and encouragement, and for the amazing opportunities that have arisen as a result of you giving me the chance to be a part of this awesome project. Your constant enthusiasm, not only for my work, but also for our common interests, such as beer and rugby, has made your friendship very valuable to me. I must also thank you for providing me with additional scholarship funding and for bringing me on board as a staff member at the University of Waikato. Your trust and generosity does not go unnoticed and it is very much appreciated.

I must acknowledge the numerous other staff members, both technical and administrative, at the University of Waikato that have helped shaped my doctorate and thank them for their efforts. I would like to thank Dr. Mark Lay and Prof. Kim Pickering, as co-supervisors, for their time and insights; Mary Dalbeth for all of her effort in assisting with admin; Ivan Bell for his help at the Science Store; Helen Turner for assistance with microscopy and for being a friendly Northerner to gossip with; Chris Wang and Yuanji Zhang for all their assistance in LSL with equipment and instruments; Lisa Li for help with sourcing materials and purchasing; and Cheryl Ward for tracking down testing standards and obscure journal articles.

I am particularly thankful to be have been part of the 'Extrusion Plus' project, and for the financial support of Scion and MBIE. I must also acknowledge the New Zealand Synchrotron Group for providing travel funding allowing me to be involved with research at the Australian Synchrotron in Melbourne, Australia.

I have been fortunate enough to work alongside some fantastic people in a great research group over the last four years, of whom there are too many to name, but they know who they are. I must thank them for their assistance with my research, for the interesting conversations and for their friendships. Many of this group who have moved on to other things, and to those who continue to work on their respective research, I wish them all the best in their future endeavours. I must also thank the cohort of 4th year engineering students and those on summer research scholarships who have been a big help with my work.

I must thank my in-laws, Marie & Charlie and all of the Norman family for your support. Thank you to my sister, Rachel, for the long chats and being there when I need to bounce ideas off you. To my parents, Tim and Bridget, I have to thank you for all of your love, and for the interest that you take in everything that I do, despite the great distance and time difference. You are amazing people and incredible parents.

Lastly but most certainly not least I have to thank my wonderful, incredible wife Ally. The last few years have most certainly been a struggle for us at times; PhD study has not only been emotionally (and financially) draining on me, but also on you, so I thank you for allowing me to undertake this doctorate and support me unconditionally. Thank you for being my sounding board, and for your constant advice. You truly are a wise little penguin. Without your constant love and motivation, or the ability to get my arse into gear or pull me out of a slump when I needed it most, I certainly would not have finished this journey. I consider myself very lucky to have you in my life, and I am eternally grateful and forever indebted to you for everything that you have done and continue to do for me.

Contents

1

Introduction

Introduction

Novatein is a bio-based, biodegradable and compostable thermoplastic, partly due to its hydrophilic nature.[1] Its tensile strength and modulus have been compared to low density polyethylene[2] and can be altered using different combinations of plasticizers and additives,[3] as well as through blending with both synthetic and bio-based polymers.[4-6]

During the processing of animals for meat, blood is collected, steam-coagulated, dried and milled to form a powder, known as bloodmeal. Bloodmeal is a commodity by-product which is typically used as fertilizer or animal feed. It has an exceptionally high protein content (90 - 95 %) which, coupled with its low cost and high availability, means that it is suitable as a raw material for protein-based biodegradable thermoplastics. Bloodmeal must be treated for the protein chains to have sufficient mobility for thermoplastic processing by disrupting hydrogen bonds, hydrophobic interactions and covalent crosslinks.[7,8] This treatment converts bloodmeal into an extrudable and injection mouldable plastic, similar to conventional petrochemical thermoplastics. Novatein® thermoplastic protein has been patented by the University of Waikato[9] and has been commercialised by Aduro Biopolymers LP[10] for the manufacture of products used in the New Zealand and Australian agricultural and horticultural sectors, as well as renderable products used in meat processing.

Like many other biopolymers, such as polylactic acid (PLA) and thermoplastic starch (TPS), Novatein has poor impact resistance and requires modification to widen the variety of applications. There are a number of strategies aiming to improve impact resistance such as rubber/elastomeric particle toughening, polymer blending and fiber reinforcement. However, there are significant challenges

associated with these techniques. For example, when blending two or more polymers, consideration must be given to the induced morphology, which is dictated by processing temperature (and hence polymer viscosity), the surface tension of the polymers in the melt, the miscibility and reactivity of components towards one another and the weight fraction of each component in the blend. Similarly, the success of particle and fiber reinforced polymers can be linked to the interfacial adhesion, the ability for debonding to occur and the subsequent ability of the matrix to deform under a high rate of loading.

Any of these strategies could potentially be applied to improve the impact strength of Novatein. Blending with other polymers has previously been successful, however morphology was not necessarily conducive to improved impact resistance, hence tailoring the phase structure is desirable. Furthermore, understanding how Novatein fractures compared to conventional thermoplastic materials, in addition to its processing-morphology-mechanical properties relationship in blends, are important for developing a strategy to manipulate the most important factors influencing impact resistance.

As such, this thesis specifically aimed at improving the impact strength of Novatein through the following routes:

1. Incorporating pre-synthesized elastomeric core-shell particles.
    o   Based on literature, it is known that incorporation of rubber or elastomeric polymers is an effective method of increasing impact strength, hence this technique was applied to Novatein. This also allowed for the analysis of the fracture mechanisms in thermoplastic protein, something that is not described in depth in other studies.

2. Blending with various commonly available functionalized polyethylenes.

   o The commercial availability of commodity polymers that are functionalized with reactive groups allows for compatibilization *in-situ*, and the wide variety of reactive functionalities available meant that extensive investigations could be conducted with Novatein to establish the most appropriate functionalities. Similarly, different grades of polyethylene are available with varying molecular weight (and hence viscosity), and the inclusion of reactive groups alters the surface energy of the polymer, both factors which contribute heavily to morphology development in polymer blends (viscosity ratio and interfacial tension).

3. Blending with polybutylene adipate-co-terephthalate (PBAT), an elastomeric biodegradable polymer.

   o Part of the appeal of Novatein is its biodegradability and compostability, hence blends of Novatein and other biodegradable polymers which exhibit good impact strength and energy absorbing properties are desirable. The learning done in the first two objectives, regarding morphology development and the significant factors in this process, as well as the requirements for improvements in impact resistance, was applied to Novatein/PBAT blends.

These objectives were addressed in six experimental chapters, in addition to a literature review and a concluding discussion. A thesis outline is presented in Scheme 1.

Chapter 2 critically examines the literature regarding polymer blending, impact strength modification of polymers and the application of these theories with regards to biopolymer blends. It aims to outline the interaction between phases in polymer blends, the mechanisms of morphology development and how these relate to increased energy absorption as a result of these interactions.

All experimental chapters, which have been published as articles in peer-reviewed journals, are preceded by a summary page containing a short overview and copyright information. The experimental chapters are concluded by a discussion pertaining to the overarching theme of the thesis in Chapter 9, namely the impact strength modification of Novatein, the problems associated with this and the steps taken to successfully produce Novatein with high impact strength and energy absorbing properties. This chapter also touches on recommendations for future work.

PROBLEM
Novatein becomes brittle after production due to desorption of plasticizer, causing low energy absorption during fracture

THESIS AIM
Modify impact strength and energy absorbing properties of Novatein without compromising other mechanical properties

Thesis starting point:
Impact modified biopolymers through blending with functionalized polyethylene

CHAPTER 4 – CORE-SHELL PARTICLE REINFORCED NOVATEIN
Feasibility of modifying impact strength using functionalized pre-synthesized particles, with no need for morphology control

AND

CHAPTER 5 – FUNCTIONALISED POLYETHYLENE/NOVATEIN BLENDS
Feasibility of producing morphology conducive to improved impact strength *in-situ* in binary blends of Novatein/functionalized PE

Highlights complexity of Novatein blends and the importance of viscosity ratio, interfacial tension and chemical interaction

CHAPTER 3 – DSC REACTION KINETICS STUDY
Examine feasibility of Novatein/epoxy reactions using model compound

CHAPTER 6 – SYNCHROTRON FTIR
What causes improvements in Chapters 4 & 5?

Dual energy absorption mechanism in core-shell blends, morphology effects in PE blends

Synthetic polymers negate biodegradable nature of Novatein – apply previous learnings to Novatein blends with biodegradable PBAT

CHAPTER 7 – COMPATIBILIZATION OF NOVATEIN/PBAT BLENDS
Dual compatibilizer systems; epoxy chain extender/imidazole catalyst and PEOX/pMDI (used in a previous Novatein blending study)
Improved properties achieved, but coalescence occurs at very low PBAT wt. %

AND

CHAPTER 8 – MORPHOLOGY MANIPULATION IN NOVATEIN/PBAT BLENDS
Blend composition kept constant (PBAT and compatibilizer wt. %) whilst Novatein formulation changed to alter viscosity ratio and interfacial tension, aiming to change morphology
Tailoring morphology by using learnings from Chapters 3 – 7; i.e. controlling viscosity ratio, interfacial tension and chemical reactivity

Tailored morphology for improved impact strength is possible

Viscosity ratio, interfacial tension and chemical reactivity all need to be considered for morphology development, but composition can override these

Critical composition for impact modification appears to be > 20 wt. % reinforcement

Scheme 1. Thesis outline

References

[1]   C.J.R. Verbeek, T. Hicks, and A. Langdon, *J. Polym. Environ.* **2012**, *20*, 1.

[2]   C.J.R. Verbeek and L.E. van den Berg, *Macromol. Mater. Eng.* **2011**, *296*, 6.

[3]   J.M. Bier, C.J.R. Verbeek, and M.C. Lay, *Macromol. Mater. Eng.* **2013**

[4]   K.I.K. Marsilla and C.J.R. Verbeek, *J. Appl. Polym. Sci.* **2013**, *130,*

[5]   K.I.K. Marsilla and C.J.R. Verbeek, *Macromol. Mater. Eng.* **2014**, *299*, 7.

[6]   K.I.K. Marsilla and C.J.R. Verbeek, *Macromol. Mater. Eng.* **2015**, *300*, 2.

[7]   C.J.R. Verbeek and L.E. van den Berg, *Macromol. Mater. Eng.* **2010**, *295*, 1.

[8]   C.J.R. Verbeek and L.E. van den Berg, *J. Polym. Environ.* **2011**, *19*, 1.

[9]   C.J.R. Verbeek, K.L. Pickering, C. Viljoen, and L.E. Van den Berg, *Plastics Material*, U.P. Applications, Editor. 2010, Novatein Limited: United States.

[10]   Aduro Biopolymers LP. *Novatein, Aduro Biopolymers*. 2017 [cited 2017 February]; Available from: http://www.adurobiopolymers.com/Novatein.

2

Energy Absorption Mechanisms and Impact Strength Modification in Multiphase Polymer and Biopolymer Systems

A literature review

Abbreviations

ABS	Acrylonitrile butadiene styrene copolymer
BR	Polybutadiene rubber
EPDM	Ethylene-propylene-diene terpolymer
EVA	Ethylene vinyl acetate copolymer
GMA	Glycidyl methacrylate
MA	Maleic anhydride
PA6/PA66	Polyamide 6/Polyamide 66
PBAT	Polybutylene adipate-co-terephthalate
PC	Polycarbonate
PCL	Polycaprolactone
PE	Polyethylene (HDPE – high density PE; LDPE – low density PE)
PEA	Polyesteramide
PEI	Polyethyleneimine
PHA	Polyhydroxyalkanoates
PHB	Polyhydroxybutyrate
PHV	Polyhydroxyvalerate
PLA	Polylactic acid
PMMA	Polymethyl methacrylate
PP	Polypropylene
PS	Polystyrene
PSF	Thermoplastic polysulfone
PTAT	Polytetramethylene adipate-co-terephthalate
PVA	Polyvinyl acetate
PVC	Polyvinyl chloride
SEBS	Styrene-ethylene/butylene-styrene triblock copolymer
TPS	Thermoplastic starch

2.1 Introduction

Polymers are commonplace in everyday life with a global market of ~ USD 60 billion in 2016 growing at ~ 7 % annually, with the majority being polyethylene and polystyrene.[1] However, specific applications may require material properties that cannot be met by existing polymeric materials. Synthesizing new polymers with the desired properties for a target application can be costly and time consuming. A suitable alternative is polymer blending, whereby two or more polymers are mixed together to produce a material with properties intermediate of the components, or enhancing specific properties in particular. The morphology formed in polymer blends is brought about by an intricate balance of rheology, composition, processing conditions and interfacial tension, and can be tailored by altering these parameters.[2]

A major drawback of some polymers is the low impact resistance and ability to absorb energy during fracture, such as in PS, PMMA and PVC. Several techniques are used in an attempt to toughen or modify impact resistance of brittle polymers, including reinforcement such as fibers and particles, or the incorporation of an elastomeric second phase. Rigid particles can be effective modifiers, but only when debonding from the matrix occurs, whereas stress transfer between a brittle matrix and an elastomeric particle or region can significantly improve energy absorption. Similarly, modification in the form of plasticization or altering molecular weight and entanglement density can have a substantial effect on fracture.[3]

Whilst synthetic polymers can provide desirable properties for a wide variety of applications, there is a large environmental impact associated to those produced through petrochemical routes. Firstly, plastics tend to be discarded or incinerated at the end of their lifecycle,[4] and while recycling has increased drastically over recent

years, landfill space is still at a premium and this problem is compounded by increasing plastic waste.[5] Secondly, the use of crude oil for various processes (not only polymer production) places a large demand on fossil fuel resources; oil demands are forecast to reach 116 million barrels per day in 2030.[6] Hence, in recent decades, much emphasis has been placed on polymer systems from renewable resources, as well as those able to undergo biodegradation due to enzymes and microbes. Biodegradability is not necessarily an indication of a bio-derived polymer though, as there are a number of synthetic biodegradable polymers such as PBAT and PCL.

Biopolymers come in many forms; naturally occurring in biomass such as starches and proteins, brought about through fermentation (PLA) or developed synthetically like PCL (Figure 1). Despite the differences in source and material properties, the similarity that all of these polymers have is that they are biodegradable and able to be broken down through the action of microbes and organisms leaving little to no residuals behind.[7]

Biodegradable polymers exhibit a wide variety of properties suitable for a number of applications. PLA, for example, is the most widely used and researched biopolymer due to its high strength and modulus, good processability, availability and low cost comparative to other biopolymers. However, PLA is brittle and absorbs little energy before fracture. In contrast, PBAT shows high elongation and good impact resistance, yet its low stiffness and strength, as well as high cost, limit the applications. Blending of biodegradable polymers is an area of high interest due to the promise shown in these materials and the potential for the replacement of petro-chemical based polymers, although the ability of these materials to absorb high levels of energy during fracture whilst maintaining other acceptable mechanical properties remains an issue.
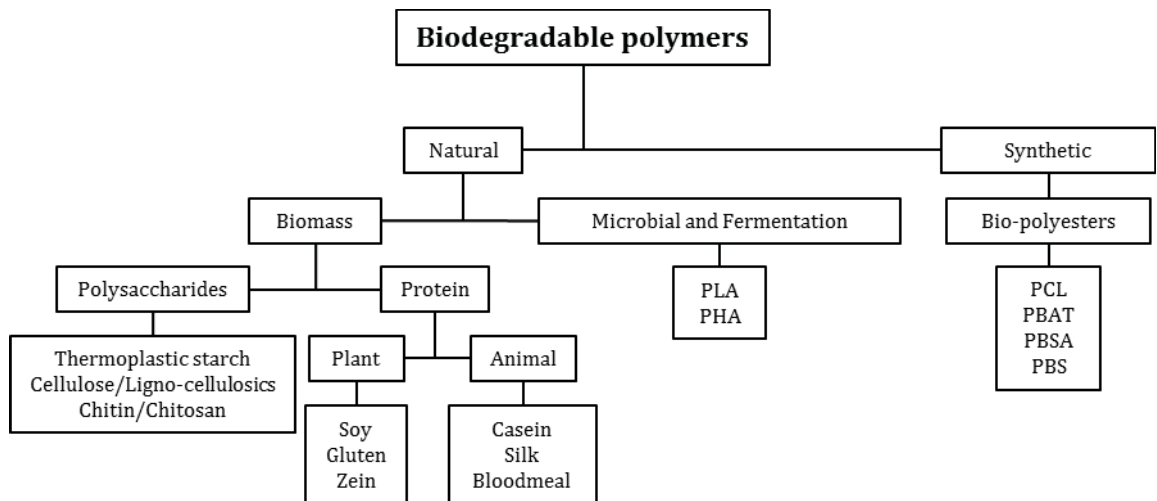
Figure 1. Classifications of biodegradable polymers.

The ability to produce biodegradable polymer blends, with superior impact strength is potentially lucrative. The success of this is related to the interaction between polymer phases, the morphology developed during processing and increased energy absorption as a result of this interaction. This review aims to outline relevant literature regarding polymer blending, morphology development and impact strength modification, and link these topics to the formation of impact strength modified biopolymer blends.

2.2   Polymer blending

Polymer blending is a solution for improving material properties in a cost effective manner. The synthesis of new polymers demands substantial time and investment, whereas blending two polymers has been used to significantly improve material traits such as mechanical and thermal properties, depending on the desired application.

The majority of polymers are immiscible, meaning thermodynamically they will not mix. Miscibility is an important concept in polymer blending as the interaction between the polymers will determine the blend properties; hence, immiscible polymers with little to no interaction tend to produce a material with sub-standard performance. Miscibility is typically described by the Gibbs free energy of mixing, which has the relationship (Equation 1)

$$\Delta G_m = \Delta H_m - T\Delta S_m \qquad (1)$$

where G_m is the free energy of mixing, H_m is the enthalpy of mixing, T is temperature and S_m is the entropy of mixing. For a system to be considered miscible, the value of the free energy of mixing must be negative, and as entropy increases in a system during mixing and hence is always positive, miscibility is driven by the enthalpy of mixing.

However, whilst some polymers may be miscible at one composition and temperature, they may become immiscible when these factors are altered causing phase separation. The phase separation occurs in the miscible polymer blend by spinodal or binodal decomposition, which is described on a temperature vs. composition plot (Figure 2). As temperature increases, or the fraction of polymer A in polymer B increases, the region of miscibility decreases. However, polymer-

polymer mixtures tend to have a lower critical solution temperature (LCST) (whilst polymer-solvent mixtures exhibit an upper critical solution temperature) whereby any temperature below the LCST produces a single miscible phase.
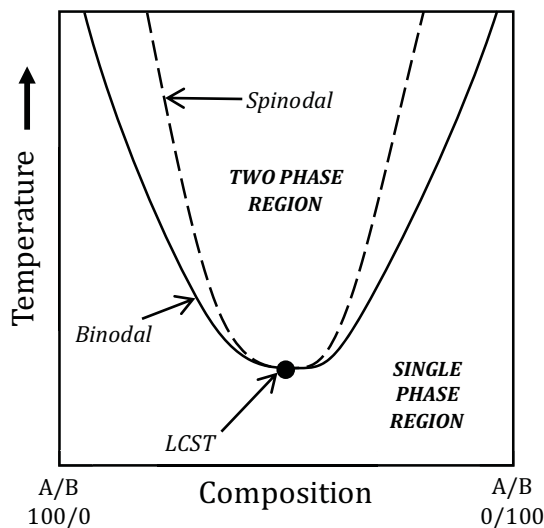

Figure 2. Phase diagram of binary blend showing lower critical solution temperature and spinodal and binodal boundaries.

2.2.1 Compatibilization

One way of promoting interaction between polymers is through compatibilization. The compounds used as compatibilizers typically have a graft or block structure, containing functional units either miscible or reactive towards the heterogeneous blend components. These compounds are either added as separate components to the blend, or produced in-situ as a result of reactions during processing. Schematically, the compatibilization of a blend of polymers A and B can be with a block/graft copolymer of any composition, usually A/B, but it is possible for A/C, B/D etc. to be used, providing that C and D are miscible with the targeted block (Figure 3). Although phase A is a solvent for block A, if using block C for compatibilization, the miscibility between polymers becomes very important. The coupling of phases decreases interfacial tension between phases A and B, hence

deformation of the minor phase occurs more easily, and the presence of the compatibilizer at the interface prevents coalescence of the dispersed minor phase.
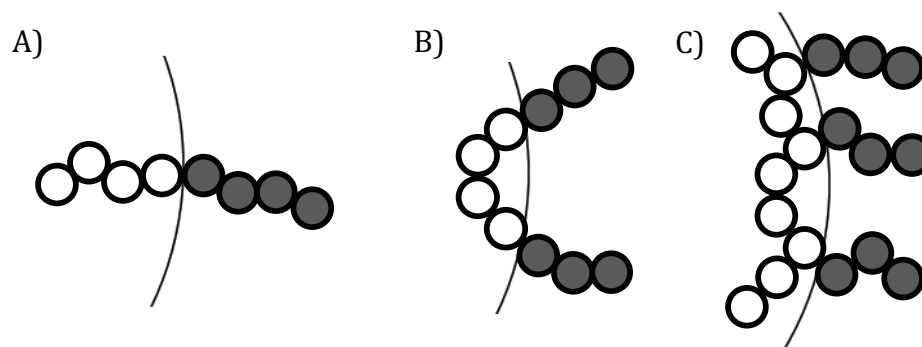

Figure 3. Conformation of copolymers for compatibilization at the interface of a heterogeneous polymer blend; A) diblock; B) triblock; C) graft. Reprinted (adapted) with permission from C. Koning, M. Van Duin, C. Pagnoulle, and R. Jerome, *Prog. Polym. Sci.* **1998**, *23*, 4. © (1998) Elsevier Science Ltd.[10]

This was shown by Souza and Demarquette, who studied the effect of different block copolymers (EPDM, EVA and SEBS) on the morphology and interfacial tension in PP/HDPE blends. It was shown that whilst all compatibilizers had a significant effect on both reducing particle size and interfacial tension in the blend, EPDM had the greatest influence attributed to the presence of both PE and PP regions in the compatibilizer.[11]

2.2.2 *In-situ* reactive compatibilization

An alternative to compatibilization using pre-made graft and block copolymers is the formation of copolymers at the interface as a result of reactions during processing. Reactive groups can be present in the blend through grafting, either as pendant or terminal groups, or as a separate component which is miscible with one phase and reactive towards the other. There are a number of reactive species that are suitable for compatibilization, which have been studied considerably. The review of Koning et al.[10] describes the reaction products of a number of reactive

15

groups typically used for compatibilization in polymer blends (Figure 4). Orr et al.[12] investigated the reaction kinetics of various reactive pairs in functionalized PS, such as comparisons between the conversion of aliphatic and aromatic amine with epoxies and anhydrides. The full comparison of reactive pairs tested by Orr et al. is presented in Table 1.[12] It was conclusively shown that aliphatic amine reactions with anhydride and isocyanate were extremely fast, with full conversion occurring in less than 30 seconds. Jeon & Macosko et al.[13] examined the effect of reactive group location along the polymer backbone, showing that the effect of steric hindrance meant that reactions of functionalities located in the middle of the polymer chain were slower than those end-functional polymers. The same authors also described how flow under steady shear in a melt mixer greatly enhanced reaction rates due to the constant creation of new interfaces,[14] hence compatibilization during extrusion melt blending is a useful route for improved material performance due to the flow fields imposed and good mixing capability. It must be noted though, that the occurrence of branching and network structure formation can occur as a result of high levels of reaction leading to embrittlement and a subsequent decrease in mechanical performance.[10]

Ionomers are another classification of polymer used for blend compatibilization. These are ion-containing polymers, with low numbers of pendant ionic groups. These ionic groups are usually formed through neutralization of acid groups by monovalent (Na^+, K^+) or divalent (Zn^{2+}) metal cations.[10] Ionic groups tend to associate with themselves forming aggregates which act as physical crosslinks between the polymer chains in the ionomer. At high temperature, these ionic aggregates can be reorganized, and when this is combined with sufficient mixing and other reactive species, such as in a twin screw extruder, new ionic reactions can form at the interface between the two polymers.
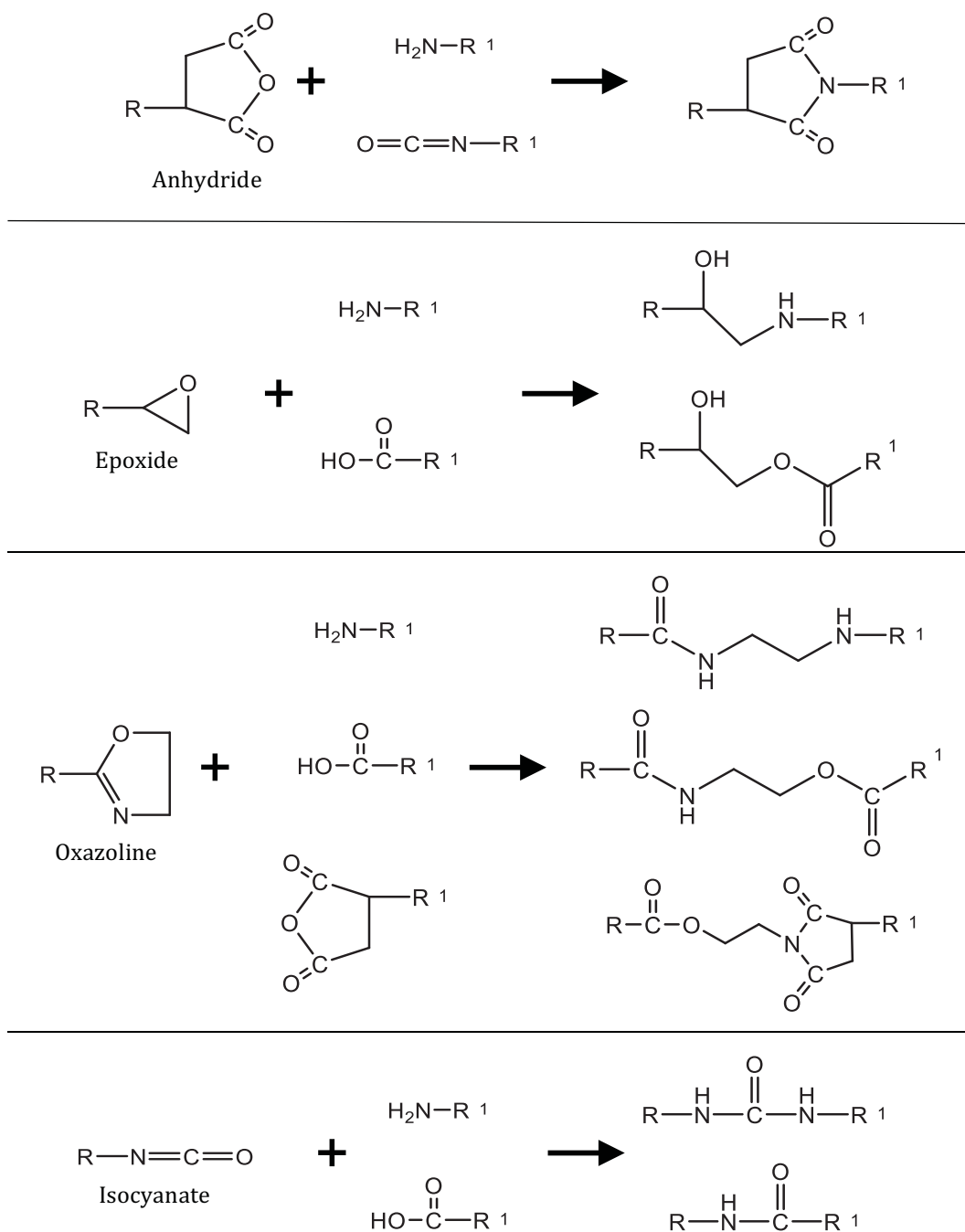
Figure 4. Examples of reactive groups found on polymer chains used for compatibilization (anhydride, epoxide, oxazoline and isocyanate) and their potential reaction products after reaction with functionalities present on other polymer chains (amine, isocyanate, carboxyl, anhydride). R and R^1 denote polymer chains. Reprinted (adapted) with permission from C. Koning, M. Van Duin, C. Pagnoulle, and R. Jerome, *Prog. Polym. Sci.* **1998**, *23*, 4. © (1998) Elsevier Science Ltd.[10]

Choi et al.[15] studied the formation of a thermoplastic elastomer of EPDM-*g*-MA, which included zinc oxide in order to form a Zn^{2+} ionomer. The method of ionomer formation proposed was the formation of ionic bonds between ZnO and hydrolysed anhydride pendant groups. However, the introduction of either stearic acid or zinc stearate improved the material properties due to the further formation of heteroionic bonds with the acid groups, separate to those formed by ZnO (Figure 5). These results were confirmed through crosslink density determination via solvent swelling. The initial introduction of ZnO to EPDM-*g*-MA showed a positive linear correlation of crosslink density to increasing ZnO content, which was further increased with the addition of zinc stearate and stearic acid, respectively.

In a similar study, Liu et al.[16] investigated the effect of metal ion type in PLA/ionomer blends. The ternary blends comprising of PLA, EBA-GMA (an ethylene/butyl acrylate/GMA copolymer) and ionomers based polyethylene-co-methacrylic acid (EMAA) incorporated different metal ions, namely zinc (Zn^{2+}), sodium (Na^+), lithium (Li^+) and magnesium (Mg^{2+}), to promote ionic interaction at the phase interface. It was observed that Zn^{2+} ionomers had the greatest influence on impact strength and the highest catalyzing effect promoting compatibilization between PLA and EBA-GMA. Notched Izod impact strength rose to over 800 J/m with just 5 wt. % Zn ionomer, compared to ~ 100 J/m without. Lithium and magnesium ionomers had little influence on impact resistance, whilst Na^+ containing blends were intermediate. There was a clear difference in toughening efficiency between monovalent and divalent ionomers, attributed to the higher reactivity and better compatibilizing effect of the Zn^{2+} and Mg^{2+} ionomers.

Table 1. Comparison of reactive pairs. Reprinted (adapted) with permission from C.A. Orr, J.J. Cernohous, P. Guegan, A. Hirao, H.K. Jeon, and C.W. Macosko, *Polymer.* **2001**, *42*, 19. © (2001) Elsevier Science Ltd.[12]

| Reactive group 1	Reactive Group 2	Conversion after 2 mins at 180 °C (%)	Rate Constant (k) (kg/mol min)
Carboxylic acid	Aliphatic amine	0	-
Aromatic amine	Aliphatic epoxy	0.6	0.1
Aromatic amine	GMA epoxy	0.7	0.15
Aliphatic amine	Aliphatic epoxy	1.1	0.28
Aliphatic amine	GMA epoxy	1.8	0.34
Carboxylic acid	Oxazoline	2.1	0.92
Carboxylic acid	GMA epoxy	9.0	2.1
Aromatic amine	Cyclic anhydride	12.5	3.3
Aliphatic amine	Cyclic anhydride	99	$\sim 10^3$
Aliphatic amine	Isocyanate	99	$> 10^5$ (at 25 °C)
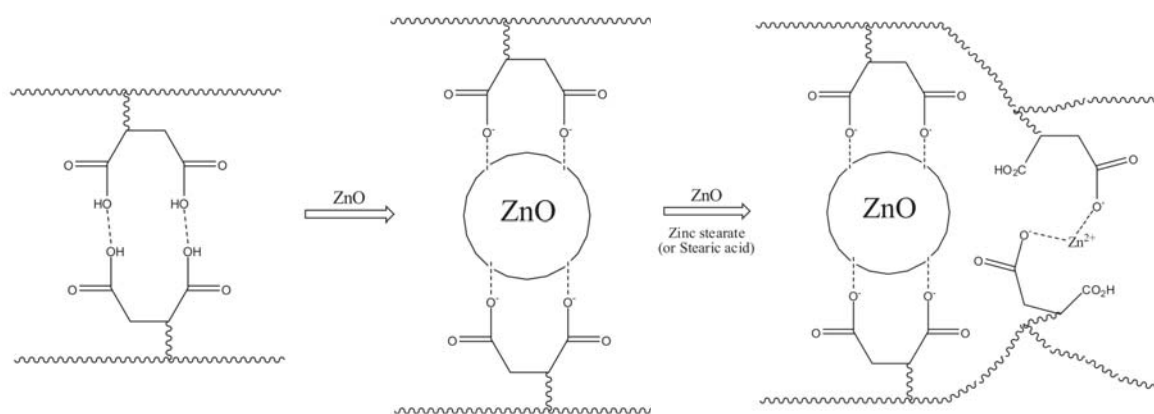
Figure 5. Formation of ionomer between EPDM-*g*-MA and ZnO, and the subsequent formation of heteroionic bonds with the addition of zinc stearate or stearic acid. Reprinted (adapted) with permission from S.S. Choi, H.M. Kwon, Y. Kim, J.W. Bae, and J.S. Kim, *J. Ind. Eng. Chem.* **2013**, *19*, 6. © (2013) The Korean Society of Industrial and Engineering Chemistry. Published by Elsevier B.V.[15]

2.2.3 Morphology development

Polymer blending begins with pellets or powders usually undergoing melting during extrusion processing. Throughout this process, the components are subject to distributive and dispersive mixing to form fine phase structures usually in the range of microns. Scott and Macosko schematically described this process[17] (Figure 6). After melting, the initial deformation of the minor phase is through stretching into long sheets and ribbons which begin to break up as a result of interfacial instability. The continued elongation and deformation of the sheets leads to long thin cylinders which if thin enough, become subject to Rayleigh disturbances, bringing about the break-up of the elongated structures into droplets.

In polymer blending there is a fine balance between viscosity ratio (λ), interfacial tension (γ_{12}), and chemical reactivity to achieve the desired morphology. For binary blends, the break-up of the minor phase during processing is often governed by the ratio of shear stress to the interfacial stress, otherwise known as the capillary number (Ca).[18] Shear stress during processing is the driving force for the minor phase deformation, whereas γ_{12} resists the deformation. Hence, droplets will continue to break up during mixing as long as the shear stress is greater than the interfacial stress, a point which is quantified by the critical capillary number (Ca$_{crit}$).[19] In contrast, λ governs the break-up time, which is why droplet formation is favored when λ is lower and close to unity.[20]

(1) Sheet/ribbon of the dispersed phase forms
(2) Holes form in the sheet due to instability
(3) Size and concentration of holes increases
(4) Dispersed phase sheet breaks into elongated, irregularly shaped structures
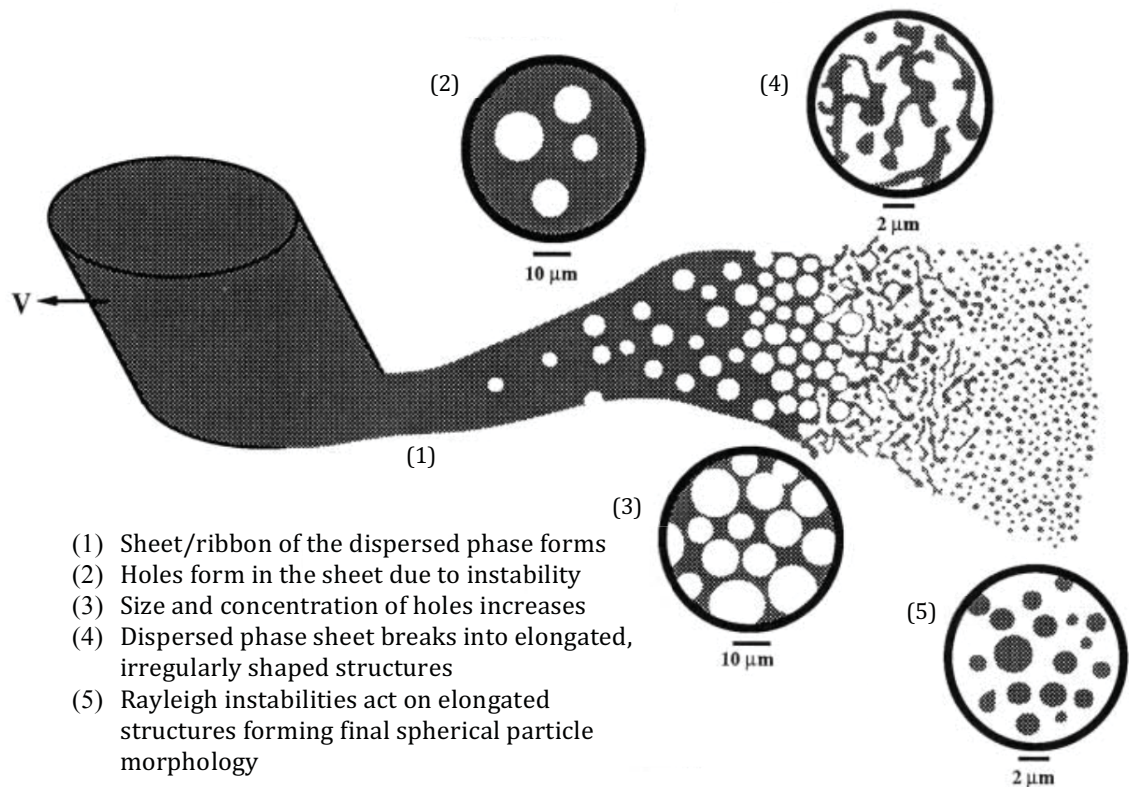(5) Rayleigh instabilities act on elongated structures forming final spherical particle morphology

Figure 6. Proposed mechanism of morphology development in polymer blends. Reprinted (adapted) with permission from C.E. Scott and C.W. Macosko, *Polymer.* **1995**, *36*, 3. © (1995) Elsevier Science Ltd.[17]

When one blend component (polymer A) is present as a low percentage of the composition, it will typically be dispersed as small droplets in the other blend component (polymer B), the matrix phase. As the fraction of the polymer A increases, these domains coalesce and percolate into a three-dimensional space. When all the domains of polymer A have coalesced forming an interconnected network it is said to have become continuous. If this coincides with polymer B not yet becoming dispersed, the morphology formed is defined as co-continuous, where neither phase is the matrix and neither is dispersed. With a further increase in polymer A, a phase inversion occurs, where polymer B becomes dispersed in a matrix of polymer A (Figure 7). However, prediction of morphology in extrusion processing, particularly in non-Newtonian polymers, is complicated due to the

viscoelastic nature of the material which changes with temperature, and the complex flow fields (shear and elongational) during processing.[20]

In a classic work, Wu[20] states the relationship between λ and the Weber number. The Weber number is defined as the ratio of inertial forces to stabilising forces, and is calculated as (Equation 2)

$$G\eta_m a_n / \gamma_{12} \qquad (2)$$

where G is the shear rate, η_m is the matrix viscosity and a_n is the number average particle diameter. This relationship shows that, when plotted against one another (Weber number vs λ) a minimum value of the Weber number is observed when λ is close to 1. Wu also stated that particle size was directly proportional to $a_n^{0.84}$ for $\lambda > 1$ and $a_n^{-0.84}$ for $\lambda < 1$.
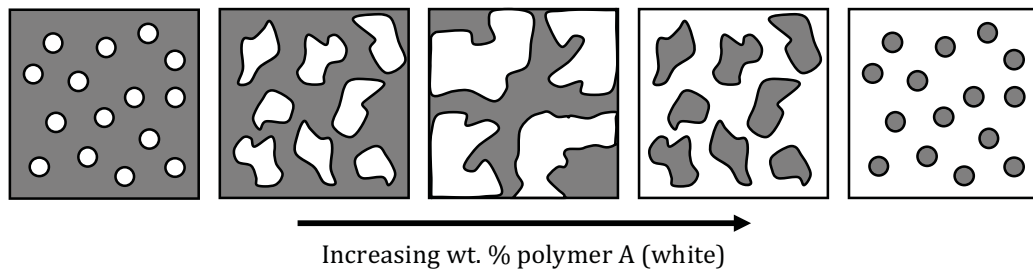

Increasing wt. % polymer A (white)

Figure 7. Change in morphology with increasing weight fraction of polymer A (white regions)

Lee and Han[21] studied the development of morphology at different stages along a twin screw extruder for a variety of blends. Typically, one would expect that a less viscous polymer would form the continuous phase when blended with a more viscous polymer. This study showed that in blends of PMMA/PS, when composition was asymmetric (i.e. 70 wt. % PMMA/30 wt. % PS and vice versa), the major phase formed the continuous matrix regardless of viscosity, and that at equal fraction (or nearly equal, i.e. 50/50) the viscosity ratio governed which phase was dispersed.

22

Morphology development becomes more complex in ternary blends and phase structure is governed by the spreading coefficients and wettability of phases towards one another.[22] Complex morphologies such as core-shell structures[23] and triple percolated (co-continuous) phase structures[24] can be produced in ternary blends depending on the balance of γ_{12}, λ and chemical interaction. It has also been stated that viscosity ratio plays less of a role in morphology development in ternary blends than interfacial tension.[25]

2.2.4 Co-continuity

Of the morphologies that can be formed in a polymer blend, co-continuous phase structures offer the unique advantage of having major contributions to material properties from both phases, in particular elastic modulus.[26] However, the detection of a purely co-continuous structure can be difficult. At low fractions of the minor phase, dispersion can be clearly indicated through electron microscopy and inferred through indirect methods such as dynamic mechanical analysis (DMA). However, with an increase in minor phase content, the onset of percolation and coalescence of discrete phases means that analysis of morphology must be done in 3-D, with a number of supplementary techniques; for example, electron microscopy can identify phase structure in two dimensions, selective phase extraction provides data about the interconnectedness of the minor phase and DMA provides information regarding the contribution to the elastic modulus of blend components. However, on their own these techniques would elucidate (in most cases) false conclusions about the morphology of the blend, hence a number of methods need to be employed for a full morphological analysis.

It was long believed that co-continuous structures only formed near the phase inversion point; the composition at which the continuous matrix becomes dispersed

and vice versa and is often at near equal proportions of the components. However, it has been demonstrated that continuous minor phases can be formed at much lower concentration, and the region in which full co-continuity occurs can be over a large range of compositions.[27] In binary polymer blends, experimental data tends to show that the onset of continuity of the minor phase, or the 'critical percolation threshold volume fraction' (φ_{cr}), falls between 0.1 and 0.3 (however, miscibility or interfacial modification tends to increase this value as coalescence is resisted).[28] It has been shown that reactive blends delay the onset of phase inversion due to steric hindrance at the interface, meaning that co-continuous morphologies can be present for long periods of time during mixing over large composition ranges, rather than breaking down into a dispersed phase structure.[29]

The classical expression for the phase inversion point, and subsequently the point at which co-continuity could be expected, is based on sample composition and λ as (Equation 3)

$$\varphi_1/\varphi_2 = \eta_1/\eta_2 = \lambda \qquad (3)$$

where φ_1 and φ_2, and η_1 and η_2 are the volume fraction and viscosities of polymer 1 and 2, respectively. However, this relationship failed to take into account interfacial interaction. Willemse et al. suggested that γ_{12} can play a significant role in the formation of co-continuous morphologies and that the volume fraction at which full co-continuity occurs increases with increasing γ_{12}, narrowing the region of co-continuity.[30]

Bhadane et al.[31] investigated the effect of viscosity ratio and shear stress on blends of EPDM and PP, which is an immiscible blend with very low interfacial tension. It was found that viscosity ratio, altered over a range of 0.7 to 5, had virtually no impact on phase size and coarseness, and level of continuity. The full continuity

diagram showed excellent symmetry and little deviation with changing λ. However, increasing composition brought about an increase to phase size and shape, changing from dispersed spheres to elongated stable fibers, and finally to a fully co-continuous phase (Figure 8)

Li et al.[32] classified co-continuous structures into three distinct groups based on the blend interfacial tension. Firstly, they categorised those with low interfacial tension whereby the network structure was formed through thread-thread coalescence as Type I blends. Second was high interfacial tension systems, where morphology development was dominated by droplet-droplet coalescence (Type II). Lastly, Type III systems had partial miscibility and emulsification, whereby droplet-droplet coalescence was responsible for co-continuity of the minor phase, albeit with an onset at a higher volume fraction of the minor phase. The morphology of Type II blends was shown to be strongly dependent on composition, whereas phase size in Type I and III was less dominated by this variable. Type I blends were said to have the broadest region of co-continuity due to high stability of the thread-like minor phase, whilst Type III blends had the narrowest co-continuous region.[32]
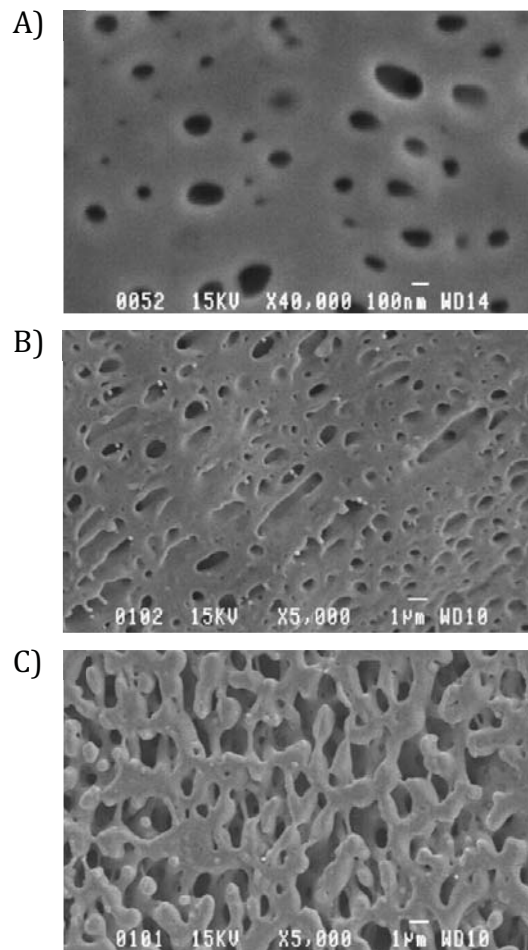
Figure 8. Scanning electron microscope images of EPDM morphology development in EPDM/PP blends. A) 10 wt. % EPDM; B) 30 wt. % EPDM; C) 50 wt. % EPDM. N.B Scale in image A is 0.1 μm, whereas in B and C the scale is 1 μm. Reprinted (adapted) with permission from P.A. Bhadane, M.F. Champagne, M.A. Huneault, F. Tofan, and B.D. Favis, *Polymer.* **2006**, *47*, 8. © (2006) Elsevier Ltd.[31]

2.2.5 Reactive extrusion

Reactive blending can take place in a two-step process where chemical modification of polymers prior to processing allows for interfaces to be created, however this can be an expensive and time consuming process. Typically, reactive extrusion is used to circumvent these issues and has been proven to provide very good mixing capabilities as well as forming new interfaces through chemical reactions occurring in-situ. The formation of these interfaces is crucial in the perceived success of the blend.

Extruder design, along with the screw design and process parameters, have a significant effect on the morphology produced. Co-rotating twin screw extruders are usually favored over single screw extruders or counter-rotating twin screw extruders as the co-rotating action of the screws combined with the self-wiping capabilities (due to the close intermeshing of screws) allows for folding and reorientation of polymers with no areas of stagnant, unmixed material (Figure 9).[33]
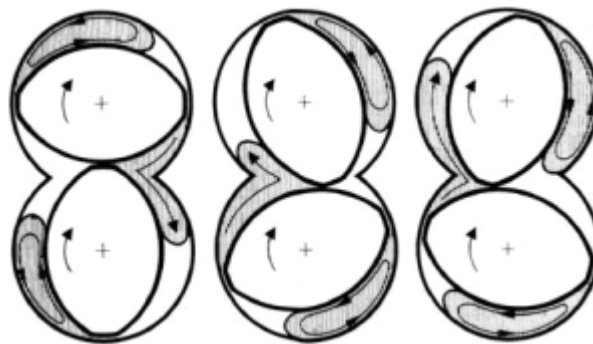

Figure 9. Flow pattern of material as a result of kneading blocks in a co-rotating twin-screw extruder. Reprinted (adapted) with permission from P.G. Andersen, *Mixing Practices in Co-Rotating Twin Screw Extruders*, in *Mixing and Compounding of Polymers*, I. Manas-Zloczower, Editor. 2009, Hanser Publications: Ohio, USA. p. 947. © (2009) Carl Hanser Verlag, Munich.[33]

The configuration of the screw within the twin screw extruder plays a big part in determining mixing and reaction efficiencies when concerned with reactive extrusion. Screw flights are the main conveying elements in the extrusion process responsible for the movement of the material through the barrel, whilst kneading blocks provide mixing despite restricting flow somewhat. Varying the number of mixing (kneading) zones can have significant effects on the level of mixing achieved during extrusion processing. Graiver[34] stated that optimal mixing of compatibilized soy protein and biodegradable polyester was achieved by using a screw configuration containing a high amount of kneading block elements. The increased number of mixing zones increased the reactive zone whereby the material

was exerted to high shear forces at high temperatures causing protein unfolding, and consequently increased interactions with the compatibilizing agent. Furthermore, it was shown in grafting of starch with propylene oxide to form hydroxypropylated starch, that extra mixing zones in the screw profile increased the grafting efficiency compared to a screw containing only conveying elements.[35]

Changing the design of these mixing zones, rather than just increasing the amount of them, can alter mixing. For instance, wider elements promote dispersive mixing because more of the polymeric mixture comes into contact with surfaces that induce high levels of shear, therefore increasing the energy applied to the material. This causes viscous dissipation (an increase in internal energy, observed as heating, as a result of fluid deformation under shear forces). However, an increase in dispersive mixing leads to a decrease in distributive mixing due to splitting of the polymer flow, and vice versa. Changing the angle of kneading blocks has an effect on the conveying ability of the mixing zone. Depending on the composition of the kneading element the mixing zones can have positive, negative or no conveying action on the polymer melt. These areas promote interactions between component polymers in the blend by exerting high shear forces on the material as well as restricting flow whilst reorienting material. Mixing zones with discs perpendicular to each other offer no conveying effect and material is caused to flow as a result of pressure from material flow at earlier points in the barrel.[33]

Processing parameters are considered highly important during the reactive extrusion process. Emin and Schuchmann[18], in their study describing droplet break up and coalescence within starch blends, describe how increasing screw speed decreased viscosity of the blend due to the increased shear stress and the subsequent degradation of starch, thereby reducing molecular weight of the starch phase. It was

also highlighted that additional mixing sections in the screw caused an increase in droplet break-up of the minor due to additional shear forces being created.

Additionally, the degree of fill in the screw channel, stagger angle of kneading blocks and residence time in the extruder can also play significant role in reactive extrusion. Fang et al.[36] showed that for the grafting of MA onto LDPE, higher stagger angle of kneading blocks (which corresponds to a negative conveying effect) correlated to a higher degree of grafting and smaller particle size. These two observations go hand in hand, as a decrease in droplet size provides increased interfacial area between polymer components, meaning the potential for chemical reactions at the interface is greatly improved. The onset of melting occurred when degree of filling was increased, and when melting occurred earlier, grafting degree was shown to improve. However, mean residence time was not proportional to degree of grafting, showing that reactions in-situ are complex and dependent on a number of variables.

2.3   Impact strength modification

The impact strength of a material is the ability to withstand a sudden load at high speed without failure. There are many influences on a polymers' impact resistance, both external (rate and mode of loading, thermal and chemical effects) and internal (polymer chain length and entanglement density, crystallinity). In many polymers, their applications are limited by poor impact strength, hence the topic of impact strength modification in both thermoplastics and thermosets is vast. It is possible to alter this material property in a number of ways; incorporating an elastomeric phase, the addition of reinforcement, or altering crystallinity (in semicrystalline polymers) have all proven to be effective forms of impact strength modification.[3]

Polymers were classified into two categories by Wu and co-workers;[37-39] brittle and pseudoductile. The failure mechanism in brittle, glassy polymers, and also in some semi-crystalline polymers, is typically crazing whereby the materials exhibit both low crack initiation and propagation energy. Crazing initiates at points of high stress concentration, often material flaws, or in the case of modified polymer this stress concentration is induced in the form of particles. In these areas, microvoids are formed, and under increasing applied stress these microvoids deform in the axis of the stress. The material between voids elongates to form fibrils, drawing material from the bulk matrix. Due to the highly oriented nature of fibrils the crazes are able to bear a load, hence an increase in energy can be absorbed by the material with increasing levels of crazing. Above a certain stress the fibrils fracture and a crack will propagate, resulting eventually in material failure. Craze formation is described in Figure 10. Despite energy absorption increasing with greater levels of crazing, it is negligible compared to the energy absorbed through extensive yielding of the matrix.[40]

MATRIX

CRACK   FIBRIL DEFORMATION   MICROVOID FORMATION
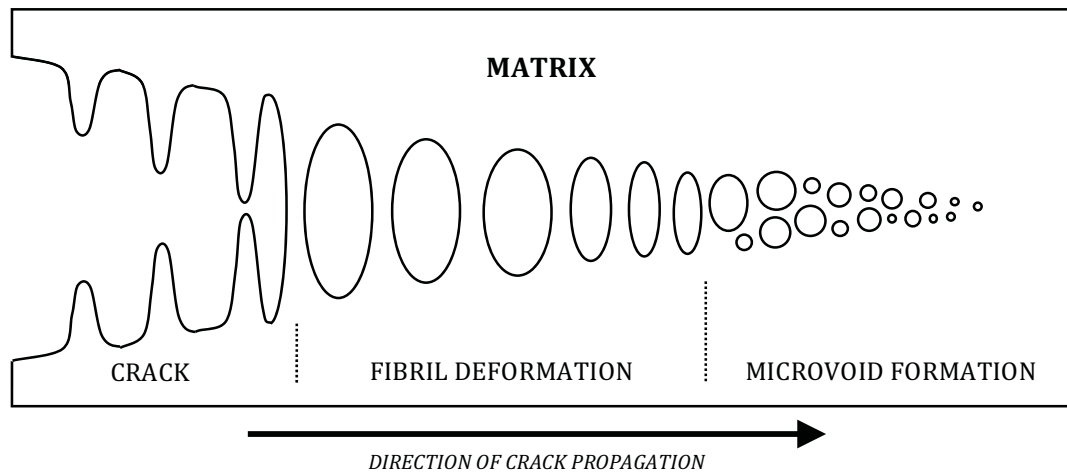
DIRECTION OF CRACK PROPAGATION

Figure 10. Formation of a craze. Reprinted (adapted) with permission from S.I. Krishnamachari, *Beyond Elastic Behavior*, in *Applied Stress Analysis of Plastics: A Mechanical Engineering Approach*. **1993**, Van Nostrand Reinhold: New York, USA. p. 146. © (1993) Van Nostrand Reinhold.[41]

In contrast, ductile materials fail through yielding, with high crack initiation energy (and therefore high unnotched impact strength) but low crack propagation energy and are therefore notch sensitive. Yielding is a complex process defined through the stress state of the material under load. Above the yield stress (providing this is below the craze initiation stress) plastic flow will occur, however the extent of plastic deformation is dependent on rate of strain and temperature. Yielding is isotropic, whereby the volume of material is constant during deformation. This is in contrast with crazing, where volume changes throughout the process.

The mechanism of fracture is related to the craze initiation stress, otherwise known as the brittle stress (σ_B), and yield stress (σ_y) of the material. If $\sigma_B < \sigma_y$, crazes initiate, propagate and break down into cracks causing catastrophic failure within the part, as crazing is able to absorb very little energy compared with shear yielding. In contrast, if $\sigma_B > \sigma_y$, then failure will occur by yielding and far more energy is able to be absorbed during fracture.[3, 40]

31

Julien et al.[42] stated that there was a number of transitions of crack growth during fracture; from fully stable, to partially stable, and lastly fully unstable. As loading rate increased during the compact tension testing of PMMA, crack growth mechanism changed from partially stable at low rates to fully unstable at fast rates. The introduction of rubber particles into the PMMA matrix stabilized crack growth at lower testing rates due to cavitation and shear yielding of the matrix thereby inducing a larger plastic zone at the crack tip, evident through an increase in K_{IC} fracture toughness over that of neat PMMA. At high testing speeds, however a decrease in K_{IC} was observed due to the time dependent nature of polymer chain relaxation.

The presence of a notch or defect in polymers can alter the type of fracture, from ductile to brittle. This can also be based on σ_y and σ_B, as polymers can fall into three categories;

1. Brittle; when $\sigma_B < \sigma_y$,
2. Ductile when unnotched, but brittle when notched (notch sensitive); $\sigma_y < \sigma_B < 3\sigma_y$,
3. Fully ductile regardless of notch; $3\sigma_y < \sigma_B$

The stress required to produce deformation in compression, from a flat punch on a plate, was shown to be $(2 + \pi)K$, where K is the shear yield stress. When working under the constraints of the von Mises yield criterion this value is $2.82\sigma_y$, which is hence approximated to $3\sigma_y$.[43] This was applied to notched plates, and described that for a deep, sharp notch the yield stress is roughly three times larger, hence brittle fracture is more likely at lower stresses.

Cho et al.[40] proposed a model for the notch sensitivity of ductile polymers, whereby the influence of a semi-circular notch was investigated with relation to the area at the notch tip that is able to yield. For untoughened PC, it was shown that

impact strength increased linearly with the square of the notch radius due to the increase in size of the plastic yielding zone around the notch tip. However, this was not true for the rubber toughened PC, as rubber particles reduced notch sensitivity and had greater toughening effects at lower notch radii.[40]

Wu[39] stated that the failure mechanisms in neat polymer matrices were governed by two intrinsic properties; characteristic ratio (C_∞), defined as a measure of flexibility and rigidity of an unperturbed polymer chain, and entanglement density (v_e) which is described as the ratio of the amorphous mass density to the molecular weight of an entanglement strand. It was shown experimentally that glassy polymers will craze when $v_e \leq \sim 0.15$ mmole/cc and $C_\infty \geq \sim 7.5$, and vice versa for ductile polymers which are prone to yielding. Therefore, as entanglement density increases so too does ductility past a critical point.

2.3.1 Particle reinforcement

Particulate reinforcement is a popular method of toughening polymers. When aiming to toughen a polymer matrix, a number of routes can be followed to incorporate the reinforcement, depending on whether rigid or elastomeric particles are being used. Rigid particles, such as calcium carbonate or silica have to be compounded during melt processing, however elastomeric particles can be formed through polymer blending (reactive and non-reactive) *in-situ*, eliminating a processing step.

2.3.1.1 Elastomeric particles/inclusions

The inclusion of elastomeric spherical particles is a well-documented example of impact strength modification. The main aim of the elastomeric particles is to facilitate and enable the dissipation of energy during fracture. The classic example,

and what was one of the first in-depth investigations into rubber toughening, is blends of nylon-66 and rubber, done by Wu in the late 1980's.[38] In these blends, it was shown that a brittle-to-ductile transition (BDT) occurred at critical number-average particle diameters, which changed depending on rubber content (10, 15, 25 wt. %) (Figure 11 A). However, when impact strength was plotted against the surface-to-surface interparticle distance (otherwise described as the matrix ligament thickness, τ) the BDT was found at one critical value (τ_c) (Figure 11 B). Therefore it was stated that provided $\tau < \tau_c$ then the material would be effectively toughened. Wu states this value to be independent of rubber particle size and content, and is a material property of the matrix, calculated by (Equation 4)

$$d_c = \tau_c \left[k(\pi/6\phi_r)^{1/3} - 1 \right]^{-1} \qquad (4)$$

where d_c is the critical particle diameter, k a geometric constant (k =1 for cubic lattice particle packing) and ϕ_r the rubber volume fraction. The reason stated for the toughening effect when $\tau < \tau_c$ is a transition of the matrix material from a state of plane-strain to plane-stress. When the matrix polymer is said to be in plane-strain, it is under triaxial stresses (brought about as a result of shrinkage during cooling) and unable to elongate in one plane due to being constrained elastically, therefore strain in that plane is equal to zero. As the ligament thickness decreases, a transition to plane-stress is seen; the elastic constraint is removed and the triaxial stresses have been relieved, meaning the material can freely elongate, causing stress in the plane of elongation to equal zero.[44]

Whilst it is often desirable to think that tensile energy-to-break (area under the tensile stress-strain curve) and impact resistance are directly linked, this correlation is not always predictable.[3] Similarly, mechanical damping as determined from dynamic mechanical analysis also does not show a predisposition to high impact

strength,[45] although links have been established between secondary transitions below the T_g and good impact properties, but only if these are major chain motions and not those of side chains.[3] A relationship was determined, however, between τ_c and the product of tensile yield stress (σ_y) and yield strain (ε_y), whereby as $\sigma_y\varepsilon_y$ increased, τ_c decreased.[46] Furthermore, τ_c was also shown to increase as the BDT temperature of the matrix decreased, which was brought about in this study through an increase in plasticizer. The more ductile the matrix is, the larger τ_c is as the matrix is more susceptible to shear yielding.
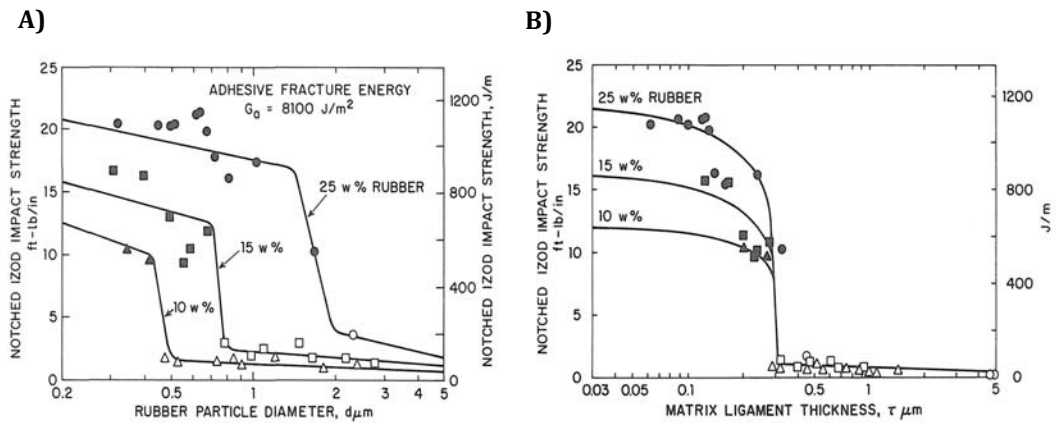

Figure 11. Notched Izod impact strength of PA66/rubber blends plotted against; A) number-average particle diameter; B) matrix ligament thickness. Reprinted (adapted) with permission from S. Wu, *J. Appl. Polym. Sci.* **1988**, *35*, 2. © (1988) John Wiley & Sons, Inc.[38]

Margolina and Wu[37] extended Wu's original ligament thickness theory, stating that stress volume spheres occupied the space around the rubber particles. The diameter of these spheres (S_c) is defined as (Equation 5)

$$S_c = d_c + \tau_c \qquad (5)$$

When the criteria for τ_c is met, or at the BDT, spheres of adjacent particles overlap. At this point, the rate of chain relaxation is accelerated in the overlapping region and shear yielding can occur in these areas. This is highly dependent on strain rate

and in the past this phenomenon has been labelled as "strain-accelerated relaxation".[44]

The intrinsic properties that affect the matrix BDT, C_∞ and v_e, also heavily affect τ_c and the optimal rubber particles size in blends (d_{opt}). With decreasing v_e, d_{opt} increases, hence larger particles are preferred for brittle polymers and vice versa, whilst increasing C_∞ corresponding to highly rigid, inflexible polymer chains correlates to a decreasing τ_c.[39]

2.3.1.2 Core-shell particles

To improve adhesion between the elastomeric particle and the matrix, composite droplets, otherwise known as core-shell particles, can be used. Typically a core of one polymer is encapsulated by a shell comprising a different polymer which is either miscible or compatible with the matrix, or that has been functionalized with groups reactive towards the matrix. These can be formed *in-situ* as a result of morphology development in ternary blends, or due to immiscibility in block copolymers with glassy and elastomeric blocks. It is also possible to incorporate commercially available pre-synthesized particles into materials during processing.

Ke et al.[47] investigated the effect of a thin rubber layer encapsulating an LDPE core in PA6, in effect a LDPE-*g*-BR-*g*-MA/PA6 blend, in comparison to LDPE/PA6 and polyolefin elastomer/PA6 binary blends compatibilized with maleic anhydride. It was shown that at temperatures as low as - 15 °C, the blend containing the LDPE/BR core-shell particles had an impact strength three times higher than neat PA6, and at room temperature impact strength increased to over 1000 J/m (compared with ~ 65 J/m for PA6). It was concluded that despite the rubbery shell, the more rigid core contributed to the maintenance of tensile strength

along with the huge increase in energy absorption, however elastic modulus decreased significantly at high particle loading.

In a further study by the same authors,[48] a comparison between LDPE and PP encapsulated by the same BR-*g*-MA was conducted in order to address the issue of reduction in elastic modulus. It was found that although impact strength did not improve as much as with the LDPE core, decreases in elastic modulus were not as drastic at high particle loading. The lower level of improvement in impact strength was attributed to the lack of deformation by the PP core, meaning that any stress transfer during fracture became discontinuous as the fibrils formed by the rubbery shell broke at high strain rates. In comparison, the LDPE core deformed as the elastomeric shell did, meaning that energy absorption was greater.

Memon[49] proposed that core-shell particles in the matrix cover a much greater fraction of the blend than just the volume fraction of the particles. The interaction between the matrix and the functional groups (on the surface of the particles) forms an interphase, effectively increasing the particle volume fraction. In highly filled blends, the large effective volumes of the particles overlap, forming a network structure of particles. It was shown through low-frequency plate–plate rheometry of PC and core-shell particles that almost 100 % of the matrix was interacting with the inclusions at 20 wt. % modifier content.[49]

Schneider et al. investigated the toughening of polystyrene using natural rubber-based composite particles.[50] The extensive study looked at the architecture of the particle and the effect on PS toughening. It was concluded that the particle must deform rather than particle/matrix separation in order to achieve toughening; this was improved by incorporating rigid subinclusions into the elastomeric particle core, allowing for greater plastic deformation before failure. They also concluded

that cavitation of particles, and hence greater plastic deformation, was harder in particles which had a crosslinked rubber core, and therefore improvements in impact strength were not as great as non-vulcanised rubber particles.

2.3.2 Fiber reinforcement

Fiber reinforced materials tend to have reasonable impact strength if the applied load is perpendicular to the orientation of the fibers. If load is applied in a parallel plane, impact resistance tends to be compromised heavily. Failure in composites is often a complex process involving a number of mechanisms; simplified to matrix failure and fiber failure coupled with fiber-matrix debonding and fiber pull out.[51]

2.3.2.1 Synthetic fiber reinforcement

Glass fiber reinforced polymers (GFRP) are common place in everyday life, being utilised for products in various settings such as aerospace, automotive and electronics industries. E-glass is the most commonly used grade of glass fiber in GFRP, whilst S-glass is also used for applications requiring higher strength and modulus such as in aviation. E-glass has a tensile strength of around 2 GPa, compared with up to 4.5 GPa for S-glass

The low impact strength of PP has been a subject of interest in glass fiber composite research. Studies have shown the correlation between improved fracture energy values, tested through falling weight and pendulum impact tests, with the incorporation of long glass fibers in a PP matrix. It has been stated that short fibers (~ 0.4 mm) may not offer any significant toughening as the energy absorbed through crack bridging and fiber debonding/pull out is low.[52] In contrast, longer fibers (> 2.5 mm) bring about increases to impact resistance with increasing fiber length up to ~ 6 mm, after which impact strength reaches a plateau.[53] The correlation is also

apparent for fiber content and impact strength. Thomason and Vlug[53] showed the impact strength of glass fiber reinforced PP increased almost linearly with increasing fiber concentration (as high as 60 wt. %), whilst the rate of increase becomes more pronounced with longer fibers (up to 12 mm).

In contrast to glass fibers, carbon fibers have roughly twice the tensile strength and approximately three times the modulus of E-glass, as well as a much lower density, meaning the strength/weight and stiffness/weight ratios are exceptionally good.[54] Carbon fiber reinforcement is typically used in thermosetting resins, through processes like resin transfer moulding (RTI), or vacuum assisted RTI. Mats of carbon fiber woven together that are already impregnated with resin (known as 'prepregs') do not involve resin transfer and can be moulded readily into complex shapes upon the application of pressure and heat. Similar downfalls to GFRP's are a problem though, such as poor interfacial adhesion and matrix brittleness.

Interesting work into carbon fiber compounding into PA6 showed that a bilayer sample composition produced by 'film insert moulding', whereby one layer of PA6/carbon fiber was moulded with a PA6/rubber second layer, had a threefold increase in impact strength and a good balance between tensile and impact strength (compared to the PA6/rubber blend prepared through conventional injection moulding). The treatment of the fibers with nitric acid brought about the most improved interlaminar shear strength (ILSS) compared to untreated, plasma treated and liquid nitrogen treated fibers, attributed to the increase of polar functional groups at the fiber surface.[55]

The grafting of PEI onto carbon fiber brings about better interfacial adhesion between the fiber and an epoxy matrix; PEI is rich in amine and imine functionalities which can readily react with epoxy groups. The impact strength of

the carbon fiber/epoxy composite was improved by ~ 35 % when PEI was conventionally grafted onto the fiber, however when a method for PEI grafting utilising supercritical methanol as the reaction medium was employed, impact strength increased almost 50 % compared to the unmodified composite.[56] Similarly, the performance of an epoxy-carbon fiber composite was greatly improved with a two-fold approach; the addition of PSF to the epoxy, and silane treatment of the carbon fibers. This caused energy dissipation to increase through better interfacial adhesion of matrix and fiber (as a result of silane treatment), as well as crack growth arrest and plastic deformation of the PSF. The fracture energy (G_{IC}) required to propagate a crack almost doubled with the treatment.[57]

Whilst the performance of synthetic fiber composites is high, the production of these materials is seen to be energy intensive and not sustainable, hence renewable natural based fibers have also been explored.

2.3.2.2 Natural fiber reinforcement

Increasing interest has developed in using natural fibers as reinforcement in polymer matrices. The renewable and sustainable nature of these fibers is attractive, as well as their carbon neutrality and low density. However, the tensile strength and modulus of such fibers are far below the carbon and glass fiber equivalents (barring some exceptions).[54] A comparison of selected natural fiber mechanical properties is displayed in Table 2.

A number of studies have successfully improved impact strength using natural fibers as reinforcement for composites. For example, in 1:1 blends of glycerol plasticized soy flour/PTAT, the addition of up to 40 wt. % raw Indian grass fiber brought about increases in both tensile strength and modulus, but no change was seen in impact strength. However, after alkali treatment of the grass fibers with

sodium hydroxide, tensile strength, modulus and impact strength all improved significantly compared with the raw fiber composite. This was attributed to the decrease in fiber size as a result of alkali treatment allowing for better fiber orientation during processing. Furthermore, alkali treatment causes the removal of hemicellulose and lignin, meaning the greater number of hydroxyl (-OH) groups present on the fiber allowed for improved interaction (hydrogen bonding and polar interactions) between fiber and matrix.[58]

Table 2. Selected mechanical properties of natural fibers. Reprinted (adapted) with permission from A.K. Bledzki and J. Gassan, *Prog. Polym. Sci.* **1999**, *24*, 2. © (1999) Elsevier Science Ltd.[54]

Fiber	Density (g/cm^3)	Tensile Strength (MPa)	Elongation (%)	Modulus (GPa)
Cotton	1.5	290 - 600	7 – 8	5.5 – 12.6
Jute	1.3	390 - 770	1.5 - 1.8	26.5
Flax	1.5	345 - 1035	2.7 - 3.2	27.6
Hemp	-	690	1.6	-
Ramie	-	400 - 940	3.7	60 - 130
Sisal	1.5	510 - 635	2 - 2.5	10 - 22

The impact strength of PP was modified with the inclusion of jute fibers. There was a good correlation between increased fiber content (up to 40 wt. %) and improved impact resistance, while this was further improved with the incorporation of maleic anhydride-grafted-PP as a compatibilizer.[59] A similar relationship was described in composites of sisal fiber and Mater-Bi (a commercial starch based blend), whereby increased fiber content correlated to a greater impact energy, determined from a falling weight test. Furthermore, it was stated that the random orientation of the sisal fibers brought about greater K_{IC} values than when aligned transverse or longitudinally.[60]

2.3.3 Polymer blending for impact strength

As has been established, the morphology of a polymer blend can have a large influence on the impact strength it exhibits. The intrinsic properties of the matrix influence whether a polymer is glassy or ductile, therefore characteristic ratio (C_∞) and entanglement density (v_e) play a significant role in impact modification. Based on these factors it is more feasible to impact modify ductile polymers than brittle ones. When aiming to toughen thermoplastic polymers through blending, one would not usually consider a rigid polymer as the minor phase, although this is known to offer toughening in thermosets provided that rigid particle cavitates during fracture. A rigid inclusion tends to increase modulus and strength, but energy absorption usually decreases.

The toughening efficiency of the minor phase in a blend is dependent on a number of factors. Firstly, the blend should be processed such that the optimum particle size, d_{opt}, is achieved. Dispersed spherical particles of size d_{opt} bring about $\tau < \tau_c$ and therefore stress spheres overlap, hence during deformation triaxial stresses around the particle are relieved and yielding occurs. This can be brought about by altering processing parameters such as shear rate (or screw speed in extrusion) and temperature, or through material properties such as viscosity ratio (λ) and interfacial tension (γ_{12}). Processing parameters and material properties are interconnected; for example increasing temperature typically decreases polymer viscosity, hence changes to λ are expected which may move it closer to unity. Similarly increasing shear rate, and subsequently shear stress during processing allows for the deformation of the minor phase for longer, overriding the effect of γ_{12}, which resists the deformation, linked to the capillary (Ca) and Weber number.

The effect of chemical interaction and miscibility also has influence on impact strength modification in polymers. During blending, the introduction of reactive functionalities in the form of compatibilizers, or partial miscibility through block copolymers, reduces interfacial tension and in turn promotes phase size reduction and potentially homogeneity. Good interfacial adhesion is important between minor and matrix phases as the ability to transfer stress from the matrix to the dispersed phase during fracture promotes energy absorption. However, excessive interaction in the way of crosslinking may be detrimental. Cavitation and debonding of particles is an energy absorbing mechanism and facilitates matrix yielding, so high levels of reaction between phases may actually cause embrittlement. The influence of these parameters in biopolymer blends with relation to impact strength is explored in section 2.4.

2.4   Impact strength modification of biopolymers through polymer blending

Similar to the multiphase systems described with synthetic polymers, biodegradable and bio-based systems have also received considerable attention, albeit with the aim of producing high performance materials with no compromise on degradability.

The complex structure of some biopolymers can make them challenging to process into thermoplastics. Typically the degradation temperature of many biopolymers is close to the transition temperature required for reorganization of the polymer chains and hence thermoplastic processing. Therefore, processing without additives is near impossible.[9] For example, native starch is made up of a combination of linear and branched forms of glucose; amylose and amylopectin. The processability of starch is based upon the ratio of amylose to amylopectin, as amylose is preferred due to its linear structure, and the ability to disrupt crystalline regions in a process known as gelatinization. Gelatinization is often done through plasticization with water and glycols.[61] Similarly, proteins have a complex structure of folded amino acids, and depending on the composition and sequence of those amino acids, a large number of inter- and intra-molecular forces must be disrupted prior to processing.[62]

Biopolymers are also typically expensive to produce and process, and that expense has limited the commercial uptake of them. For example, biopolymers such as PLA and PBAT are often > 3 USD/kg, whilst the likes of PCL can be up to ~ 20 USD/kg. In contrast, commodity polymers such as PE and PP can be bought for ~ 1 USD/kg, if not less. Until biopolymers are able to be produced on mass for equivalent to that of conventional synthetic polymers, it is unlikely that there will be a major replacement of non-biodegradable plastics with biopolymers.

Another challenge already eluded to is the sub-standard mechanical properties of many biodegradable polymers (Table 3). Many studies conducted into these materials investigate tensile properties, yet impact properties are largely forgotten. These materials tend to lack balance in terms of strength and stiffness compared to elongation, toughness and impact strength. For example, the tensile strength of PLA may be 70 MPa, yet it fractures at an elongation of < 5 %, whilst PBAT may reach an extension of up to 1000 % but stiffness and strength are lacking. Much of the research into this field aims to find that suitable balance, whereby improvement of one property is not detrimental to others.

Table 3. Selected mechanical properties of biodegradable polymers

Material	Tensile Strength (MPa)	Strain at break (%)	Modulus (MPa)	Impact Strength Izod (J/m)	Charpy (kJ/m^2)	Ref
PLA	65 - 70	5 - 11	~ 1875	15 - 20	~ 2	[63-65]
PBAT	11	> 500	40	54	-	[63]
PHBV	30	4	1.5	23	-	[66]
PBS	22	45	400	-	-	[67]
PCL	19	> 1000	190	-	No break	[68, 69]
Thermoplastic starch films	50	2 - 4	3600	-	-	[70, 71]
Soy protein	5 - 8	27	250	30 - 40	-	[58, 72]
Peanut protein film	6 - 8	50 - 65	150	-	-	[73]
Wheat gluten film	7	120	51	-	-	[74]

2.4.1 Biopolyesters

A number of biodegradable polyesters are available which can be classified as synthetic or natural. For example, PHA's such as PHB and PHV are known as bacterial polyesters as they are produced in the cells of microbes, as a result of nutritional deficiencies.[75] In contrast, biodegradable polyesters such as PBAT,

PBS (trans-esterification) and PCL (ring opening polymerization) are produced synthetically. Low T_g biopolyesters like PBAT and PCL can be used as impact modifiers themselves due to their good energy absorbing properties (Table 2), whilst it's been shown that the impact resistance of PHA's can be effectively modified, typically through the inclusion of elastomeric particles or by plasticization.

2.4.1.1 Polylactic acid (PLA)

PLA is an aliphatic polyester manufactured via ring opening polymerization of lactide, a dimer of lactic acid produced through microbial fermentation of carbohydrate rich sources. It has great potential to replace synthetic polymers in many applications due to its good mechanical properties, processability, sustainability and biodegradability. However, the high T_g, sensitivity to moisture and inherent brittleness limit the use of PLA.[76]

Many attempts have been made to combat the poor energy absorbing properties of PLA, with a number proving successful. A number of routes have been followed to improve impact strength and energy absorption, with blending appearing to be fairly successful. Typically, in those studies following the blending route, compatibilization has a significant effect, due to the level of interfacial adhesion achieved during blending.

For PLA blends, GMA is often used as a compatibilizing agent, either as a monomer, or grafted to a longer chain polymer. The reason for the popularity of GMA in PLA blends is the exceptionally high reactivity of the epoxy ring present, facilitated further by the high PLA processing temperatures (> 180 °C) compared with biopolymers such as starch and protein. Comparing low and high molecular weight PLA in blends of PLA and PE-*g*-GMA showed that large increases in energy

absorption were correlated to particle size. At 20 wt. % PE-*g*-GMA, the minor phase was much more finely dispersed in the high Mw PLA (50 – 100 nm domain size) compared to the low Mw PLA (100 – 300 nm), attributed to increases in shear stress generated during mixing, caused by the higher viscosity of PLA (Figure 12). However, the larger PE-GMA particles in the low Mw PLA actually brought about better impact properties, corroborated by the fact that τ_c as described by its relationship with v_e and C_∞ is 100 – 300 nm for PLA. Increased crystallinity after annealing also contributed to improvements in impact strength in low Mw PLA/PE-*g*-GMA.[65]
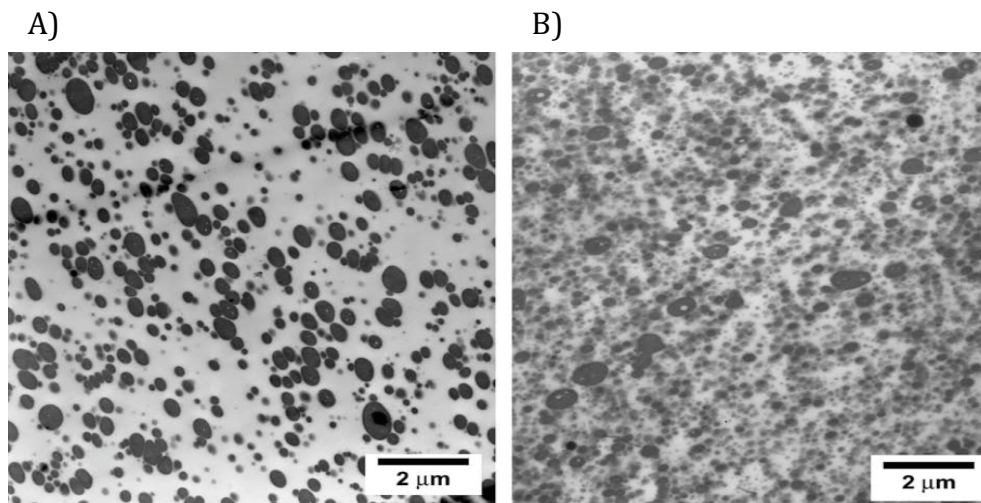
Figure 12. TEM micrographs of PLA/PE-GMA blends stained by ruthenium tetroxide; A) low Mw PLA/PE-GMA; B) high Mw PLA/PE-GMA. Reprinted (adapted) with permission from H.T. Oyama, *Polymer.* **2009**, *50*, 3. © (2008) Elsevier Ltd.[65]

Particulate reinforcement has also been shown to be effective in modifying PLA toughness when particles are functionalized with GMA. An improvement of 27 times the neat PLA Izod impact strength was brought about in a PLA/ABS-*g*-GMA blend with the inclusion of just 1 wt. % GMA.[77] Similarly, the use of GMA monomer as a compatibilizer for PLA blends has proven effective in PLA/PBAT blends of varying composition and with different wt. % GMA,[63, 78] although the

compatibilizing efficiency decreased above 5 wt. % GMA due to excessive crosslinking of epoxy groups and functional groups present on PBAT and PLA. A much greater improvement in impact resistance is seen in the ABS-*g*-GMA blends due to the efficient stress transfer and smaller particle size being much closer to the optimum particle diameter (Figure 13).

A number of other compatibilizers have led to improvements in impact resistance in PLA blends; the introduction of 0.5 wt. % lysine triisocyanate in PLA/polybutylene succinate (PBS) blends caused impact strength to triple,[79] whilst small additions of PCL to PLA/TPS also brought about significant improvements to ductility and impact resistance.[80]

On the other hand, some blends still exhibit greater impact resistance than neat PLA even in the absence of a compatibilizer. For example, synthesized random aliphatic copolyester (poly(ε-caprolactone-co-δ-valerolactone)) incorporated into PLA at 10 wt. % caused impact strength to triple,[81] whilst the in-situ polymerization of polyethylene glycol (PEG) and polymeric methylene diphenylene diisocyanate (pMDI) during reactive extrusion with PLA produced a blend containing crosslinked polyurethane particles in a PLA matrix with an impact strength up to 30 times greater than neat PLA.[64]
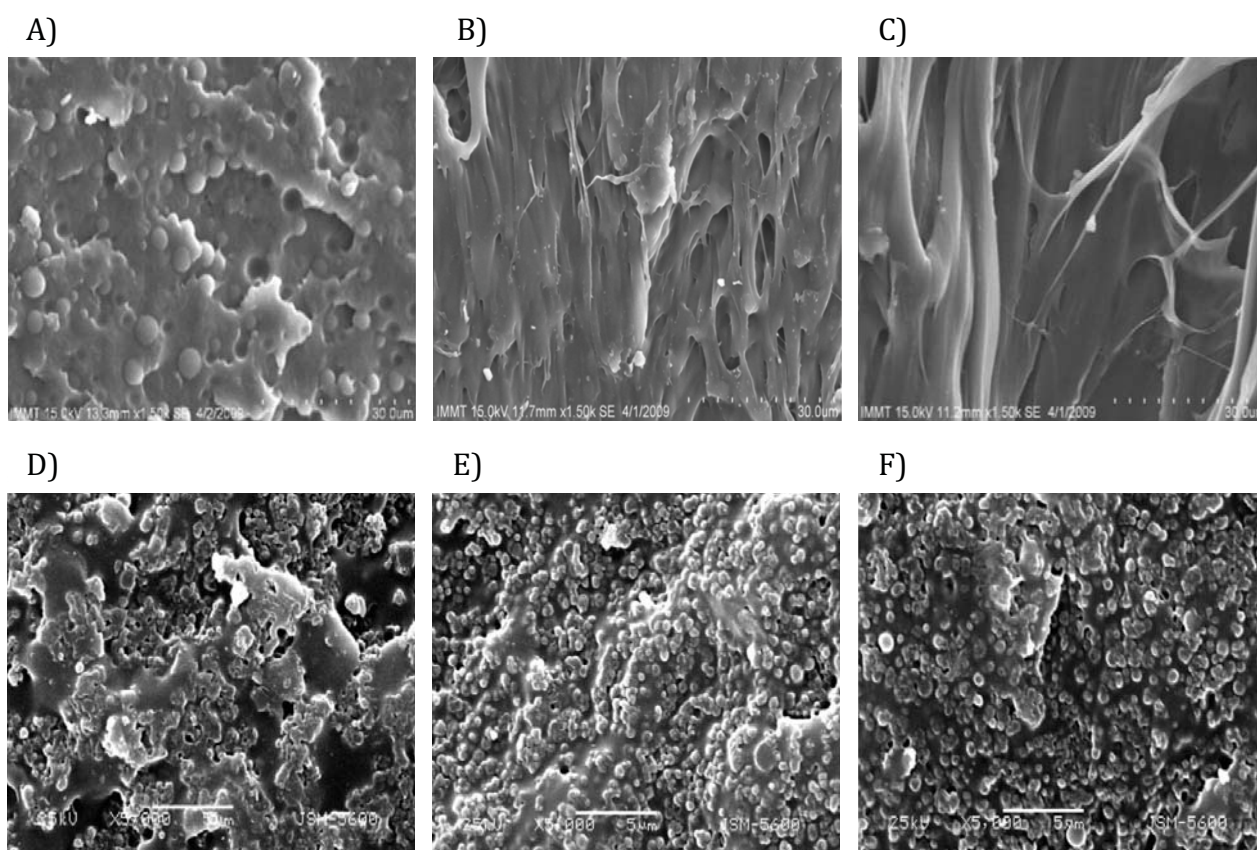
Figure 13. SEM micrographs of; A) PLA/PBAT/GMA (75/25/0 w/w); B) PLA/PBAT/GMA (72/25/3); C) PLA/PBAT/GMA (70/25/5); D) PLA/ABS-*g*-GMA (70/30/0); E) PLA/ABS-*g*-GMA (67/30/3); F) PLA/ABS-*g*-GMA (65/30/5). Scale bar in A – C is 30 μm and in D – F is 5 μm. Reprinted (adapted) with permission from M. Kumar, S. Mohanty, S.K. Nayak, and M. Rahail Parvaiz, Bioresource Technol. **2010**, *101*, 21 and S. Sun, M. Zhang, H. Zhang, and X. Zhang, *J. Appl. Polym. Sci.* **2011**, *122*, 5. © (2010) Elsevier Ltd., and (2011) Wiley Periodicals, Inc., respectively.[63, 77]

2.4.1.2 Polyhydroxyalkanoate (PHA)

Neat PHB was effectively toughened with the inclusion of epoxidized natural rubber (ENR) and BR-*g*-MA.[82] The notched Izod impact strength of PHB (~ 20 J/m) increased to over 120 J/m at an optimal inclusion of 30 wt. % ENR and 10 wt. % BR-*g*-MA. The molecular weight and maleic anhydride content of BR-*g*-MA also affect impact resistance, as lower Mw along with lower functionality of the BR-*g*-MA resulted in lower impact strength (~ 60 J/m).

PHB was also effectively toughened with natural rubber (poly(cis-1,4-isoprene), otherwise known as PIP), shown through an increase in strain at break and energy to break. However toughening was only seen when PIP was grafted with PVA, which is known to be miscible with PHB. Impact strength more than doubled with the inclusion of 20 wt. % PIP-*g*-PVA. This was attributed to a decrease in particle size and improved interfacial adhesion, brought about due to the decrease in interfacial tension between PIP and PHB as a result of PVA. Furthermore, the melt viscosity of PIP-*g*-PVA was lower than neat PIP, suggesting that viscosity ratio moved closer to unity with the inclusion of PVA (Figure 14).[83]

It has been shown that with co-polymers of PHB and PHV, polyhydroxybutyrate-co-valerate (PHBV), an increase in the hydroxyvalerate content increases notched Izod impact strength,[84] whilst it can also be impact strength modified with different epoxidized oils. A comparison of epoxidized soybean oil, epoxy soyate (the esterified form of epoxidized soybean oil with a chemical name 2-ethylhexyl epoxy soyate) and epoxidized linseed oil showed that epoxy soyate had the greatest effect on impact strength. This was attributed to the structure of the epoxy soyate, as during esterification through treatment with alcohol, molecular weight decreased allowing for better interaction as a plasticizer. There was little difference between unmodified PHBV and that with epoxidosed soybean oil or linseed oil. The further inclusion of polyhedral oligomeric silsesquioxane (POSS), a silicon based compound used for nanocomposites and as a precursor to ceramics, provided additional reinforcement and a further increase in impact properties at 5 wt. %. However, the greatest toughening effect was seen with the combination of both epoxy soyate and POSS.[66]
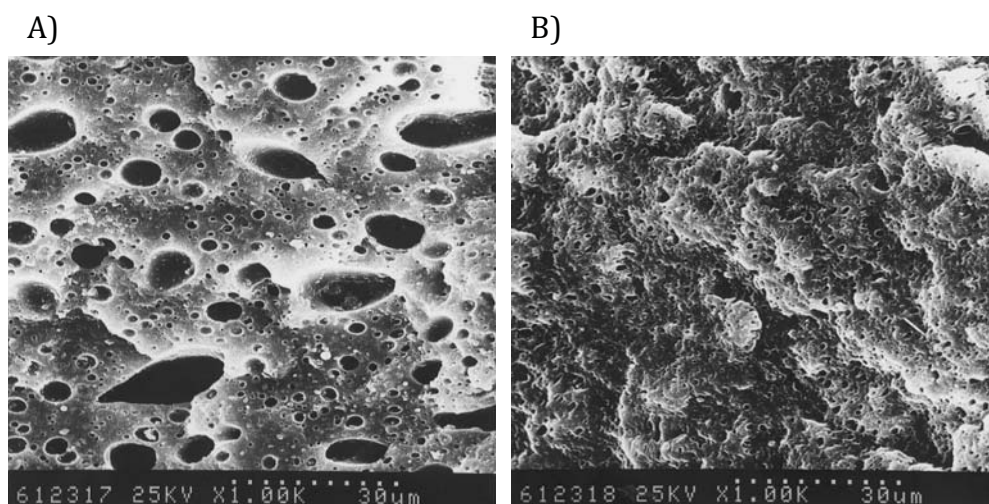
Figure 14. SEM micrographs of fracture surfaces from; A) PHB/PIP (80/20 w/w); B) PHB/PIP-*g*-PVA (80/20). Reprinted (adapted) with permission from S.Y. Lee, *Biotechnol. Bioeng.* **1996**, *49*, 1. © (1996) John Wiley & Sons, Inc.[83]

2.4.2 Thermoplastic starch

Thermoplastic starch is highly compostable at room temperature due to its hydrophilic nature, with ~ 60 % of the available carbon from TPS able to be mineralized in 14 weeks.[85] This high level of biodegradation, coupled with the high reactivity of the hydroxyl functional groups of both amylose and amylopectin,[86] makes TPS an attractive material for blending. A commercially available starch based material is Mater-Bi; a blend of TPS and PCL, produced by Novamont Ltd (Italy). Mater-Bi is typically used in packaging, agriculture and other consumer goods. It is appropriate for film blowing and foaming (depending on grade)[87] meaning the potential applications are large.

Thermoplastic starch materials have been produced which are particularly ductile, with elongation at break values up to ~ 125 % and 'no break' results quoted for impact strength. However, these materials have particularly low tensile strength and modulus. It was shown that these properties were heavily dependent on plasticizer

content (glycerol and water). These below par mechanical properties were able to be remedied somewhat by blending with PCL, without compromising the good impact properties.[68] The same authors found very similar results when blending TPS with PEA.[88]

Martin and Avérous[89] showed that for low PLA contents in blends of TPS/PLA the Charpy impact strength was improved when plasticizer content was higher in the starch phase. This correlated to a finer PLA phase structure in the more highly plasticized starch matrix, attributed to a decrease in viscosity ratio between TPS and PLA. However, from the SEM analysis (Figure 15) it was observed that the PLA phase was not fully dispersed, hence the co-continuous morphology of the blend means that PLA was likely to contribute highly to the blend properties.
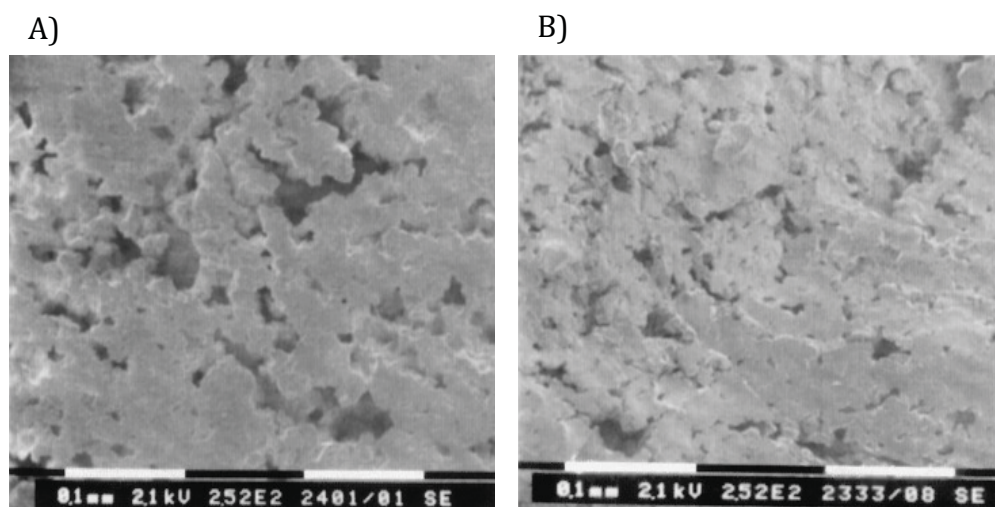

Figure 15. SEM images of TPS/PLA (75/25 w/w) blends after solvent extraction of PLA phase. A) Low plasticizer content TPS; B) High plasticizer content TPS. Scale bar is 100 μm. Reprinted (adapted) with permission from O. Martin and L. Avérous, *Polymer.* **2001**, *42*, 14. © (2001) Elsevier Science Ltd.[89]

2.4.3 Thermoplastic protein

Proteins are one of the most naturally occurring polymers, found in many plant and animal based sources. How the protein interacts with its environment is dependent on the make-up of different proteins, and the chemical functional groups found along the protein backbone vary depending on the particular amino acid, therefore dictating the conformation of the protein in its folded secondary, tertiary and quaternary states. However these reactive groups, providing that inter- and intra-molecular interactions are inhibited through denaturants and plasticizers, are able to interact and form bonds with other molecules. For example, primary amines, carboxylic acids, sulfhydryl and carbonyl groups can all be targeted for chemical interaction.[90] Secondary structures, the initial folding of the basic amino acid chain into ordered α-helices and β-sheets, have been shown to be linked to thermoplastic protein mechanical properties. For example, protein materials with high β-sheet content such as spider silk have been shown to have very high strength,[91] whilst high α-helix content is linked to good ductility and subsequently the ability to blow films from the thermoplastic protein.[92] Unordered structures have also been shown to transform into more ordered structures (α-helices and β-sheets) as a result of drawing and deformation.[93]

Sources of protein for thermoplastics are plentiful, from both plant and animal sources. Plant proteins such as soy, whey, casein, corn gluten, peanut and sunflower meal, and animal proteins such as bloodmeal, meat and bone meal, collagen, keratin, chitosan and gelatin have all been used for the production of thermoplastic materials, with varying degrees of success.[94] Due to the sub-standard properties of many thermoplastic proteins, blending has become a common route with the aim of improving the performance of these materials.

2.4.3.1 Impact properties of thermoplastic protein

Many studies have been concerned with the production of thermoplastic protein using both plant and animal-based material as the raw material source. However few deal directly with the impact properties of the material.

Tummala et al.[95] investigated the effect of different plasticizers on ~ 2:1 blends of soy protein thermoplastic and PEA. The best impact properties were observed in blends plasticized with glycerol, however compatibility of the blend was poor and the improvements in impact resistance could mainly be attributed to local ductile fracture of PEA. In contrast, the inclusion of sorbitol as a plasticizer caused greater tensile strength and modulus, but poor impact resistance, caused by strong hydrogen bonding between protein and PEA. The storage modulus (E') of the glycerol plasticized blend was much lower than the sorbitol plasticized blend, and tan δ showed a prominent peak below ambient temperature attributed to the T_g of PEA. This observation suggests a co-continuous morphology formed, and this could be confirmed through the SEM analysis (Figure 16) whereby the large areas of yielding were assigned to PEA, whilst the protein phase remained undeformed.

In a similar study from the same authors,[72] the same soy protein/PEA blend was reinforced with hemp fiber to produce a biocomposite. In comparison to the previous work the tensile strength and modulus, flexural strength and modulus, and impact strength all improved significantly with the incorporation of the fibers, although there was a large decrease in tensile strain at break.

Aithani and Mohanty[96] showed that blends of PCL and corn gluten meal (denatured by guanidine hydrochloride) had better elongation at break and impact strength than HDPE. This was attributed to the increased compatibility between PCL and corn gluten meal as a result of protein denaturation.
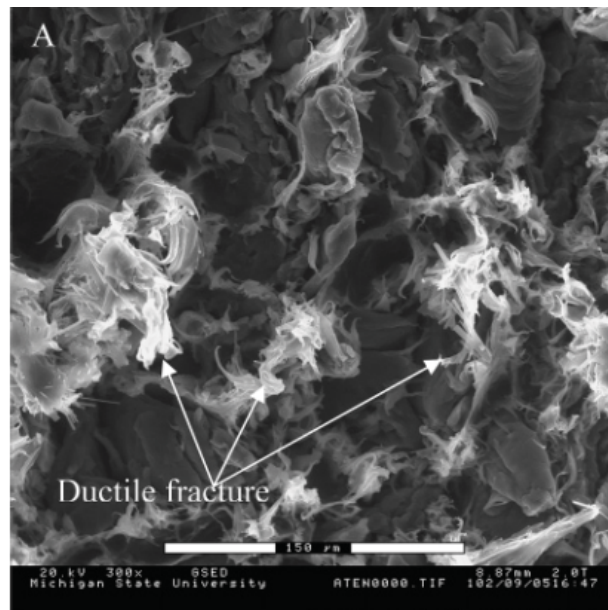
Figure 16. SEM micrograph of tensile fracture surface of glycerol plasticized soy protein/PEA blend. Scale bar is 150 μm. Reprinted (adapted) with permission from P. Tummala, W. Liu, L.T. Drzal, A.K. Mohanty, and M. Misra, *Ind. Eng. Chem*. **2006**, *45*, 22. © (2006) American Chemical Society.[95]

2.4.3.2 Novatein Thermoplastic Protein

Novatein thermoplastic protein, produced by Aduro Biopolymers LP (New Zealand), is a biopolymer that requires impact strength modification.[97] This material is produced from bloodmeal, a waste by-product of the meat processing industry with exceptionally high protein content (~ 90 wt. %). Novatein is very hydrophilic, and highly degradable in green composting situations, losing ~ 45 % mass in 12 weeks.[98] The tensile strength and modulus of Novatein have been compared to LDPE,[99] yet it has poor energy absorbing properties such as strain at break and impact resistance. The tensile properties of Novatein can be successfully modified depending on plasticizer content and the inclusion of additives. Blending of Novatein with both synthetic and biopolymers has proven successful due to the high level of reactive amino acids present among the protein backbone, coupled with appropriate compatibilization.[67, 100, 101] Novatein is currently being used for

renderable products, used in meat processing, that break down into protein meal during the rendering process. These Novatein products have the potential to replace single-use petrochemical-based equivalents which must be disposed of before rendering.

There appears to be a significant gap in the areas around the impact resistance of thermoplastic protein, including the protein structure-property relationships and morphology-property relationships when concerned with thermoplastic protein blends. However, based on literature regarding impact strength modification of other biopolymer systems through blending, similar approaches to synthetic polymers can be employed for improvements in impact resistance. The development of impact strength modified, biodegradable polymeric materials made from protein is potentially lucrative, and an understanding into the fundamentals around this topic would fill the gap in the current knowledge. Novatein thermoplastic protein is already in use for applications in the agricultural sector, and modification of the energy absorbing properties, primarily impact strength, could allow it to be used in a wider variety of applications.

2.5 References

[1]   Market-Research-Future. *Polymer Resin Market Report - Forecast to 2022*. 2016   [cited   2017   4   July];   Available   from: https://www.marketresearchfuture.com/reports/polymer-resin-market.

[2]   B.D. Favis, *Factors influencing the morphology of immiscible polymer blends in melt processing*, in *Polymer Blends Volume 1: Formulation* D.R. Paul and C.B. Bucknall, Editors. 2000, John Wiley & Sons, Inc.: New York. p. 501.

[3]   W.G. Perkins, *Polym. Eng. Sci.* **1999**, *39*, 12.

[4]   K.F. Mulder, *Technol. Forecast. Soc.* **1998**, *58*, 1-2.

[5]   S.M. Al-Salem, P. Lettieri, and J. Baeyens, *Waste Manage. (Oxford, U. K.)*. **2009**, *29*, 10.

[6]   S. Shafiee and E. Topal, *Energy Policy*. **2008**, *36*, 2.

[7]   M. Ratajska and S. Boryniec, *React. Funct. Polym.* **1998**, *38*, 1.

[8]   L. Avérous and E. Pollet, *Biodegradable Polymers*, in *Environmental Silicate Nano-Biocomposites*, L. Avérous and E. Pollet, Editors. 2012, Springer London. p. 13.

[9]   C.J.R. Verbeek and J.M. Bier, *Synthesis and Characterization of Thermoplastic Agro-polymers*, in *A Handbook of Applied Biopolymer Technology: Synthesis, Degradation and Applications*, S.K. Sharma and A. Mudhoo, Editors. 2011, Royal Society of Chemistry: London. p. 197.

[10]   C. Koning, M. Van Duin, C. Pagnoulle, and R. Jerome, *Prog. Polym. Sci.* **1998**, *23*, 4.

[11]   A.M.C. Souza and N.R. Demarquette, *Polymer*. **2002**, *43*, 14.

[12]   C.A. Orr, J.J. Cernohous, P. Guegan, A. Hirao, H.K. Jeon, and C.W. Macosko, *Polymer*. **2001**, *42*, 19.

[13]   H.K. Jeon, C.W. Macosko, B. Moon, T.R. Hoye, and Z. Yin, *Macromolecules.* **2004**, *37*, 7.

[14]   C.W. Macosko, H.K. Jeon, and T.R. Hoye, *Prog. Polym. Sci.* **2005**, *30*, 8–9.

[15]   S.S. Choi, H.M. Kwon, Y. Kim, J.W. Bae, and J.S. Kim, *J. Ind. Eng. Chem.* **2013**, *19*, 6.

[16]   H. Liu, X. Guo, W. Song, and J. Zhang, *Ind. Eng. Chem.* **2013**, *52*, 13.

[17]   C.E. Scott and C.W. Macosko, *Polymer.* **1995**, *36*, 3.

[18]   M.A. Emin and H.P. Schuchmann, *J. Food. Eng.* **2013**, *116*, 1.

[19]   F. Chen and J. Zhang, *ACS Appl. Mater. Interfaces.* **2010**, *2*, 11.

[20]   S. Wu, *Polym. Eng. Sci.* **1986**, *27*, 5.

[21]   J.K. Lee and C.D. Han, *Polymer.* **2000**, *41*, 5.

[22]   P. Le Corroller and B.D. Favis, *Polymer.* **2011**, *52*, 17.

[23]   H. Ohishi, *J. Appl. Polym. Sci.* **2004**, *93*, 4.

[24]   J. Zhang, S. Ravati, N. Virgilio, and B.D. Favis, *Macromolecules.* **2007**, *40*, 25.

[25]   S. Shokoohi and A. Arefazar, *Polym. Advan. Technol.* **2009**, *20*, 5.

[26]   P. Pötschke and D.R. Paul, *J. Macromol. Sci. Polym. Rev.* **2003**, *43*, 1.

[27]   T.S. Omonov, C. Harrats, P. Moldenaers, and G. Groeninckx, *Polymer.* **2007**, *48*, 20.

[28]   J. Lyngaae-Jørgensen, K.L. Rasmussen, E.A. Chtcherbakova, and L.A. Utracki, *Polym. Eng. Sci.* **1999**, *39*, 6.

[29]   N.D.B. Lazo and C.E. Scott. *Isolating the Effect of Reaction on the Phase Inversion of Model PA/PS Blends (564)*. in *Technical Papers of the Annual Technical Conference - Society of Plastics Engineers Incorporated*. 2000. Orlando, USA.

[30] R.C. Willemse, A.P. de Boer, J. van Dam, and A.D. Gotsis, *Polymer.* **1999**, *40*, 4.

[31] P.A. Bhadane, M.F. Champagne, M.A. Huneault, F. Tofan, and B.D. Favis, *Polymer.* **2006**, *47*, 8.

[32] J. Li, P.L. Ma, and B.D. Favis, *Macromolecules.* **2002**, *35*, 6.

[33] P.G. Andersen, *Mixing Practices in Co-Rotating Twin Screw Extruders*, in *Mixing and Compounding of Polymers*, I. Manas-Zloczower, Editor. **2009**, Hanser Publications: Ohio, USA. p. 947.

[34] D. Graiver, L.H. Waikul, C. Berger, and R. Narayan, *J. Appl. Polym. Sci.* **2004**, *92*, 5.

[35] R.A. De Graaf and L.P. Janssen, *Adv. Polym. Tech.* **2003**, *22*, 1.

[36] H. Fang, X. Ma, L. Feng, K. Wang, and B. Cao, *J. Appl. Polym. Sci.* **2008**, *108*, 6.

[37] A. Margolina and S. Wu, *Polymer.* **1988**, *29*, 12.

[38] S. Wu, *J. Appl. Polym. Sci.* **1988**, *35*, 2.

[39] S. Wu, *Polym. Eng. Sci.* **1990**, *30*, 13.

[40] K. Cho, J.H. Yang, B. Kang, and C.E. Park, *J. Appl. Polym. Sci.* **2003**, *89*, 11.

[41] S.I. Krishnamachari, *Beyond Elastic Behavior*, in *Applied Stress Analysis of Plastics: A Mechanical Engineering Approach.* **1993**, Van Nostrand Reinhold: New York, USA. p. 146.

[42] O. Julien, P. Béguelin, L. Monnerie, and H.H. Kausch, *Loading-Rate Dependence of the Fracture Behavior of Rubber-Modified Poly(methyl methacrylate)*, in *Toughened Plastics II*, C. K. Riew and A.J. Kinloch, Editors. **1996**, American Chemical Society: Washington D. C., USA. p. 233.

[43]   I.M. Ward and D.W. Hadley, *Breaking Phenomena*, in *An Introduction to the Mechanical Properties of Solid Polymers*. 1993, John Wiley & Sons Ltd: Chichester, England. p. 246.

[44]   A.F. Yee and R.A. Pearson, *J. Mater. Sci.* **1986**, *21*, 7.

[45]   C. Grein, K. Bernreitner, and M. Gahleitner, *J. Appl. Polym. Sci.* **2004**, *93*, 4.

[46]   W. Jiang, D. Yu, and B. Jiang, *Polymer.* **2004**, *45*, 19.

[47]   Z. Ke, D. Shi, J. Yin, R.K.Y. Li, and Y.W. Mai, *Macromolecules.* **2008**, *41*, 20.

[48]   D. Shi, E. Liu, T. Tan, H. Shi, T. Jiang, Y. Yang, S. Luan, J. Yin, Y. Mai, and R.K.Y. Li, *RSC Adv.* **2013**, *3*, 44.

[49]   N.A. Memon, *J. Polym. Sci. Pol. Phys.* **1998**, *36*, 7.

[50]   M. Schneider, T. Pith, and M. Lambla, *J. Mater. Sci.* **1997**, *32*, 23.

[51]   N.L. Hancox, *An overview of the impact behaviour of fiber-reinforced composites*, in *Impact Behaviour of Fiber-Reinforced Composite Materials and Structures*, S.R. Reid and G. Zhou, Editors. 2000, Woodhead Publishing Limited: Cambridge, England. p. 1.

[52]   B. Yu, C. Geng, M. Zhou, H. Bai, Q. Fu, and B. He, *Compos. Part B-Eng.* **2016**, *92*,

[53]   J.L. Thomason and M.A. Vlug, *Compos. Part A-Appl. S.* **1997**, *28*, 3.

[54]   A.K. Bledzki and J. Gassan, *Prog. Polym. Sci.* **1999**, *24*, 2.

[55]   S.Y. Kim, S.J. Baek, and J.R. Youn, *Carbon.* **2011**, *49*, 15.

[56]   L. Ma, L. Meng, G. Wu, Y. Wang, M. Zhao, C. Zhang, and Y. Huang, *Compos. Sci. Technol.* **2015**, *114*,

[57]   H. Carrillo-Escalante, A. Alvarez-Castillo, A. Valadez-Gonzalez, and P. Herrera-Franco, *Carbon Lett.* **2016**, *19*, 1.

[58] W. Liu, A.K. Mohanty, L.T. Drzal, and M. Misra, *Ind. Eng. Chem.* **2005**, *44*, 18.

[59] A.K. Rana, A. Mandal, and S. Bandyopadhyay, *Compos. Sci. Technol.* **2003**, *63*, 6.

[60] V. Alvarez, A. Vazquez, and C. Bernal, *J. Compos. Mater.* **2006**, *40*, 1.

[61] H. Liu, F. Xie, L. Yu, L. Chen, and L. Li, *Prog. Polym. Sci.* **2009**, *34*, 12.

[62] C.J.R. Verbeek and L.E. van den Berg, *Recent Patents on Materials Science.* **2009**, *2*, 3.

[63] M. Kumar, S. Mohanty, S.K. Nayak, and M. Rahail Parvaiz, *Bioresource Technol.* **2010**, *101*, 21.

[64] G.-C. Liu, Y.-S. He, J.-B. Zeng, Y. Xu, and Y.-Z. Wang, *Polym. Chem.* **2014**, *5*, 7.

[65] H.T. Oyama, *Polymer.* **2009**, *50*, 3.

[66] M.O. Seydibeyoglu, M. Misra, and A. Mohanty, *Int. J. Plast. Technol.* **2010**, *14*, 1.

[67] K.I.K. Marsilla and C.J.R. Verbeek, *Macromol. Mater. Eng.* **2014**, *299*, 7.

[68] L. Avérous, L. Moro, P. Dole, and C. Fringant, *Polymer.* **2000**, *41*, 11.

[69] G. Li and B.D. Favis, *Macromol. Chem. Phys.* **2010**, *211*, 3.

[70] W. Qiangxian, W. Zhengshun, T. Huafeng, Z. Yu, and C. Shuilian, *Ind. Eng. Chem.* **2008**, *47*, 24.

[71] Y. Zhang, L. Huang, H. Zhou, P. Zhang, M. Zhu, B. Fan, and Q. Wu, *Starch/Staerke.* **2013**, *65*, 5-6.

[72] A.K. Mohanty, P. Tummala, W. Liu, M. Misra, P.V. Mulukutla, and L.T. Drzal, *J Polym Environ.* **2005**, *13*, 3.

[73] N. Reddy, L. Chen, and Y. Yang, *Ind. Crops Prod.* **2013**, *43*, 0.

[74] L. Chen, N. Reddy, X. Wu, and Y. Yang, *Ind. Crop. Prod.* **2012**, *35*, 1.

[75]   X.Z. Tang, P. Kumar, S. Alavi, and K.P. Sandeep, *Crit. Rev. Food Sci.* **2012**, *52*, 5.

[76]   K.M. Nampoothiri, N.R. Nair, and R.P. John, *Bioresource Technol.* **2010**, *101*, 22.

[77]   S. Sun, M. Zhang, H. Zhang, and X. Zhang, *J. Appl. Polym. Sci.* **2011**, *122*, 5.

[78]   Z. Naiwen, W. Qinfeng, R. Jie, and W. Liang, *J. Mater. Sci.* **2009**, *44*, 1.

[79]   M. Harada, T. Ohya, K. Iida, H. Hayashi, K. Hirano, and H. Fukuda, *J. Appl. Polym. Sci.* **2007**, *106*, 3.

[80]   P. Sarazin, G. Li, W.J. Orts, and B.D. Favis, *Polymer.* **2008**, *49*, 2.

[81]   J. Odent, J. Raquez, E. Duquesne, and P. Dubois, *Eur. Polym. J.* **2012**, *48*, 2.

[82]   Y. Parulekar and A. Mohanty, *Green Chem.* **2006**, *8*, 2.

[83]   J.S. Yoon, W.S. Lee, H.J. Jin, I.J. Chin, M.N. Kim, and J.H. Go, *Eur. Polym. J.* **1999**, *35*, 5.

[84]   S.Y. Lee, *Biotechnol. Bioeng.* **1996**, *49*, 1.

[85]   G. Li, P. Sarazin, W.J. Orts, S.H. Imam, and B.D. Favis, *Macromol. Chem. Phys.* **2011**, *212*, 11.

[86]   G. Moad, *Prog. Polym. Sci.* **2011**, *36*, 2.

[87]   C. Bastioli, *Polym. Degrad. Stabil.* **1998**, *59*, 1–3.

[88]   L. Avérous, N. Fauconnier, L. Moro, and C. Fringant, *J. Appl. Polym. Sci.* **2000**, *76*, 7.

[89]   O. Martin and L. Avérous, *Polymer.* **2001**, *42*, 14.

[90]   P. Gupta and K.K. Nayak, *Polym. Eng. Sci.* **2015**, *55*, 3.

[91]   J.M. Gosline, M.E. DeMont, and M.W. Denny, *Endeavour.* **1986**, *10*, 1.

[92]   M. Oliviero, E. Di Maio, and S. Iannace, *J. Appl. Polym. Sci.* **2010**, *115*, 1.

[93] T. Kurose, K. Urman, J.U. Otaigbe, R.Y. Lochhead, and S.F. Thames, *Polym. Eng. Sci.* **2007**, *47*, 4.

[94] C.J.R. Verbeek and L.E. van den Berg, *Macromol. Mater. Eng.* **2010**, *295*, 1.

[95] P. Tummala, W. Liu, L.T. Drzal, A.K. Mohanty, and M. Misra, *Ind. Eng. Chem.* **2006**, *45*, 22.

[96] D. Aithani and A.K. Mohanty, *Ind. Eng. Chem.* **2006**, *45*, 18.

[97] C.J.R. Verbeek, K.L. Pickering, C. Viljoen, and L.E. Van den Berg: US8277553 (**2010**)

[98] C.J.R. Verbeek, T. Hicks, and A. Langdon, *J. Polym. Environ.* **2012**, *20*, 1.

[99] C.J.R. Verbeek and L.E. van den Berg, *Macromol. Mater. Eng.* **2011**, *296*, 6.

[100] K.I.K. Marsilla and C.J.R. Verbeek, *J. Appl. Polym. Sci.* **2013**, *130*, 3.

[101] K.I.K. Marsilla and C.J.R. Verbeek, *Macromol. Mater. Eng.* **2015**, *300*, 2.

3

Nonisothermal Curing of DGEBA with Bloodmeal-based Proteins

A paper published in

Industrial & Engineering Chemistry Research

By

M. J. Smith, C. J. R. Verbeek & M. C. Lay

Nonisothermal Curing of DGEBA with Bloodmeal-based Proteins

In Chapter 3, the reaction kinetics between Novatein and a model compound for epoxy functionalized polymers (DGEBA epoxy resin) was studied using nonisothermal DSC. The results were used to assess the viability of reactive extrusion of Novatein with epoxy functionalized polymers by determining parameters such as onset temperature of reaction, reaction rates, and allowed for the modelling of conversion as a function of time for bloodmeal protein-epoxy reactions, which are important in reactive extrusion.

As first author of this paper, I prepared the initial draft manuscript, which was refined and edited in consultation with my supervisors, who have been credited as co-authors

Nonisothermal Curing of DGEBA with Bloodmeal-based Proteins

Matthew J. Smith,* Casparus J. R. Verbeek, and Mark C. Lay

School of Engineering, University of Waikato, Private Bag 3105, Hamilton 3240, New Zealand

S *Supporting Information*

ABSTRACT: Differential scanning calorimetry (DSC) was used to study the curing reaction of bisphenol A diglycidyl ether (DGEBA) and Novatein thermoplastic protein (NTP). NTP is made from bloodmeal and is ~60% protein. Activation energy (E_a), pre-exponential factor ($\ln A_o$) and order of reaction ($m + n$) were calculated using the Kissinger, model-free isoconversional and autocatalytic models. Curing kinetics were almost independent of concentration and the addition of plasticizers and protein denaturants to bloodmeal caused a decrease in E_a of ~50%. Increasing protein denaturants had little effect on the reaction; however, inclusion of salt proved detrimental. At NTP's maximum processing temperature (~450 K), using an equal molar ratio of epoxy groups to reactive amino acids, 75% conversion can be reached in 3 min based on the modeling done here.

INTRODUCTION

Synthetic polymer production has overshadowed commercial production of natural polymers due to their superior mechanical properties and cost. At the same time, increasing waste has caused plastics produced from renewable and sustainable sources to regain some credibility.[1−3] A large variety of biopolymers can be processed into thermoplastic materials, and a particular area of interest is thermoplastics produced from proteins.[4−11] Bloodmeal is a byproduct of the meat processing industry and has a protein content of ~90 wt %.[11] Bloodmeal can be converted into a thermoplastic, and has been commercialized as Novatein thermoplastic protein (NTP).[12] The tensile strength and modulus of NTP are comparable to linear low density polyethylene (LLDPE);[13] however, it has a low energy-to-break and impact strength.

Reactive compounding is a common strategy for toughening brittle polymers and could potentially be used to improve NTP. By controlling the morphology of a polymer blend, energy absorption during fracture can be modified.[14] Impact modifiers are typically rubbery microdomains with lower T_g than that of the matrix material. The low T_g of these domains allows them to deform more than the matrix under loading, increasing energy absorption before material failure (e.g., high impact polystyrene).[15]

If this principle is applied to NTP, it would require the introduction of a second, more flexible phase into the NTP matrix, such as polyethylene. Functionalized polyethylene, containing highly reactive epoxide groups, has been used in impact modified PLA.[16,17] The three membered epoxy ring is reactive toward functional groups present on peptides;[18,19] however, the reactivity of epoxides with long chain proteins is less studied.

Primary and secondary amines found in amino acid functional groups (proline, histidine, asparagine, glutamine, lysine and arginine) react with epoxides to form secondary and tertiary amines, respectively. Hydroxyls and carboxyls (tyrosine, threonine, serine, glutamic acid and aspartic acid) react with epoxides to form ethers and esters, respectively. Furthermore, sulfhydryl groups on cysteine residues also react with epoxides forming covalent bonds between sulfur and carbon. Because all of these reaction mechanisms produce a hydroxyl group (reactive toward epoxide rings itself), opening of epoxy rings is considered autocatalytic.[18]

Reaction Kinetics. Bisphenol A diglycidyl ether (DGEBA) can be cured using both hydrolyzed protein[18,19] as well as amino acids[20] due to the prevalence of chemical side chains that are reactive toward oxiranes. The kinetic parameters of epoxy resin curing using hydrolyzed proteins (1.4−6.5 kDa) have been determined by El-Thaher et al.[18] using nonisothermal DSC. Kinetic parameters were calculated using the Kissinger equation and the model-free isoconversional method. Furthermore, the order of reaction was obtained by modeling conversion and rate of reaction data, and comparing this with experimental results.

Studying kinetic parameters of curing reactions using DSC assumes that the rate of reaction is proportional to the heat flow recorded. Therefore, by recording the heat flow of a curing reaction using a dynamic scan, the temperature at which the exothermic peak is at its highest can be used to calculate activation energy (E_a) because this is the point at which the reaction rate is maximum. The Kissinger method is commonly used in reaction kinetic studies as it does not require the reaction order to calculate activation energy, unlike many other kinetic models. The Kissinger method assumes that the curing reaction is first-order, dependent on temperature and independent of conversion (α). E_a and the pre-exponential factor (A_o) can be calculated using the maximum exothermic peak temperature (T_p) and heating rate (β).[21] This is expressed as

$$\Delta \ln\left(\frac{\beta}{T_p^2}\right) \Big/ \Delta\left(\frac{1}{T_p}\right) = -\frac{E_a}{R} \tag{1}$$

where R is the universal gas constant (8.314 J/mol). A plot of the values $\ln(\beta/T_p^2)$ vs $1/T_p$ for all heating rates produces a

Table 1. Sample Formulations Tested

mass ratio (NTP:DGEBA)	molar ratio (epoxy groups: reactive amino acid functional groups)[a]	additive/condition
1:1	~2	
7:3	~1	
1:1	~1.5	bloodmeal:DGEBA
1:1	~2	NTP (no TEG):DGEBA
1:1	~2	NTP:DGEBA + 5 pph NaCl
1:1	~2	NTP:DGEBA + 5 pph SDS

[a]Calculated from the amino acid structure of bovine hemoglobin and bovine serum albumin[25] using the reactive amino acids mentioned previously, assuming these are available for reaction.

straight line with a slope of E_α/R and y-intercept of $\ln(A_oR/E_\alpha)$. Using these E_α values it is also possible to calculate the temperature dependent rate constant (k) using the Arrhenius equation.

During epoxy curing, heat flow is proportional to the consumption of reactants and it is possible to plot the change in conversion by integrating the area under the DSC exotherm.[22] However, care must be taken in defining a consistent baseline and curve onset temperature. The model-free isoconversional method can be used to assess E_α and A_o at different points throughout the reaction with regards to conversion. By applying the Kissinger method to temperatures relating to different conversions, it can be shown how E_α and $\ln A_o$ change in comparison to the original Kissinger values, assumed to be constant throughout the reaction.

Finally, by selecting an appropriate reaction model, it is possible to simulate the reaction rate ($d\alpha/dt$) and conversion and compare these to experimental data. The rate of reaction is dependent on both concentration of reactants and temperature and takes the form

$$\frac{d\alpha}{dt} = \beta\frac{d\alpha}{dT} = kf(\alpha) = A_o\exp^{(-E_\alpha/RT)}f(\alpha) \quad (2)$$

where k is the temperature dependent rate constant, t is time and $f(\alpha)$ is a function of conversion. The conversion function, $f(\alpha)$, can take many forms depending on the type of reaction. Epoxy curing is considered autocatalytic which is modeled using the Sestak−Berggren model[23] whereby $f(\alpha)$ takes the form

$$\alpha^m(1-\alpha)^n[-\ln(1-\alpha)]^p \quad (3)$$

where ($m + n$) is the order of reaction and $[-\ln(1-\alpha)]^p$ is a function of pressure. The mechanisms of epoxy curing using proteins do not produce any gaseous byproducts, therefore the pressure function of the model is redundant and can be ignored. The advantage of the Sestak−Berggren model is that kinetic parameters E_α and $\ln A_o$, as well as the order of reaction ($m + n$), can be calculated simultaneously using a least-squares regression method.[24] Conversion can be simulated for reactive extrusion processes at various temperatures by numerically integrating the rate equation using the temperature dependent rate constant (k) as calculated from the Arrhenius equation and $f(\alpha)$ as calculated from the Sestak−Berggren model (eq 2).

Determining the reaction kinetics of the protein−epoxy system is important for successful reactive extrusion between NTP and epoxy functionalized polyethylene. Due to the low number of epoxide groups present on functionalized polyethylene, a low molecular mass, bifunctional epoxy resin commonly used in thermosetting material can be used as a model compound for the protein−epoxy reaction. The reaction between hydrolyzed short chain protein and epoxy resin has

previously been characterized;[18,19] however, a protein−epoxy system using longer chain bloodmeal-based protein has not.

This study analyses and models the curing reaction between long chain bloodmeal-based proteins and DGEBA epoxy resin using a nonisothermal DSC method. The concentration dependence of the protein−epoxy reaction, and the effect of plasticizers, denaturants and accelerators on the curing reaction are also examined.

■ EXPERIMENTAL SECTION

Materials. Bisphenol A diglycidyl ether epoxy resin (Epoxy R180 Resin) was acquired from Nuplex Composites, a division of Nuplex Industries (Auckland, NZ). Bloodmeal used in NTP preparation was acquired from Wallace Corporation (Te Aroha, NZ). Technical grade sodium dodecyl sulfate (SDS), analytical grade sodium sulphite (SS) and triethylene glycol (TEG) were procured from Merck (NZ).

Sample Preparation. SDS and SS (both 3 $pph_{bloodmeal}$) were dissolved in distilled water (25 $pph_{bloodmeal}$) at approximately 343 K using a magnetic stirrer and mixed with bloodmeal (100 parts) in a high speed mixer (Kenwood FP950 series) until a homogeneous powdery material was formed. For applicable formulations, TEG (20 $pph_{bloodmeal}$) was added to the bloodmeal/protein mixture and then mixed further in the high speed mixer until homogeneous material was obtained (NTP). The powder was stored overnight to equilibrate in a refrigerated environment (~277 K) before mixing with the epoxy resin.

A number of different testing conditions and material ratios were investigated (Table 1). For each testing condition a master batch was produced (~10 g) by adding NTP powder to epoxy resin. Other additives, such as NaCl and additional SDS, were dry blended at this point. A subsample was taken from this master batch for testing, and it was ensured that proper mixing had taken place. Sample formulations were selected to establish concentration dependence of reaction kinetics, and also to determine the effect of plasticizers, protein denaturants and additives on reaction kinetics.

Differential Scanning Calorimetry. Differential scanning calorimetry (DSC) was conducted using a PerkinElmer DSC 8500 equipped with a liquid nitrogen cooling system. Samples (3−7 mg) were placed in aluminum pans with an aluminum cover placed on top. Pans were not sealed as NTP degradation temperatures and TEG boiling point (as shown by previous TGA analysis[26]) are below the maximum DSC scan temperature and would therefore cause a sealed pan to rupture during scanning. Dynamic heating scans were conducted under nitrogen atmosphere at 5, 10, 15, 20 and 25 K/min, respectively from 293 to 573 K. Scans were conducted in triplicate for each heating rate. Nitrogen purge gas was used at a rate of 50 mL/min.
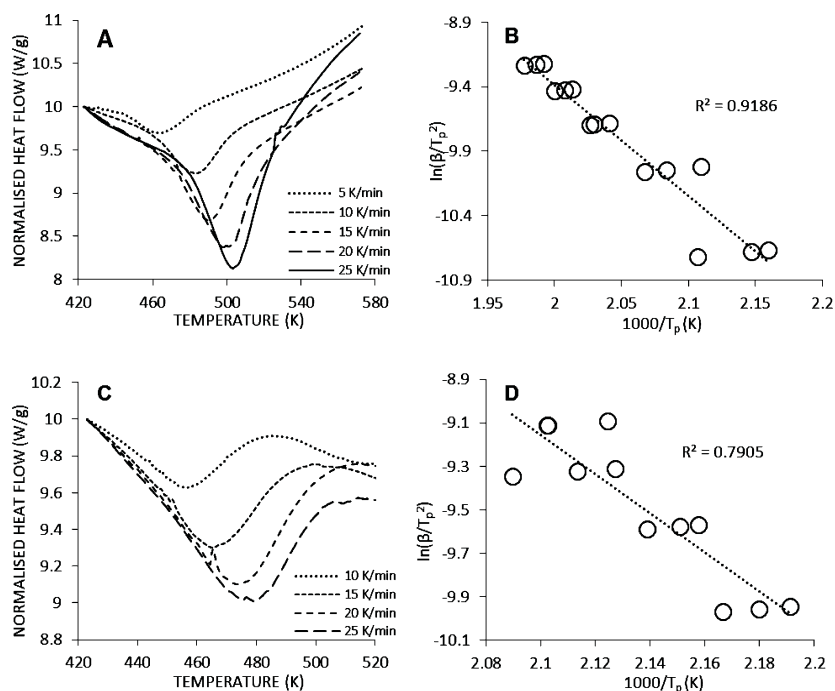
Figure 1. DSC curves and constructed Kissinger plots for different DGEBA:protein ratios (A and B) 1:1 and (C and D) 7:3.

■ RESULTS AND DISCUSSION

Concentration Dependence. Nonisothermal DSC of NTP−DGEBA mixtures revealed an increase in exothermic peak temperature with scan rate (Figure 1a,c). Using the exothermic peak temperatures across the range of scan rates, Kissinger plots were constructed (Figure 1b,d) and the activation energy (E_α) and pre-exponential factor (A_o) were calculated.

The activation energy and pre-exponential factor were almost independent of DGEBA concentration (Table 2). This may be

Table 2. Calculated Kissinger Parameters for Different Mass Ratios of NTP to DGEBA

mass ratio (NTP:DGEBA)	average T_p (K) (β = 25 K/min)	E_α (kJ/mol)	ln A_o (1/min)
1:1	503.74	71.7	16.92
7:3	473.98	74.9	18.87

attributed to the excess epoxy functional groups over reactive amino acid side groups in the 1:1 system and the almost equal ratio in the 7:3 system (Table 1). E_α and A_o values obtained for NTP are comparable to those from other research for epoxy resin cured with protein hydrolysate.[18] This can be expected as in both cases the number of available protein side groups reactive toward the oxirane are increased compared to protein in its native conformation or aggregated state where the side groups inside the protein or aggregate are protected. Although results presented in Figure 1 B and D suggest some variability because of a low R^2 value, a one way ANOVA test of exothermic peak temperature against heating rate states that the difference in values statistically significant.

Using the Kissinger method can introduce some error (reported to be less than 5%, provided $E_\alpha/RT > 10$)[27] between model and experimental results, because it assumes that the reaction is independent of conversion and first-order, making E_α and ln A_o constant throughout the reaction. When the
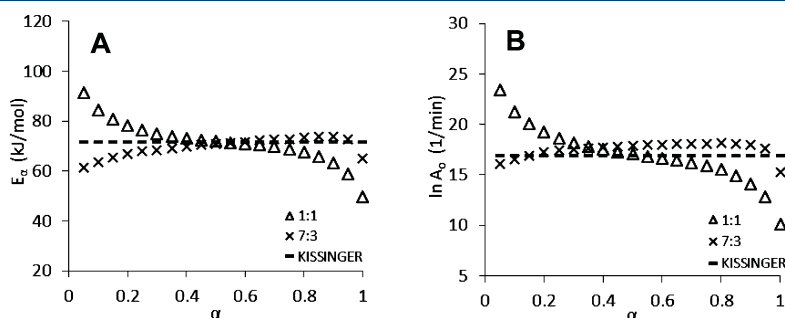

Figure 2. Dependency of (A) E_α and (B) ln A_o on conversion for the two mass ratios of NTP−DGEBA resin curing. Kissinger values are from the 1:1 NTP−DGEBA system.

68

model-free isoconversional method was used to examine the dependency of E_α and $\ln A_o$ on conversion (Figure 2), it showed that E_α and $\ln A_o$ were not constant throughout the reaction and were different for the two mass ratios of NTP:DGEBA trialled, suggesting the reaction is not first-order. If the reaction was independent of concentration of DGEBA and protein reactive groups, the shape of the individual plots in Figure 2 would be the same. A decrease in E_α and $\ln A_o$ with increasing conversion (after a conversion of 0.8 for a mass ratio of 7:3) could be attributed to vitrification within NTP, where protein chain mobility is reduced due to the curing reaction locking the protein chains in place, limiting DGEBA diffusion, and restricting the reaction.[28]

The average E_α and $\ln A_o$ values calculated using the model-free isoconversional method were all comparable to the values established using the Kissinger method. The average activation energies calculated were 71.8 and 69.7 kJ/mol for mass ratios of 1:1 and 7:3, respectively. The relationship between $\ln A_o$ and conversion was similar, with calculated values of 16.99 and 17.50 1/min for mass ratios of 1:1 and 7:3. The activation energy and pre-exponential factors were fairly constant in the middle stages of reaction ($\alpha = 0.2$ to 0.8) whereas they varied considerably at both high and low conversions (Figure 2). The constant E_α and $\ln A_o$ in the middle stages of reaction may be attributed to increasing energy given to polymer chains due to increasing temperature during the DSC scan overcoming the increased rigidity of the protein chains due to vitrification.[28] The decrease in $\ln A_o$ toward the end of the reaction in all cases can be attributed to the decrease in available reactive groups on the reactants as conversion increases.[19]

The curing of epoxy resins involves the formation of hydroxyl groups after proton transfer from the reactive group on the hardener to the oxygen in the epoxy ring. As hydroxyl groups are reactive toward oxiranes, epoxy curing is considered autocatalytic. These reactions are well modeled using the Sestak–Berggren model. By using finite difference methods the reaction order ($m + n$), E_α and $\ln A_o$ can be determined (Table 3) by fitting model data to the experimental data (Figure 3).

Table 3. Calculated Kinetic Parameters for Different Mass Ratios of NTP to DGEBA Using the Sestak–Berggren Model

mass ratio (NTP:DGEBA)	E_α (kJ/mol)	$\ln A_o$ (1/min)	($m + n$)
1:1	70.3	17.60	1.76
7:3	68.4	18.87	1.45
PEP220:DGEBA (1:1)[18]	63.0	14.60	1.37

The modeled data shows a very good fit with all experimental data, for both conversion and reaction rate ($d\alpha/dt$) as a function of temperature; therefore, the Sestak–Berggren model is suitable for modeling epoxy curing with NTP.

The reaction order ($m + n$), E_α and $\ln A_o$ values for curing of DGEBA using NTP are slightly higher than for a 1:1 ratio of DGEBA to hydrolyzed protein from other research (Table 3).[18] This may be attributed to a higher level of protein chain interaction and entanglement for NTP, decreasing the number or accessibility of reactive sites. These values are much lower than that of the curing reaction between DGEBA and unmodified bloodmeal (Table 5).

Effect of Additives on Reaction Kinetics. Unmodified bloodmeal and bloodmeal with denaturants but no plasticizer were also used as a curing agent for DGEBA as a comparison to NTP (Figure 4). Although bloodmeal is cross-linked due to heating during rendering and drying, enough reactive groups are present on the protein chain for curing. In both systems, the exothermic peak temperature, activation energy and pre-exponential factor were all high compared to NTP and would appear to be dependent on the mobility of the protein chains or the availability of reactive groups (Table 4).

The inclusion of protein denaturants (SS and SDS) caused a reduction of all the kinetic parameters (NTP (no TEG) in Table 4). This is attributed to the decrease in disulfide, hydrogen and hydrophobic bonding between amino acid residues on the protein chains, thereby increasing chain flexibility, possibly exposing more reactive groups. Furthermore, the inclusion of water and TEG, both known plasticizers for bloodmeal (and proteins in general) allows for increased protein chain mobility.[29] This increased level of mobility suggests that the reactions occurring between the reactive side groups of the protein and the oxiranes in the system are not limited to local interaction with groups in close proximity. This would therefore explain the decrease in E_α and $\ln A_o$ seen in the NTP system containing no TEG compared to the bloodmeal system.

Unbound water is evaporated at 373 K, while bound water can remain in the system up to 423 K.[26] Because both bound and unbound water leave the protein–epoxy blend prior to the onset of reaction there is only a limited level of plasticization available in the system after 373 K. Therefore, the addition of TEG during NTP processing increases the level of plasticization and even after the evaporation of water, allows the protein chains to move more freely until reaction with the epoxy group on DGEBA. This increased level of plasticizer is the reason that the kinetic parameters in the NTP–epoxy system containing TEG are lower.

Work conducted by El-Thaher et al.[19] explored the effect of protein denaturants (SDS and urea) on the reaction kinetics of protein hydrolysate and DGEBA. The inclusion of SDS brought about a large reduction in E_α and $\ln A_o$, whereas adding urea actually increased these kinetic parameters. Furthermore, Janssen et al. stated that the reaction between epoxy resins and amine hardeners can be accelerated using metal salts of inorganic acids.[30] Therefore, this work also explored the addition of SDS and sodium chloride (NaCl) to the NTP–epoxy system.

Although, further addition of SDS slightly decreased the average peak temperature, it did not have any significant effect on the reaction kinetics of the NTP–epoxy reaction. However, adding NaCl increased E_α and $\ln A_o$ (Table 4).

SDS is a protein denaturant, and although the inclusion of small amounts to the protein–epoxy system is proven to decrease E_α and $\ln A_o$, the additional SDS added later in the processing does not have the same effect as the SDS in solution. This is because the additional SDS may not be mixed fully into the system, as it is dry blended with DGEBA first, which is then mixed with NTP. The SDS in solution used in NTP processing is far more likely to disrupt interactions between polymer chains than the SDS in powder form; therefore, little change is seen in the kinetic parameters associated with this blend.

The addition of NaCl to the NTP–epoxy blend caused an increase in all the kinetic parameters. Other literature is contradictory regarding the effect of salt on the epoxy curing reaction. Janssen et al. provided a number of examples whereby the gelling time of an epoxy/amine hardener system is greatly reduced at room temperature (from 90 min to as low as 9 min
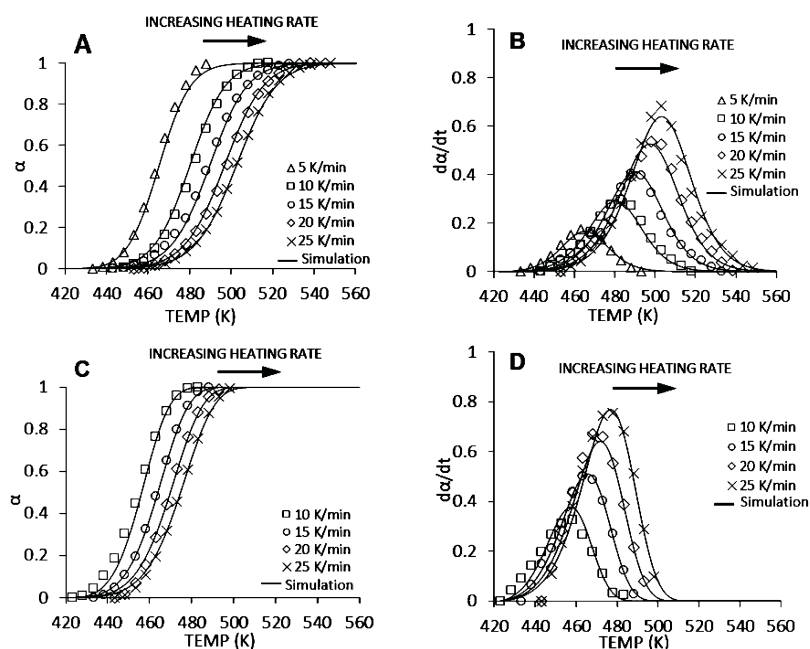
Figure 3. Experimental and simulated data for conversion (α) and reaction rate ($d\alpha/dt$) as a function of temperature for different mass ratios of NTP−DGEBA (A and B) 1:1 (C and D) 7:3.
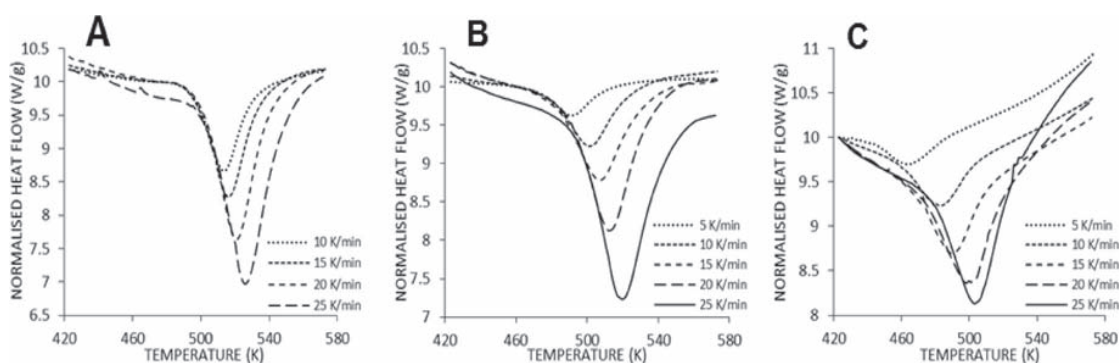

Figure 4. DSC traces of epoxy curing reaction with bloodmeal and NTP (A) 1:1 bloodmeal−epoxy system, (B) 1:1 NTP (no TEG)−DGEBA system and (C) 1:1 NTP−DGEBA system.

Table 4. Maximum Exotherm Peak Temperature (T_p) and Calculated Kissinger Parameters As Determined from DSC

curing agent	mass ratio (hardener:epoxy)	average T_p (K) (β = 25 K/min)	E_α (kJ/mol)	ln A_o (1/min)
bloodmeal	1:1	526	145.5	33.78
NTP (no TEG)	1:1	520.18	110.7	25.89
NTP (with TEG)	1:1	503.74	71.7	16.92
NTP (with TEG) + 5 pph SDS	1:1	494.30	74.3	17.94
NTP (with TEG) + 5 pph NaCl	1:1	512.42	96.1	22.71

in some systems) due to the inclusion of various metal salts.[30] In contrast, El-Thaher et al.[18] reported that protein hydrolysate extracted using a salt solution (predominantly NaCl) showed higher kinetic parameters regardless of hydrolysis temperature. The Kissinger parameters calculated for hydrolyzed protein extracted using salt solution (E_α = 89.4 kJ/mol and ln A_o = 22.83 1/min) are similar to the values seen in the NTP−epoxy system containing NaCl (96.1 kJ/mol and 22.71 1/min). This suggests that NaCl did not accelerate the reaction but instead

hindered the interaction between reactive protein side groups and epoxy groups. The hindrance was likely caused due to Na$^+$ and Cl$^-$ ions interacting with protein functional groups (COO$^-$, NH$_3^+$). These interactions need to be disrupted first before the reaction between the epoxy ring and protein functional group can occur.[18,19] This results in a higher activation energy, as demonstrated here.

The model-free isoconversional method was used to establish the dependency of E_α and ln A_o on conversion (Figure 5).
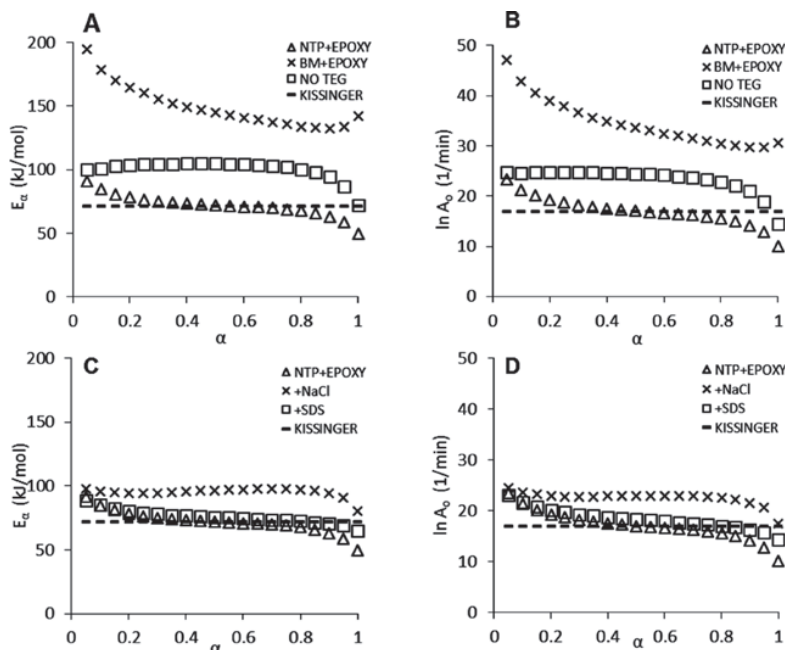
Figure 5. Dependency of E_α and $\ln A_o$ on conversion (α) for (A and B) systems with different denaturants and plasticizers, and (C and D) NTP−DGEBA systems with different additives. Kissinger values are from the 1:1 NTP−DGEBA system.

Similar to the previous results, it appeared that the change in pre-exponential factor was proportional to the change in activation energy. This may suggest that a decrease in activation energy at high conversion (as seen in the denatured, plasticized systems) is accompanied by a decrease in $\ln A_o$ as vitrification limits the interactions between protein and epoxy to local reactive sites. Even highly plasticized chains (as a result of TEG in the system), while having a much higher chain mobility, will still be cross-linked by reactions with DGEBA, bringing about similar behavior at high conversion. At all conversions, E_α and $\ln A_o$ decreased with the inclusion of protein denaturants. A further decrease was evident after plasticization. In both cases the rate of reaction is higher (Figure 6), suggesting that increased protein chain mobility had a similar effect to catalyzing the reaction.

Additional SDS has very little effect on the dependency of E_α and $\ln A_o$ on conversion. The shapes of the plot indicate the dependency is very similar, which is to be expected due to the comparable Kissinger parameters. The addition of NaCl on the other hand results in values that are particularly linear for α = 0.2 to 0.9. The values for this blend are a lot more constant than other systems, varying only 7 kJ/mol over the entire reaction. This value is very small in comparison to the bloodmeal−epoxy system and the plasticized NTP−epoxy system, which both varied by over 40 kJ/mol as the reaction progressed. The reasoning for this stable E_α could be that the reaction reaches a "dynamic balance" whereby factors affecting the reaction achieve a compromise as the decreasing frequency of reaction is effectively canceled out by the formation of hydroxyls during reaction (promoting autocatalysis).[28,31]

The autocatalytic nature of the curing reaction meant that kinetic parameters were calculated using the Sestak−Berggren model and the least-squares regression method. It is apparent that through denaturing the protein, the reaction kinetics decreased, thereby decreasing reaction temperature. For
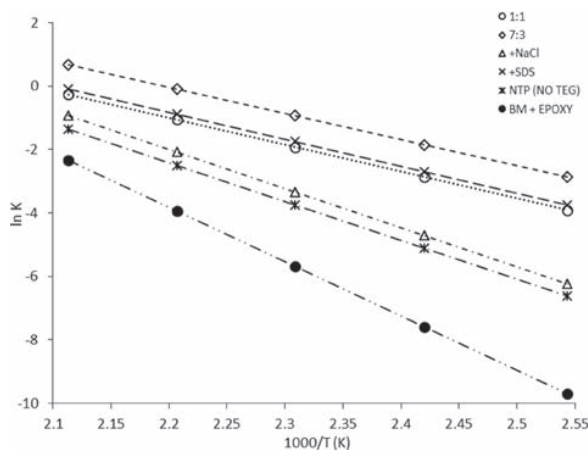

Figure 6. Temperature dependence of reaction rate for different NTP−DGEBA systems.

example, the unmodified bloodmeal−epoxy reaction parameters were much higher than the NTP−epoxy system, which contained TEG as plasticizer while that of NTP with SS and SDS but no TEG were intermediate. The order of reaction is significantly higher with less plasticizer and denaturant, but never exceeded 2. This suggests that by disrupting the inter- and intramolecular reactions in the protein, the reaction between functional groups on the protein and epoxy functionalities would become more feasible during extrusion processing.

The NTP−epoxy system and that with additional SDS had very similar calculated kinetic parameters using the Sestak−Berggren model. This was expected due to the similarity between both the Kissinger values and dependency of E_α and $\ln A_o$ on conversion. However, the NTP−epoxy system with

71

Table 5. Calculated Kinetic Parameters for NTP−DGEBA Systems with Different Additives Using the Sestak−Berggren Model

additive/blend	mass ratio (hardener:epoxy)	E_α (kJ/mol)	ln A_o (1/min)	(m + n)
bloodmeal−DGEBA	1:1	142.3	33.81	1.99
NTP (no TEG)−DGEBA	1:1	101.6	24.45	1.93
NTP−DGEBA	1:1	70.3	17.60	1.76
NTP−DGEBA + 5 pph SDS	1:1	70.8	17.90	1.60
NTP−DGEBA + 5 pph NaCl	1:1	102.4	25.11	1.76
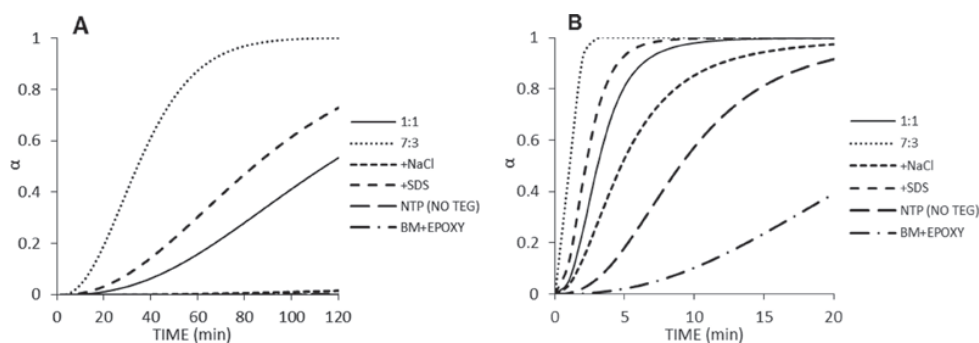
Figure 7. Conversion (α) as a function of time for different NTP−DGEBA systems at (A) 393 K and (B) 473 K.

added NaCl exhibited increased activation energy and pre-exponential factor, yet a comparable order of reaction. This was attributed to the bonding of salt ions with amino acid residues which are expected to react with the epoxy functional group.[19] The reaction parameters calculated suggest that the order of reaction is dependent on protein chain mobility, whereas E_α is dependent on the availability of reactive amino acids (Table 5).

The model provided a good fit to all experimental data, similar to that shown in Figure 3, for both conversion as a function of temperature and reaction rate ($d\alpha/dt$), which supports the argument that the reaction follows an autocatalytic mechanism. Detailed plots are displayed in the Supporting Information.

Conversion and Reaction Rate as a Function of Time. Using the E_α and ln A_o values obtained and the Arrhenius equation to calculate K, a plot of ln K vs $1000/T$ highlights the system's temperature dependence (Figure 6). It is apparent that the 1:1, 7:3 and additional SDS blends had higher rate constants regardless of temperature. However, the temperature dependence of the rate constant appears much greater in those systems that have higher activation energies, i.e., additional NaCl, NTP (no TEG) and, in particular, the bloodmeal plus epoxy system.

Reaction rates and the changes in conversion as a function of time are required for designing reactive extrusion processes. Residence time for NTP extrusion is normally limited to matter of minutes due to moisture loss and protein cross-linking as a result of shear.[11] The reaction rate should therefore be fast enough to allow for the required conversion.

For different mass ratios, conversion in the system with excess protein, regardless of temperature, will progress faster than the blend with an equal mass ratio. This can be attributed to the increase in number of reactive functional groups on the protein chain that are available for reaction with the epoxide ring. Varying the denaturant and plasticizer content had a large effect on conversion (Figure 6). The inclusion of NaCl greatly inhibited the reaction due to the formation of hydrophic interactions between the salt and protein functional groups. The additional SDS had a slight accelerating effect on the

reaction, particularly in the middle conversion region. The accelerating feature of the additional SDS may be attributed to the disruption of hydrophobic bonding between protein chains, as well as similar interactions and hydrogen bonding between the protein chains and DGEBA.

The calculated kinetic parameters can be used to simulate conversion as a function of time for the different systems (eq 2). At 393 K (Figure 7a), even the fastest reaction will take around 100 min to reach full conversion. Obviously, this amount of time is not feasible for the reactive extrusion of NTP. With a processing temperature of 473 K (Figure 7b), the 7:3 system will reach full conversion at around 3 min. However, high temperature extrusion may not be possible, as it will lead to excessive moisture loss and cross-linking.

■ CONCLUSION

The reaction kinetics of DGEBA curing with NTP were almost independent of concentration, attributed to the molar excess of DGEBA reactive groups to reactive amino acids present on the protein molecule in both ratios tested. The kinetic parameters were, however, comparable to DGEBA curing with protein hydrolysate. DGEBA cured with unmodified bloodmeal displayed kinetics much larger than that of the NTP−DGEBA reaction. The addition of TEG as a plasticizer to the bloodmeal protein brought about a decrease in kinetic parameters, and the further addition of protein denaturants (SS and SDS) caused another reduction. Additional SDS caused a decrease in E_α and ln A_o in DGEBA curing with protein hydrolysate; however, in this case, it made no significant difference, most likely as it was not in solution and would therefore not disrupt hydrophobic bonding in the protein effectively. It was found that the inclusion NaCl to the NTP−DGEBA system had a detrimental effect on the curing reaction, bringing about an increase in E_α and ln A_o, which is consistent with literature. Those systems with higher kinetic parameters, i.e., the unmodified bloodmeal, additional NaCl and no TEG systems, had a much greater temperature dependence than the other systems, although those other systems were found to have higher reaction rates regardless of

temperature. This is highly applicable to reactive extrusion; simulations show that at temperatures around 473 K full conversion could obtained in a number of minutes. However, the extrusion of NTP is limited by a number of factors, namely moisture loss and protein cross-linking as a result of excessive shear forces, which therefore restricts processing temperatures.

■ ASSOCIATED CONTENT

Ⓢ Supporting Information

Plots of experimental and simulated data for conversion (α) and reaction rate ($d\alpha/dt$) as a function of temperature for systems with different additives. The Supporting Information is available free of charge on the ACS Publications website at DOI: 10.1021/acs.iecr.5b00580.

■ AUTHOR INFORMATION

Corresponding Author

*M. J. Smith. E-mail: matthewjsmith90@gmail.com.

Notes

The authors declare no competing financial interest.

■ REFERENCES

(1) Al-Salem, S. M.; Lettieri, P.; Baeyens, J. Recycling and recovery routes of plastic solid waste (PSW): A review. *Waste Manage. (Oxford, U. K.)* **2009**, *29*, 2625.

(2) Mulder, K. F. Sustainable consumption and production of plastics? *Technol. Forecast. Soc.* **1998**, *58*, 105.

(3) Shafiee, S.; Topal, E. An econometrics view of worldwide fossil fuel consumption and the role of US. *Energy Policy* **2008**, *36*, 775.

(4) Cuq, B.; Gontard, N.; Guilbert, S. Thermoplastic properties of fish myofibrillar proteins: Application to biopackaging fabrication. *Polymer* **1997**, *38*, 4071.

(5) Graiver, D.; Waikul, L. H.; Berger, C.; Narayan, R. Biodegradable soy protein-polyester blends by reactive extrusion process. *J. Appl. Polym. Sci.* **2004**, *92*, 3231.

(6) Liu, W. J.; Mohanty, A. K.; Askeland, P.; Drzal, L. T.; Misra, M. Modification of soy protein plastic with functional monomer with reactive extrusion. *J. Polym. Environ.* **2008**, *16*, 177.

(7) Lukubira, S.; Ogale, A. A. Thermal processing and properties of bioplastic sheets derived from meat and bone meal. *J. Appl. Polym. Sci.* **2013**, *130*, 256.

(8) Marsilla, K. I. K.; Verbeek, C. J. R. Properties of bloodmeal/linear low-density polyethylene blends compatibilized with maleic anhydride grafted polyethylene. *J. Appl. Polym. Sci.* **2013**, *130*, 1890.

(9) Reddy, N.; Chen, L.; Yang, Y. Thermoplastic films from peanut proteins extracted from peanut meal. *Ind. Crops Prod.* **2013**, *43*, 159.

(10) Svenson, J.; Walallavita, A. S.; Verbeek, C. J. R. Evaluation of fishmeal as starting material for producing biodegradable protein-based thermoplastic polymers. *Waste Biomass Valorization* **2013**, *4*, 147.

(11) Verbeek, C. J. R.; van den Berg, L. E. Development of proteinous bioplastics using bloodmeal. *J. Polym. Environ.* **2011**, *19*, 1.

(12) Pickering, K. L.; Verbeek, C. J. R.; Viljoen, C.; Van den Berg, L. E. (Novatein Limited). Plastics material. U.S. Patent US 2010/0234515 A1, September 16, 2010.

(13) Verbeek, C. J. R.; van den Berg, L. E. Mechanical properties and water absorption of thermoplastic bloodmeal. *Macromol. Mater. Eng.* **2011**, *296*, 524.

(14) Vasile, C. Reactive blending. In *Handbook of Polymer Blends and Composites*; Vasile, C., Kulshreshtha, A. K., Eds.; Smithers Rapra Technology: Shrewsbury, U. K., 2003.

(15) Fryling, C. F. (Koppers Company, Inc.). High impact polystyrene. U.S. Patent US 3144420 A, August 11, 1964.

(16) Flexman, E. A.; Uradnisheck, J. (E. I. du Pont de Nemours and Company). Toughened poly(lactic acid) compositions. U.S. Patent US 7381772 B2, March 6, 2008.

(17) Plimmer, P.; Tanner, C. Reactive polymeric mixture. U.S. Patent US 20120259028 A1, November 10, 2012.

(18) El-Thaher, N.; Mekonnen, T.; Mussone, P.; Bressler, D.; Choi, P. Nonisothermal DSC study of epoxy resins cured with hydrolyzed specified risk material. *Ind. Eng. Chem. Res.* **2013**, *52*, 8189.

(19) El-Thaher, N.; Mussone, P.; Bressler, D. C.; Choi, P. Y. K. Kinetics study of curing epoxy resins with hydrolyzed proteins and the effect of denaturants urea and sodium dodecyl sulfate. *ACS Sustainable Chem. Eng.* **2014**, *2*, 282.

(20) Motahari, A.; Omrani, A.; Rostami, A. A.; Ehsani, M. Preparation and characterization of a novel epoxy based nanocomposite using tryptophan as an eco-friendly curing agent. *Thermochim. Acta* **2013**, *574*, 38.

(21) Kissinger, H. E. Reaction kinetics in differential thermal analysis. *Anal. Chem. (Washington, DC, U. S.)* **1957**, *29*, 1702.

(22) Harsch, M.; Karger-Kocsis, J.; Holst, M. Influence of fillers and additives on the cure kinetics of an epoxy/anhydride resin. *Eur. Polym. J.* **2007**, *43*, 1168.

(23) Roşu, D.; Caşcaval, C. N.; Mustaţă, F.; Ciobanu, C. Cure kinetics of epoxy resins studied by non-isothermal DSC data. *Thermochim. Acta* **2002**, *383*, 119.

(24) Zhang, J.; Dong, H.; Tong, L.; Meng, L.; Chen, Y.; Yue, G. Investigation of curing kinetics of sodium carboxymethyl cellulose/epoxy resin system by differential scanning calorimetry. *Thermochim. Acta* **2012**, *549*, 63.

(25) UniProt. The Universal Protein Resource (UniProt). http://www.uniprot.org/ (accessed December 10, 2014).

(26) Verbeek, C. J. R.; van den Berg, L. E. Structural changes as a result of processing in thermoplastic bloodmeal. *J. Appl. Polym. Sci.* **2012**, *125*, 347.

(27) Criado, J. M.; Ortega, A. Non-isothermal transformation kinetics: Remarks on the Kissinger method. *J. Non-Cryst. Solids* **1986**, *87*, 302.

(28) Wan, J.; Li, C.; Bu, Z. Y.; Xu, C. J.; Li, B. G.; Fan, H. A comparative study of epoxy resin cured with a linear diamine and a branched polyamine. *Chem. Eng. J. (Amsterdam, Neth.)* **2012**, *188*, 160.

(29) Verbeek, C. J. R.; Bier, J. M. Synthesis and Characterisation of Thermoplastic Agro-polymers. In *A Handbook of Applied Biopolymer Technology: Synthesis, Degradation and Applications*; Sharma, S. K.; Mudhoo, A., Eds.; Royal Society of Chemistry: London, 2011.

(30) Janssen, P.; Vogt, W.; Richtzenhain, H. (Dynamit Nobel AG). Epoxy resin hardening process using inorganic metal salt accelerators. U.S. Patent US 3492269 A, January 27, 1970.

(31) Vyazovkin, S.; Sbirrazzuoli, N. Mechanism and kinetics of epoxy-amine cure studied by differential scanning calorimetry. *Macromolecules (Washington, DC, U. S.)* **1996**, *29*, 1867.

Non-isothermal curing of DGEBA with bloodmeal-based proteins

Matthew J. Smith*, Casparus J. R. Verbeek and Mark C. Lay

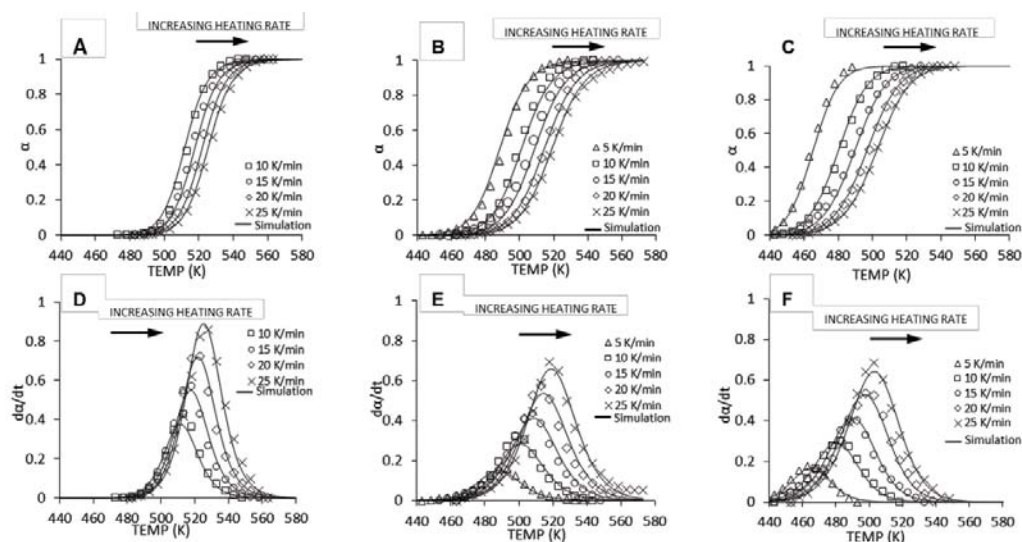School of Engineering, University of Waikato, Private Bag 3105, Hamilton, 3240, New Zealand

Figure S1. Experimental and simulated data for conversion (α) and reaction rate (dα/dt) as a function of temperature for systems with different denaturants and plasticisers (A and D) Bloodmeal - DGEBA (B and E) NTP (No TEG) – DGEBA (C and F) NTP - DGEBA
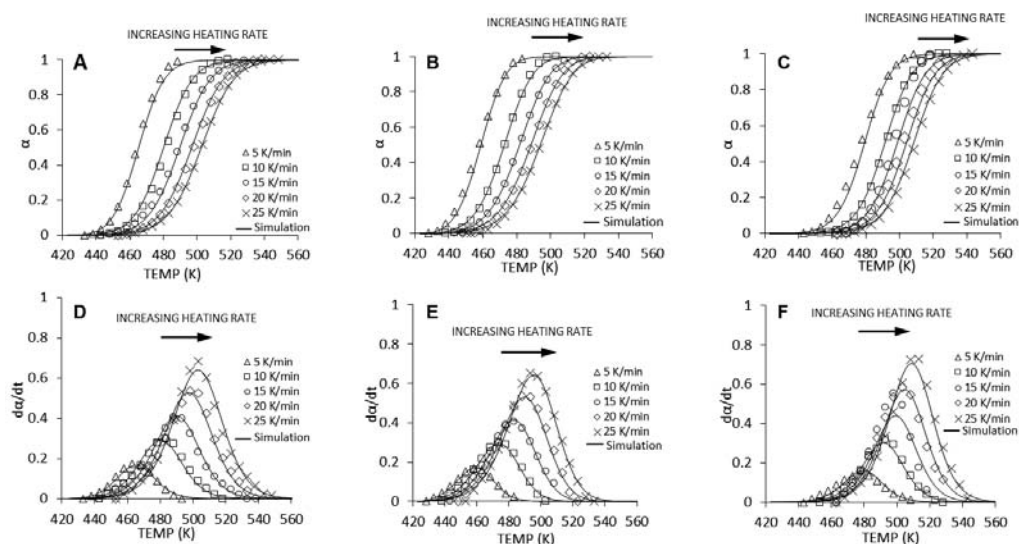

Figure S2. Experimental and simulated data for conversion (α) and reaction rate (dα/dt) as a function of temperature for NTP-DGEBA systems with different additives (A and D) NTP - DGEBA (B and E) NTP - DGEBA + 5 pph SDS (C and F) NTP – DGEBA + 5 pph NaCl

4

Impact Modification and Fracture Mechanisms of Core–Shell Particle Reinforced Thermoplastic Protein

A paper published in

Macromolecular Materials & Engineering

By

M. J. Smith & C. J. R. Verbeek

Impact Modification and Fracture Mechanisms of Core-Shell Particle Reinforced Thermoplastic Protein

Chapter 4 aimed to investigate the impact strength modification of Novatein when morphology was not dependant on blend composition as the incorporation of pre-synthesized glycidyl methacrylate-modified core-shell particles meant the dispersed minor phase was spherical in shape. This chapter aimed to show that theories relating to rubber toughening and impact strength in conventional polymers could also be applied to Novatein, and how the incorporation of epoxy functionalities on the particle influenced particle dispersion and mechanical properties.

As first author of this paper, I prepared the initial draft manuscript, which was refined and edited in consultation with my supervisor, who has been credited as co-author.

Impact Modification and Fracture Mechanisms of Core–Shell Particle Reinforced Thermoplastic Protein

Matthew J. Smith,* Casparus J. R. Verbeek

Mechanical properties and fracture mechanisms of Novatein thermoplastic protein and blends with core–shell particles (CSPs) have been examined. Novatein is brittle with low impact strength and energy-to-break. Epoxy-modified CSPs increase notched and unnotched impact strength, tensile strain-at-break, and energy-to-break, while tensile strength and modulus decrease as CSP content increases. T_g increases slightly with increasing CSP content attributed to physical crosslinking. Changes to mechanical properties are related to the critical matrix

ligament thickness and rate of loading. Novatein control samples display brittle fracture characterized by large-scale crazing. At high CSP content a large plastic zone and a slow crack propagation zone in unnotched and tensile samples are observed suggesting increased energy absorption. Notched impact samples reach critical craze stresses easily regardless of CSP content reducing impact strength. It is concluded that the impact strength of thermoplastic protein can be modified in a similar manner to traditional thermoplastics.
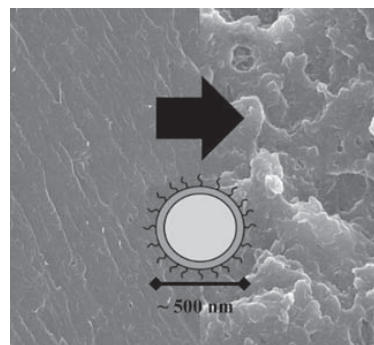
1. Introduction

Proteins are naturally occurring biopolymers and offer a green alternative to some petrochemical thermoplastics. Many protein resources are noncompetitive with food streams, are waste or by-products of other processes, and are biodegradable when in thermoplastic form. For example, proteins such as wheat, soy, peanut, meat and bone meal and fish meal have all been precursors for thermoplastic material.[1–6] Another example is bloodmeal, a by-product of the meat processing industry which has a very high protein content (≈90 wt%) making it suitable

for thermoplastic processing.[7] This material, known as Novatein thermoplastic protein, has a tensile strength (9.6 MPa) and modulus (534 MPa) comparable to low density polyethylene (LDPE) but a much lower impact strength (0.9 kJ m^{-2}) and strain- and energy-to-break (12% and 0.8 MPa).[8] Novatein is mostly used in the meat industry during animal slaughtering for devices preventing meat contamination. The nature of Novatein causes it to become brittle after production due to the evaporation of water, which is used as a plasticizer during processing.

Impact modification of polymers can be achieved in a number of ways. Rigid particles, such as nanoscale $CaCO_3$, have been shown to effectively toughen and modify impact strength of semi-crystalline polymers. Hard particles act as stress concentration points in the matrix and are only deemed effective if cavitation and debonding of the particle is possible allowing matrix yielding. However, these particles can greatly increase the modulus of

M. J. Smith, Prof. C. J. R. Verbeek
University of Waikato
Private Bag 3105, Hamilton 3240, New Zealand
E-mail: matthewjsmith90@gmail.com

the composite for only a small relative change in impact strength and toughness.[9]

Second phase rubber toughening is another prevalent technique used in engineering plastics. The idea of using a dispersed phase to improve the impact strength of both thermoplastics and thermosetting resins is common practice.[10] Core–shell particles (CSPs) can be used to offer improved interaction at the interface between the elastomeric and matrix phases of immiscible blends. CSPs have a core formed typically of an elastomeric polymer, covered by a shell of a different, more rigid polymer. These particles can be synthesized through emulsion polymerization to have shells that are specifically miscible with the intended matrix, or they can be functionalized with chemical groups that can react with the matrix polymer. Reactive groups present on the shell of the particle also aid dispersion during melt blending, as reactive compatibilizers act as emulsifying agents preventing coalescence.[11] Both examples here suggest that the interfacial adhesion between matrix and modifier is extremely important.

Brittle failure is often characterized by extensive crazing of the matrix, whereas the primary mechanism seen in ductile failure is plastic shear yielding. Shear yielding in polymers is desirable as it is more efficient at dissipating energy than crazing.[12] The inclusion of rubbery particles typically aids this transition from crazing to shear yielding. Wu[13] stated that the critical parameter for promoting impact strength or toughness with rubber particles was the surface-to-surface interparticle distance (matrix ligament thickness, τ) rather than particle size or volume fraction alone. However, τ is dependent on particle size and volume fraction (Equation 1). For a given particle diameter, D, and volume fraction, φ_r, τ can be calculated using Equation (1)[13]

$$\tau = D\left[\left(\pi / \left(6\phi_r\right)\right)^{(1/3)} - 1\right]$$

(1)

At a critical ligament thickness, τ_c, a brittle to ductile transition has been observed. For rubber-toughened nylon 6,6 this was 0.3 µm.[13] This theory has since been extended to show that the percolation of "stress spheres" surrounding particles, and therefore the stress state of the ligaments, is the governing factor.[14] It was established that below a certain thickness these ligaments could undergo shear yielding as a result of the transition from plane strain to plane stress, thereby dissipating energy more efficiently.[15] However, there is still some disagreement as particle size and composition, along with the inherent ductility of the matrix, influence the brittle to ductile transition.[10,16]

Cho et al.[17] showed that CSPs in polycarbonate increased the size of the plastic deformation zone at the tip of the notch in impact testing. An increase in the size of the plastic zone decreases the mean stresses at the crack tip and also ensures that craze initiation stresses are not reached in the matrix. Large amounts of energy are therefore absorbed at the crack tip before catastrophic failure. Furthermore, cavitation of particles also offers additional impact resistance as debonding of particles relieves triaxial stresses within the matrix. The disappearance of triaxial stress causes a matrix to behave as if under plane-stress conditions, similar to decreasing the ligament thickness, allowing shear yielding of the matrix.[18] The subsequent void formation acts as a further stress concentration point, however as voids are unable to bear a load, they will only offer limited toughness modification.[10]

The modulus of the particle is important for toughening polymers. A low modulus core will allow for more efficient stress transfer and deform more. High modulus cores tend to have low strength, causing a decrease in overall composite strength.[19] For example, Schneider et al. showed that a prevulcanized (higher modulus) natural rubber (NR) core in a poly(methyl methacrylate) (PMMA)/NR CSP was less effective at toughening polystyrene than a lower modulus noncrosslinked NR core.[12] Similarly the inherent ductility of the matrix will affect the influence that rubbery inclusions will have on the material. If a matrix is more prone to shear yielding and cold drawing it is able to be toughened much more greatly than a brittle polymer.[20]

Julien et al.[21] postulated that there was a number of transitions of crack growth during fracture; from fully stable to partially stable and finally fully unstable. It was observed that as loading rate increased during the compact tension testing of PMMA, the crack growth mechanism changed from partially stable at low rates to fully unstable at fast rates. The introduction of rubber particles into the PMMA matrix stabilized crack growth at lower testing rates due to cavitation and shear yielding of the matrix thereby inducing a larger plastic zone at the crack tip. This was evident through an increase in K_{IC} fracture toughness over that of neat PMMA. However at high testing speeds, a decrease in K_{IC} was observed due to the time dependent nature of polymer chain relaxation.

Many bioderived thermoplastics have undesirable mechanical properties. They are typically brittle, with low elongation, energy-to-break and impact resistance. However, the addition of plasticizers, second polymer components, and reinforcing agents such as particles and fibers can have a desirable effect on energy absorbing properties.[22]

In this study, CSPs consisting of an elastomeric butyl acrylate and 2-ethylhexyl acrylate core and a poly(methyl methacrylate) shell were used to modify the impact strength of Novatein thermoplastic protein. Novatein is

a newly developed material and its fracture mechanism, with and without modification, was also assessed using epoxy functionalized and regular CSPs.

2. Experimental Section

2.1. Materials

Pre-extruded injection molding grade of Novatein IR3020 was acquired from Aduro Biopolymers (Hamilton, NZ) in powder form. Two grades of core–shell impact modifiers (CSPs), DOW Paraloid EXL 2390 and EXL 2314, were acquired from Plastral (Auckland, NZ) in powder form. Both grades had a crosslinked elastomeric core consisting of butyl acrylate and 2-ethylhexyl acrylate, and a rigid PMMA shell. The EXL 2314 grade was modified with a glycidyl methacrylate (GMA) functionality on the PMMA shell while EXL 2390 had no functionality. Individual CSPs had been measured as ≈500 nm in diameter using scanning electron microscopy (SEM).

2.2. Sample Preparation

Initial blends included 10 and 20 parts of either EXL 2390 (2390–10 and 2390–20) or EXL 2314 (2314–10 and 2314–20) per hundred parts Novatein (pph$_{NTP}$). After these scoping trials, blends containing different amounts of just EXL 2314 were produced up to 30 pph$_{NTP}$, with the number of the blend name denoting the amount of CSPs in pph$_{NTP}$ (2314–5, 2314–10, 2314–15, 2314–20, 2314–30).

Pre-extruded Novatein powder was tumble mixed with one of the Paraloid impact modifiers in a zip lock bag before extrusion. Blends were prepared by melt blending in a LabTech corotating twin screw extruder (L/D 44:1) with a screw speed of 200 rpm. Temperature profile increased over 11 barrel heating sections, from 70 °C at the feed throat to 100 °C along the main barrel, and increasing to 120 °C at the die. Blends were granulated using a triblade granulator with a 4 mm plate (Castin Machinery, NZ).

Tensile bars (ASTM D368) and impact bars (ISO 179) were produced in a BOY 35A injection molding machine, with a temperature profile of 100, 135, 150, 150, 150 °C from feed to nozzle. Mold temperature was kept constant at 50 °C. Notches for notched impact samples were cut according to ISO 179 using an automated notch cutter. All test pieces were conditioned at 50% relative humidity and 23 °C for 7 d before testing.

2.3. Analysis

Tensile testing was conducted according to ASTM D638 on an Instron model 33R4204 tensile testing rig. A crosshead speed of 10 mm min^{-1} was used with an extensometer with a 50 mm gauge length. Notched and unnotched Charpy impact testing was conducted on a Ray-Ran Pendulum Impact System. A hammer weighing 0.457 kg with a test speed of 2.9 m s^{-1} was used for all tests, equating to a pendulum energy of 2 J. Notched and unnotched testing was conducted in an edgewise orientation.

Dynamic mechanical analysis (DMA) was conducted on sections of impact bar (thickness of ≈4 mm and width of ≈9.5 mm)

using a Perkin Elmer DMA8000 instrument. Scans were run in triplicate using a single cantilever configuration at 1 Hz from −100 to 180 °C. A free length of ≈13 mm was used at a dynamic displacement of 0.05 mm. Data collected were analyzed using Perkin Elmer's Pyris software.

Morphology of Novatein and blends containing CSPs was assessed using fractured ends of tested samples mounted on aluminum studs. The samples were then sputter coated with platinum using a Hitachi E-1030 ion sputter coater. SEM was carried out using a Hitachi S-4700. An accelerating voltage of 3 or 20 kV was applied, however, this did not affect resulting images. Optical images were obtained at a magnification of either × 16 or × 40 using a Nikon Digital Sight DS-U1 camera mounted on a Wild Heerbrugg M3B optical microscope, using similar fractured surfaces.

3. Results and Discussion

3.1. Effect of Surface Modification

Tensile data for surface modified and unmodified blends (Figure 1) showed a decrease in tensile strength and modulus with increasing CSP content. The decrease in strength and modulus in rubber-modified polymers is typically accompanied by an increase in elongation due to increased plastic yielding (covered in later sections). This was evident in the blends containing epoxy modified CSPs (2314–10 and 2314–20) whereby a significant increase in strain-at-break was seen. However, the blends containing unmodified CSPs actually showed a decrease in strain-at-break, as well as a far greater decrease in tensile strength than EXL 2314 blends.

In the case of 2314–10 and 2314–20, the increase in strain-at-break far outweighed the decrease in tensile strength bringing about a large increase in energy-to-break (up to 4.59 MPa compared to 0.22 MPa for Novatein). In contrast, the blends with unmodified particles displayed a decrease in energy-to-break. It was apparent from notched Charpy impact testing that unmodified
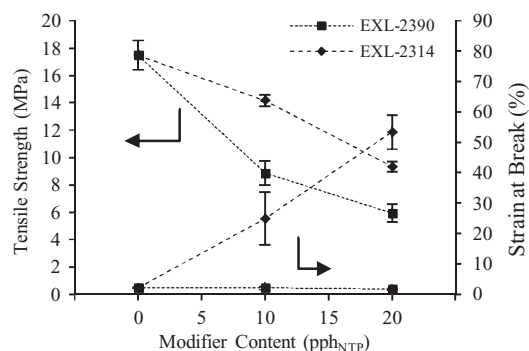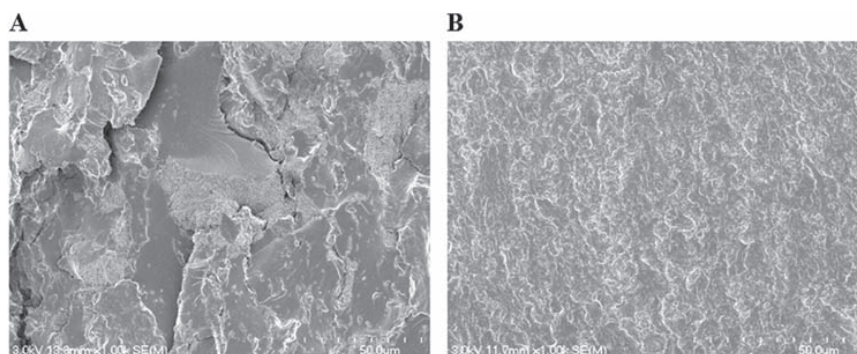

Figure 1. Selected mechanical properties of blends containing modified and unmodified core–shell impact modifiers.

■ *Figure 2.* Impact fracture surface of A) 2390–20; B) 2314–20.

CSPs were far less efficient at improving impact strength than the epoxy modified CSPs. The inclusion of 20 pph_{NTP} EXL 2390 caused a reduction in impact strength compared to that of Novatein (0.75 kJ m^{-2} compared to 0.9 kJ m^{-2}, respectively). In contrast, the notched impact strength for 2314–20 ($\approx$2.5 kJ m^{-2}) was much larger than the Novatein control.

The fracture surface of 2390–20 shows that while unmodified CSPs were agglomerated, these agglomerations were well distributed throughout the sample. In contrast the 2314–20 fracture surface revealed good distribution of CSPs through the sample, as well as good dispersion of individual particles. Agglomeration resulted in no toughening effect, as large cracks can readily propagate through the material with little resistance. Furthermore, the large crazes present in 2390–20 do not appear to terminate in the rubbery CSPs, as is the case in 2314–20 (Figure 2). The fracture surfaces suggest that interfacial adhesion is good in both cases. There appears to be little debonding and cavitation of CSPs, therefore the toughening mechanism seen in the epoxy modified particle blends is not only as a result of the increased adhesion, but as a function of better dispersion and the increased level of crazing of the matrix (Figure 2B).

In contrast to these results, Li et al.[23] found that the inclusion of Paraloid EXL 2330 (unmodified CSP similar in composition to Paraloid EXL 2390) in polylactic acid (PLA) produced a greater increase in impact strength than blends containing the epoxy functionalized CSPs used in this study. The difference in impact strength was attributed to the presence of the GMA functionality causing a change in rubber particle size, quality of dispersion and adhesion to the matrix, however no concrete evidence was given. There was a similar decrease in tensile strength and modulus between the two PLA blends, however, strain-at-break was higher in the modified particle blend. It is likely that the reactive functionality, while acting like a crosslinking point which potentially decreases chain mobility, may also have increased interfacial adhesion.

Therefore, at a high rate of loading (impact testing) the CSPs will be less likely to cavitate and behave in a more brittle fashion, similar to thermosetting resins. In contrast, under a low rate of loading (tensile testing), despite the physical crosslinking caused by the reactive functionality, cavitation of particles and yielding of the matrix is more likely, due to the time dependent nature of chain relaxation and fracture. This induces shear yielding due to the transition from plane strain to plane stress.

3.2. Effect of Composition

Due to the superior mechanical properties of blends containing Paraloid EXL 2314, the effect of composition was restricted to blends containing these CSPs only. Higher CSP content resulted in higher impact resistance (Figure 3A,B), regardless of whether a sample was notched or unnotched. In notched samples very little change in impact strength was seen up to 10 pph_{NTP} however an increase was seen after this. By including 30 pph_{NTP} CSPs, the notched impact strength of increased by $\approx$300%. In contrast, the unnotched impact strength of pure Novatein was approximately doubled with the inclusion of 10–15 pph_{NTP} CSPs, and increased by an order of magnitude after 20 pph_{NTP} CSPs.

The absolute values of the unnotched samples are far higher than those of the notched samples, but this is to be expected due to the high level of stress concentration and pre-existing defects at the notch tip. Also, the relative changes in impact strength are far greater in unnotched testing. This observation suggests that Novatein and blends containing the CSPs are sensitive to the effect of the notch. It must be noted that the standard deviation in the impact results is large, particularly at high loading. Even with a larger sample size (15–20 specimens), a large variation was observed, however the standard error of the mean was decreased greatly. A Student's *T*-test showed that for both notched and unnotched conditions there were significant differences (p value < 0.05) between the control (pure Novatein) and all sample

Materials
Views
www.MaterialsViews.com

Macromol. Mater. Eng. **2016**, *301*, 992–1003
© 2016 WILEY-VCH Verlag GmbH & Co. KGaA, Weinheim
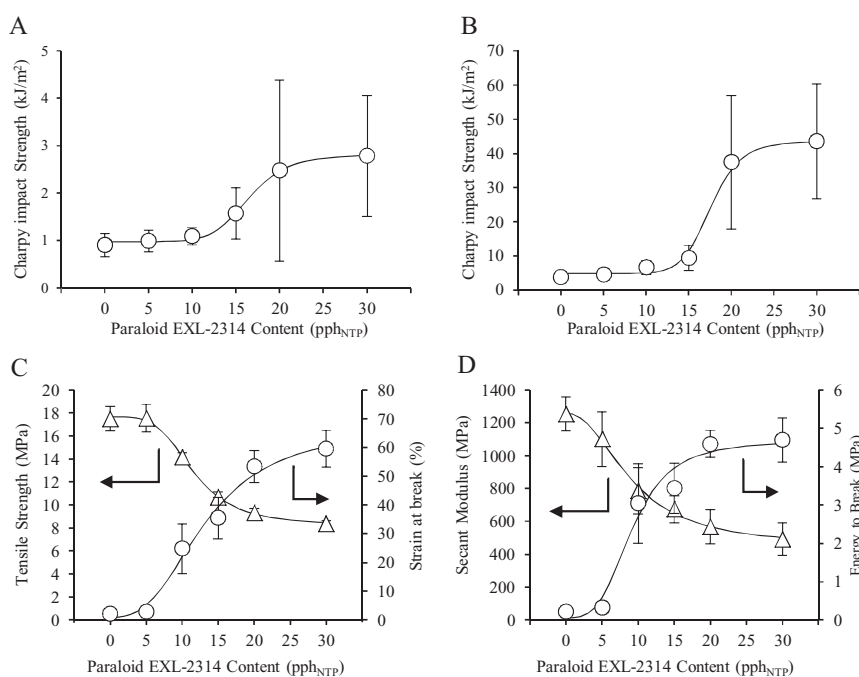
Macromolecular
Journals

81

Figure 3. Mechanical properties of Novatein as a function of modifier content A) notched impact strength; B) unnotched impact strength; C) tensile strength and strain-at-break; D) secant modulus and energy-to-break.

groups, except 2314–5 which could be expected due to the negligible effect of the CSPs at this low inclusion level. In the notched samples, there are no significant differences between sample groups until an inclusion of over 10 pph$_{NTP}$, which corresponds well to the brittle to ductile transition observed in the mechanical data. Furthermore, there was no significant difference between sample groups at the higher CSP content (i.e., between 2314–20 and 2314–30 values). The mechanical data presented suggest that the values reach a plateau between 20 and 30 pph$_{NTP}$ CSPs. This can be considered a positive result in terms of potential upscaling for commercial applications, as an increase of expensive CSPs above 20 pph$_{NTP}$ will not be required. The inclusion of particles can cause "crack bowing," whereby microscopic crazes and cracks change direction depending on the positioning of the particles.[24] By increasing the distance that the crack travels and thus the surface area over which the impact energy is calculated, a difference in impact energy can be seen from sample to sample, hence the large variation at high CSP content. This mechanism is not present at all, or negligible, in low CSP content samples and therefore little variation is seen. This mechanism has not been explored in this manuscript and can be the subject of further investigation.

For some unnotched 2314–20 and 2314–30 samples, the sample did not break during impact testing, but instead stopped the hammer fully. The recorded values for these samples was taken as the maximum energy that the hammer can fully exert on the sample ($\approx$50 kJ m^{-2}). These values were included in the calculations for the averages in Figure 3B.

The matrix ligament thickness for toughening the protein matrix can be determined from Equation (1). In theory according to Wu, to reach τ_c (0.3 µm),[13] $\approx$10 pph$_{NTP}$ CSPs are required. However, for Novatein, even at a ligament thickness of less than 0.3 µm (15 pph$_{NTP}$), no increase in impact strength was observed. The main toughening effect was seen above 17 pph$_{NTP}$ and would give a matrix ligament thickness of 21 µm (based on inflection point, Figure 3A,B). This would suggest that ligament thickness is not the only variable that affects toughness and impact resistance.

Tensile testing results supplement the impact testing data and support the theory that energy absorption of the material increases as ligament thickness decreases. However, this increase in energy absorption occurs at much lower CSP content (the inflection point is seen at $\approx$10 pph$_{NTP}$) (Figure 3C,D). This brittle to ductile transition is also evident from the tensile stress–strain curves as there are clear yield points in blends with greater than 5 pph$_{NTP}$ CSPs (Figure S1, Supporting Information). This difference in inflection point between tensile results and impact results is due to rate of loading and will be
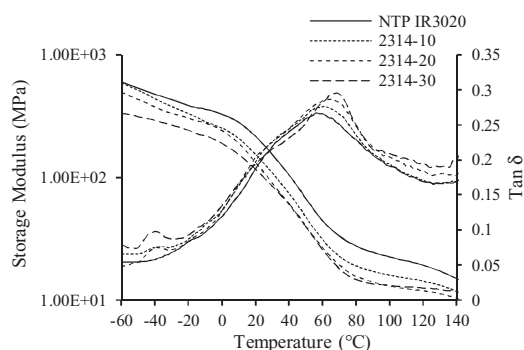
Figure 4. Dynamic mechanical analysis of impact modified Novatein.

addressed later. It must also be noted that strain softening occurs in the blend containing 10 pph$_{NTP}$ CSPs. This is consistent with rubber toughened epoxies that show strain softening as a result of low T_g inclusions.[18]

A brittle to ductile transition with increasing CSP content is often observed for rubber-toughened polymers. At this transition, strain-at-break and energy-to-break drastically increase, while modulus and tensile strength significant decrease. The properties of the inclusion often dictate the properties of the overall material in particulate reinforced composites.[19] The same behavior was observed for Novatein reinforced with CSPs.

3.3. Thermal Analysis

DMA revealed a decrease in relative storage modulus over the entire temperature range with increasing CSP content. This is to be expected with rubber modified polymers,[19] where the contribution of the rubbery core is to lower the blend's average modulus.

The tan δ plots (Figure 4) show a clear T_g at ≈−40 °C attributed to the rubbery core of the CSP. The magnitude of this peak increases with an increase in CSP content. In a similar fashion, the magnitude of the large tan δ peak at ≈60 °C increases in magnitude with increasing CSPs. This can be attributed to the increased damping ability of the blends as a result of the rubbery inclusions that has a much lower T_g than the matrix. It is well documented that β-transitions seen in tan δ below the T_g of a material can be related to its impact resistance.[25] In this case, it appears that the β-transition of Novatein is masked by the CSP T_g and therefore this relationship cannot be confirmed. It is interesting to note that the magnitude of the tan δ peak at the matrix T_g (60 °C) also increases in magnitude with increasing CSP content. However, the relationship between increasing α-transition peak magnitude and impact strength at higher CSP content cannot be confirmed and may be the subject of further investigation.

There is a clear increase in the T_g of the Novatein matrix (taken to be the large peak in tan δ at ≈60 °C) with increasing CSP content. This could be attributed to the chemical reaction or interaction between the epoxy groups on the PMMA shell and reactive amino acids along the protein chain. Usually, in rubber modified thermoplastics, an increase in T_g would not be expected, however with strong interactions, the "crosslinking" effect of the nanoparticles has a similar effect to increasing crosslink density or chain entanglement.[25]

Memon[26] suggested that CSPs in the matrix covers a much greater fraction of the blend than just the volume fraction of the inclusion. The interaction between the matrix and the functional groups (on the surface of the particles) forms an interphase, effectively increasing the particle volume fraction. In highly filled blends, the large effective volumes of the particles overlap, thereby forming a network structure of particles. It was shown through low-frequency plate–plate rheometry of polycarbonate and CSPs that almost 100% of the matrix was interacting with the shell of the inclusions at 20% modifier content, decreasing as a function of decreasing modifier content.[26] The shift in T_g seen in for Novatein could be due to this large effective area of the epoxy functionalized CSPs and the subsequent network structure formed. This in turn is likely to cause decreased chain mobility in the protein matrix which will require more energy for the onset of chain movement.

3.4. Fracture Behavior

As with the mechanical properties, the mechanism of fracture changes as the level of reinforcement changes (Figure 5). However, while there were differences as a result of filler loading, there were also differences in failure mechanisms as a result of the rate of loading, i.e., impact testing versus tensile testing.

3.4.1. Impact Testing

As interparticle distance decreases, thin matrix ligaments are more prone to plastic yielding. This is particularly evident when comparing a pure Novatein impact-fracture surface with a sample containing 30 pph$_{NTP}$ CSPs (Figure 6). The impact fracture surface of the Novatein sample is characterized by a number of large, uninterrupted crazes running parallel with the direction of impact. In contrast, at high particle content there is a much greater level of crazing, which is interrupted by the rubbery CSPs. The CSPs act as both nucleation and termination sites for the microscopic crazes. The blends containing up to 15 pph$_{NTP}$ CSPs exhibit similar behavior to Novatein, with uninterrupted crazing dominating despite the inclusion of CSPs. However, above this point, blends behave in a similar fashion
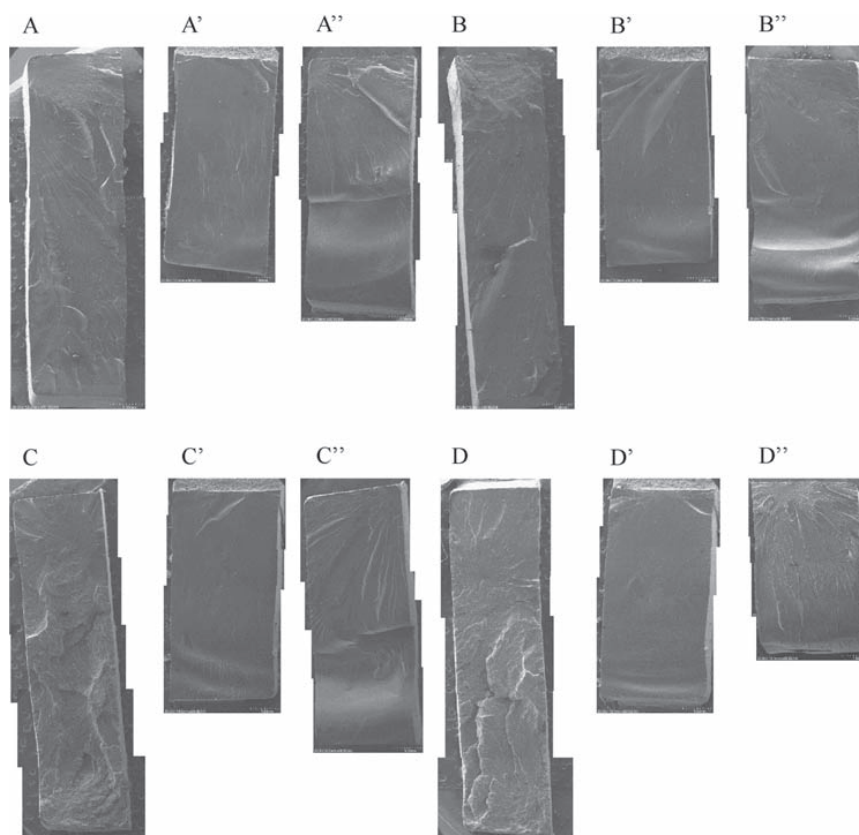
Materials
Views
www.MaterialsViews.com

Macromol. Mater. Eng. **2016**, *301*, 992–1003
© 2016 WILEY-VCH Verlag GmbH & Co. KGaA, Weinheim

Macromolecular
Journals

83

Figure 5. Tensile, notched, and unnotched fracture surfaces, respectively of A,A′,A″) Novatein; B,B′,B″) 2314–5; C,C′,C″) 2314–15; D,D′,D″) 2314–30.

to 2314–30. This is to be expected however, by examining the impact testing results (Figure 3A,B). Those blends below the inflection point behave in a brittle manner, as Novatein, while those above the inflection point begin to behave in a ductile fashion.

Notched and unnotched impact tests were considered to evaluate the effect of severe stress concentration on the

fracture behavior of Novatein. The plastic zone is the area of plastic deformation where fracture initiates and from where cracks propagate (Figure 7). If sufficient stress is reached in this area, crazes will begin to propagate slowly in a radial fashion. The size of this slow propagation region is dependent on the critical craze stress and matrix yield stress. Once the critical craze stress is reached,
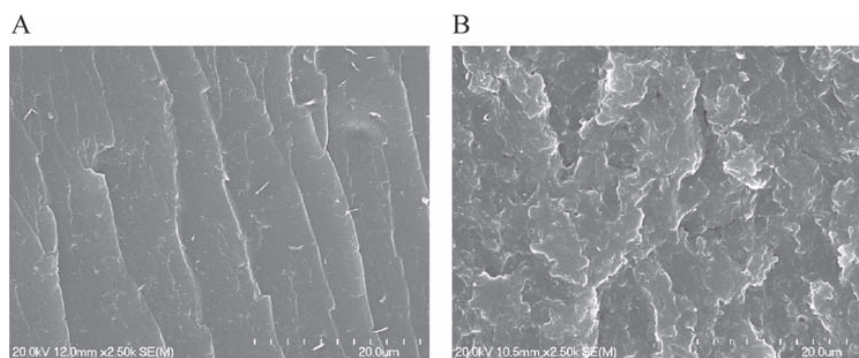
Figure 6. Unnotched impact fracture surfaces of A) Novatein; B) 2314–30.
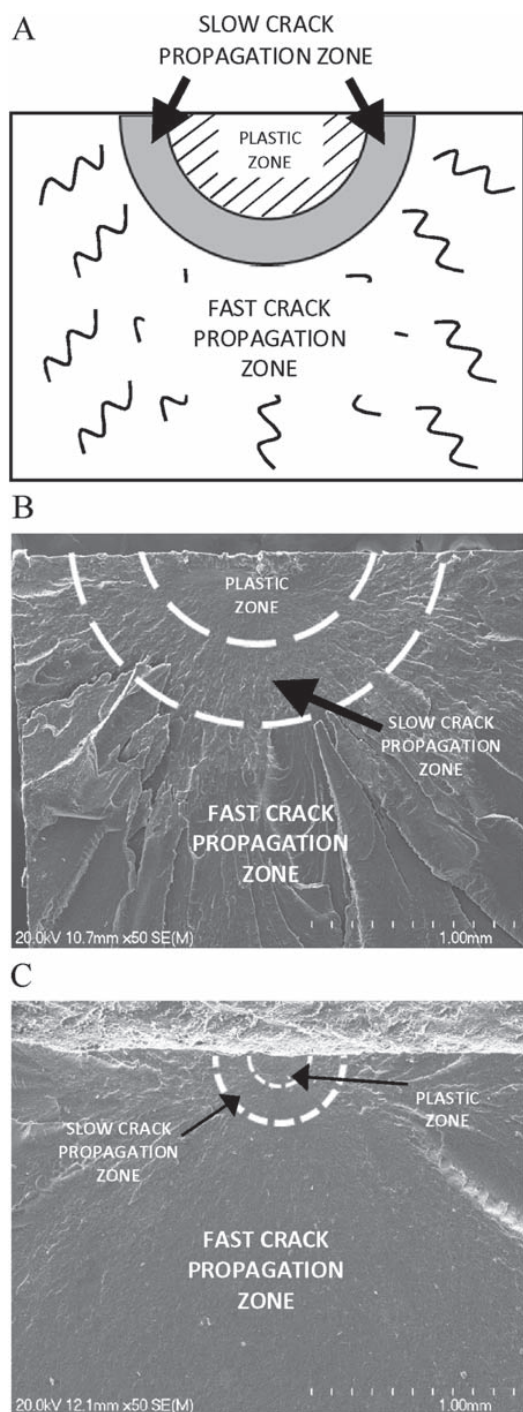
www.MaterialsViews.com

84

Figure 7. Identified regions during crack propagation and fracture: A) schematic diagram; B) example of regions in unnotched 2314–30; C) example of regions in notched 2314–30.

catastrophic crazing will occur and the material will fail. For unnotched samples, the absence of the intentional stress concentration (i.e., the v-notch) allows for increased plastic flow and yielding, therefore the increase in impact resistance as a function of composition was far greater for unnotched samples.

The increased impact strength with increased CSP content was attributed to more effective dissipation of energy in the plastic zone, a greater level of slow crack propagation and more chaotic crazing (random termination and nucleation of microscopic crazes, e.g., Figure 6B). Due to the dispersed nature and good adhesion to the matrix there is effective stress transfer, and although the rate of loading may be too high for sufficient chain realignment and yielding, the matrix ligaments in the plastic zone are more prone to plastic deformation as a result of plane stress conditions.

The introduction of CSPs causes both stress concentrations to form in the matrix and also the transition from plane strain to plane stress of matrix ligaments that are thinner than τ_c. With a decrease in ligament thickness, stress concentrations around particles may overlap, and the rate of chain relaxation is accelerated in the overlapping region and shear bands may form in these regions. This is highly dependent on strain rate and in the past this phenomenon has been labeled "strain-accelerated relaxation."[18] This supplements the argument that the transition from plane strain to plane stress allows thin ligaments of the matrix to yield. When the matrix polymer is said to be under plane strain it is constrained under triaxial stresses and unable to elongate in one plane, therefore strain in that plane is equal to zero. As the ligament thickness decrease, a transition to plane stress is seen and the material can freely elongate as the triaxial stresses have been relieved, causing stress in the plane of elongation to equal zero. Therefore, the thin matrix ligaments, now in plane stress, can yield plastically,[13,27] forming the plastic zone.

Cho et al.[17] states that the total energy absorbed during deformation and fracture is comprised of energy from yielding plus the energy from crazing. However, as crazing is a feature of brittle fracture and typically absorbs very little energy, the total energy absorbed is said to be approximately the energy absorbed during yielding. The size of the plastic zone can therefore be related to the total energy absorbed during fracture. The plastic deformation zone will be small, or not present at all, if the critical craze initiation stress is below the yield stress of the material. The tensile yield stress for Novatein is at the break point (≈18 MPa) which decreases to ≈8 MPa when using 30 pph_{NTP} CSPs. When examining the tensile stress–strain curves of all blends (Figure S1, Supporting Information) it can be assumed that the critical craze

Materials
Views
www.MaterialsViews.com

Macromol. Mater. Eng. **2016,** *301,* 992–1003
© 2016 WILEY-VCH Verlag GmbH & Co. KGaA, Weinheim

Macromolecular
Journals

85

stress in Novatein must fall between 18 and 14.5 MPa, as significant yielding occurs in 2314–10 suggesting that the critical craze stress is not immediately met. It must be noted that these values are for tensile testing and not impact testing, and the variation of rate of loading will affect this.

The large stress concentration in notched samples means that the critical craze stress is reached very easily and only limited yielding can occur. In this case, the material showed highly brittle fracture through large-scale crazing, thereby absorbing very little energy in contrast to unnotched samples with less stress concentration. The slow crack propagation zone is also much larger than in the notched blends, further increasing energy absorption (Figure S2, Supporting Information). The influence of the particles is seen further away from the plastic zone, whereby those with high loading are more prone to cold drawing and yielding.

This can be detected by a change in color of the material as seen under the optical microscope (for color figure the reader is directed to the Supporting Information, Figure S3). In a gray-scale image however, this change in the material can be seen by producing a binary copy (Figure 8). The areas of high deformation (and which are orange in Figure S3, Supporting Information) are seen as dark regions while the bulk matrix appears white. This change of color in the physical sample is brought about by the refraction of light in the cold drawn material and it is clear that there is a separation between the dark sections of the matrix and the orange filament-type structures (Figure S3C, Supporting Information).

It is evident in the optical microscopy images of notched impact samples (Figure S3D,E, Supporting Information) that the main mechanism of fracture is large-scale crazing. There is very little of the orange colored drawn material as seen in the equivalent unnotched samples. However, it is clear that there is some level of yielding and drawing at the edge of the sample, with

crazing dominating through the center of the sample. This edge yielding is likely due to plane stress conditions that exist at the edge of the sample and ductile elongation appears to dominate. In contrast, the constraint of the material in the center of the sample it is likely to bring about plane strain, making it unlikely to yield and hence brittle crazing dominates.

This edge yielding is much more prevalent in the sample with high CSP content (Figure S3E, Supporting Information) due to the decreased ligament thickness, but was not observed along the whole length of the fracture surface. The energy of the hammer remains unchanged throughout the impact, but the cross sectional area (which is able to absorb this energy) decreases as the cracks propagate. Therefore, at some distance from the notch, the critical craze stress will be reached and large-scale crazing will become the main fracture mechanism, rather than mixed mode yielding and crazing.

3.4.2. Tensile Testing

The brittle to ductile transition seen in the tensile mechanical properties (Figure S1, Supporting Information) is supported through observations in the blend fracture surfaces. Novatein exhibited highly brittle crazing throughout the sample, similar to what was seen in the impact fracture surface. It does display low levels of shear banding, however large-scale yielding is not seen (which is also evident from a low strain-at-break). The same behavior is seen at low filler content (2314–5); both exhibit a plastic zone (top section of Figure 5A,B), but these are small and it is clear that crazing dominates the fracture. Even though Novatein and 2314–5 exhibit plastic zones, this is the only area of significant deformation which accounts for the low strain-at-break during tensile testing (Figure 5A,B). At high particle content ductile fracture and large-scale yielding dominate, but this is to be expected after analyzing the tensile data.
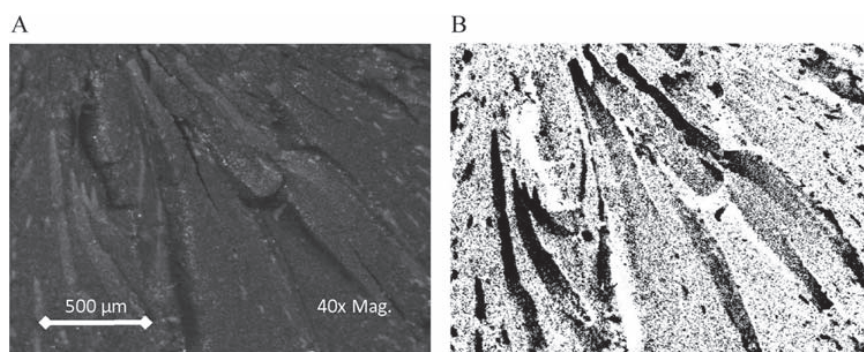

Figure 8. A) Optical microscope image of unnotched impact fracture surface from 2314–30. B) Binary representation of image in panel (A) highlighting regions of high deformation.

www.MaterialsViews.com

Using tensile testing or impact testing, a different τ_c was observed. For tensile data, 10 pph_{NTP} CSPs was identified as the minimum CSP level to bring about a brittle to ductile transition, while this was 15 pph_{NTP} for impact strength; the difference being rate of loading. The very low rate of loading in the tensile tests allowed for reorientation of protein chains along the axis of the applied force, allowing the thin matrix ligaments to yield excessively (at 15 pph_{NTP} CSPs or more). Also, the point at which significant yielding occurred (brittle to ductile transition) was almost identical to the value that Wu stated to be the critical ligament thickness (0.3 μm for nylon yielding in

a nylon/rubber blend).[13] In this study it was shown that yielding of the Novatein matrix (and thus the ligaments) occurred at a calculated ligament thickness of 0.33 μm.

From previous literature[21] it is possible to establish how stable crack propagation is during fracture in Novatein. During impact testing, pure Novatein and low CSP content blends show fully unstable crack growth, meaning that crazing is dominant, concurrent with other results. The introduction of elastomeric particles into the matrix (higher CSP content) stabilizes crack growth somewhat and induces cavitation and shear yielding of the matrix thereby inducing a larger plastic zone and more
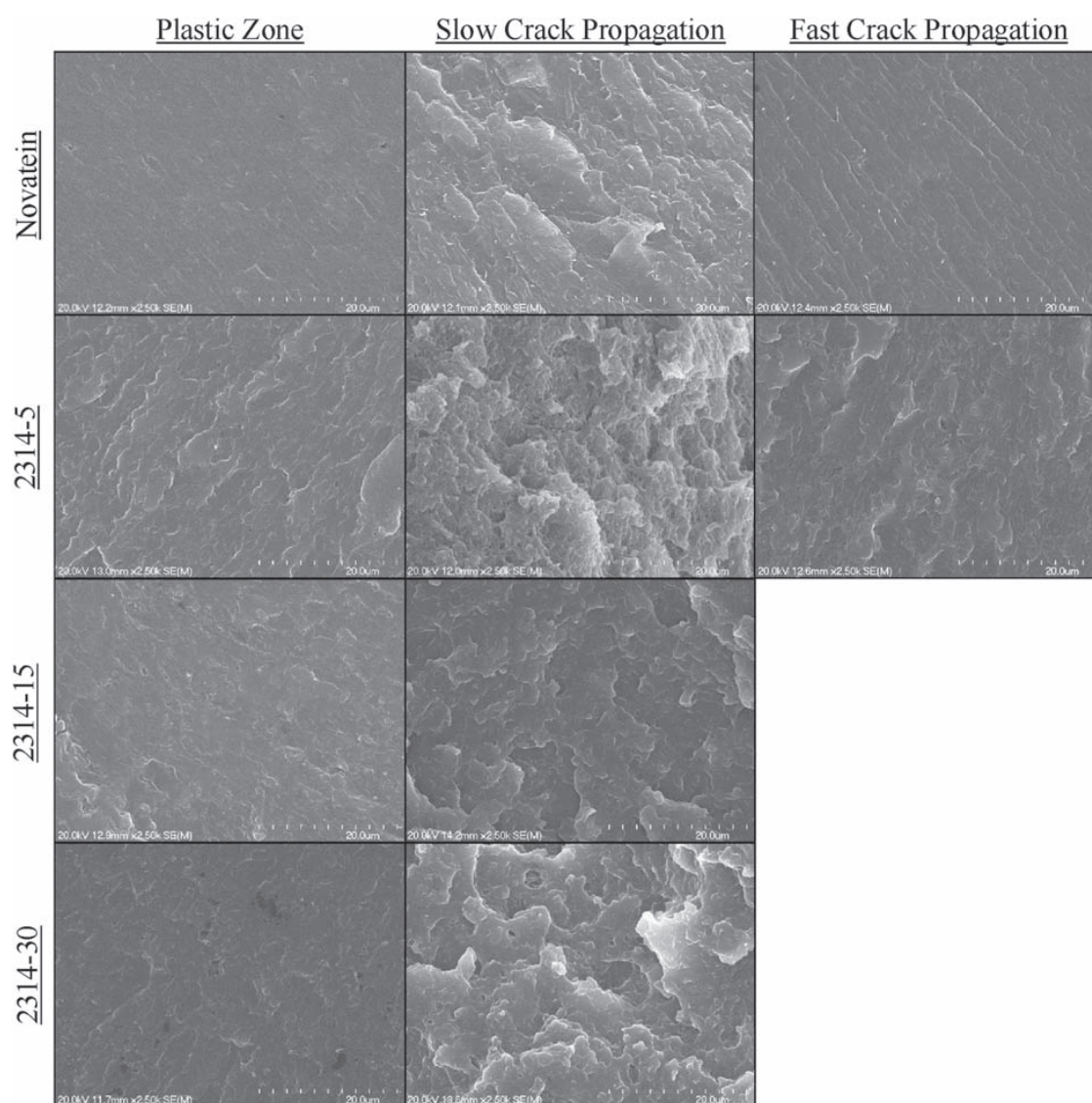

Figure 9. Microscopic features of plastic zone, slow crack propagation, and fast crack propagation regions in selected tensile fracture samples.

effective dissipation of energy. In contrast, tensile testing appears to bring about partially stable crack growth in Novatein and 2315–5, while the increase in CSP content causes the fracture to become fully stable, as there does not appear to be large-scale brittle fracture. This means that the critical craze stress is not reached and yielding as a result of thin matrix ligaments and cavitation dominates.

3.4.3. Microscopic Features of the Plastic, Slow, and Fast Propagation Zones

It is apparent that the plastic zone for Novatein and low CSP content samples were very similar, while intermediate and high CSP content samples also had a similar plastic zone, again pronouncing the brittle-to-ductile transition (Figure 9). The inclusion of CSPs for all samples brought about an increase of interrupted crazing, however this appears to become more pronounced at higher CSP content. The level of crazing in the slow crack propagation region appears to increase over that of the plastic zone, although this is to be expected as fracture progresses. Compared to Novatein, the high CSP content blend displayed large-scale plastic deformation and yielding, with no transition from ductile to brittle fracture. In the fast crack propagation region of Novatein and 2314–5, crazes appear large and uninterrupted as described previously, leading to a low level of energy absorption during tensile fracture.

Cavitation is also present in all samples containing CSPs, however it had a greater influence in samples that also showed significant yielding. At high magnification, the cavitation of CSPs is clearly visible (Figure 10) and when compared to a region of fast fracture it is evident that far more plastic deformation occurs, thereby facilitating energy absorption.

It has been argued that cavitation and debonding of particles is the main mechanism of toughening in thermosetting resins rather than a decrease of ligament thickness.[18] However, both features relieve triaxial stresses

in the matrix and allow plastic yielding of ligaments. It must be noted that in a ductile matrix that is able to yield without cavitation, the debonding of particles will offer additional toughening, although the void formed as a result of this is not load bearing and the additional influence will not be drastic.

4. Conclusions

The mechanical properties and fracture mechanisms of Novatein thermoplastic protein were heavily influenced by the introduction of CSPs. Epoxy modified CSPs were better dispersed than unmodified CSPs and brought about better mechanical properties. The introduction of CSP's at a content of greater than ≈15 pph_{NTP} significantly increased the impact strength in both notched and unnotched samples. A CSP content of ≈10 pph_{NTP} caused a decrease in tensile strength and modulus, while strain-at-break and energy-to-break drastically increased. DMA revealed that both the peak in tan δ associated with the T_g of the CSP rubber core, and the magnitude of the tan δ peak associated with Novatein increased in magnitude with increasing CSP content. However, for Novatein it did shift to higher temperatures, attributed to the large effective area of the epoxy functionalized particles and resulting physical crosslinking, thereby causing decreased chain mobility in the protein matrix.

Novatein control samples in both tensile and impact testing showed highly brittle fracture, dominated by large-scale crazing with very little yielding. The high impact strength with increased CSPs was attributed to more effective energy dissipation in the plastic zone, a greater level of slow crack propagation and more chaotic crazing. Unnotched impact samples had a larger plastic zone than notched samples, yet the slow propagation zone size did not appear to change significantly as the CSP content varied. Plastic zones for unnotched and tensile samples were very similar for the Novatein
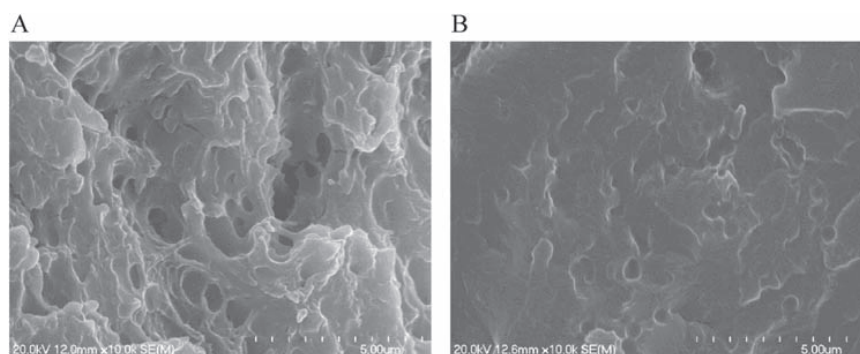

■ *Figure 10.* A) Cavitation in the plastic zone of 2314–5; B) fast crack propagation of 2314–5.

www.MaterialsViews.com

88

control. The intermediate and high CSP content blends, while appearing similar to each other, had plastic zones very different to Novatein due to the effect of the CSPs. There was variation in the plastic zones of the unnotched impact and tensile samples of the low CSP content blend attributed to rate of loading.

The large stress concentration in notched impact samples meant that the critical craze stress is easily reached and only limited yielding occurred. In this case, all blends showed highly brittle fracture through large-scale crazing, thereby absorbing very little energy in contrast to unnotched samples. Similarly, the Novatein control and low CSP content samples exhibited brittle behavior during tensile testing, while a CSP content of greater than 10 pph_{NTP} brought about large-scale yielding, cavitation, and little evidence of fast propagation, particularly at high CSP content. The introduction of CSPs caused stress concentrations to form in the matrix and also led to the transition from plane strain to plane stress of thin matrix ligaments that are thinner than τ_c, causing significant yielding.

Supporting Information

[1] L. Chen, N. Reddy, X. Wu, Y. Yang, *Ind. Crops Prod.* **2012**, *35*, 1.
[2] B. Cuq, N. Gontard, S. Guilbert, *Polymer* **1997**, *38*, 16.
[3] D. Graiver, L. H. Waikul, C. Berger, R. Narayan, *J. Appl. Polym. Sci.* **2004**, *92*, 5.
[4] S. Lukubira, A. A. Ogale, *J. Appl. Polym. Sci.* **2013**, *130*, 1.
[5] N. Reddy, L. Chen, Y. Yang, *Ind. Crops Prod.* **2013**, *43*, 159.
[6] J. Svenson, A. S. Walallavita, C. J. R. Verbeek, *Waste Biomass Valorization* **2013**, *4*, 1.
[7] C. J. R. Verbeek, L. E. van den Berg, *J. Polym. Environ.* **2011**, *19*, 1.
[8] C. J. R. Verbeek, L. E. van den Berg, *Macromol. Mater. Eng.* **2011**, *296*, 6.
[9] B. Cotterell, J. Y. H Chia, K. Hbaieb, *Eng. Fract. Mech.* **2007**, *74*, 7.
[10] W. G. Perkins, *Polym. Eng. Sci.* **1999**, *39*, 12.
[11] S. Bruce Brown, in *Polymer Blends Handbook* (Eds: L. A. Utracki, C. A. Wilkie), Springer, Dordrecht, The Netherlands **2014**, pp. 517–675.
[12] M. Schneider, T. Pith, M. Lambla, *J. Mater. Sci.* **1997**, *32*, 23.
[13] S. Wu, *J. Appl. Polym. Sci.* **1988**, *35*, 2.
[14] J. Z. Liang, R. K. Y. Li, *J. Appl. Polym. Sci.* **2000**, *77*, 2.
[15] A. Margolina, S. Wu, *Polymer* **1988**, *29*, 12.
[16] R. Bagheri, R. A. Pearson, *Polymer* **2000**, *41*, 1.
[17] K. Cho, J. H. Yang, B. Kang, C. E. Park, *J. Appl. Polym. Sci.* **2003**, *89*, 11.
[18] A. F. Yee, R. A. Pearson, *J. Mater. Sci.* **1986**, *21*, 7.
[19] D. Shi, E. Liu, T. Tan, H. Shi, T. Jiang, Y. Yang, S. Luan, J. Yin, Y.-W. Mai, R. K. Y. Li, *RSC Adv.* **2013**, *3*, 21563.
[20] R. A. Pearson, A. F. Yee, *J. Mater. Sci.* **1989**, *24*, 7.
[21] O. Julien, P. Béguelin, L. Monnerie, H. H. Kausch, in *Toughened Plastics II* (Eds: C. K. Riew, A. J. Kinloch), American Chemical Society, Washington, DC, USA **1996**, pp. 233–249.
[22] B. Imre, B. Pukánszky, *Eur. Polym. J.* **2013**, *49*, 6.
[23] T. Li, L. Turng, S. Gong, K. Erlacher, *Polym. Eng. Sci.* **2006**, *46*, 10.
[24] R. J. Zhou, T. Burkhart, *J. Mater. Sci.* **2010**, *45*, 11.
[25] K. P. Menard, *Dynamic Mechanical Analysis: A Practical Introduction*, 2nd ed., CRC Press, Florida, USA **2008**.
[26] N. A. Memon, *J. Polym. Sci. Polym. Phys.* **1998**, *36*, 7.
[27] D. Roylance, *Mechanics of Materials*, John Wiley & Sons, New York, USA, **1996**, p. 258.

Supporting Information

Impact Modification and Fracture Mechanisms of Core–Shell Particle Reinforced Thermoplastic Protein

Matthew J. Smith* and Casparus J. R. Verbeek

Impact modification and fracture mechanisms of core-shell particle reinforced thermoplastic protein

Matthew J. Smith*, Casparus J. R. Verbeek

Journal: Macromolecular Materials & Engineering

M. J. Smith, Associate Prof. C. J. R. Verbeek
University of Waikato, Private Bag 3105, Hamilton, 3240, New Zealand
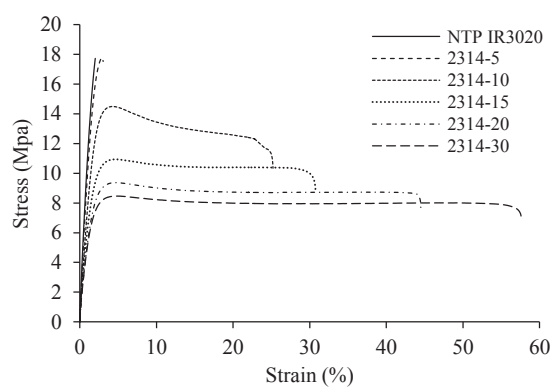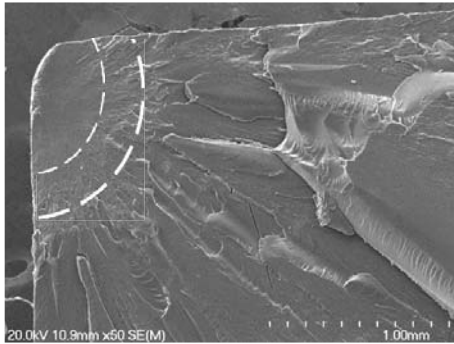E-mail: matthewjsmith90@gmail.com

Figure S1. Stress-strain curves of Novatein blends containing epoxy modified impact modifier.
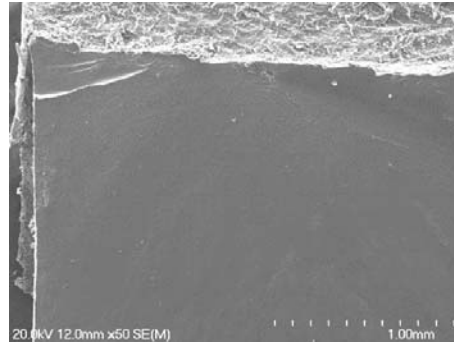
Notched Impact Fracture

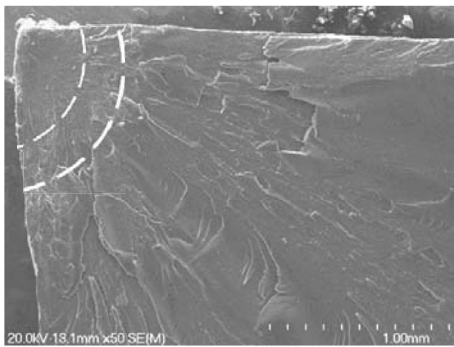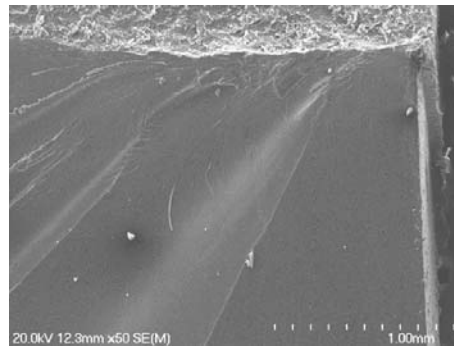*Figure S2*. Initiation points of unnotched and notched impact fracture. A and B) Novatein; C and D) 2314-5; E and F) 2314-15; G and H) 2314-30. N.B White dashed lines denote regions identified in Figure 10.
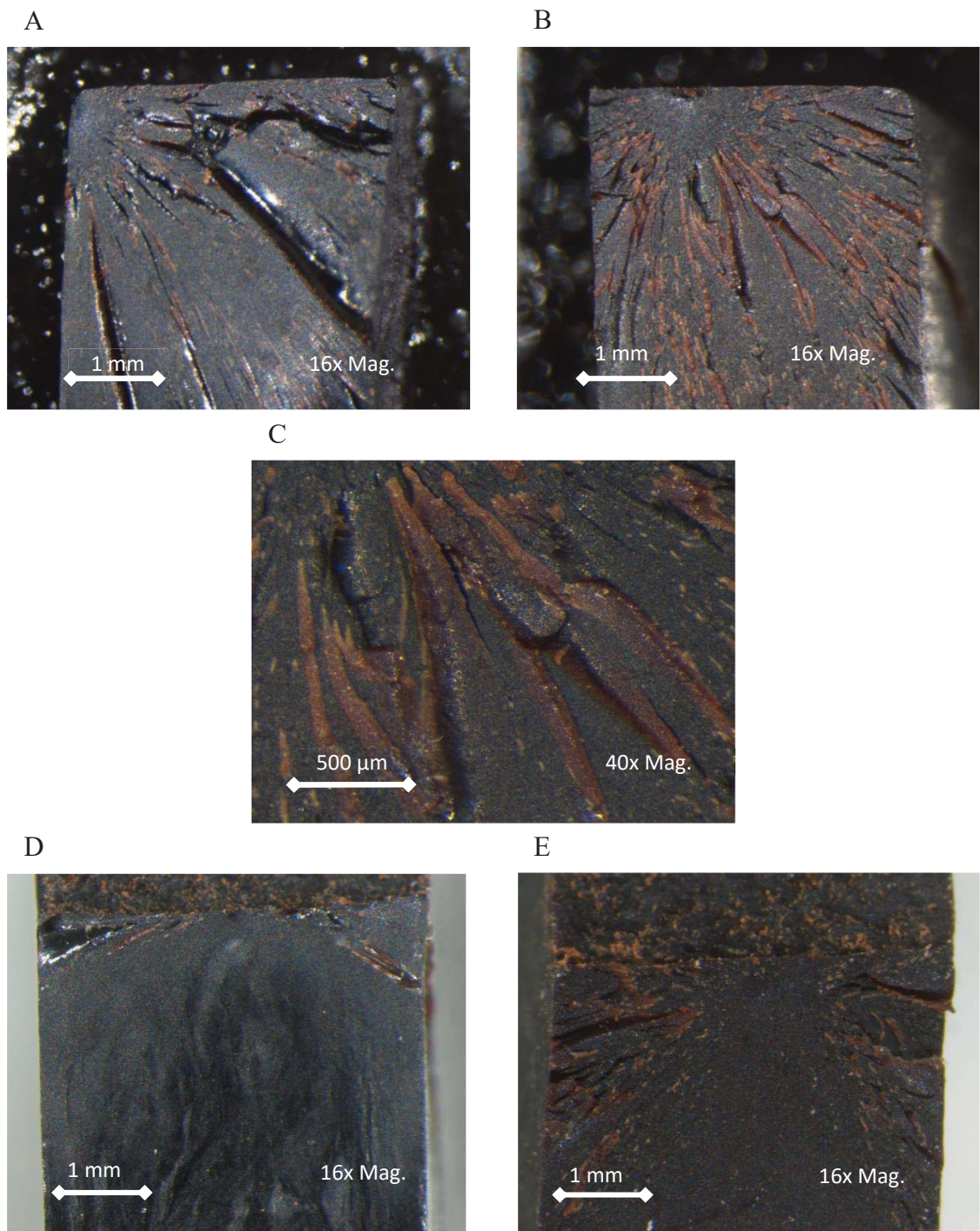
Figure S3. Optical microscope images of impact fracture surface from A) Unnotched Novatein. B) Unnotched 2314-30. C) Increased magnification of image B, displaying cold drawn fibril-like structures, D) Notched Novatein E) Notched 2314-30.

5

The relationship between morphology development and mechanical properties in thermoplastic protein blends

A paper published in

Advances in Polymer Technology

By

M. J. Smith & C. J. R. Verbeek

The relationship between morphology development and mechanical properties in thermoplastic protein blends

Chapter 5 investigated the morphology development in blends of Novatein and polyethylene functionalized with different reactive groups, and the relationship with mechanical properties. The reactive functionalities included on the polyethylene were either epoxides in the form of glycidyl methacrylate, carboxylic acid functionalities partially neutralised to produce zinc carboxylate salts, or maleic anhydride functionalities, all of which are to be reactive towards functional groups found on amino acids within the protein's primary structure. With regard to the main thesis objectives, this chapter highlighted the difficulty of morphology control in Novatein blends, and the effect that morphology has on mechanical properties as a result of the critical balance between viscosity ratio, interfacial tension, chemical interaction and composition.

As first author of this paper, I prepared the initial draft manuscript, which was refined and edited in consultation with my supervisor, who has been credited as co-author.

RESEARCH ARTICLE

The relationship between morphology development and mechanical properties in thermoplastic protein blends

Matthew J. Smith [ID] | **Casparus J. R. Verbeek** [ID]

University of Waikato, Hamilton,
New Zealand

Correspondence
Matthew J. Smith, University of Waikato,
Hamilton, New Zealand.
Email: matthew.smith@waikato.ac.nz

Abstract

Novatein thermoplastic protein was blended with modified polyethylene (containing either epoxy, carboxylic acid functionalities partially neutralised to produce zinc carboxylate salts, or maleic anhydride functionalities) to alter blend morphology and to manipulate thermal and mechanical properties. Up to 40 $pph_{Novatein}$ polyethylene (PE) was blended with Novatein by extrusion and injection moulding. Using zinc ionomer resulted in optimal properties and was compatible with a finely dispersed morphology at high content; high interfacial tension (σ) and a viscosity ratio (λ) of ~1 was observed. Unmodified blends and those containing epoxy functionalities showed co-continuity at low PE content. Whilst co-continuity appeared to increase impact resistance, other mechanical properties decreased due to lack of phase interaction. Maleic anhydride-grafted-polyethylene blends showed a finely dispersed PE phase, yet was less compatible. Zinc ionomer was deemed to be the most appropriate for modification of mechanical properties in Novatein.

KEYWORDS

biopolymers, blends, morphology, thermoplastic protein

1 | INTRODUCTION

A variety of bio-based polymers can be processed into thermoplastic materials and of particular interest for this work is thermoplastics produced from proteins. Novatein is produced from bloodmeal and has a tensile strength and modulus comparable to low density polyethylene (LDPE), but is highly brittle and has low impact resistance.[1] Products produced from Novatein are used to preserve meat quality during meat processing.[2]

Blending two polymers is an inexpensive strategy that could lead to improvements in mechanical properties.[3–5] The majority of polymers are immiscible, or partially miscible, leading to a variety of possible morphologies.[6–8]

The viscosity ratio ($\eta_A/\eta_B = \lambda$) between blend components plays a major part in morphology development where the breakup of the minor phase into dispersed droplets is most favourable when $\lambda = 1$.[9,10] However, the final morphology also depends on interfacial tension, chemical interaction, mixing time, composition and stresses associated with flow.[9,11] Altering interfacial tension by introducing a compatibilizer can reduce the effect of λ.[12] In contrast to a dispersed morphology, co-continuity occurs when both components in the blend have some degree of an interconnecting, continuous structure that is present throughout the entire system.[13]

It was long believed that co-continuous structures only formed near the phase inversion point; the composition at which the continuous matrix becomes dispersed and vice versa and is often at near equal proportions of the components. However, it has been demonstrated that continuous minor phases can be form at much lower concentration, and the region in which full co-continuity occurs can be over a large range of compositions.[10] For a continuous network to form, deformation of the minor phase (above a critical concentration) must occur for it to contact other regions of the same phase. It is believed that the typical mechanism creating a continuous path throughout the major phase is when stable

elongated thread-like structures of the minor phase coalesce (thread-thread coalescence).[9,11,12] However, it has been argued that it is unlikely for a minor phase to break up during processing and subsequently coalesce. Rather, a breakup of sheets or ribbons of the minor phase is responsible for the creation of a network structure.[7,14]

Li et al.[12] classified co-continuous structures and their development into those with low interfacial tension which is formed through thread-thread coalescence (Type I); high interfacial tension systems, dominated by droplet-droplet coalescence (Type II); and systems with partial miscibility and emulsification whereby droplet-droplet coalescence is responsible for co-continuity of the minor phase, albeit with an onset at a higher volume fraction of the minor phase (Type III). The morphology of Type II blends is strongly dependant on composition, whereas phase size in Type I and III is less dominated by this variable. Type I blends were said to have the broadest region of co-continuity due to high stability of the thread-like minor phase, whilst Type III were the narrowest.[12]

Despite being sustainable and biodegradable some biopolymers still have insufficient mechanical properties. Biopolymer blends, for the most part, are in agreement with synthetic polymer blends in that mechanical properties can be tailored depending on morphology. For example, polylactic acid (PLA) was blended with functionalized polyethylene (PE) to improve PLA's low impact resistance.[15,16] The reactive PE phase formed a dispersed spherical phase with a low T_g, with an increase of impact strength up to 3,000%.[15] Yield stress and elongation at break in blends of thermoplastic soy protein (SP) and poly(butylene adipate-co-terephthalate) (PBAT) were highly sensitive towards the aspect ratio of the dispersed phase. The coalescence of SP at relatively low content (~30 wt.%) to form a network through the continuous PBAT phase caused a large increase in yield strength and decrease in elongation due to the unique properties of SP.[17]

Modification of Novatein has mainly been focused on polymer blending, with the aim of overcoming the poor energy absorbing properties. In uncompatibilized blends of Novatein and biodegradable polybutylene succinate (PBS),[18] high energy to break at a 50/50 composition was observed, attributed to a co-continuous morphology at the phase inversion point. Compositions either side of this phase inversion point saw a decrease in energy to break due to the breakup of the minor phase into a dispersion, thereby interfering with interactions in the matrix, showing that the window for co-continuity in Novatein/PBS blends is very narrow. The inclusion of compatibilizers (poly(2-ethyl-2-oxazoline) and poly(phenyl isocyanate-co-formaldehyde)) caused increased tensile strength, modulus and adhesion between phases, as well as retarding phase coalescence which subsequently decreased phase size. Similar results were observed in blends of Novatein and linear low density polyethylene (LLDPE)

compatibilized by polyethylene-*graft*-maleic anhydride (PE-g-MA)[19] whereby PE-g-MA caused a drastic reduction in phase size and led to favourable mechanical properties when compared to the uncompatibilized blend. Whilst these studies used compatibilizers to improve blend properties, there has not been any investigation into blends of Novatein with commercially available polymers that are modified to contain reactive functionalities as part of a block copolymer.

In this study, a number of commercially available polyethylene grades were blended with Novatein. Unmodified LDPE was used as a control, whilst the inclusion of PE-g-MA was also used as a comparison of a ternary blend. Cyclic anhydrides, acid based ionomers and epoxy functional groups are reactive towards specific functionalities in bio-based polymers such as hydroxyls, amine and carboxyls, making them appropriate for use as reactive groups in protein blends.[20–22] Other commercially available PE's were chosen to contain glycidyl methacrylate (GMA) or carboxylic acid partially neutralised with zinc oxide to manipulate compatibility, interfacial adhesion and ultimately the morphology. Although using PE may compromise its biodegradability. This can be mitigated by using as little as possible petrochemical polymer or by replacing with a bio-based alternative, however cost and chemical functionality currently limits the use of bio-based alternatives.

Due to the poor energy absorbing properties of Novatein, the overarching aim of this study was to use modified polyethylene to manipulate the morphology of Novatein blends and to link this to changes in mechanical properties. Of particular interest is improving energy absorbing properties such as strain at break and impact strength.

2 | EXPERIMENTAL

2.1 | Materials

Novatein® thermoplastic protein, manufactured from bloodmeal and a proprietary blend of additives and plasticisers,[23] was acquired from Aduro Biopolymers LP, New Zealand. The amino acid composition of bloodmeal is well documented and remains unchanged during Novatein production and processing.[24] Lotader AX8900 (LOT) is a random terpolymer of ethylene, acrylic ester (24 wt.%) and glycidyl methacrylate (8 wt.%), with an MFI (2.16 kg, 190°C) of 6 g/10 min. It was produced by Arkema, France, and acquired through Nuplex Specialties, New Zealand. Surlyn 9320 (SUR) is a zinc ionomer thermoplastic resin, otherwise described as an ethylene/acid/acylate terpolymer in which some of the methacrylic acid groups have been partially neutralised with zinc oxide. Surlyn has an MFI (2.16 kg, 190°C) of 0.8 g/10 min; it was produced by Du Pont and acquired through IMCD, New Zealand. Cotene 3901 (CTN) is unmodified LLDPE with an MFI (2.16 kg, 190°C) of 4 g/10 min which was obtained from Elastochem, New
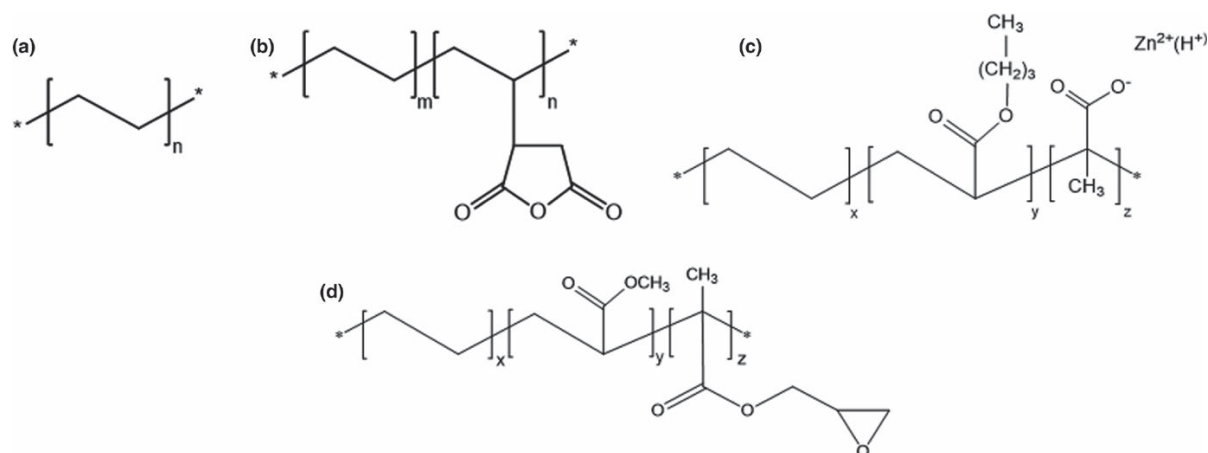
FIGURE 1 PE chemical structures. (a) Cotene 3901; (b) Polyethylene-graft-maleic anhydride; (c) Surlyn 9320; (d) Lotader AX8900

Zealand. Maleic anhydride grafted polyethylene (PE-g-MA) (MA content ~0.5 wt.%) was purchased from Sigma-Aldrich, New Zealand. The chemical structures of polyethylene grades used in this study are presented in Figure 1.

2.2 | Processing

As received Novatein granules were tumble mixed with polyethylene depending on the composition in a zip lock bag before extrusion. In all cases, the concentration of PE modifier was 6, 10, 20 and 40 $pph_{Novatein}$ selected to bring about a range of possible morphologies. For blends containing Cotene 3901 and maleic anhydride grafted polyethylene (CTNMA), the two PE modifiers were present in equal amounts, i.e., CTNMA10 contains 5 $pph_{Novatein}$ CTN and PE-g-MA, respectively. Initial scoping work suggested that a 1:1 ratio of CTN and PE-g-MA was optimal for CTNMA blends. Blends of Novatein and polyethylene were prepared by melt blending in a LabTech corotating twin screw extruder (L/D 44:1) with a screw speed of 200 rpm. Temperature profile increased over 11 barrel heating sections, from 70°C at the feed throat, 100°C along the main barrel, increasing to 120°C at the die. Blends were granulated using a tri-blade granulator with a 4 mm aperture (Castin Machinery, New Zealand).

Tensile bars (ASTM D368) and impact bars (ISO 179) were produced on a BOY 35A injection moulding machine, with a temperature profile of 100, 115, 120, 120, 120°C from feed to nozzle. Mould temperature was kept constant at 50°C. All test pieces were conditioned at 50% RH and 23°C for 7 days before mechanical testing.

2.3 | Analysis

Tensile testing was conducted according to ASTM D368 on an Instron model 33R4204 tensile testing rig with a crosshead speed of 10 mm/min. The modulus presented is a secant modulus, calculated from the raw data between a strain of 0.05% and 0.25%. Notched and unnotched charpy impact testing was conducted on a Ray-Ran Pendulum Impact System. A hammer weight of 0.952 kg and hammer speed of 2.9 m/s was used for all blends, equating to a pendulum energy of 4 J. All mechanical testing was conducted on samples that had been conditioned at 50% RH and 23°C for 7 days.

Dynamic mechanical analysis (DMA) was conducted on conditioned samples using a Perkin Elmer DMA8000 instrument. Sections of injection moulded impact bars with a thickness of ~4 mm and width of ~9.5 mm were scanned in triplicate using a single cantilever configuration at 1 Hz from −100 to 180°C. The conventional S/W of ~3.5 was not used for convenience of using an impact bar. This causes the storage modulus obtained to become closer to a shear modulus than a Young's modulus. A free length of ~13 mm was used at a dynamic displacement of 0.05 mm. Data collected was analysed using Perkin Elmer's Pyris software.

Morphology of Novatein/PE blends was assessed using scanning electron microscopy (SEM) in a Hitachi S-4700 at an accelerating voltage of 20 kV. Cryofractured samples were sputter coated with platinum using a Hitachi E-1030 ion sputter coater. Optical images of samples after digestion were obtained at a magnification of ×6.4 using a Nikon Digital Sight DS-U1 camera mounted on a Wild Heerbrugg M3B optical microscope.

Extraction of the Novatein phase from the blends was done using a method adapted from Caroli et al.[25] Samples containing low (6 $pph_{Novatein}$) and high (20 $pph_{Novatein}$) PE content were selected for extraction to highlight the difference in continuity of the second phase. Samples taken from injection moulded impact bars were digested for ~12 hr in 50 ml centrifuge tubes using a 2:1 mixture of H_2O_2 and 70% HNO_3. After this, centrifuge tubes containing samples and solution were

TABLE 1 Viscosity ratio and interfacial tension of Novatein/polyethylene blends

Polymer pair	Viscosity ratio ($\eta_A/\eta_B = \lambda$)	Interfacial tension, σ (mN/m)
Novatein/Cotene	1.19	8.37
Novatein/Lotader	2.81	7.74
Novatein/Surlyn	0.91	9.16
Novatein/CTNMA	14.20	8.70

heated at 60°C for 90 min. Digested samples were washed with distilled water and dried in desiccators for a minimum of 24 hr before imaging. Mass loss of the Novatein phase from the blend was calculated using Equation 1, where m_i is sample mass before extraction, m_f is the mass after extraction and w_{NTP} is the weight fraction of Novatein in the blend.

$$\text{Mass Loss (\%)} = \frac{m_i - m_f}{m_i \times w_{NTP}} \times 100 \quad (1)$$

Capillary rheometry was carried out using an in-house built rheometer mounted into an Instron model 33R4204 tensile testing rig. Barrel and piston diameter were both 20 mm. Four capillary lengths were used (0, 10, 20 and 30 mm) with a capillary diameter of 2 mm. Pressure transducers recorded pressure data at the entrance to the capillary during testing whilst measurements conducted using the orifice die allowed corrections to be made for entrance pressure effects. Tests were conducted at a barrel temperature of 120°C at a rate of 100 mm/min (i.e., a single fixed shear rate was used for all the materials tested). Data collected was used to calculate viscosity ratio ($\eta_N/\eta_P = \lambda$) between blend components, where η_N is the Novatein viscosity and η_P is the polyethylene phase viscosity.

Calculation of blend interfacial tension required surface energy determination of each material using dynamic contact angle measurements with three solvents; one non-polar (diiodomethane) and two polar (water and ethylene glycol). An FTA1000B instrument (First Then Angstorm, USA) was used to place a droplet of solvent on the material. Contact angles for each solvent were calculated from an average of 6 drops on the material. Surface energy of each material was calculated using the Young-Dupré equation,[26] and subsequently the interfacial tension was determined based on the harmonic mean equation.[27]

3 | RESULTS AND DISCUSSION

3.1 | Viscosity ratio, interfacial tension and chemical functionality

Viscosity ratio (λ) plays an important role in blend morphology and when $\lambda = 1$, minor phase break up is favoured to produce a dispersed droplet morphology.[9] From the viscosity ratios calculated here (Table 1), it is apparent that the most favourable blends for a morphology where the minor phase is dispersed are SUR and CTN. However, the divalent zinc ion in Surlyn makes interactions with the protein phase through co-ordination with the amine groups. This means that the morphology of CTN and SUR blends were different. LOT and CTNMA blends had a less favourable λ for discrete PE domains to form, and in particular the addition of PE-g-MA resulted in a significant increase in λ (compared to CTN blends) as a result of its very low melting temperature.

Interfacial tension (σ) also plays a role in phase structure development of blends. It can be seen that for all Novatein blends σ is particularly high (Table 1). This is apparent when values observed here are compared to a number of conventional polymer blends or even other biopolymer blends, such as starch/PLA blends.[28,29] An increase in σ is known to shift the full co-continuity range to higher compositions[30] therefore it would be expected that polyethylene would begin to percolate at a higher composition in SUR and CTNMA blends. However, the calculated interfacial tension may not be the true value of σ in the blend. Chemical interaction at the interface during processing causes in situ changes to σ, affecting phase behaviour that cannot necessarily be measured.

The assumptions can be made that SUR blends would have a high onset of co-continuity and display a dispersed domain structure due to favourable λ and σ. On the other hand, whilst CTN and LOT have a λ that suggests a dispersed phase structure it is likely that coalescence will occur at low compositions due to the unfavourable σ. This is evidence of interfacial tension overriding the effect of viscosity ratio where little or no chemical interaction occurs.[12] With regards to CTNMA blends, λ and σ give contradicting evidence, suggesting that percolation occurs at a high composition yet viscosity ratio is not conducive to a dispersed phase structure. In the case where λ and σ are in contradiction, chemical interaction is the driving force for morphology development when chemically reactive groups are present. In spite of this, Marsilla and Verbeek[19] showed conclusively that the addition of PE-g-MA to a Novatein/PE blend decreased the PE domain size and improved dispersion, suggesting that interfacial tension may be more important in Novatein blends.

It has to be appreciated however, that λ and σ cannot be the only influencing factor on morphology in this situation. The chemical functionality present on the PE in the blend is an integral part of the morphology development, and the influence that morphology has on mechanical properties. For example, CTN may have a viscosity ratio and interfacial tension that suggest a dispersed droplet morphology, but the lack of reactivity limits interfacial adhesion. In the case of LOT, the epoxy group of glycidyl methacrylate can ring open, as can the maleic anhydride functionality of PE-g-MA, and

become reactive towards a number of amino acids present in the protein. However, the epoxy will only react with protein at high temperature[21] whilst MA will develop acid-base or covalent interaction with the protein, provided the anhydride is hydrolysed and ring opens. In contrast, depending on the state of the divalent zinc ion present in SUR, ionic interactions will form with a number of charged amino acids such as arginine, histidine, lysine, aspartic acid and glutamic acid. Furthermore, terminal end groups of the amino acid chains are also available for interaction. This improved interaction in the SUR blend is evidenced in the morphology discussed below.

In highly reactive systems such as proteins, selecting a compatibilizer should primarily be chosen based on reactivity rather than viscosity ratio or interfacial tension as these play a secondary role in blend morphology development.

3.2 | Morphology development

The fracture surface of Novatein is highly dependent on rate of loading. A full analysis of the fracture mechanisms displayed in Novatein is presented by Smith and Verbeek.[31] The micro-morphology displayed in polymer blends is often studied using high magnification electron microscopy,
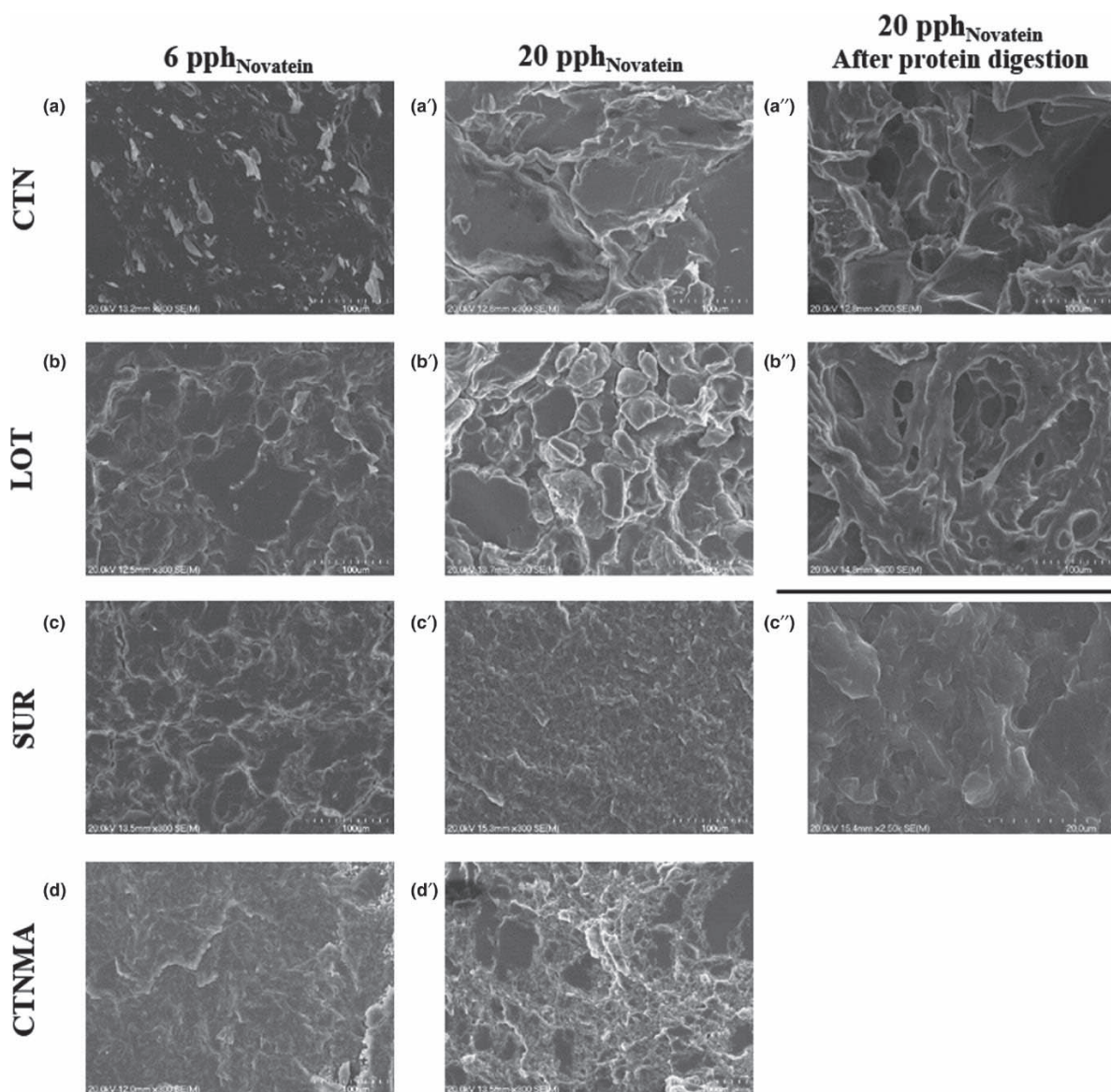

FIGURE 2 Scanning electron microscopy micrographs (×300 magnification) of cryofracture surfaces. (a, a′, a″) Novatein-Cotene blends; (b, b′, b″) Novatein-Lotader blends; (c, c′, c″) Novatein-Surlyn blends; (d, d′) Novatein-CTNMA blends. N.B. - C″ is high magnification cryofracture surface of SUR20
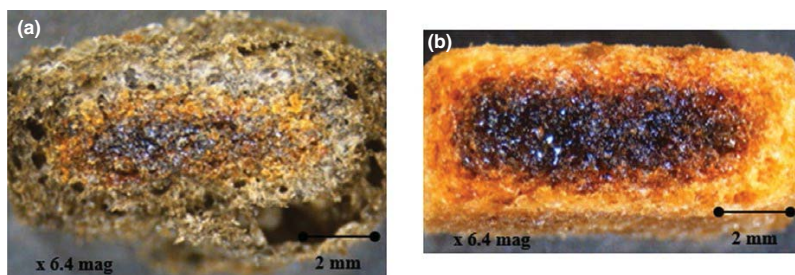
FIGURE 3 Optical micrographs of selected samples after Novatein phase extraction; (a) CTN20, (b) LOT20

TABLE 2 Data from extraction tests

Blend	Mass Loss (%)	
	6 pph$_{Novatein}$	20 pph$_{Novatein}$
COT	94.6 ± 3.8	77.0 ± 2.2
LOT	60.1 ± 10.2	39.8 ± 4.6
SUR	98.0 ± 0.7	87.0 ± 4.0
CTNMA	96.2 ± 4.7	87.2 ± 9.7

Standard deviation included (±).

but this only offers a two dimensional view of a sample. Extraction of one phase sheds light on the level of phase continuity in the NTP-PE system. Full co-continuity in a polymer blend is when one phase can be fully extracted, leaving the second phase intact. Therefore, the region from 100% phase extraction to disintegration is known as the co-continuity window.[9] Whilst phase extraction provides insight into the level of co-continuity, it does not consider changes to phase shape or coarseness, so this technique is best done in conjunction with microscopy.[7]

The introduction of PE into Novatein brought about drastic changes in morphology; however, this was highly dependent on PE fraction, viscosity, interfacial tension and chemical reactivity. In the CTN blends it was apparent that there was phase separation and very little interaction at the interface. On a micro scale, the morphology of CTN blends at low PE content (6 pph$_{Novatein}$) appeared consistent with a dispersed droplet morphology found in conventional blends at a viscosity ratio (λ) ~1 and low minor phase content (Figure 2a). This was consistent with capillary rheometer findings (Table 1). Droplets of CTN were inconsistent in size, ranging approximately between 2 and 50 μm. There was evidence of cavitation of the PE domains, however these features were also reminiscent of fibre pull out in fibre reinforced composites. In comparison, it is evident from the high content CTN blend (20 pph$_{Novatein}$) that, unlike the droplet type morphology in CTN6, there was a high level of encapsulation of Novatein by the PE phase which no longer appeared dispersed (Figure 2a′). The protein phase digestions showed that while the structure of the PE phase is maintained after extraction (Figure 3a—for colour figure refer to online version) the Novatein phase was also accessible to the solvent

(Table 2). This suggested that polyethylene formed a network through the sample at low content and that the droplets seen in CTN6 were actually elongated structures extending into the sample, forming a three dimensional network.

Introducing epoxy functionalities (Lotader), brought about a variation in morphology over that of uncompatibilized blends. At both low and high LOT contents (6 and 20 pph$_{Novatein}$) polyethylene was encasing regions of Novatein suggesting a co-continuous network (Figure 2b,b′). It is known that when a polymer blend includes both a high and low viscosity component (Novatein and PE, respectively, in this case) then the co-continuity threshold is shifted towards lower contents of the low viscosity phase, otherwise known as an asymmetric phase inversion.[32] Interaction at the interface improved over CTN blends, although a chemical reaction between the epoxy functionality and Novatein was not confirmed. It has been shown that the reaction of the epoxy functional group and reactive amino acids on the protein chain will only begin at around 180°C, so it is unlikely that high reaction efficiencies are present in the system.[21,33] However, the epoxy group could ring open, providing a more hydrophilic group that could assist in compatibilization.

The addition of just 6 pph$_{Novatein}$ LOT caused the percentage of Novatein removed from the blend during digestion to decrease dramatically compared with CTN6, whilst the Novatein removed from LOT20 was less than half the mass of the sample (Table 2). Optical analysis of the blends (Figure 3—for colour figure refer to online version) showed that not all the protein phase was extracted from LOT20 and therefore must have formed a combination of discrete particles and a continuous network. The LOT phase encased discrete domains of Novatein and in turn protected it from the digestion solution, confirmed through the SEM analysis (Figure 2b,b′). This is a similar asymmetric phase inversion to the one seen by Li and Favis.[11] The variation in continuity between CTN and LOT blends was attributed to the higher viscosity ratio of LOT blends, lower σ and the presence of the epoxy functional groups. However, it was possible to see from SEM analysis that both CTN and LOT blends, after extraction, displayed an elongated fibrillar-type structure (Figure 2a″,b″). These elongated structures are more apparent as PE content increased, attributed to increased coalescence during mixing.

In contrast to other blends, SUR formed a highly compatible blend at both low and high loading levels (Figure 2c,c′). At 20 pph$_{Novatein}$ the PE formed very finely dispersed domains that were well adhered to Novatein (Figure 2c″). The viscosity ratio between Novatein and Surlyn is the lowest out of all the blends, suggesting it would be the most favourable for droplet formation or a very well dispersed PE phase. It is well documented that a lower viscosity ratio between blend components becomes more favourable for a dispersed morphology; increased compatibility and interaction at the interface allows for better dispersion of the minor phase and a more stable phase structure.[7] Phase extraction data complimented the SEM analysis for SUR blends; very little PE was retrieved after extraction and the amount of Novatein digested was actually more than the weight fraction of protein in the blends, suggesting high levels of compatibility between the two phases. The PE that was retrieved did not hold its structure at both low and high levels meaning that the PE phase had not yet started to percolate throughout the Novatein phase. It was not possible to image the recovered PE fraction.

Instead of having pre-functionalised reactive block copolymers to facilitate interfacial reactions in the polymer blend, a third reactive component can be added to unreactive blend components. Novatein/LLDPE blends can be compatibilized using PE-g-MA[19] where the cyclic anhydride is hydrolysed to form maleic acid, behaving similarly to Surlyn. It is well documented that the amine/anhydride pairing is one of the most reactive systems used in polymer blends.[22,33] The introduction of PE-g-MA into the NTP-CTN system caused a drastic change in morphology compared with CTN and LOT blends (Figure 2d,d″). The discrete domains of polyethylene observed in CTN blends were no longer present and distinguishing between two phases became difficult. This was as a result of the compatibilizing nature of maleic anhydride, also confirmed by Marsilla and Verbeek.[19] The inclusion of the maleic anhydride caused increased dispersion of the polyethylene phase, despite a higher σ and very high λ. In this case the high viscosity ratio suggested that phase separation and coalescence was likely, however the high reactivity of maleic anhydride towards Novatein negates this effect and caused the PE to become dispersed, facilitating interactions between the two phases. There are, however, some large regions of Novatein which did not appear to interact with the PE phase which could be as a result of regions excessive cross-linking in the bloodmeal protein during drying. The retrieval of Novatein from CTNMA blends through digestion showed almost identical results as SUR blends, highlighting the similarity in the effect of the cyclic anhydride and zinc ionomer when reacting with the protein matrix.

It is plausible for a minor second phase to coalesce during annealing, or cooling from a high temperature. This static annealing occurs when there is high interfacial mobility; unlikely in Novatein systems as it does not flow (or form a conventional melt) without the application of heat, shear and pressure. Therefore, coalescence seen in the blends shown here was dynamic, or occurred as a result of shear and flow.[11] In this case, dynamic coalescence was likely to occur during the extrusion step, progressing further during the injection moulding process.

From the SEM micrographs of fracture surfaces, and the samples after phase extraction (Figure 2), both CTN and LOT blends can be classified as Type II systems as they are uncompatibilized binary blends (despite the epoxy functionality in LOT) with high interfacial tension. This would imply that the method of morphology development is dominated by droplet-droplet coalescence. In Figure 2a droplet-like features were observed for CTN6 and droplet coalescence occurred at a very low PE content (consistent with the observations of Li et al.[12]), with coalescence occurring in LOT blends below 6 pph$_{Novatein}$. The low reactivity of the epoxy functionality towards Novatein at the processing temperatures used in this study[21,22,33] would be a contributing factor as to why CTN and LOT behave in a similar fashion, where there was a distinct lack of interaction between the two phases.

For CTN and LOT blends, the low viscosity PE phase also acts as a lubricant during extrusion, as low viscosity additives segregate to high shear regions during processing.[34] Furthermore, this segregation reduces the energy available for softening of the major phase (Novatein) leading to large regions of Novatein suspended in the PE phase.

SUR blends behave as a Type III blend (compatible ternary system), similar to the one presented by Li et al.[12] One can then conclude that the ionic interaction between SUR and Novatein is directly responsible for the compatibility observed. The onset of continuity of the minor phase was at a much later stage than the Type II uncompatibilized binary blend and continuity development would appear to be dominated by droplet-droplet coalescence rather than thread-thread coalescence or sheet breakup, as suggested by the presence of the very finely dispersed PE phase at 20 pph$_{Novatein}$. Blends containing both Cotene and PE-g-MA (CTNMA) behaved in the fashion expected for a ternary compatibilized blend (Type III). The onset of co-continuity was above 20 pph$_{Novatein}$ and interestingly, the continuity values of SUR and CTNMA blends were very similar to those presented by Li et al.[12] for a Type II blend of HDPE and PS at ~15–20 wt.%.

Li and Favis[11] showed that polycaprolactone (PCL) preferentially encapsulated thermoplastic starch (TPS) due to the elasticity and pseudo-crosslinked nature of starch. This system showed an asymmetric phase inversion whereby the full co-continuity region was 55–67 vol.% TPS. Furthermore, it was shown through solvent extraction that at just 25 vol.% PCL, the minor phase is 80% continuous. This is similar
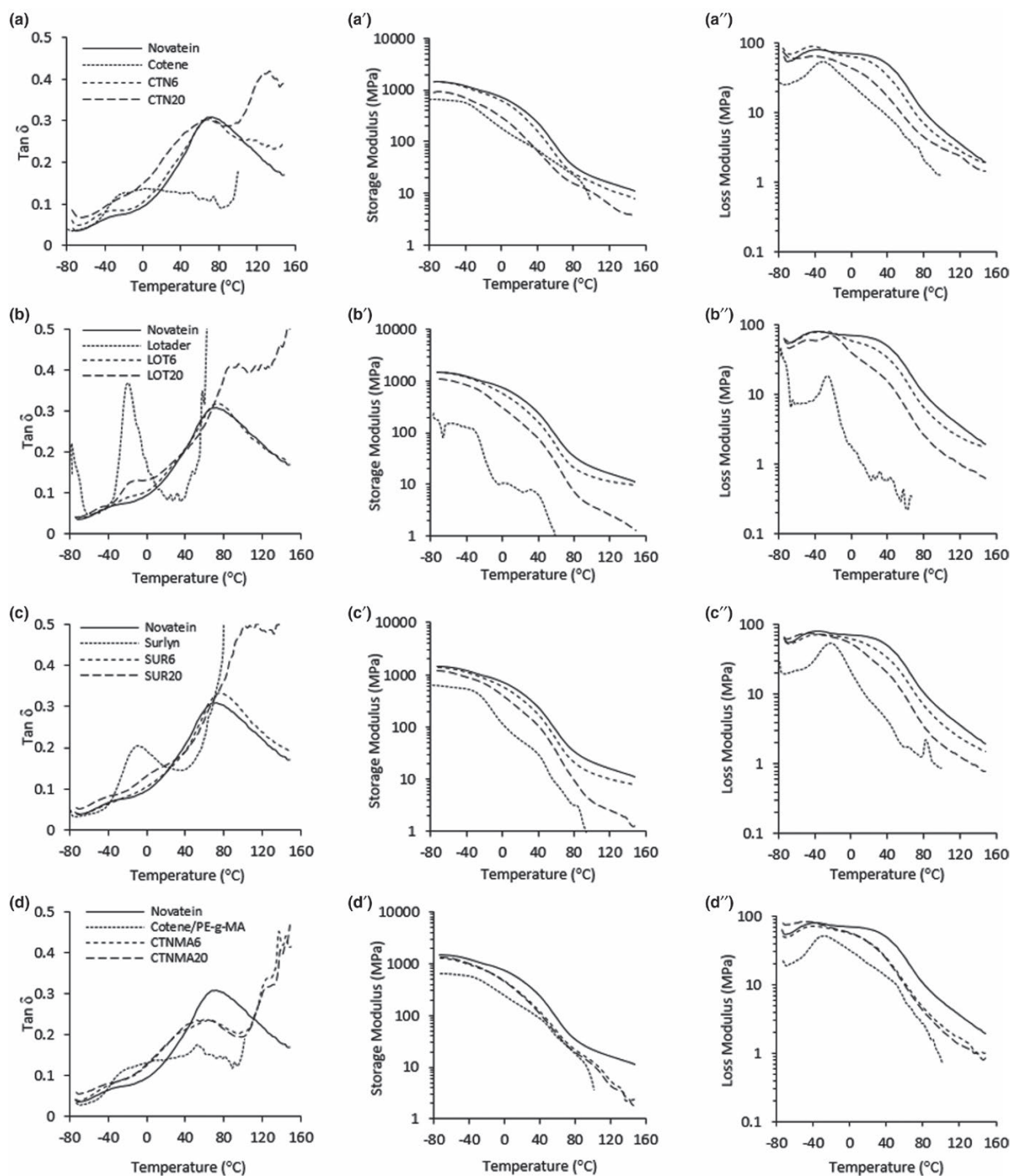
FIGURE 4 Tan δ, storage modulus and loss modulus for (a, a′, a″) Novatein-Cotene blends; (b, b′, b″) Novatein-Lotader blends; (c, c′, c″) Novatein-Surlyn blends; (d, d′, d″) Novatein-CTNMA blends

to NTP-PE systems whereby at low polyethylene content a significant level of continuity was observed.

Reactive protein systems rely heavily on interactions at the interface to form a finely dispersed morphology, hence the Novatein blends containing more functionalities that are reactive at low temperature provided stable dispersions and good interfacial adhesion (CTNMA and SUR). This compatibility was confirmed and supported through dynamic mechanical analysis.

TABLE 3 Selected mechanical properties for Novatein and NTP-PE blends. Standard deviation included (±). [Correction added on 3 July 2017, after first online publication: The grouping of data in Table 3 for Novatein values will be as follows. The shading for CTN will begin from 3rd row and end with 6th row, similarly for SUR the shading will begin from 11th row and end with 14th row]

Blend	$pph_{Novatein}$	Tensile strength (MPa)	Strain at break (%)	Secant modulus (MPa)	Notched impact strength (kJ/m^2)	Unnotched impact strength (kJ/m^2)
Novatein	n/a	4.47 ± 0.05	41.37 ± 3.67	199.79 ± 19.31	1.32 ± 0.71	9.70 ± 4.71
CTN	6	4.19 ± 0.23	4.25 ± 1.16	313.02 ± 30.34	0.74 ± 0.24	1.34 ± 0.21
	10	3.50 ± 0.28	3.49 ± 1.21	303.77 ± 34.14	1.82 ± 0.47	3.42 ± 1.35
	20	2.17 ± 0.17	3.66 ± 0.64	224.83 ± 19.06	3.14 ± 0.62	3.59 ± 0.88
	40	1.94 ± 0.13	23.25 ± 21.61[a]	130.86 ± 17.58	9.18 ± 3.98	13.50 ± 4.55
LOT	6	3.40 ± 0.17	1.59 ± 0.44	342.11 ± 45.00	0.75 ± 0.12	1.63 ± 0.47
	10	2.34 ± 0.11	2.66 ± 0.92	196.99 ± 22.04	1.52 ± 0.25	4.06 ± 0.98
	20	1.73 ± 0.05	4.81 ± 0.67	147.50 ± 5.48	2.46 ± 0.27	3.93 ± 0.77
	40	1.18 ± 0.12	9.71 ± 5.12[a]	71.03 ± 13.35	5.42 ± 3.24	7.38 ± 3.39
SUR	6	4.04 ± 0.11	2.07 ± 0.24	330.70 ± 24.12	1.13 ± 0.18	3.18 ± 0.59
	10	3.55 ± 0.04	2.17 ± 0.14	264.50 ± 23.43	1.09 ± 0.24	3.38 ± 0.53
	20	3.35 ± 0.07	9.49 ± 0.89	151.83 ± 6.47	2.31 ± 0.22	10.37 ± 1.03
	40	3.41 ± 0.04	78.01 ± 4.98	116.42 ± 8.49	6.17 ± 0.59	36.68 ± 2.28
CTNMA	6	6.01 ± 0.79	1.87 ± 0.41	506.36 ± 46.63	0.79 ± 0.13	2.43 ± 0.59
	10	5.24 ± 0.53	1.82 ± 0.36	455.50 ± 12.47	1.16 ± 0.30	3.71 ± 1.41
	20	4.94 ± 0.11	4.16 ± 0.37	280.58 ± 22.50	1.45 ± 0.02	4.45 ± 0.67
	40	3.88 ± 0.04	22.99 ± 3.14	135.93 ± 7.88	3.74 ± 0.37	11.67 ± 1.92

[a]Fracture was inconsistent due to highly continuous nature of PE. During testing of some samples the PE phase would still be elongating after the Novatein phase appeared to fracture, hence high standard deviation.

3.3 | Dynamic mechanical thermal analysis

As with rheology testing, dynamic mechanical analysis is a useful technique to assess the morphology of immiscible polymer blends.[7] One would expect the shape of a DMA curve to reflect that of the continuous phase. As the blend is made more compatible the shape of the curve becomes more intermediate of the two polymers.

The observations made from DMA thermograms (Figure 4) clearly separates into two effects; miscibility and composition. CTN and LOT blends were clearly immiscible as determined from microscopy, while SUR was intermediate to CTN and the CTNMA blend. These observations are confirmed by the DMA thermograms. For CTN and LOT, the tan δ and loss modulus curves mirrored that of Novatein at low PE content, suggesting Novatein is the continuous phase. Only at higher PE content did these curves become intermediate of Novatein and PE, as the phase morphology shifted from dispersed to co-continuous.

On the other hand, the curves for SUR and CTNMA were much more intermediate to Novatein and PE controls, even at low content, suggesting compatibility, as observed by SEM. This was most evident in the CTNMA material where the 6 and 20 $pph_{Novatein}$ curves were indistinguishable from one another, suggesting that the blends were compatible enough that morphology was not influenced by composition. This behaviour was almost matched by that of the SUR blends.

One other interesting observation is that for the highly incompatible blends (CTN and LOT), at 20 $pph_{Novatein}$, two distinct α-transitions were observed between −50 and 150°C. These transitions merged into one transition for CTNMA and SUR, providing further evidence of improved compatibility. At 20 $pph_{Novatein}$, SUR was the only blend where the DMA data suggested that Novatein was the continuous phase, even with a high level of compatibility.

The conclusions drawn from DMA show that there was greater compatibility in the blends containing maleic anhydride and zinc ionomer. The presence of water in Novatein allows the anhydride ring to hydrolyse and form interactions with reactive amino acids on the protein, whilst ionic interactions can form readily with charged amino acids in SUR blends. These assumptions were further confirmed using mechanical testing.

3.4 | Mechanical properties

The tensile and impact properties of Novatein are altered significantly by the inclusion of polyethylene (Table 3). With the exception of CTNMA, all blends have a tensile strength less than that of the Novatein control regardless of PE content. As polyethylene content increases it would be expected that the values become similar to those of the neat PE samples. However, this was not the case because after yielding neat polyethylene would typically undergo extensive strain hardening, which was

not evident in the blends. The tensile strength at 40 pph$_{Novatein}$ for SUR and LOT were strikingly similar to the yield strengths of the neat PE (σ_y = ~3 and ~1.5 MPa for neat Surlyn 9320 and Lotader AX8900, respectively). In contrast the tensile strength of CTN40 (~2 MPa) is approximately half the yield strength of neat CTN (~4 MPa) whilst at low PE content the value for CTNMA reflects the σ_y of neat CTNMA (~7 MPa). Increasing the level of PE in all blends caused a drastic decrease in tensile strength, as a result of polyethylene interrupting strong protein-protein interactions. It must also be noted that whilst SUR and CTNMA had similar digestion results, large Novatein inclusions are present in CTNMA blends which act as major stress concentrations during fracture. This contributed to the low elongation and impact strength when compared with SUR blends.

Strain at break (ε_b) was compromised heavily in the majority of blends. The Novatein control exhibited an initial ε_b value of 41%, but this was decreased to less than 5% with the inclusion of 6 pph$_{Novatein}$ regardless of functionality present. With further addition of PE, almost all values remained under that of Novatein, even though there were slight increases in ε_b with an increase in PE content. This was due to weak or insufficient interactions at the interface (highlighted by the morphology analysis). However, at high PE content, ε_b for SUR blends improved due to the fine dispersion of the PE phase. The principle mechanism causing this large increase in ε_b is a transition in the matrix from plane strain to plane stress and effective stress transfer from Novatein to the PE phase.[31]

At low PE inclusions all blends showed an increase in secant modulus. The secant modulus of CTNMA more than doubled over that of the Novatein control, whilst CTN, LOT and SUR all had a similar increase of over 50% (>300 MPa). At low polyethylene content all the experimental data is much higher than the Novatein control suggesting that whilst the Novatein phase dominated, there were some synergistic effect provided by the inclusion of the PE hindering chain movement in the elastic region. It is known that a co-continuous structure has the maximum contribution of the blend components to the modulus suggesting why all blends exhibit high modulus at low PE content.[7] As the PE content increased, modulus decreased, but this is to be expected as the PE grades used all have a lower secant modulus than Novatein. At the highest level of PE, all blends had a lower modulus than Novatein but were still much higher than the neat PE modulus values.

The impact resistance of the blends showed a clear increase in both notched and unnotched impact strength with increasing PE content. In notched samples the introduction of low levels of PE in all blends caused a decrease in impact strength compared with neat Novatein. However, above this level, the impact strength improved or was comparable to Novatein, with the biggest increase being ~370% with the addition of 40 pph$_{Novatein}$ of Surlyn.

In contrast, the unnotched samples were greatly affected with the inclusion of PE. Almost all blends displayed a lower impact

strength than Novatein; only CTN 40, SUR 20, SUR 40 and CTNMA 40 had a greater impact strength. The greatest increase was again seen in SUR 40 (~280% increase). It is assumed that the co-continuous morphologies displayed caused disruption of the strong protein-protein interactions thereby decreasing the level of energy absorbed during impact. With a high rate of loading (2.9 m/s) the elongation of PE is not as severe as compared to tensile samples tested at low loading rates. However, fibrillation of phases in a co-continuous morphology is known to dissipate energy and increase impact resistance,[35] as shown here at higher PE content. It is interesting to note that those blends which are heavily phase separated (CTN and LOT) showed less of a difference between notched and unnotched impact resistance, whereas SUR and CTNMA blends showed much more variation. The effect of the stress concentration as a result of the notch is less in those phase separated blends highlighting how changes in morphology can be related how the blend behaves under impact.

Considering mechanical properties alone, 20 pph$_{Novatein}$ Surlyn would be considered as the optimal formulation. It could be argued that SUR40 would be the optimal composition, however, for scale up, this blend would not be feasible due to the high cost of the zinc ionomer. Of all the 20 pph$_{Novatein}$ blends, SUR20 was shown to have the highest impact strength and the tensile strength was least compromised with PE addition. It also had the highest elongation at break with a modulus comparable to that of Novatein. These observations were ascribed to its morphology; an apparent continuous Novatein phase with a very small PE domain size. The PE phase was finely dispersed (as confirmed by SEM) leading to the improvement in impact strength. The interfacial interaction between Novatein and Surlyn brought about the divalent zinc ion allowed for efficient stress transfer during fracture, leading to the observed increase in mechanical properties.

The morphology development of unreactive systems can be generalised in terms of λ and σ, as with blends containing Cotene. However, when chemically reactive functionalities are introduced the combination of λ, σ and chemical interaction all need to be considered to establish a full picture of the morphology that will form. In the case of Novatein, chemical interaction is the driving force for morphology development but only in conjunction with the other two factors. It is also likely that the influence of chemical functionalities is the driving force in other reactive protein systems, and this can be the focus of future work.

4 | CONCLUSION

The morphology of Novatein/polyethylene blends was successfully altered and characterised through the use of modified polyethylene containing reactive functionalities (epoxy, carboxylic acid partially neutralised with zinc oxide or maleic anhydride). Morphology is not necessarily dominated by one component of the blend properties, i.e., composition, chemical reactivity,

viscosity ratio or interfacial tension; rather it is a combination of these factors. SUR blends had the most optimal properties at high PE content, attributed to the formation of micro-domains which increased impact resistance and elongation at break. The blend's viscosity ratio (~1) and higher interfacial tension facilitated this morphology development, yet the improved mechanical properties can be attributed to the interactions at the interface, brought about by the presence of divalent zinc ions in Surlyn and reactive amino acids present in Novatein. This compatibility was evidenced in the dynamic mechanical analysis and microscopy. On the other hand, unmodified blends and those containing glycidyl methacrylate (LOT) had a highly continuous polyethylene phase, even at low PE content. This was attributed to the lower blend interfacial tension, promoting coalescence of the minor phase. There was also a lack of interaction at the interface, causing a detrimental effect on mechanical properties. An intermediate effect was seen in blends containing maleic anhydride grafted polyethylene. Despite the compatibility evidenced through DMA and solvent extraction data, the existence of large, undispersed Novatein domains acted as stress concentrations and had a negative effect on mechanical properties.

Manipulation and tailoring of morphology in Novatein blends is a complex balance of viscosity ratio, interfacial tension and chemical interaction. For any prediction to be made on the morphology formed, all three factors must be considered. For blends of Novatein to exhibit a finely dispersed morphology, with the aim of altering material properties, the second phase must contain functionalities highly reactive towards protein, and the blend must have a viscosity ratio close to one with a high interfacial tension. Furthermore, in order for greatest energy absorption during deformation or impact, the second phase must be elastomeric and exhibit good adhesion to the protein matrix.

ACKNOWLEDGMENTS

REFERENCES

[1] C. J. R. Verbeek, L. E. van den Berg, *Macromol. Mater. Eng.* **2011**, *296*, 524.

[2] Novatein, Aduro Biopolymers, http://www.adurobiopolymers.com/Novatein (accessed: February 2017).

[3] Z. Bartczak, A. S. Argon, R. E. Cohen, M. Weinberg, *Polymer* **1999**, *40*, 2347.

[4] R. Y. Hong, H. P. Fu, Y. J. Zhang, L. Liu, J. Wang, H. Z. Li, Y. Zheng, *J. Appl. Polym. Sci.* **2007**, *105*, 2176.

[5] M. W. L. Wilbrink, A. S. Argon, R. E. Cohen, M. Weinberg, *Polymer* **2001**, *42*, 10155.

[6] W. G. Perkins, *Polym. Eng. Sci.* **1999**, *39*, 2445.

[7] P. Pötschke, D. R. Paul, *J. Macromol. Sci. Polym. Rev.* **2003**, *43*, 87.

[8] H. Veenstra, P. C. J. Verkooijen, B. J. J. van Lent , J. van Dam, A. P. de Boer, A. P. H. J. Nijhof, *Polymer* **2000**, *41*, 1817.

[9] F. Chen, J. Zhang, *ACS Appl. Mater. Interfaces* **2010**, *2*, 3324.

[10] T. S. Omonov, C. Harrats, P. Moldenaers, G. Groeninckx, *Polymer* **2007**, *48*, 5917.

[11] G. Li, B. D. Favis, *Macromol. Chem. Phys.* **2010**, *211*, 321.

[12] J. Li, P. L. Ma, B. D. Favis, *Macromolecules* **2002**, *35*, 2005.

[13] J. Lyngaae-Jørgensen, K. L. Rasmussen, E. A. Chtcherbakova, L. A. Utracki, *Polym. Eng. Sci.* **1999**, *39*, 1060.

[14] C. E. Scott, C. W. Macosko, *Polymer* **1995**, *36*, 461.

[15] E. A. Flexman, J. Uradnisheck, (E. I. du Pont de Nemours and Company), *US 7381772* **2008**.

[16] P. Plimmer, C. Tanner, *US 20120259028 A1* **2012**.

[17] F. Chen, J. Zhang, *Polymer* **2009**, *50*, 3770.

[18] K. I. K. Marsilla, C. J. R. Verbeek, *Macromol. Mater. Eng.* **2014**, *299*, 885.

[19] K. I. K. Marsilla, C. J. R. Verbeek, *J. Appl. Polym. Sci.* **2013**, *130*, 1890.

[20] J. M. Raquez, R. Narayan, P. Dubois, *Macromol. Mater. Eng.* **2008**, *293*, 447.

[21] M. J. Smith, C. J. R. Verbeek, M. C. Lay, *Ind. Eng. Chem. Res.* **2015**, *54*, 4717.

[22] C. W. Macosko, H. K. Jeon, T. R. Hoye, *Prog. Polym. Sci.* **2005**, *30*, 939.

[23] C. J. R. Verbeek, K. L. Pickering, C. Viljoen, L. E. Van den Berg, (Novatein Limited), *US 2010/0234515 A1* **2010**.

[24] S. L. Kramer, P. E. Waibel, B. R. Behrends, S. M. El Kandelgy, *J. Agr. Food Chem.* **1978**, *26*, 979.

[25] S. Caroli, G. Forte, M. Alessandrelli, R. Cresti, M. Spagnoli, S. D'Ilio, J. Pauwels, G. N. Kramer, *Microchem. J.* **2000**, *67*, 227.

[26] B. Mesic, M. Lestelius, G. Engström, *Packag. Technol. Sci.* **2006**, *19*, 61.

[27] R. N. Shimizu, N. R. Demarquette, *J. Appl. Polym. Sci.* **2000**, *76*, 1831.

[28] G. Biresaw, C. J. Carriere, *J. Polym. Sci., Part B: Polym. Phys.* **2001**, *39*, 920.

[29] G. Guerrica-Echevarría, J. I. Eguiazábal, J. Nazábal, *Polym. Test.* **2000**, *19*, 849.

[30] R. C. Willemse, A. P. de Boer, J. van Dam , A. D. Gotsis, *Polymer* **1999**, *40*, 827.

[31] M. J. Smith, C. J. R. Verbeek, *Macromol. Mater. Eng.* **2016**, *301*, 992.

[32] E. Schwach, L. Averous, *Polym. Int.* **2004**, *53*, 2115.

[33] C. A. Orr, J. J. Cernohous, P. Guegan, A. Hirao, H. K. Jeon, C. W. Macosko, *Polymer* **2001**, *42*, 8171.

[34] H. E. Burch, C. E. Scott, *Polymer* **2001**, *42*, 7313.

[35] U. Niebergall, J. Bohse, B. L. Schürmann, S. Seidler, W. Grellmann, *Polym. Eng. Sci.* **1999**, *39*, 1109.

6

Structural Changes and Energy Absorption Mechanisms during Fracture of Thermoplastic Protein Blends Using Synchrotron FTIR

A paper published in

Polymer Engineering & Science

By

M. J. Smith & C. J. R. Verbeek

Structural Changes and Energy Absorption Mechanisms during Fracture of Thermoplastic Protein Blends Using Synchrotron FTIR

The study presented in Chapter 6 aimed to use synchrotron FT-IR to map the phase distribution of impact strength modified blends of Novatein produced in Chapters 4 and 5. The investigation examined protein secondary structure within the blends and assessed if structural changes can be correlated with changes in energy absorption, or if morphology was responsible for changes to mechanical properties. Furthermore, the study aimed to determine if protein secondary structure was altered during fracture, and whether this changed with type and content of the second phase.

As first author of this paper, I prepared the initial draft manuscript, which was refined and edited in consultation with my supervisor, who has been credited as co-author.

Structural Changes and Energy Absorption Mechanisms During Fracture of Thermoplastic Protein Blends Using Synchrotron FTIR

Matthew J. Smith [ORCID], Casparus J. R. Verbeek [ORCID]
School of Engineering, University of Waikato, Hamilton, New Zealand

Novatein thermoplastic protein embrittles quickly after processing due to desorption of plasticizer, leading to poor energy absorbing properties such as impact strength. However, impact modified Novatein blends, containing functionalized polyethylene or nano-scale core-shell particles exhibit increased energy absorbing properties. The phase distribution of reinforced blends, and the protein secondary structure changes as a result of blending and fracture was investigated using synchrotron FT-IR microspectroscopy. Morphological changes in Novatein/polyethylene blends were responsible for variations in mechanical properties, rather than changes in secondary structure. In contrast, a greater impact strength was correlated to an increase of disordered secondary structures in core-shell particle reinforced Novatein. Blends which exhibited greater elongation or yielding during fracture showed a significant difference between protein secondary structure in the bulk matrix and the yielded material after fracture. It was concluded that the change in conformation of protein structures during fracture is an energy absorbing mechanism that acts in conjunction with the free elongation of the matrix due to decreasing interparticle distance for materials reinforced with nano-particles. POLYM. ENG. SCI., 00:000–000, 2017. © 2017 Society of Plastics Engineers

INTRODUCTION

A number of protein sources, such as soy, wheat, pea, and sunflower proteins, have been the subject of investigation for thermoplastic processing, with varying degrees of success [1–3]. Novatein thermoplastic protein, a biodegradable polymer produced from bloodmeal [4], has poor energy absorbing properties depending on plasticizer content and protein denaturant levels. The injection molding grade of Novatein shows high tensile strength and modulus but has low strain at break and impact strength [5]. In comparison, increased plasticizer and protein denaturant content brings about better energy absorbing properties in Novatein, but a reduction in strength and modulus are observed [6].

Mechanical properties of polymers can be tailored by blending; however, the changes observed are heavily dependent on the morphology formed. The addition of an elastomeric polymer into a rigid matrix, either through blending or the incorporation of synthesized particles are common techniques for improving

energy absorption [7]. Impact modification of Novatein has been achieved in a number of ways; nano-scale core-shell particles with an elastomeric core and rigid shell were shown to improve the unnotched impact strength by an order of magnitude [5]. Similarly, reactively blending high contents (~40 wt%) of modified polyethylene (PE) with Novatein, doubled the elongation at break and increased impact strength by ~350%, while decreasing tensile strength by less than 25% [6]. Whether these changes in energy absorption could be correlated to changes in protein structure, or if morphology effects were the sole reason for the improved properties, is still unknown.

Fourier transform infrared spectroscopy (FTIR) is commonly used in polymer blends to determine the interactions forming during processing. Coupling reactions can be identified through changes to peak heights signifying the consumption of reactive functionalities, or vibrational peaks arising from new covalent interactions. This technique is useful in toughened blends, as interactions between the phases may indicate increased stress transfer during fracture [8].

Synchrotron FTIR has been used extensively in the characterization of Novatein to gain an understanding of the protein structure and how this affects, and is affected by, thermoplastic processing [9–14]. The highly focused beam of light produced from a synchrotron source allows for much smaller apertures to be used when scanning, providing high spatial resolution (~1 μm) [15]. Hence, this technique is useful in applications where small vibrations are detected and fine spatial resolution is required, such as changes to protein secondary structure. The primary structure of the protein will dictate how the protein interacts, folds and subsequently forms α-helix, β-sheet or random coil arrangements. When processing into a thermoplastic, these structures must be rearranged to allow the material to flow and the protein backbone to reorder; forming new interactions upon the application of shear, heat, and pressure during processing [16].

Protein secondary structure can be identified through analysis of amide I, II, and III regions (1,600–1,700 cm^{-1}, 1,480–1,575 cm^{-1}, and 1,200–1,350 cm^{-1}, respectively) [17]. Higher α-helix content in thermoplastic proteins often allows for a more ductile material, as in the case of blown films [18], while increased β-sheet content is typical of protein materials exhibiting high strength, such as spider silk [19]. By assessing the content of these structures within a thermoplastic protein, it may be possible to comment on the ability of such materials to absorb energy during fracture and alter protein structure to allow for this in the future.

This study aims to use synchrotron FTIR to map the phase distribution of impact modified blends of Novatein containing PE, modified PE and nano-scale core shell particles. The investigation will examine protein secondary structure within the blends and assess if structural changes can be correlated with

TABLE 1. Sample compositions.

Blend name	Novatein Grade	Mass fraction Novatein (%)	Second phase	pph$_{Novatein}$
Novatein Crude	—		—	—
Novatein IR3020	—		—	—
CTN	Crude	83	Cotene 3901	20
LOT	Crude	83	Lotader AX8900	20
SUR	Crude	83	Surlyn 9320	20
CTNMA	Crude	83	Cotene 3901/PE-g-MA	10/10
CS5$_{C/I}$	IR3020	95	Paraloid EXL 2314	5
CS15$_{C/I}$	IR3020	87	Paraloid EXL 2314	15
CS30$_{C/I}$	IR3020	77	Paraloid EXL 2314	30

changes in energy absorption. Lastly, this study will aim to determine if protein secondary structure is altered as a result of fracture, and whether this changes with type and content of the second phase.

EXPERIMENTAL

Materials

Two grades of Novatein thermoplastic protein, Novatein Crude and Novatein IR3020 (both proprietary grades produced from bloodmeal, plasticizer and protein denaturants), were supplied by Aduro Biopolymers LP, Hamilton, New Zealand [20]. It is known that Novatein Crude contains a higher content of plasticizer and protein denaturants than Novatein IR3020. Lotader AX8900 (LOT) is a random terpolymer of ethylene, acrylic ester (24 wt%), and glycidyl methacrylate (GMA, 8 wt%), produced by Arkema, France, and acquired through Nuplex Specialties, New Zealand. Surlyn 9320 (SUR) is a zinc ionomer thermoplastic resin (described elsewhere as ethylene/acid/acylate terpolymer with partial neutralization of methacrylic acid groups by zinc oxide) produced by Du Pont and acquired through IMCD, New Zealand. Cotene 3901 (CTN) is unmodified LLDPE obtained from Elastochem, New Zealand. Maleic anhydride grafted polyethylene (PE-g-MA) (MA content ∼0.5 wt%) was purchased from Sigma-Aldrich, New Zealand. The core–shell impact modifier used was DOW Paraloid EXL 2314, which was acquired from Plastral, New Zealand, in powder form. Paraloid EXL 2314 has a crosslinked elastomeric core consisting of butyl acrylate and 2-ethylhexyl acrylate, and a rigid PMMA shell modified with a GMA functionality. Individual particles had been measured as ∼500 nm in diameter using scanning electron microscopy (SEM).

Sample Preparation

In the case of Novatein/PE blends, granules of Novatein Crude and PE were tumble mixed in a ziplock bag before extrusion [6]. Novatein/core-shell particle blends were produced from Novatein IR3020 and Paraloid EXL 2314 which was incorporated during the Novatein production stage [5]. Tested controls and blends, containing parts per hundred of the second phase used (pph$_{Novatein}$), are displayed in Table 1.

The subscript after core-shell reinforced blends, C or I, corresponds to the way in which the sample was fractured, whether

cryo-fracture under liquid nitrogen or through Charpy impact testing (pendulum energy = 2 J). All other blends were cryo-fractured under liquid nitrogen.

Compositions were melt blended using a LabTech corotating twin screw extruder (L/D 44:1). The barrel temperature profile increased from 70°C at the feed throat, to 100°C along the main barrel sections, and finally to 120°C at the die. Screw speed remained constant at 200 rpm. Extrudate was granulated to < 4 mm in size using a tri-blade granulator (Castin Machinery, New Zealand).

Injection molded samples were produced using a BOY 35A injection molding machine. A barrel temperature profile ranging from 70°C at the feed throat, to 120°C at the nozzle was used. This low processing temperature aimed to avoid protein cross-linking and excessive plasticizer loss. Mold temperature was kept constant at 50°C. Charpy impact bars to be used in synchrotron analysis were conditioned at 50% RH and 23°C for 7 days before freeze drying for at least 48 h in a Labconco Free-Zone 2.5 L Benchtop system.

Scanning Electron Microscopy

Morphology and phase distribution of Novatein and blends was assessed using SEM in a Hitachi S-4700. The surfaces of interest from cryo-fractured or impact fractured samples were mounted on aluminium discs and sputter coated with platinum using a Hitachi E-1030 ion sputter coater prior to imaging. Images were captured at an accelerating voltage of 3, 5, or 20 kV, although this did not affect the quality of the image.

Synchrotron FTIR Microspectroscopy

Spatially resolved FTIR was conducted on the mid-infrared micro-spectroscopy beamline at the Australian Synchrotron facility, Victoria, Australia. FTIR spectra were collected in transmission mode using a Bruker Hyperion 3000 with an MCT collector and motorized XY stage. The stage was purged with nitrogen gas during spectra collection. Opus 7 software was used for data collection. For each sample, video images were initially captured to allow definition of grids to be scanned depending on sample morphology. These grids were 40 × 5, 30 × 7 for blends and 10 × 10 or 5 × 5 for controls where each individual grid point was 5 μm × 5 μm. Thirty-two spectra were collected and averaged for each grid point with a resolution of 4 cm^{-1}, with scans being collected between 3,900 and 700 cm^{-1}. Two repeats of the same grid size were mapped on each sample. For impact fractured samples (CS5$_I$, CS15$_I$, CS30$_I$), three grids were mapped; one in the bulk matrix, one in the filament-type structure brought about through deformation during impact, and one in the transition region between the bulk and filament (Fig. 1).

Microtomed sections of freeze dried impact bars were cut using stainless steel blades (TBS^{TM}) on a TBS Cut 4060 RE microtome (TBS^{TM}). These sections were then flattened between two diamond cells and transferred to a barium fluoride window for analysis.

Data Analysis

Two stages of analysis were conducted using Opus 7.2 software; first, determining the phase distribution of the blend and
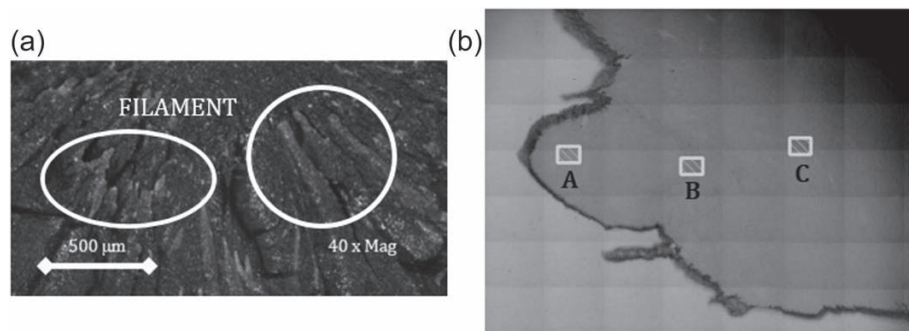
FIG. 1. (a) Example optical micrograph of CS30$_I$ showing filament structures used for mapping; (b) Example optical image of CS15$_I$ before scanning highlighting grid maps; (A) filament; (B) transition; (C) bulk matrix.

second, determining the secondary structure of the Novatein phase within the blends. As the introduction of core-shell particles caused the largest relative increase in impact strength, an analysis of protein secondary structure after fracture in CS samples was also conducted.

Phase Distribution Analysis

The ratio of Opus J-type integral (peak height) of the Novatein N─H stretching region to characteristic bands in polyethylene and Paraloid EXL 2314 were calculated across the map. Using peak ratios made any thickness variations across the sample redundant. Different bands used in the identification of the second phase were also selected for analysis to confirm the original phase maps. The integration limits for the initial and confirmation maps are displayed in Table 2. Typical FTIR spectra from Novatein, Cotene 3901 (unmodified polyethylene) and Paraloid EXL 2314 (core-shell particles) are presented in Fig. 2. The FTIR spectra for Lotader AX8900, Surlyn 9320 and maleic anhydride-grafted-polyethylene do differ slightly from Cotene, but for mapping phase distribution, the identifying bands are present in all four grades of PE.

In the cases where the same band was found in both phases (i.e., peak b and peak c), a correction was made for the overlapping peak height to avoid over-estimation of the PE mass fraction in the blend when using the ratio of peak b to peak a. The peak ratios used for initial phase distribution analysis were a/c and a/e. To confirm these results, peak ratios a/d and a/f were also calculated.

To establish the dispersion and distribution of the second phase, histograms of the Novatein mass fraction across the grids were produced. This allowed the determination of the Novatein content in the Novatein rich domains, and the transition region between Novatein rich and Novatein poor regions. These histograms were used to select the data points for secondary structure analysis based on the average Novatein content across the map (Table 1).

Secondary Structure Analysis

The second derivative of the absorbance spectra for the blends was calculated with the Savitzky–Golay algorithm in Opus 7.2 using nine-point smoothing, and inverted by dividing through negative one. Similarly, the inverted second derivative of the absorbance spectra for the neat second phase in the blend was also calculated. This was then used to correct for the mass fraction of second phase across the whole map, eventually giving the corrected second derivative spectra of the Novatein phase in the blend.

The secondary structures under investigation were α-helices, turns, random coils and β-sheets which have FTIR band assignments of 1,330–1,300 cm^{-1}, 1,295–1,270 cm^{-1}, 1,270–1,250 cm^{-1}, and 1,245–1,220 cm^{-1}, respectively [9, 25]. The maximum peak height of the inverted second derivative for the wavenumbers associated with the secondary structures was used to calculate the ratios A''_α/A''_β, A''_t/A''_β, and A''_r/A''_β through the Opus J-type integral. The subscripts α, β, t, and r denote α-helices, β-sheets, turns, and random coils, respectively. The fractional composition of secondary structures for each grid point was calculated using *Equations* (1–5).

$$\alpha + \beta + t + r = 1 \tag{1}$$

TABLE 2. Band assignments used in phase distribution analysis.

Material	Functionality	Integration limits for analysis (cm^{-1})	Notation in Fig. 2	Ref #
Novatein	N─H stretch	3000–3600	a	[21]
	C─H stretch (CH$_2$, CH$_3$)	2800–3000	b	
Polyethylene	C─H stretch (CH$_2$, CH$_3$)	2800–3000	c	[21]
	PE bending deformation (Con.)[a]	1430–1480	d	
Core-shell particles	C═O (Ester bond)	1710–1755	e	[22, 23]
	C─O─C (Con.)	1140–1200	f	[24]

[a]The note (Con.) shows the bands used for confirming maps found in Supporting Information Figure S1.
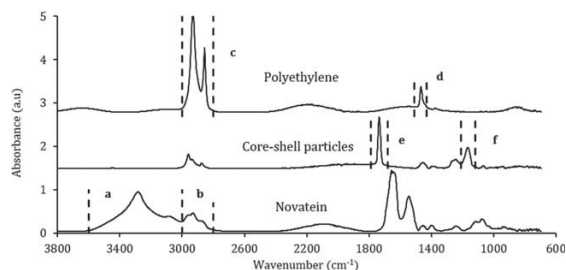
FIG. 2. Typical synchrotron FTIR spectra for unmodified polyethylene, core-shell particles, and Novatein IR3020, displaying integration limits for phase distribution mapping.

$$\beta = \frac{1}{A''_\alpha/A''_\beta + A''_t/A''_\beta + A''_r/A''_\beta} \quad (2)$$

$$\alpha = \beta \frac{A''_\alpha}{A''_\beta} \quad (3)$$

$$t = \beta \frac{A''_t}{A''_\beta} \quad (4)$$

$$r = \beta \frac{A''_r}{A''_\beta} \quad (5)$$

Only the grid points that were deemed to be "Novatein-rich" in the phase analysis were used to calculate the average secondary structure composition for the blends. These were the points that were between 1 and 0.05 less than the average Novatein mass percentage across both maps.

RESULTS AND DISCUSSION

Mechanical Properties and Morphology of Novatein Blends

Depending on plasticizer and additive content, Novatein can have poor and inconsistent energy absorbing properties such as strain-at-break (ε_b) and impact resistance. Hence, importance has been placed on modifying Novatein using elastomeric, low T_g second phase inclusions. This has proven to be successful by incorporating modified PE or core-shell particles, however composition affects the level of improvement [5, 6]. For all PE blends, the inclusion of 40 pph$_{Novatein}$ produced the best energy absorbing properties [6]. It is not feasible to produce blends with that amount of modified PE although, as it is uneconomic. Therefore, blends containing 20 pph$_{Novatein}$ PE were chosen in this study to investigate the effect of morphology. At high

particle content, however, core-shell particles have a much greater toughening efficiency compared with PE, although a large decrease in tensile strength accompanied this improved impact resistance [5] (Table 3).

The secondary structure of protein material can also have a large influence on the mechanical properties. For example, spider silk is known to have a high β-sheet content and actually has higher strength per unit weight than high tensile steel [19]. In contrast, highly amorphous, disordered regions in protein material are conducive to ductility and elasticity [26]. Bloodmeal (and decolored bloodmeal) secondary structure has been extensively studied by Bier et al. [9, 11] and Hicks et al. [12, 13] using synchrotron FTIR. However, secondary structure changes as a result of blending and fracture has not been studied previously.

Novatein appears homogenous when observing the cryo-fracture surface (Fig. 3a). The flat, featureless surface is characteristic of brittle fracture, absorbing very little energy, supported by the mechanical properties. Blending modified polyethylene (PE) brings about varying morphologies dependent on the chemical functionality present on the PE, composition, viscosity ratio, and interfacial tension. This was extensively investigated by Smith and Verbeek [6]. LDPE has been shown to be highly incompatible with Novatein (CTN blends), forming a continuous second phase at low content (Fig. 3b), as shown through solvent extraction of the Novatein phase [6]. The modification of LDPE to include reactive GMA functionalities (LOT blends) did not improve compatibility due to the low reactivity of epoxides and functional amino acids at the chosen processing temperature [27] (Fig. 3c). The optimal blend of Novatein was with a zinc ionomer, which had PE as the polymer backbone and methacrylic acid functionalities partially neutralized by zinc oxide (SUR blends). This blend had the optimum viscosity ratio and interfacial tension for a dispersed morphology, while the good interfacial adhesion (brought about by the presence of the divalent zinc ion) allowed for sufficient stress transfer, bringing about good energy absorbing properties (Fig. 3d). Some compatibility was displayed with the incorporation of maleic anhydride-grafted-polyethylene to the Novatein/LDPE blend (CTNMA blends), due to miscibility of the polyethylene components and high reactivity of maleic anhydride toward the amino acids present in Novatein. However, large domains of Novatein were present in the sample (Fig. 3e), acting as significant stress concentrations and subsequently hindering impact strength improvement.

TABLE 3. Selected mechanical properties of Novatein and blends.

Blend[a]	Tensile strength (MPa)	Strain at break (%)	Notched impact strength (kJ/m²)	Unnotched impact strength (kJ/m²)	Ref #
Novatein Crude	4.47 ± 0.05	41.37 ± 3.67	1.32 ± 0.71	9.70 ± 4.71	[6]
CTN	2.17 ± 0.17	3.66 ± 0.64	3.14 ± 0.62	3.59 ± 0.88	[6]
LOT	1.73 ± 0.05	4.81 ± 0.67	2.46 ± 0.27	3.93 ± 0.77	[6]
SUR	3.35 ± 0.07	9.49 ± 0.89	2.31 ± 0.22	10.37 ± 1.03	[6]
CTNMA	4.94 ± 0.11	4.16 ± 0.37	1.45 ± 0.02	4.45 ± 0.67	[6]
Novatein IR3020	17.49 ± 1.06	2.13 ± 0.25	0.90 ± 0.25	3.72 ± 1.34	[5]
CS5	17.55 ± 1.21	2.95 ± 0.82	0.99 ± 0.22	4.48 ± 1.67	[5]
CS15	10.71 ± 0.42	35.47 ± 7.20	1.57 ± 0.54	6.60 ± 2.03	[5]
CS30	8.41 ± 0.25	59.55 ± 6.39	2.78 ± 1.27	43.49 ± 16.82	[5]

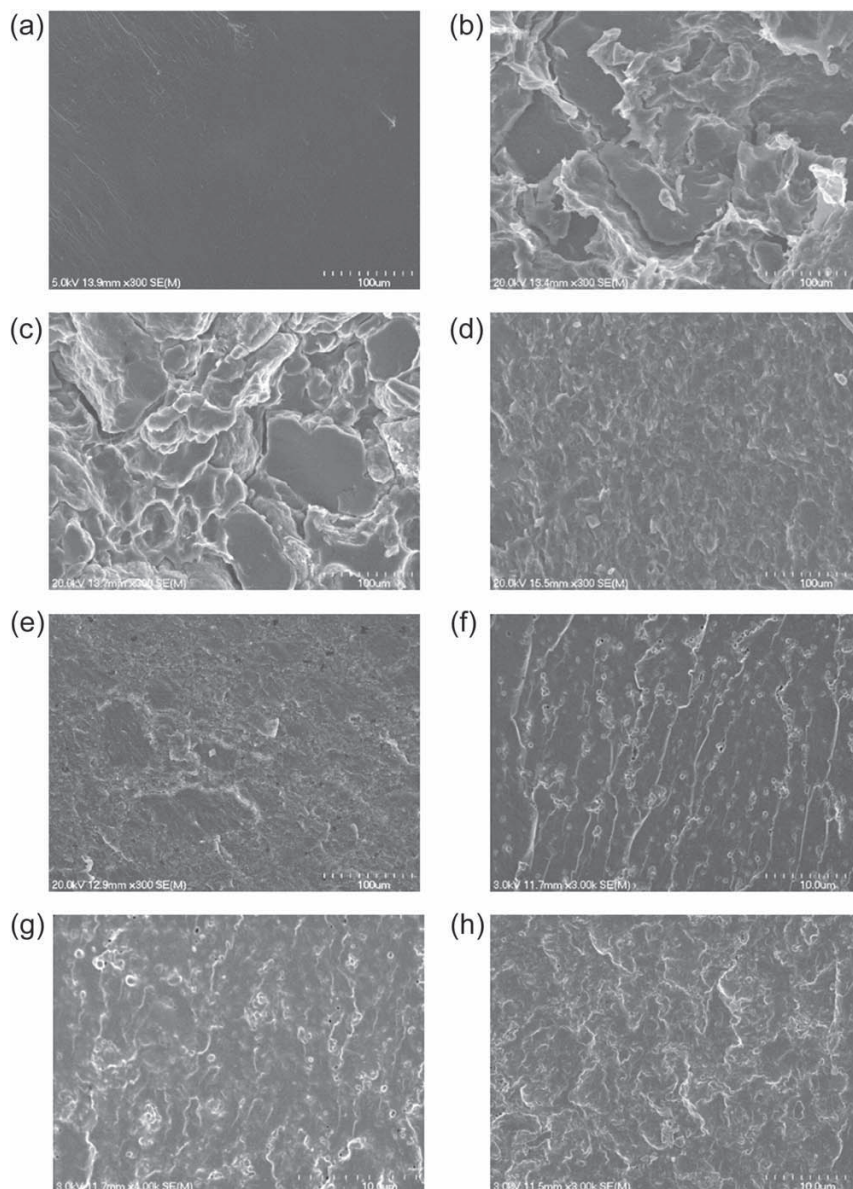[a]Second phase inclusion and pph$_{Novatein}$ are as in Table 1.

FIG. 3. SEM micrographs of (a) Novatein; (b) CTN20; (c) LOT20; (d) SUR20; (e) CTNMA20; (f) CS5$_I$; (g) CS15$_I$; (h) CS30$_I$. N.B. The different magnification of images a–e and images f–h is purely to highlight phase separation. No comparison should be made between phase size for images a–e and f–h.

In contrast, the introduction of core-shell particles, whereby morphology is fixed in the form of a dispersion of particles, also increased the energy absorbing properties of Novatein. By increasing the content of these elastomeric particles above a critical point, the interparticle distance becomes such that the matrix material is no longer elastically constrained and can therefore elongate freely under stress (provided it is above the yield stress and below the critical craze stress) [5]. Therefore, CS5$_I$ blends (Fig. 3f), showed negligible change compared to Novatein, whereas CS15$_I$ and CS30$_I$ (Fig. 3g and h, respectively) showed a large increase in energy absorption.

The phase separation in both Novatein/polyethylene blends and core-shell particle reinforced Novatein appears to be directly responsible for the changes in mechanical properties observed. Using synchrotron FTIR, it is possible to map the phase distribution accurately, as well as establishing if protein structural changes affected energy absorption.

Phase Distribution Mapping

Using the ratio of peak heights a/c and a/e (Table 2), it is possible to determine the phase distribution of the polymer
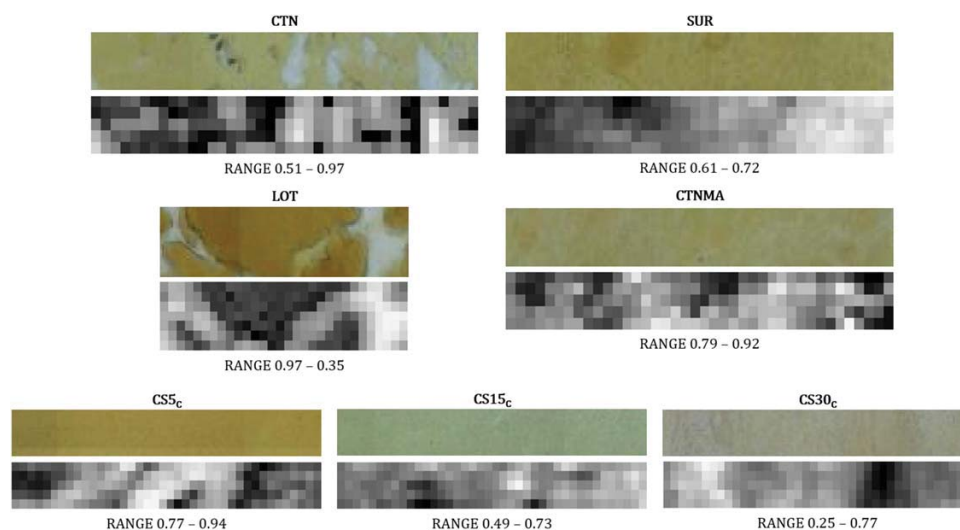
FIG. 4. Optical microscopy image from Opus software and corresponding phase distribution maps on independent scales. Peak ratios used; CTN, LOT, SUR, CTNMA – a/c; CS5, CS15, CS30 – a/e. [Color figure can be viewed at wileyonlinelibrary.com]

blend. Optical microscope images taken before scanning showed varying levels of phase separation within the blends (Fig. 4, for color figure readers are directed to the online version of this article). Despite being a dark brown/red color in the thermoplastic form, once flattened between the diamond cells, Novatein appears yellow in color. Hence, in the optical microscopy images, the yellow regions are Novatein and the white/transparent areas are the second phase (where visible). This phase separation, or lack of separation in those more compatible blends, correlates to the morphological analysis presented in previous work [6].

The phase distribution maps for the ratios a/c and a/e are shown in Fig. 4. Dark areas are indicative of a high ratio and are rich in Novatein (light areas equal Novatein poor regions). The distribution of Novatein rich and poor areas corresponds well to the phase separation visible in the optical image. The initial maps are shown on an independent scale (Fig. 4), that is, changes in Novatein rich and poor regions in each sample are presented irrespective of other maps. However, when compared to the other samples by plotting all maps on the same scale (Fig. 5, inset), it can be seen that those blends displaying less phase separation (SUR, CTNMA, CS5$_C$, CS15$_C$, CS30$_C$) showed a more homogenous phase structure, whereas CTN and LOT maps still appear heterogeneous. This is to be expected in compatible Novatein/PE blends and well dispersed core-shell particles in a Novatein matrix. There are still Novatein-rich regions in the more compatible blends (Fig. 4), possibly caused by aggregated crosslinked bloodmeal particles that are less likely to reorder due to the presence of strong protein-protein interactions that have not become reordered by the processing additives.

An interesting observation from the maps is the presence of a gradient at the interface, or an interphase, between Novatein and PE in the phase separated blends (Fig. 4). A 5 μm grid is too large to quantify the actual size of this interphase, but it may be suggested that the gradual change from one phase to the other signifies some diffusion at the interface during processing, rather than complete immiscibility due to poor interfacial adhesion and compatibility as described previously [6].

These phase distribution plots can be confirmed by mapping the peak ratios a/d and a/f (Table 2). While there may be a small amount of variation, the same pattern regarding phase separation can be observed (Supporting Information Figure S1).

The mass fraction of Novatein for each grid point can be determined using the ratio of peak a/c and a/e depending on the blend, after correcting for overlapping peaks as explained before. A histogram of Novatein mass fractions across both repeats for each formulation is presented in Fig. 5. Knowing these mass fractions also allows for correction of the FTIR spectra at each point before deconvolution of the Amide III region for secondary structure analysis, as PE and core-shell particles also absorb in this region.

It would be expected that from the sample compositions the average Novatein mass percentage for polyethylene blends would be 83%, and for core-shell blends the average would be 95%, 87%, and 77% for CS5, CS15, and CS30, respectively. However, this is not the case (Fig. 5). This variation is because the average presented is only for the grids considered for analysis ($\sim$200 μm^2), not the average for the whole sample or even the whole microtomed section. For example, in the phase separated blends, to be able to analyze across phase boundaries maps containing visible regions of PE were considered. However, in CTN, these regions only accounted for $\sim$5% of the area mapped, whereas in LOT, the actual amount of PE was much closer to the blend composition, approximately 20%. This is applicable to the homogenous blends also. The areas mapped may be more Novatein rich or poor than other areas of the sample. Despite the good dispersion and distribution of the second phase, the phase maps (Fig. 4) show that there are areas of phase aggregation.

In the heavily phase separated blends, CTN and LOT (Fig. 5a and b), the mass percentage of Novatein throughout the grid
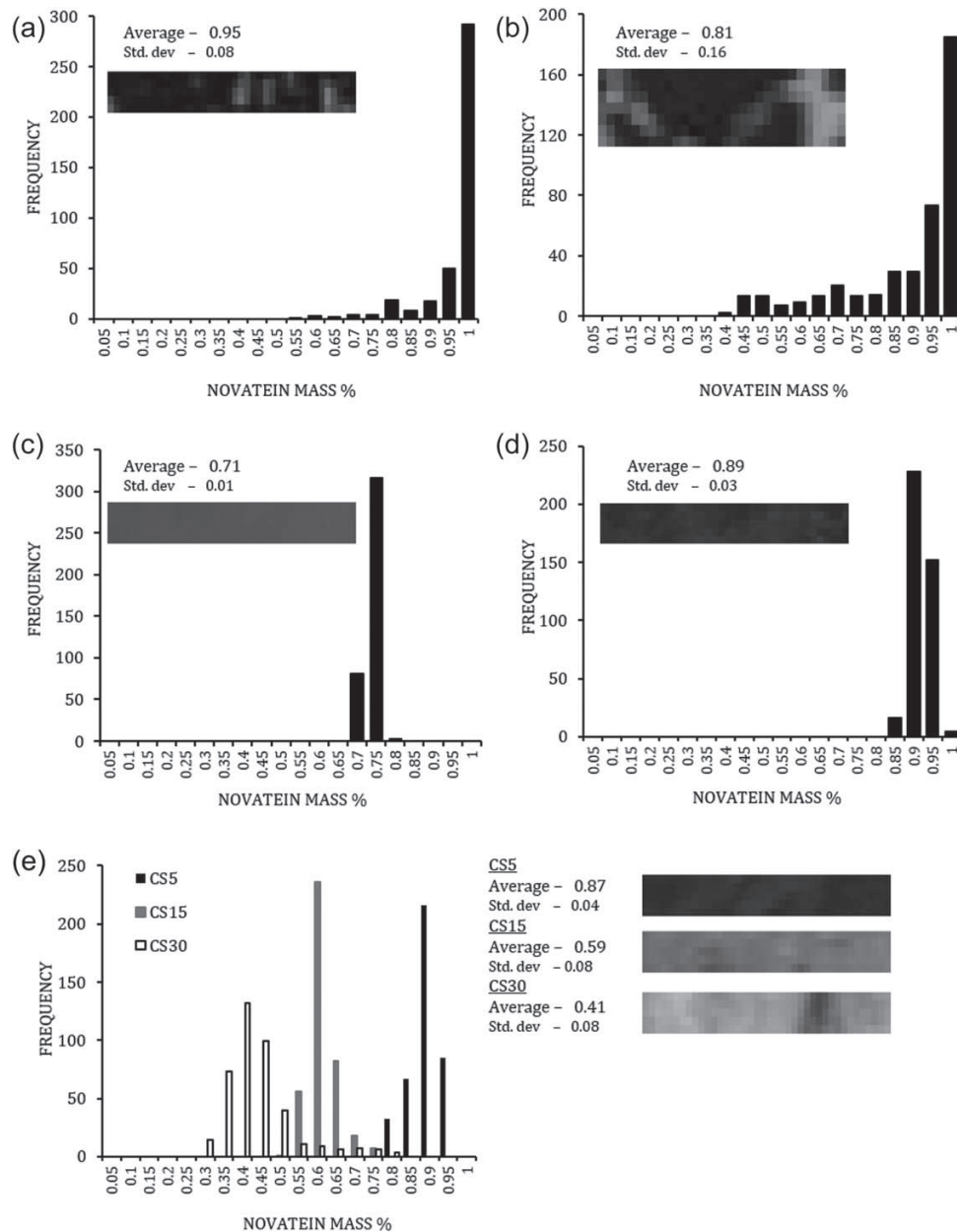
114

FIG. 5. Histogram of Novatein mass percentage across phase distribution map, and inset, phase distribution maps corresponding to those in Fig. 4 presented on a scale of 0–1. a) CTN; b) LOT; c) SUR; d) CTNMA; e) CS5, CS15, CS30.

is variable, shown through the wide distribution in the histogram. This is to be expected, as the visible phase separation suggests that regions rich in Novatein, as well as rich in PE, will be present. However, even in those regions that are classed as PE-rich, there is still a substantial amount of Novatein present (> 40%), suggesting significant levels of diffusion between phases during processing. In contrast, the distribution in grids of more compatible blends, SUR and CTNMA (Fig. 5c and d), is very narrow, with most of the points in the map showing similar

Novatein mass percentages and fewer regions rich in PE. In SUR although, the tight distribution shifts to lower Novatein mass percentages, meaning that a higher proportion of each grid point is PE. The core-shell blends (Fig. 5e) show decreasing average Novatein mass percentages with increasing particle content. Distribution is widest in CS30, likely caused by agglomeration of particles causing areas poor in Novatein, but in turn, also causing areas of Novatein-rich material. The averages stated in Fig. 5 were used to determine which points should be used for

TABLE 4. Mean fractional composition of secondary structures and *p*-values of two tailed Student *t*-tests, assuming unequal variance for all cryo-fractured blends.

	Novatein crude	CTN20	LOT20	SUR20	CTNMA20	Novatein IR3020	CS5$_C$	CS15$_C$	CS30$_C$
Total ordered	0.47	0.44	0.53	0.45	0.51	0.49	0.43	0.43	0.36
Total disordered	0.53	0.56	0.47	0.55	0.49	0.51	0.57	0.57	0.64
α-helix									
Mean	0.15	0.15	0.17	0.15	0.18	0.18	0.15	0.16	0.12
Std. dev	0.03	0.04	0.03	0.03	0.04	0.03	0.03	0.04	0.03
p value[a]	—	0.80	0.00	0.86	0.00	—	0.00	0.01	0.74
β-sheet									
Mean	0.32	0.29	0.36	0.30	0.33	0.31	0.28	0.27	0.24
Std. dev	0.05	0.06	0.07	0.04	0.07	0.06	0.06	0.08	0.07
p value[a]	—	0.00	0.00	0.00	0.60	—	0.00	0.00	0.00
β-turns									
Mean	0.06	0.06	0.09	0.10	0.07	0.05	0.09	0.15	0.15
Std. dev	0.03	0.04	0.03	0.03	0.04	0.03	0.04	0.05	0.05
p value[a]	—	0.10	0.00	0.00	0.06	—	0.00	0.00	0.00
Random coils									
Mean	0.47	0.50	0.38	0.45	0.42	0.46	0.48	0.42	0.49
Std. dev	0.05	0.06	0.06	0.04	0.07	0.05	0.05	0.07	0.09
p value[a]	—	0.00	0.00	0.04	0.00	—	0.00	0.00	0.00

[a]Note *p* values for polyethylene blends are calculated against Novatein Crude and *p* values for core-shell blends are calculated against Novatein IR3020.

secondary structure determination, to ensure areas that are rich in Novatein were analyzed.

The averages calculated from the histograms suggest that there was some bias in how grids were initially selected. The aim when selecting points to analyze was to select an area of the sample that would be representative, while also providing interesting information regarding interphases and distribution of the second phase. If time allowed, a grid of the entire microtomed section would have produced a more accurate description of phase distribution, and with advances in macro-ATR synchrotron infrared spectroscopy, this should be the focus of future work.

Based on visual inspection of the of the phase distribution maps, the corresponding optical image and the histograms, it is established that in phase separated blends (CTN and LOT) the bulk has a Novatein mass percentage of greater than 85%, while the transition region is between 60% and 85% Novatein mass percentage. The identification of this interphase allows protein secondary structures to be calculated in this region. The spatial resolution used here is not fine enough to comment on the transition region, or interphase, in SUR and CTNMA.

Mechanical Property Relationship With Protein Secondary Structure

Mean fractional composition of secondary structures in Novatein for all blends is presented (Table 4) along with *p*-values of Student *t*-tests examining statistical differences between samples. Note, a *p*-value of greater than 0.05 means that there is no significant difference between samples. Upon examination of Novatein/PE blends, there does not appear to be a pattern with regards to average secondary structures. Novatein blended with unmodified PE shows very little structural change relative to the Novatein control, suggesting minimal interaction between phases. The slight decrease in *β*-sheet content could be attributed to the diffusion suggested by the phase distribution data.

All samples containing reactive functionalities (LOT, SUR, and CTNMA) showed a decrease in random coils suggesting organization into more ordered structures. However, if structures are grouped into ordered (α-helix and *β*-sheet) and disordered (*β*-turns and random coils) then only LOT and CTNMA showed an increase in ordered structures compared to Novatein Crude. The lack of any discernible pattern suggests that while protein secondary structure is significantly affected in some cases (as shown by the *p*-values), it does not account for the changes in mechanical properties in the blends compared to Novatein. Therefore, in this instance, morphology effects brought about the changes to properties rather than secondary structure changes.

The interphase region seen in CTN and LOT showed some interesting observations. Compared to the bulk protein matrix, and the Novatein control, these regions exhibit an increase in ordered structures (Table 5). This change may be caused by the

TABLE 5. Mean fractional composition of secondary structures in the interphase region of phase separated blends.

	CTN20 Interphase	LOT20 Interphase
Total ordered	0.51	0.56
Total disordered	0.49	0.44
α-helix		
Mean	0.17	0.18
Std. dev	0.05	0.04
β-sheet		
Mean	0.34	0.38
Std. dev	0.08	0.09
β-turns		
Mean	0.07	0.11
Std. dev	0.05	0.06
Random coils		
Mean	0.42	0.33
Std. dev	0.07	0.09

116

TABLE 6. Mean fractional composition of secondary structures in varying regions of impact fractured Novatein/core-shell particle blends.

	Novatein IR3020	CS5$_I$			CS15$_I$			CS30$_I$		
		Bulk	Transition	Filament	Bulk	Transition	Filament	Bulk	Transition	Filament
Total ordered	0.49	0.42	0.43	0.46	0.29	0.31	0.34	0.26	0.27	0.39
Total disordered	0.51	0.58	0.57	0.54	0.71	0.69	0.66	0.74	0.73	0.61
α-helix										
Mean	0.18	0.12	0.13	0.12	0.08	0.08	0.07	0.10	0.10	0.12
Std. dev	0.03	0.03	0.03	0.03	0.02	0.02	0.02	0.03	0.03	0.02
β-sheet										
Mean	0.31	0.30	0.30	0.34	0.21	0.23	0.27	0.16	0.17	0.27
Std. dev	0.06	0.05	0.05	0.05	0.07	0.05	0.06	0.05	0.06	0.05
β-turns										
Mean	0.05	0.05	0.05	0.05	0.11	0.11	0.07	0.14	0.18	0.13
Std. dev	0.03	0.03	0.03	0.03	0.05	0.04	0.04	0.06	0.03	0.05
Random coils										
Mean	0.46	0.53	0.52	0.49	0.60	0.58	0.59	0.60	0.55	0.48
Std. dev	0.05	0.06	0.06	0.06	0.07	0.06	0.08	0.07	0.06	0.08

inherent incompatibility of Novatein and PE; Novatein is hydrophilic in nature while PE is highly hydrophobic. If entanglement or covalent interaction was highly prevalent, then a decrease in ordered structures may be expected as protein-polyethylene interactions took the place of protein-protein interaction.

There are some obvious trends present in the blends containing core-shell particles. For instance, across all samples the fraction of ordered structures decreased. This effect became more pronounced with increasing particle content. This is likely due to the higher number of GMA functional groups present, encouraging interactions between particles and matrix and in turn disrupting the ordered structures of Novatein. This effect is similar to the one seen for wheat gliadin films crosslinked with epichlorohydrin, whereby increasing epoxy content caused a decrease in β-sheets [21].

When related to the level of energy absorption each blend showed, there was differences between the polyethylene blends and core-shell particle blends. All of the Novatein/PE blends, when compared against one another, showed no pattern with regards to total ordered and disordered structures, or even changes to individual secondary structures. For example, LOT and CTNMA both had an increase in α-helices and a decrease in random structures, while CTN showed the opposite, yet all these samples were poor at absorbing energy during fracture. In contrast, all of the core-shell particle blends showed an increase in disordered structures compared to Novatein, with a higher relative change being observed at high particle content.

These findings suggest that in order for Novatein to exhibit increased energy absorption, the fraction of disordered secondary structures present must increase. However, in blends, this must also be coupled with adequate interfacial adhesion, efficient stress transfer between phases and a decrease matrix ligament thickness. For example, CTN and CS5$_C$ both showed a decrease in ordered structures, yet it is known that Novatein and unmodified PE are incompatible and form co-continuous morphologies at low PE content, thereby disrupting protein-protein interactions [6], while the interparticle distance (matrix ligament) in CS5 is not at the critical point where the Novatein matrix can freely elongate [5].

Changes to Secondary Structure During Fracture

While it has been shown that the incorporation of a second phase into the protein matrix can alter secondary structure, the effect of fracture upon secondary structure has not been considered. This was investigated for the core-shell particle reinforced Novatein as these blends showed a much greater relative increase in impact strength compared to Novatein/polyethylene blends. It has been reported that during impact fracture of core-shell particle reinforced Novatein, filament-type structures are formed as a result of excessive matrix yielding [5] (Fig. 1a). These filaments become more prominent with increased particle loading, thereby dissipating more energy during fracture and improving impact strength. Because these structures undergo high levels of plastic deformation, it is important to understand the effect on protein secondary structure.

Spectra was collected for three maps within impact fractured samples; one map in the bulk matrix, one map in the filament

TABLE 7. Results (p-values) of two-tailed student t-test, assuming unequal variance comparing fractional composition in impact fractured Novatein/core-shell particle blends.

	CS5$_I$		CS15$_I$		CS30$_I$	
	Bulk/Transition	Transition/Filament	Bulk/Transition	Transition/Filament	Bulk/Transition	Transition/Filament
α-helix	0.10	0.00	0.75	0.00	0.58	0.83
β-sheet	0.58	0.00	0.19	0.00	0.46	0.00
β-turns	0.82	0.08	0.97	0.00	0.02	0.00
Random coils	0.65	0.00	0.18	0.52	0.02	0.66

region, and one map between the matrix and filament, denoted the transition (Fig. 1b). Secondary structures in each of the regions in the impact fractured samples were calculated (Table 5). The values for the bulk matrix for the impact samples was different to the cryo-fractured samples, however being submerged in liquid nitrogen prior to fracture locks in the structure by being well below the materials T_g, so structural differences can be expected between cryo and impact fractured samples.

It is apparent from Table 6 that there are significant changes to protein secondary structures as a result of fracture. For all samples, the β-sheet content increased from bulk to filament, while the fraction of random coils decreased. Turns decreased at higher particle content and α-helices were relatively unaffected by fracture. As particle content increased, the relative changes seen in β-sheet and random coils became greater. The bulk and transition regions were not statistically different while the transition and filament regions showed that for CS5$_I$ and CS15$_I$, most of the structural changes occur within the filament (Table 7). There were no significant differences between all structures comparing the bulk matrix and transition region. In contrast, CS30$_I$ showed that disordered structures changed significantly between bulk and transition regions and less in the filament.

It is not a new concept to state that protein chains transform from one structure to another when placed under stress. It is well documented that α-helices transform into β-sheets when keratin is put in tension [28–30]. In the case of Novatein, the assumption is made that during fracture, random coils become aligned along the axis of force, and form new interactions with new neighboring chains, hence an increase in ordered β-sheets. This process is similar to spider silk formation in nature. Randomly aligned chains become oriented into β-sheets as a spider produces silk. This alignment is as a result of elongational flow and wall shear which produces tensile strain within the spider's silk gland. It is known that the higher the tension the spider puts on the silk, the greater the chain alignment [31]. Similarly, fiber spinning and drawing of biomimetic synthetic spider silk causes higher β-sheet content at the expense of random coils and that the effect of draw rate is similar to that of increased tension from the spider during silk production [32]. Furthermore, the orientation of α-helices and β-sheets in soy protein films was shown to increase with draw ratio, and that uniaxial drawing increased mechanical properties due to this orientation effect [33].

It is likely in reinforced Novatein with a high content of core-shell particles that it is not only the interparticle distance that encourages Novatein to deform under stress as previously suggested [2] but also the reduction in ordered secondary structures. During fracture, with Novatein free to elongate due to the plane strain to plane stress transition, there is a high level of orientation of the disordered structures. This explains why the alignment effects are more prevalent in CS30$_I$ compared to CS5$_I$; CS30$_I$ has a smaller interparticle distance and the matrix ligaments are in plane stress, whereas the matrix ligaments in CS5$_I$ are elastically constrained and unable to elongate in the same way.

It is possible to suggest that the change in conformation of protein structures during fracture is an energy absorbing mechanism. At high particle content, the effect is twofold; an increase in energy is seen due to decreased interparticle distance and free elongation of the matrix, and a further increase is brought about due to conformational changes in protein secondary structure. This theory is supported by the relative changes in disordered structures (Table 6). At low particle content, where the protein matrix is unable to freely elongate during fracture, an increase of disordered structures of $\sim$9.5% is observed from bulk to filament, while an increase of 50% is seen in the high particle blend. This is concurrent with the high relative changes in impact strength seen in the CS30 blends.

CONCLUSIONS

Synchrotron FT-IR microspectroscopy is an efficient tool for mapping the phase distribution of thermoplastic protein blends and determining the secondary structures within the blends. For Novatein/polyethylene blends, morphology was shown to cause variations in mechanical properties rather than changes to protein secondary structure. However, in core-shell particle reinforced Novatein there was a distinct correlation between increased disordered structures and greater impact resistance. The findings suggested that for Novatein blends to exhibit improved energy absorption compared to unmodified Novatein, the fraction of disordered structures must increase, interfacial adhesion must be sufficient for stress transfer between phases and the matrix ligament thickness/interparticle distance must be small enough to allow for matrix yielding.

Core-shell particle reinforced Novatein displayed an increase in ordered structures in material that yielded during fracture, compared to the bulk matrix. This was a result of orientation and elongational flow of randomly aligned structures during fracture. This transformation from one secondary structure to another requires energy, and as such, it is suggested that the transformation of secondary structures contributed to energy absorption during fracture. This phenomenon was far more pronounced in the sample with high particle content, suggesting that the ability of the matrix to freely elongate is the limiting factor in the structural transformations.

REFERENCES

1. P. Gupta and K.K. Nayak, *Polym. Eng. Sci.*, **55**, 3 (2015).

2. E. Klüver and M. Meyer, *Polym. Eng. Sci.*, **55**, 8 (2015).

3. A. Rouilly, A. Mériaux, C. Geneau, F. Silvestre, and L. Rigal, *Polym. Eng. Sci.*, **46**, 11 (2006).

4. C.J.R. Verbeek and L.E. van den Berg, *J. Polym. Environ.*, **19**, 1 (2011).

5. M.J. Smith and C.J.R. Verbeek, *Macromol. Mater. Eng.*, **301**, 8 (2016).

6. M.J. Smith and C.J.R. Verbeek, *Adv. Polym. Technol.* doi:10.1002/adv.21847

7. W.G. Perkins, *Polym. Eng. Sci.*, **39**, 12 (1999).

8. Y. Zhang, L. Huang, H. Zhou, P. Zhang, M. Zhu, B. Fan, and Q. Wu, *Starch/Staerke*, **65**, 5 (2013).

9. J.M. Bier, C.J.R. Verbeek, and M.C. Lay, *J. Appl. Polym. Sci.*, **130**, 1 (2013).

10. J.M. Bier, C.J.R. Verbeek, and M.C. Lay, *J. Appl. Polym. Sci.*, **131**, 4 (2014).

11. J.M. Bier, C.J.R. Verbeek, and M.C. Lay, *J. Therm. Anal. Calorim.*, **115**, 1 (2014).

12. T.M. Hicks, C.J.R. Verbeek, M.C. Lay, and J.M. Bier, *RSC Adv.*, **4**, 59 (2014).

13. T.M. Hicks, C.J.R. Verbeek, M.C. Lay, and J.M. Bier, *Macromol. Mater. Eng.*, **300**, 3 (2015).

14. T.M. Hicks, C.J.R. Verbeek, M.C. Lay, and M. Manley-Harris, *J. Appl. Polym. Sci.*, **132**, 26 (2015).

15. G.J. Ellis and M.C. Martin, *Eur. Polym. J.*, **81**, (2016).

16. C.J.R. Verbeek and L.E. van den Berg, *Recent Pat. Mater. Sci.*, **2**, 3 (2009).

17. J. Kong and S. Yu, *Acta Biochim. Biophys. Sin.*, **39**, 8 (2007).

18. M. Oliviero, E. Di Maio, and S. Iannace, *J. Appl. Polym. Sci.*, **115**, 1 (2010).

19. J.M. Gosline, M.E. DeMont, and M.W. Denny, *Endeavour*, **10**, 1 (1986).

20. C.J.R. Verbeek, K.L. Pickering, C. Viljoen, and L.E. Van den Berg, U.S. Patent, US20100234515A1 (2010).

21. Y. Song, L. Li, and Q. Zheng, *J. Agric. Food Chem.*, **57**, 6 (2009).

22. R.Y. Hong, H.P. Fu, Y.J. Zhang, L. Liu, J. Wang, H.Z. Li, and Y. Zheng, *J. Appl. Polym. Sci.*, **105**, 4 (2007).

23. W. Qiangxian, W. Zhengshun, T. Huafeng, Z. Yu, and C. Shuilian, *Ind. Eng. Chem.*, **47**, 24 (2008).

24. W.J. Liu, A.K. Mohanty, P. Askeland, L.T. Drzal, and M. Misra, *J. Polym. Environ.*, **16**, 3 (2008).

25. S. Cai and B.R. Singh, *Biophys. Chem.*, **80**, 1 (1999).

26. S. Rauscher, S. Baud, M. Miao, F.W. Keeley, and R. Pomès, *Structure*, **14**, 11 (2006).

27. M.J. Smith, C.J.R. Verbeek, and M.C. Lay, *Ind. Eng. Chem. Res.*, **54**, 17 (2015).

28. J. Cao, *J. Mol. Struct.*, **553**, 1 (2000).

29. J. Cao, *J. Mol. Struct.*, **607**, 1 (2002).

30. R. Paquin and P. Colomban, *J. Raman Spectrosc.*, **38**, 5 (2007).

31. O. Tokareva, M. Jacobsen, M. Buehler, J. Wong, and D.L. Kaplan, *Acta Biomater.*, **10**, 4 (2014).

32. B. An, M.B. Hinman, G.P. Holland, J.L. Yarger, and R.V. Lewis, *Biomacromolecules*, **12**, 6 (2011).

33. T. Kurose, K. Urman, J.U. Otaigbe, R.Y. Lochhead, and S.F. Thames, *Polym. Eng. Sci.*, **47**, 4 (2007).
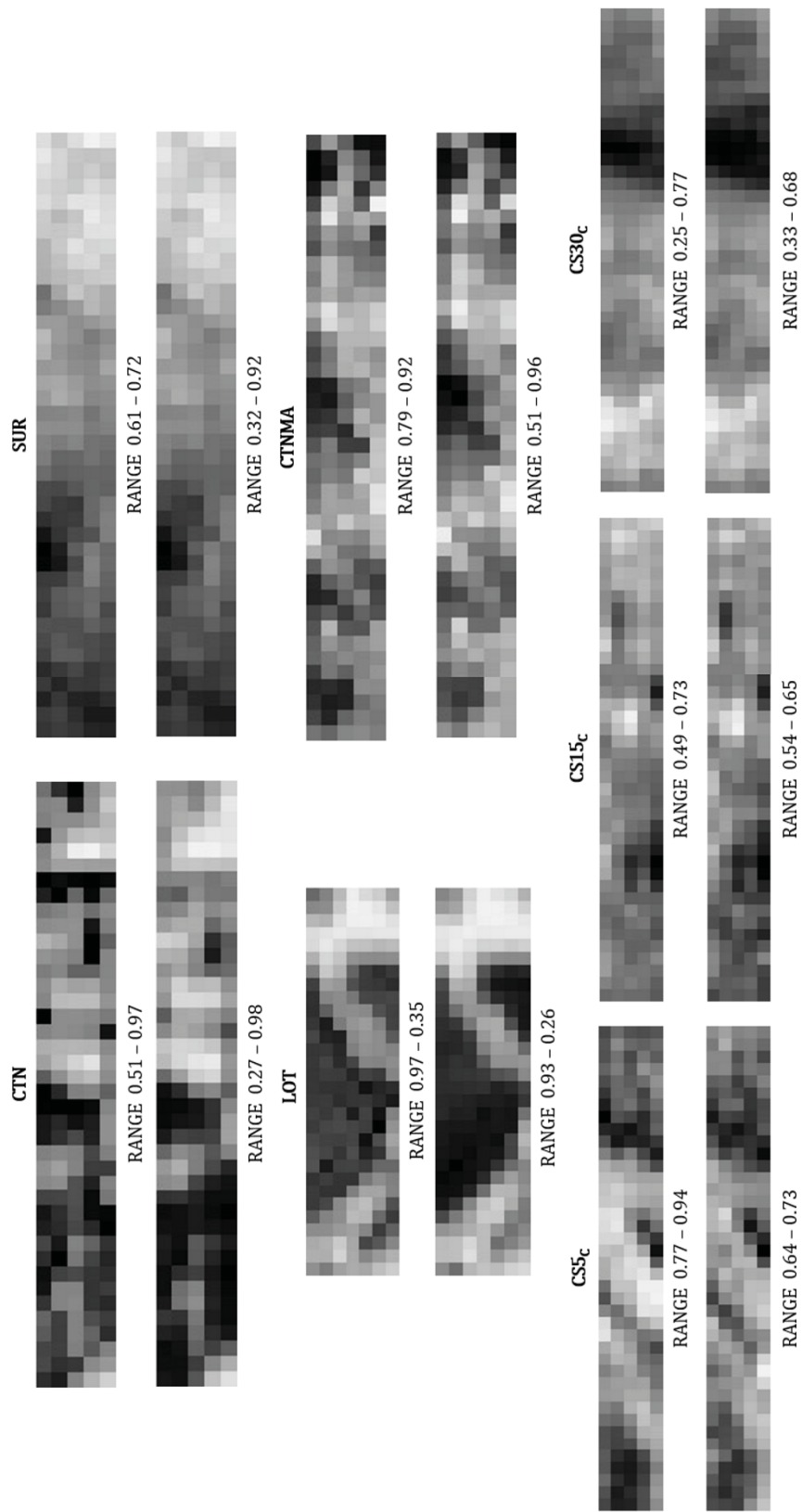
SUPPORTING INFORMATION

Figure S1. Phase distribution confirmation maps. Peak ratios A – D) a/c; A' – D') a/d; E – G) a/e; E' – G') a/f

7

Compatibilization Effects in Thermoplastic Protein/Polyester Blends

A paper published in

Journal of Applied Polymer Science

By

M. J. Smith & C. J. R. Verbeek

Compatibilization Effects in Thermoplastic Protein/Polyester Blends

Seeing that the target market for Novatein-based materials would require or desire biodegradability, focus was shifted to blends of Novatein with PBAT, a biodegradable aliphatic-aromatic copolyester known for its good energy absorbing properties. The objective was to apply the theories and ideas from Chapters 3 to 6, concerning morphology development, particle toughening and fracture mechanisms of Novatein blends, to new blends of Novatein and PBAT.

Therefore, Chapter 7 investigated the compatibilization of Novatein/PBAT blends using two different compatibilizer systems, one based on previous work of Novatein/polybutylene succinate, and one containing an epoxy functionalized chain extender with an imidazole catalyst. The aim of this chapter was to produce a blend with increased energy absorption, but at low minor phase compositions. In Chapter 4 and 5, improvements in impact strength were only observed at high weight fractions of the second phase. Therefore the hypothesis was generated that impact strength of Novatein could be improved through creating a dispersed droplet morphology by only adding small amounts of PBAT, and that compatibilizer type was particularly important in this process.

As first author of this paper, I prepared the initial draft manuscript, which was refined and edited in consultation with my supervisor, who has been credited as co-author.

Compatibilization effects in thermoplastic protein/polyester blends

Matthew J. Smith [iD], **Casparus J. R. Verbeek** [iD]

University of Waikato, Hamilton, New Zealand
Correspondence to: (E-mail: matthew.smith@waikato.ac.nz)

ABSTRACT: Novatein thermoplastic protein was extrusion blended with poly(butylene adipate-*co*-terephthalate) (PBAT) in the presence of dual compatibilizers to produce blends with greater energy absorbing properties than pure Novatein. Compatibilizer pairs were Joncryl ADR-4368 (glycidyl methacrylate-functionalized) with 2-methylimidazole (2MI), and poly-2-ethyl-2-oxazoline (PEOX) with polymeric diphenyl methane diisocyanate (pMDI). Uncompatibilized Novatein/PBAT blends had decreased tensile mechanical properties, attributed to phase separation, and poor interfacial adhesion. PBAT became finely dispersed in both compatibilized systems, but PEOX/pMDI blends showed embrittlement and large Novatein domains, which acted as stress concentrations. Tensile strength and elongation at break for Joncryl/2MI blends did not decrease compared with Novatein, even at 10 wt % PBAT, and impact strength increased threefold. Dynamic mechanical analysis and solvent extraction showed that PBAT coalesced in all systems, at compositions as low as 2 wt %. It was concluded that using Joncryl/2MI as a dual compatibilizer system can successfully produce a morphology that enhances energy absorption during fracture. © 2017 Wiley Periodicals, Inc. J. Appl. Polym. Sci. **2017**, *134*, 45808.

INTRODUCTION

Thermoplastics produced from renewable and sustainable sources have gained considerable interest in recent years. Novatein thermoplastic protein is produced from bloodmeal, a byproduct of the meat processing industry and is rich in protein (∼90%). Novatein becomes brittle over time due to the loss of plasticizer to the atmosphere, meaning it is unable to absorb high levels of energy during fracture.[1] Its impact resistance and energy-to-break can be improved by blending with elastomeric polymers, or particles containing an elastomeric core.[2,3]

The properties of many polymers can be tailored to a certain application through blending. A number of possible phase morphologies can arise depending on interfacial tension, viscosity ratio, and blend composition. Typically, a dispersed droplet morphology is favored for impact modification, although arguments have been presented that co-continuous structures can bring about similar improvements.[4,5] Co-continuity in polymer blends is expected to occur around the phase inversion point, where the composition is near equal, however, it has been shown that the onset of continuity in the minor phase can occur at very low contents of the minor phase.[6]

The majority of polymer blends are immiscible and require compatibilizers to improve interfacial adhesion between blend components. The level of energy absorption during fracture can often be linked to compatibility and interfacial adhesion. For

example, good interaction at the interface allows for efficient stress transfer between phases; particularly useful when the dispersed phase is elastomeric and can absorb higher levels of energy than the matrix.[7]

Functionalities such as glycidyl methacrylate (GMA) (containing epoxy groups), maleic anhydride, and isocyanates are commonly used for compatibilization due to their high reactivity towards several functional groups found in biopolymers (such as —NH, —OH, —COOH).[8] Many compatibilizers are multi-functional, containing several grafted functionalities along the polymer backbone, rather than just at the end groups, allowing the molecule to take part in multiple reactions and increase its compatibilization efficiency. One such compatibilizer (Joncryl) is styrene-based and has been used in a number of studies as a compatibilizer for biopolymer blends, as well as a chain extender in homopolymers with low molecular weight. Joncryl was shown to effectively compatibilize poly(lactic acid) (PLA)/poly(butylene adipate-*co*-terephthalate) (PBAT) blends at inclusions as low as 1 wt %.[9] Similarly, the addition of Joncryl to thermoplastic starch/PLA films brought about an increase in tensile strength, modulus, and elongation at break attributed to improvements in compatibility and interfacial adhesion.[10]

PBAT is a biodegradable aliphatic–aromatic copolyester and has attracted interest due to its low T_g and high elongation at break, meaning it can be used to improve the impact resistance and
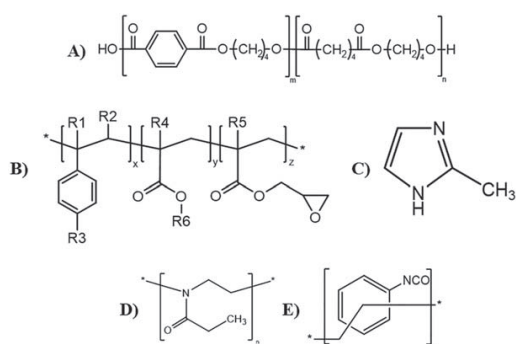
Figure 1. Structure of materials used in this study: (a) PBAT; (b) Joncryl ADR-4368, where R1–R5 is hydrogen, methyl, higher alkyl groups, or combinations of those, R6 is an alkyl group and x, y, z is 1–20[9]; (c) 2MI; (d) PEOX; (e) pMDI.

energy absorption of brittle polymers. Several studies have shown the benefit of blending bio-derived materials with PBAT.[11–15] For example, blending PBAT with PLA caused impact strength to double due to the formation of spherical PBAT micro-domains, while impact strength tripled with the addition of GMA as a compatibilizer.[16] An increase in energy absorption was also seen when thermoplastic sugar beet pulp was blended with PBAT in the presence of polymeric diphenyl methane diisocyanate (pMDI).[12]

Novatein has been blended previously with poly(butylene succinate) (PBS) using a dual compatibilizer system of poly-2-ethyl-2-oxazoline (PEOX) and pMDI.[17] This blend showed comparable elongation at break and a significantly higher tensile strength compared to neat Novatein, hence an overall increase in energy-to-break. Furthermore, the presence of the dual compatibilizers was also shown to be more effective than a single compatibilizer;[18] impact strength was not reported.

Due to PBAT's high ductility and the inherent brittleness of Novatein, the aim of this study was to produce a blend with improved energy absorbing properties compared to Novatein. This would allow Novatein to be used for a broader variety of products in the agricultural industry. Two different compatibilizer systems were used; Joncryl and 2-methylimidazole (2MI) as well as PEOX and pMDI. It is known that epoxy functionalities are reactive towards some amino acids,[19] however, this reaction occurs at a much higher temperature than the normal Novatein processing temperature, hence, 2MI was included as a catalyst for the first system. The efficiency of these compatibilizer systems was assessed by examining mechanical and thermal properties, as well as phase morphology and the onset of continuity in the minor phase.

EXPERIMENTAL

Materials

Novatein thermoplastic protein was acquired from Aduro Biopolymers LP (Hamilton, NZ). Novatein is produced from bloodmeal and a proprietary blend of plasticizers (triethylene glycol and water) and additives.[20] PBAT is a biodegradable, aliphatic–aromatic copolyester based on the monomers 1,4-

butanediol, adipic acid, and terephthalic acid in the polymer chain. This was acquired as BASF Ecoflex F blend C1200, which has a high molecular weight and long chain branched molecular structure (melt flow index = 2.7–4.9 g/10 min at 190 °C, using a weight of 2.16 kg). Joncryl ADR-4368 is a multi-functional reactive coupling agent with low molecular weight and epoxy functionalities (GMA). Joncryl has an epoxy equivalent weight of 285 g/mol. Both Ecoflex and Joncryl were acquired from Clariant (Auckland, NZ). PEOX, pMDI, and 2MI were all acquired from Sigma-Aldrich (Auckland, NZ). To emphasize the reactive functionalities, the structures of PBAT and the compatibilizer systems used are shown in Figure 1.[9,21]

Processing

Blend compositions (Table I) were established after initial scoping trials, where it was decided that a compatibilizer content of a fixed percentage of the PBAT phase was to be used. For Joncryl and 2MI, a total compatibilizer content of 70% of PBAT was used, and 50% of the PBAT phase for the PEOX/pMDI system. Adding greater than 10 wt % PBAT to Novatein was deemed uneconomical due to the relative high cost of PBAT.

For Joncryl/2MI systems, 2MI was dissolved in H_2O along with the other additives required for Novatein production, and was incorporated during Novatein extrusion. For the relevant blends, Joncryl or PEOX were added during extrusion of the Novatein/PBAT blends. To minimize hydrolysis of the isocyanate, pMDI was only added after blending Novatein and PBAT, during injection molding.

Extrusion of blends was carried out using a LabTech co-rotating twin screw extruder (L/D 44:1) with a screw speed of 200 rpm. The temperature profile increased along the barrel, from 70 °C at the feed throat to 140 °C at the die face using a 10 mm circular die. The screw configuration had one melting zone

Table I. Blend Compositions

Blend	Blend components (wt %)					
	Novatein	PBAT	Joncryl	2MI	PEOX	pMDI
Novatein	100	—	—	—	—	—
98/2-U	98	2	—	—	—	—
95/5-U	95	5	—	—	—	—
93/7-U	93	7	—	—	—	—
90/10-U	90	10	—	—	—	—
98/2-J	96.6	2	1	0.4	—	—
95/5-J	91.5	5	2.5	1	—	—
93/7-J	88.1	7	3.5	1.4	—	—
90/10-J	83	10	5	2	—	—
98/2-P	97	2	—	—	0.6	0.4
95/5-P	92.5	5	—	—	1.5	1
93/7-P	89.5	7	—	—	2.1	1.4
90/10-P	85	10	—	—	3	2

Blend numbers are based on composition (98/2 = 98 wt % Novatein and 2 wt % PBAT); letter describes the compatibilizer system (U, uncompatibilized; J, Joncryl/2MI; P PEOX/pMDI). For compatibilized blends, the compatibilizer content is described as part of the Novatein fraction.

(kneading blocks with 30° stagger) and three mixing zones (kneading blocks with 60° stagger) over the 11 barrel zones, located in zone 3 and 6, 8 and 10, respectively.

Test specimens were produced on a BOY 35 A injection molding machine with a temperature profile increasing from 100 °C at the feed throat to 150 °C at the nozzle. The mold temperature was 50 °C and the cooling time was 45 s. Before testing and analysis, all samples were conditioned at 23 °C and 50% relative humidity for 7 days.

Analysis

Tensile testing of injection molded bars was performed on an Instron 33R4204 in accordance with ASTM D368. The modulus presented is a secant modulus, calculated from the raw data between a strain of 0.05 and 0.25%. A crosshead speed of 5 mm/min was used. Charpy impact testing was done using a Ray-Ran Pendulum Impact System with an impact energy of 4 J (hammer weight of 0.952 kg and speed of 2.9 m/s) in an edge-wise orientation. Notches were cut on an in-house built automatic notch cutter in accordance with ISO 179. A minimum of six samples were tested for tensile and impact tests.

Morphology of the blends was assessed through scanning electron microscopy (SEM) in a Hitachi S-4700 instrument. Prior to imaging, cryo-fractured samples were mounted on aluminum studs and sputter coated with platinum in a Hitachi E-1030 ion sputter coater. Images were taken at an accelerating voltage of 5 kV.

Dynamic mechanical analysis (DMA) was conducted using a Perkin Elmer DMA 8000 in single cantilever mode at 1 Hz from -80 to 150 °C. Data were collected and analyzed using Perkin Elmer's Pyris software. Samples with a thickness $\sim$4 mm, width $\sim$9 mm, and free length $\sim$13 mm were subjected to a dynamic displacement of 0.05 mm. The span-to-width ratio $\sim$3.5, which is conventional, was not used for convenience of using an injection molded impact bar. This causes the storage modulus obtained to become closer to a shear modulus than a Young's modulus.

To calculate continuity of the minor phase, PBAT was removed from the blend using soxhlet extraction. Chloroform was used as the solvent and extractions lasted for 18 h. Samples of approximately 300 mg were sealed in 74-μm wire mesh during extraction. After extraction samples were air dried for 24 h and subsequently oven dried at 105 °C.

PBAT continuity was calculated from mass loss after extraction according to eq. (1).[22]

$$\text{PBAT continuity} = (m_i - m_c) \times 100 \tag{1}$$

where m_i is initial sample weight and m_c is corrected final sample mass. Novatein contains two plasticizers (water and triethylene glycol) of which water is completely removed during drying. Chloroform may also partially remove some other additives in Novatein. Corrections to mass loss were made considering the chloroform extraction of neat Novatein, accounting for the mass fraction Novatein in the blend [eq. (2)];

$$m_c = m_f + (m_i \times m_N) \times w_N \tag{2}$$

where m_f is sample weight after extraction and drying, m_N is the average percentage mass loss for pure Novatein after extraction and drying, and w_N is mass fraction of Novatein in the blend.

RESULTS AND DISCUSSION

Compatibilization Mechanisms

In Novatein, morphology development is a complex balance of viscosity ratio, interfacial tension, and chemical interactions between the phases. Chemical interactions appears to be the most important factor when producing an appropriate morphology for improved mechanical properties.[3] Novatein, comprising mostly of hemoglobin, possesses a high number of reactive amino acids along the protein backbone, which can interact with the functionalities present in the compatibilizers.

The use of dual compatibilizers in Novatein/PBAT blends aims to couple the two phases in multiple ways. Using PEOX/pMDI as a compatibilizer pair has proven successful in other studies.[17,23] PEOX interacts with Novatein through hydrogen bonding with amino acids containing functional groups such as primary and secondary amines, carboxylic acids, and sulfhydryls (although this is less likely due to disulphide bonds present in protein).[18] Furthermore, the tertiary amine structure of PEOX means it is slightly basic,[24] and with Novatein being slightly acidic, acid–base interactions are able to occur. The formation of water bridges, which also facilitates compatibilization, takes place due to the highly soluble nature and high affinity for H-bonding of PEOX.[25] In contrast, the isocyanate group in pMDI can covalently bond to the hydroxyl, carboxyl (forming urethane linkages),[26] and secondary amine groups in the protein. Similar interactions are possible with PBAT, at the terminal carboxyl and hydroxyl groups. Furthermore, hydrogen bonding is possible between PEOX (terminal —OH group) and pMDI (—NCO group), showing why these two compounds work well in a dual compatibilizer system. Examples of some possible interactions are displayed in Figure 2(A) (for color figure, readers are directed to the online version of this manuscript), although it should be noted that these are not the only feasible interactions. There are some limitations in using pMDI in Novatein systems as isocyanate groups are highly reactive towards water, which is the main plasticizing component in Novatein. This is minimized by adding pMDI just before the injection molding stage, once the effect of water has been lessened due to interactions with PEOX.

The compatibilizing reactions involving Joncryl are dependent on epoxy ring opening and subsequent interactions with functional amino acids and terminal end groups in PBAT. However, it is known that the onset of reactions between a model epoxy compound and Novatein is $\sim$180 °C, well above the processing temperature of Novatein.[19] Similarly, interactions between PBAT and Joncryl are likely to proceed much slower at the low Novatein processing temperatures, hence a catalyst is essential. Epoxy ring opening has been shown to occur at low temperatures ($\sim$120 °C), similar to Novatein processing conditions, in the presence of 2MI.[27] The inclusion of imidazole catalyses epoxy ring opening by attacking the least hindered carbon in the oxirane, forming a 1:1 adduct [Figure 2(Bi)]. In the case of 2MI, the imidazole can be regenerated through β-elimination of a hydrogen atom caused by a Hoffman reaction. This produces either hydroxyl or carboxyl functional groups depending on the rearrangement of the remaining molecule [Figure 2(B)], which
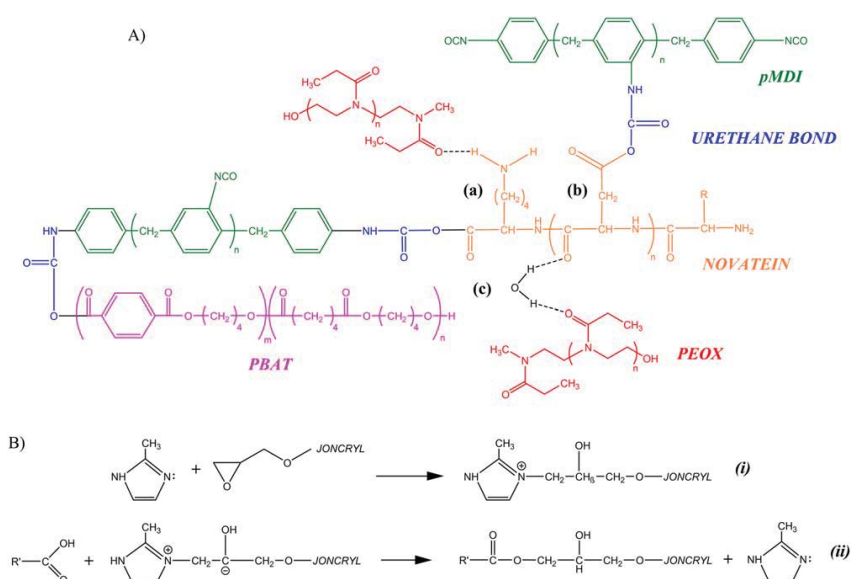
Figure 2. (A) Possible reactions and products in Novatein/PBAT blend compatibilized with PEOX/pMDI.[18] (a) Lysine; (b) aspartic acid; (c) water bridge; R = other amino acid side chains; (B) reaction mechanism and regeneration of 2MI in Novatein/PBAT blend compatibilized with Joncryl/2MI[28,29] (R′ = PBAT/Novatein terminal group or other amino acid side chain). [Color figure can be viewed at wileyonlinelibrary.com]

in turn becomes reactive toward both the protein and polyester phase or other epoxy groups.[28,29] In Figure 2(Bii), the carboxyl group displayed could also be an amine group of Novatein, and similar regeneration would take place. The formation of ester and ether linkages are the most likely reaction products. The non-consuming nature of imidazole catalysis in this situation is beneficial as the molecule can be involved in multiple reactions during processing. Furthermore, any unreacted epoxy groups are able to form strong polar bonds with carboxylic acid functionalities,[30] found prominently in both Novatein and PBAT. The potential for many reactions due to imidazole regeneration and the multi-functional nature of Joncryl leads to strong interactions at the interface as well as the likelihood of branching and increased molecular weight.

Mechanical Properties

Novatein is particularly brittle after processing and conditioning and fails to absorb energy as most synthetic polymers do. Typically, yielding and necking allow for large amounts of energy to be absorbed and dissipated during fracture. Yet, the strong protein–protein interactions present in Novatein mean that yielding may only occur when plasticizer levels are particularly high, or, as mentioned in literature, when reinforced with nano-particles causing a transition from plane strain to plane stress in the matrix.[2,3]

The incorporation of PBAT into Novatein without compatibilization, even at low levels caused a decrease in all tensile mechanical properties (Figure 3). This effect becomes more pronounced as the PBAT content increased, in an almost linear fashion. This is likely to be caused by the interruption of strong protein–protein interactions by PBAT, as well as large phase separated regions with poor interfacial adhesion, thereby leading to

stress concentrations during fracture. There was a small increase in notched impact strength in the uncompatibilized blend with 10 wt % PBAT, however this change is not significant.

The addition of PEOX and pMDI performed worse than the uncompatibilized blends with regards to tensile strength and strain at break. In contrast, secant modulus increased, suggesting that embrittlement occurred because of PEOX/pMDI. Despite this embrittlement, notched impact strength approximately doubled at 10 wt % PBAT, attributed to the energy absorption of the finely dispersed PBAT phase and increased levels of crazing during fracture (discussed later).

With regards to the Joncryl/2MI compatibilizer system, it was apparent that this blend was superior to the uncompatibilized and PEOX/pMDI systems. Tensile strength and modulus are both maintained, while a slight increase in strain at break is presented. Interestingly, notched impact strength doubled with just 2 wt % PBAT and almost tripled over Novatein at 10 wt %. These results suggest that the interfacial adhesion between Novatein and PBAT was sufficient for effective stress transfer to take place in the Joncryl/2MI system, unlike the other systems, in addition to forming an appropriate morphology (discussed later).

It should be noted that PBAT has significantly different mechanical properties to that of Novatein. For instance, PBAT undergoes yielding at ~4 MPa and strain hardens to greater than 30 MPa, as well as having an elongation at break of up to 700%. In contrast, the modulus of PBAT is much lower than Novatein (~100 and ~1100 MPa, respectively), potentially causing the decrease seen in the uncompatibilized blends in particular. However, the modulus values for both compatibilized systems would suggest otherwise, as they were comparable or
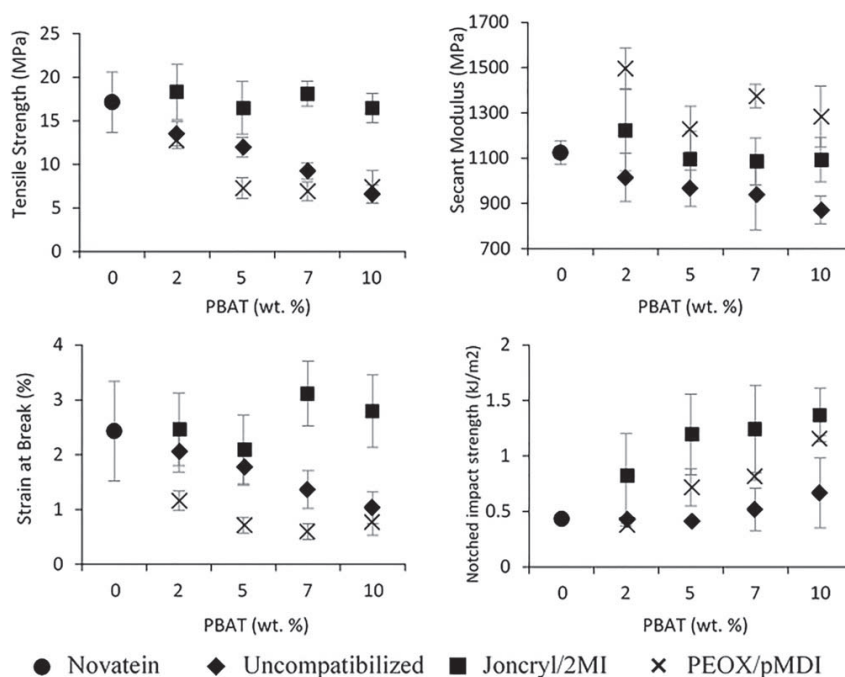
Figure 3. Selected mechanical properties of Novatein/PBAT blends.

increased over Novatein. This is likely caused by the increased interaction between PBAT and Novatein, hindering chain movement in the linear elastic region. This is evident from the difference in stress–strain plot, whereby Novatein and blends fracture before yielding, compared to PBAT which elongates extensively (Figure 4, for color figure, readers are directed to the online version of this manuscript).

The trends seen here are reminiscent of the Novatein/PBS systems with the PEOX/pMDI compatibilizer system presented by Marsilla and Verbeek,[17] whereby compatibilized blends consistently had a higher modulus than uncompatibilized blends, as seen in this work. It must be noted that in Novatein/PBS systems, superior mechanical properties were only seen at high polyester content (>30 wt %), whereas tensile properties were not compromised in this study at low PBAT levels when compatibilized with Joncryl/2MI.

Morphological Analysis

Phase separation, dispersion, and distribution is best thought of in three dimensions, however, many techniques will not fully characterize the phase behavior when employed on their own. For example, solvent extraction can establish the level of phase continuity but does not consider the phase size or coarseness; in contrast, SEM can establish how well dispersed and distributed the phases are, but only in a two-dimensional space. Therefore, it is common practice to use a number of techniques simultaneously.

SEM. Due to the brittle nature of Novatein, the fracture surface is featureless, exhibiting little evidence of plastic deformation or

yielding in the matrix even at high magnification (Figure 5). The inclusion of PBAT into Novatein without any compatibilization, caused phase separation (Figure 6), although at low content the PBAT phase appeared to have been distributed well through the matrix. The domains of PBAT ranged in size, from sub-micron to tens of microns. These larger inclusions may act as stress concentrations leading to the slight decrease in properties at low PBAT content. With increasing content, the PBAT domains coalesced, with domains increasing in size up to 100 µm. Interestingly, as the polyester content increased, the Novatein phase became encapsulated by PBAT. The interfacial adhesion in the uncompatibilized blends is poor, contributing to the decreased mechanical properties. The observations made here are in agreement with literature.[17,18]
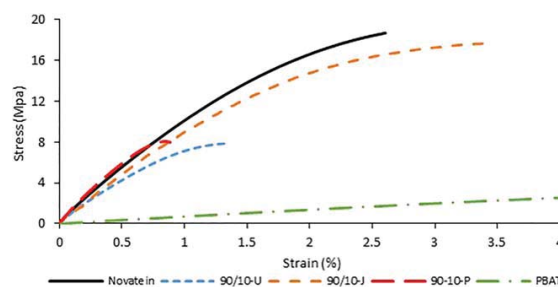

Figure 4. Stress–strain curves of Novatein, PBAT, and Novatein/PBAT blends. (N.B strain up to 4% is displayed even though PBAT yields at 4 MPa and elongates to ~700% strain). [Color figure can be viewed at wileyonlinelibrary.com]
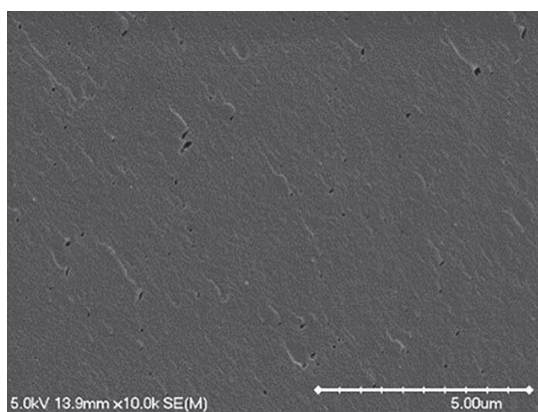
Figure 5. SEM image of Novatein fracture surface (Scale bar = 5 μm).

With regards to the compatibilized blends (Figure 6), both the Joncryl/2MI and PEOX/pMDI systems increased PBAT dispersion and interfacial adhesion, however, the Joncryl/2MI system appeared to be more efficient. For example, in the PEOX/pMDI system, large regions of Novatein can clearly be seen, as well as the formation of voids around these regions. This concurs with the observations made in Novatein/PBS blends with the same compatibilizers.[18] These large Novatein domains and voids act as stress concentrations contributing to the poor mechanical properties.

In contrast, the large Novatein regions are absent in Joncryl/2MI blends; the surface appears homogenous and no distinct

phases can be detected at this magnification. The lighter areas seen in the SEM images for these blends could be mistaken as the PBAT second phase, however these regions are crazes brought about during fracture. At higher magnification (Figure 7) the dispersed PBAT phase can be seen, with increasing domain size at 10% PBAT. Joncryl has been proven as an effective compatibilizer for blends containing PBAT and PLA, and while the epoxy groups are reactive towards proteins, uncatalyzed, this reaction only proceeds at much higher temperatures than Novatein can be processed at.[19] Therefore, the formation of a stable, dispersed morphology suggests that the presence of the imidazole had a catalytic effect on the reaction. The improvement in interfacial adhesion and more finely dispersed PBAT phase explains the ability of the blend to absorb more energy during fracture compared to unmodified Novatein.

During fracture, in both compatibilized blends, an increase in crazing is evident when compared to uncompatibilized blends and pure Novatein. This is attributed to the finely dispersed PBAT regions in PEOX/pMDI blends, or more PBAT-rich regions in Joncryl/2MI system, becoming formation and termination points of crazes. The increased energy absorption brought about through greater amounts of crazing and plastic deformation leads to the increased impact strength of compatibilized blends.

DMA. DMA can be used in conjunction with other techniques to confirm the phase behavior of polymer blends, that is, by inspecting the storage modulus curves. Typically, one would expect the storage modulus (E' curve to be similar to that of the continuous phase. However, with the onset of percolation of
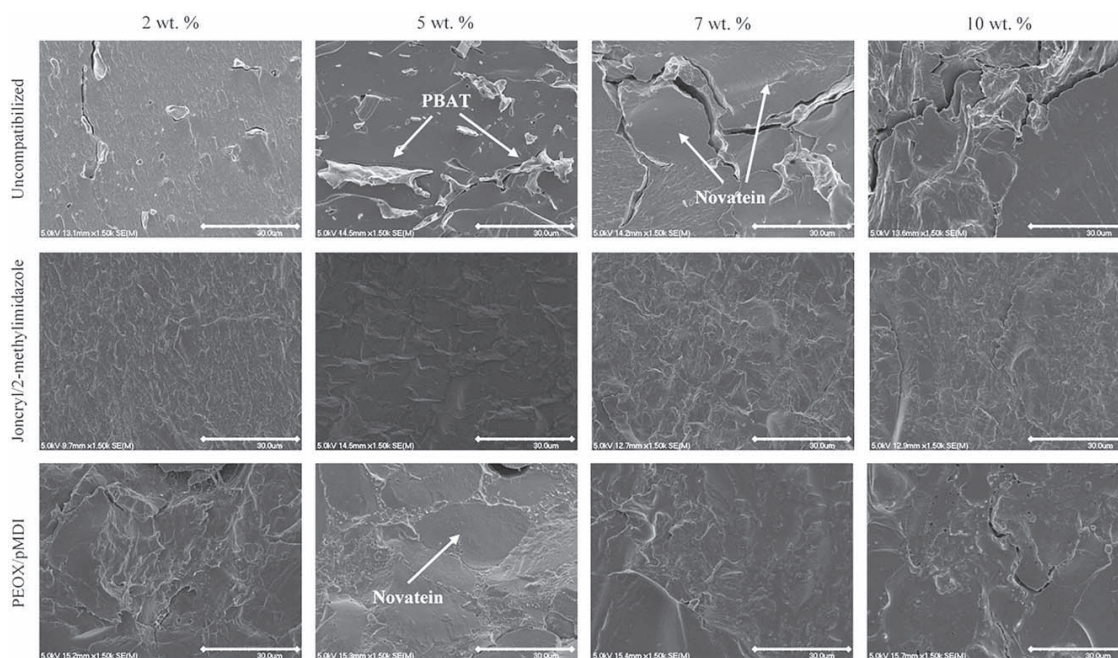

Figure 6. SEM comparison of Novatein/PBAT blends with dual compatibilizer systems, with domains pointed out for clarity (Scale bar = 30 μm).
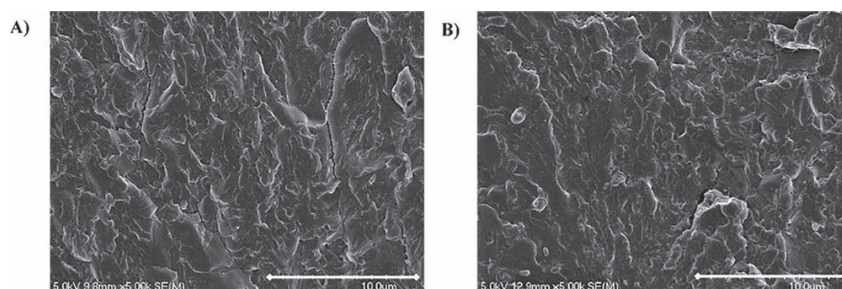
128

Figure 7. High magnification SEM images of (a) 98/2-J; (b) 90/10-J (Scale bar = 10 μm).

the dispersed phase, E' begins to tend towards the minor phase until eventually, with increasing composition there is a phase inversion, whereby E' has no influence from the original continuous phase. Also, it could be expected that thermal transitions may shift, with peaks becoming broader and lower in magnitude (tan δ and loss modulus).[18]

Novatein had a very clear peak in tan δ at ∼85 °C, attributed to the T_g. Its loss modulus curve was mostly featureless in the low temperature region, with a very broad low intensity peak around −20 °C. Pure PBAT showed a T_g at −20 °C (Figure 8, for color figure, readers are directed to the online version of this manuscript) with no other major transitions observed in the temperature range studied.

The PBAT peak in tan δ was not apparent in the uncompatibilized blends below 7 wt %, but became more prominent at 10

wt %. The Novatein T_g peak did not shift or change in magnitude suggesting there was little or no interaction between the two phases, confirming the conclusions drawn from mechanical testing and SEM analysis. At low PBAT content (2 and 5 wt %) the shape of E' resembled that of Novatein, although the magnitude did not decrease much. However, at high PBAT content (10 wt %), E' was more similar to PBAT, suggesting that the minor phase had coalesced to some degree. In between these two extremes, 93/7-U resembled that of Novatein at low temperature, but decreased more significantly at high temperature and became more like E' for PBAT. It was concluded that the onset of continuity of the PBAT was in this region. Considering the loss modulus (E''), the same can be said as for tan δ. The T_g of PBAT became more pronounced with increasing content. However, with increasing polyester content it was interesting to observe that the PBAT T_g peak at −20 °C became more
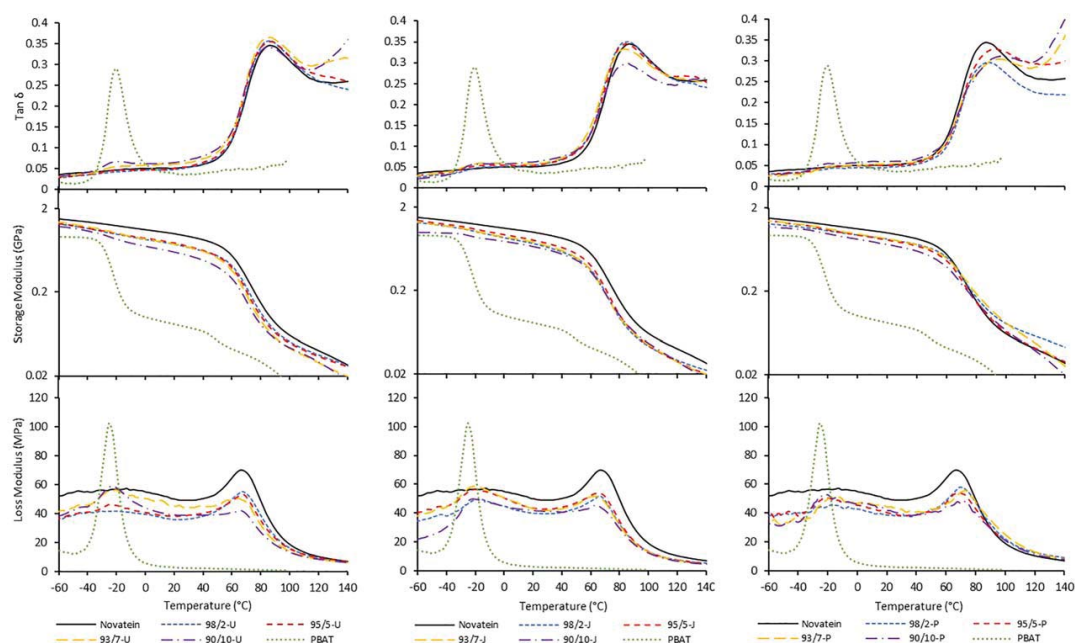

Figure 8. Dynamic mechanical analysis of Novatein, PBAT, compatibilized, and uncompatibilized blends. [Color figure can be viewed at wileyonlinelibrary.com]

129

prominent relative to the Novatein T_g peak at 85 °C, which decreased in magnitude and broadened. This was attributed to the coalescence of PBAT and encapsulation of Novatein, meaning PBAT provided a greater contribution to modulus, as with E'.

In contrast, for Joncryl/2MI compatibilized blends, PBAT's tan δ peak at −20 °C was much less pronounced across the entire composition range. The Novatein T_g peak decreased in magnitude with increasing polyester content, eluding to the fact that less protein chains took part in the transitions. The strong interaction between protein and PBAT as a result of compatibilization hindered protein chain motion and allowed greater levels of energy to be transferred to the minor phase. This is supported by the maintenance of tensile modulus in Joncryl/2MI blends with increasing PBAT content, which has a much lower modulus than pure Novatein. The slight decrease in Novatein T_g could also point to improvement in compatibility between the two polymers.

In contrast, E' for the Joncryl/2MI blends showed comparable plots to Novatein for all compositions above room temperature, only with somewhat decreased magnitude. This meant that Novatein contributed more to the modulus value even at higher content. However, at low temperature, between −60 and −20 °C, storage modulus for 90/10-J was very similar to neat PBAT, suggesting that there was a large contribution of PBAT to the modulus. The combination of these two factors would suggest that any percolation in the sample at this composition is minimal (as E' is closely linked with Novatein at higher temperature), and the PBAT contribution mostly comes from the efficient stress transfer between phases allowing for energy absorption at lower temperature. When comparing E' curve of 90/10-U against E' curve of 90/10-J it is seen that the uncompatibilized blend has a lower E' for much of the temperature range studied, highlighting the increased continuity of PBAT when no compatibilizer is included.

The E'' peak temperature relating to glass transitions in Novatein and PBAT were both strikingly similar to tan δ, with peaks at approximately 70 and −20 °C, respectively. Interestingly, Joncryl/2MI blends behaved in a similar fashion to uncompatibilized blends, with a peak at −20 °C clearly seen as well as a decrease in magnitude of the Novatein T_g peak. These were not necessarily as prominent in tan δ due to the low percentage of PBAT, with the tan δ values presented in the blend roughly 15% that of neat PBAT. The presence of the strong PBAT peak in E'' for the blend (∼50% of pure PBAT peak) suggested coalescence of the minor phase at 7–10 wt %

The tan δ plot for the PEOX/pMDI system only showed PBAT's T_g (−20 °C) at 10 wt %. However, the Novatein T_g peak shifted to a higher temperature (93 °C) at 5 and 7 wt %, and showed another increase at 10 wt % to 96 °C. The strong interaction between Novatein and PBAT as a result of dual compatibilizers hindered protein chain motion, thereby pushing the transition temperature higher. This supported the increase in tensile modulus of these blends.
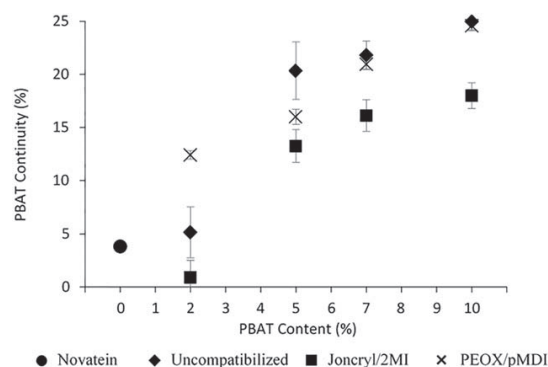

Figure 9. PBAT continuity as calculated from solvent extraction data.

E' tended towards Novatein at all temperatures, caused by the fine dispersion of PBAT, concurrent with the SEM analysis. At high temperatures, the modulus became greater than neat Novatein, again eluding to the lack of chain mobility as a result of interaction brought about by the dual compatibilizers. This is further supported by the broad peaks for the PBAT and Novatein T_gs in PEOX/pMDI blends.

The DMA results concur with the morphology analysis and support the mechanical testing data. In uncompatibilized blends, PBAT began to coalesce at low wt %, suggested by E' tending toward the minor phase, while the PEOX/pMDI system showed good interaction which subsequently hindered protein chain motion. Interestingly, despite the homogeneous appearance of the Joncryl/2MI system in the SEM images, the strong peaks at low temperature in E'' would suggest that PBAT was phase separated, but finely dispersed with good interfacial adhesion. This caused an increased energy absorption due to effective stress transfer during fracture.

Solvent Extraction. Soxhlet extraction of the minor phase can give interesting information regarding blend morphology and the extent of continuity. Chloroform was used to ensure the PBAT phase was extracted without damaging the Novatein phase. The co-continuity window is described as the composition when extraction of the minor phase becomes possible (i.e., percolation onset) to the composition where total disintegration of the sample occurs, signifying the dispersion of the phase that was initially the matrix.[6]

Novatein lost approximately 4% of its mass after extraction and drying, attributed to loss of plasticizer during drying, as well as a small protein fraction as a result of the chloroform wash (Figure 9). At low PBAT compositions, it is interesting to note that the uncompatibilized blend showed little deviation from the Novatein control (Figure 9), supporting the microscopy analysis that the PBAT is dispersed in the Novatein matrix. However, as PBAT levels increased from 2 to 5 wt %, the continuity drastically increased to >20%, meaning that despite PBAT appearing dispersed (Figure 6), these regions of PBAT were connected and percolated through the system. Further increases in PBAT content brought about small increases in continuity, caused by the

encapsulation of Novatein and increasing coalescence of the second phase.

In contrast, at 2 wt % PBAT in the PEOX/pMDI compatibilized system, PBAT continuity was roughly three times greater than the uncompatibilized blend (Figure 9). It was thought that even though PBAT was dispersed (Figure 6), these regions are still interconnected between large regions of Novatein. If the encapsulation that occurred at higher PBAT content in PEOX/pMDI systems also occurred at 2 wt % but on a much finer scale, it was thought that the discrete Novatein regions will also be washed out with the PBAT during soxhlet extraction. As seen in Figure 6, increasing PBAT content resulted in increased encapsulation, in turn causing more Novatein to be washed out as PBAT became soluble in chloroform; hence the increasing PBAT continuity (although this increase was not as drastic).

Lastly, Joncryl/2MI systems followed the same trend as uncompatibilized systems, however, continuity is significantly decreased (~5–7% less) in the compatibilized blends across all compositions (Figure 9). In fact, in the 98/2-J blend, there was less mass loss than in neat Novatein. This showed that there were significant chemical changes to Novatein, and that the extractable protein fraction was actually less with the addition of PBAT, Joncryl, and 2MI. The PBAT is also protected by the Novatein in this instance due to the very fine dispersion and strong interfacial adhesion. However, like the other blends, between 2 and 5 wt % PBAT coalesced, with further small increases in continuity with increasing polyester content. This is consistent with the material's morphology, where PBAT was finely dispersed, further supported with the DMA findings. For the Joncryl/2MI systems Novatein contributed more to the modulus of the material than the PBAT phase at low content, yet got more pronounced with increasing polyester content due to coalescence.

The asymmetric phase inversion displayed in Novatein/PBAT systems is very similar to that of plasticized wheat starch/PBAT blends, whereby the percolation threshold of the PBAT minor phase was <10 wt %, despite the high interfacial tension in the blend.[31] The early onset of coalescence was attributed to interactions, most likely hydrogen bonding, of the starch hydroxyl groups and carbonyl functionalities of PBAT, which is also feasible in the case of Novatein.

The findings of this study showed that in Novatein/PBAT blends, the use of Joncryl and 2MI as a dual compatibilizer system was beneficial not only for desirable phase morphology, but also increases in energy absorption. While energy-to-break does not change drastically there was a threefold increase in notched impact strength for the 90/10-J system. Soxhlet extraction of PBAT agrees with DMA, as well as literature, that there is an asymmetric phase inversion in all blends and that the polyester phase coalesces at low wt %, even when compatibilized. It is concluded then, that the use of a dual compatibilizer system allowed for the development of phase morphologies conducive to improved impact resistance in Novatein.

CONCLUSIONS

Uncompatibilized blends showed a decrease in all mechanical properties due to the interruption of strong protein–protein interactions and a heavily phase separated morphology. Similarly, PEOX/pMDI blends also had a decrease in tensile strength and elongation at break, but an increase in tensile modulus. This embrittlement of the material was attributed to strong interaction between Novatein and PBAT, restricting protein and polyester chain motion. In contrast, tensile strength and elongation at break for Joncryl/2MI blends did not decrease, accompanied by a threefold increase in impact strength.

Uncompatibilized blends had a heavily phase separated morphology with little interaction at the interface as well as encapsulation of Novatein by PBAT leading to the poor mechanical properties. For the compatibilized systems, PBAT appeared to be efficiently dispersed throughout Novatein, however, solvent extraction and dynamic mechanical data showed that the minor phase was well distributed, yet percolated through the sample at low content (as low as 2 wt % in PEOX/pMDI blends). Joncryl/2MI blends had lower polyester continuity and no visible stress concentrations as with other blends, leading to the conclusion that the percolation of the very finely dispersed PBAT phase produced a morphology that was conducive to greater energy absorption. Regardless of compatibilizers, asymmetric phase inversions were observed for all blends whereby the onset of percolation occurred at ~2–7 wt %.

This study successfully used a dual compatibilizer system (Joncryl/2MI) to effectively compatibilize Novatein/PBAT blends, and produce a phase morphology that allowed for greater energy absorption during fracture. Future work should be focused on the effect of viscosity ratio and interfacial tension on the blend morphology, and optimization of compatibilizer content to obtain more desirable increases in mechanical properties.

REFERENCES

1. Verbeek, C. J. R.; van den Berg, L. E. *Macromol. Mater. Eng.* **2011**, *296*, 524.

2. Smith, M. J.; Verbeek, C. J. R. *Macromol. Mater. Eng.* **2016**, *301*, 992.

3. Smith, M. J.; Verbeek, C. J. R. *Adv. Polym. Tech.* **2017**, DOI: 10.1002/adv.21847

4. Mamat, A.; Vu-Khanh, T.; Cigana, P.; Favis, B. D. *J. Polym. Sci. Pol. Phys.* **1997**, *35*, 2583.

5. Niebergall, U.; Bohse, J.; Schürmann, B. L.; Seidler, S.; Grellmann, W. *Polym. Eng. Sci.* **1999**, *39*, 1109.

6. Pötschke, P.; Paul, D. R. *J. Macromol. Sci. Polym. Rev.* **2003**, *43*, 87.

7. Perkins, W. G. *Polym. Eng. Sci.* **1999**, *39*, 2445.

8. Macosko, C. W.; Jeon, H. K.; Hoye, T. R. *Prog. Polym. Sci.* **2005**, *30*, 939.

9. Al-Itry, R.; Lamnawar, K.; Maazouz, A. *Polym. Degrad. Stabil.* **2012**, *97*, 1898.

10. Zhang, Y.; Yuan, X.; Liu, Q.; Hrymak, A. *J. Polym. Environ.* **2012**, *20*, 315.

11. Harada, M.; Ohya, T.; Iida, K.; Hayashi, H.; Hirano, K.; Fukuda, H. *J. Appl. Polym. Sci.* **2007**, *106*, 1813.

12. Liu, B.; Bhaladhare, S.; Zhan, P.; Jiang, L.; Zhang, J.; Liu, L.; Hotchkiss, A. T. *Ind. Eng. Chem.* **2011**, *50*, 13859.

13. Naiwen, Z.; Qinfeng, W.; Jie, R.; Liang, W. *J. Mater. Sci.* **2009**, *44*, 250.

14. Reddy, M. M.; Misra, M.; Mohanty, A. K. *J. Polym. Environ.* **2014**, *22*, 167.

15. Reddy, M. M.; Mohanty, A. K.; Misra, M. *J. Mater. Sci.* **2012**, *47*, 2591.

16. Kumar, M.; Mohanty, S.; Nayak, S. K.; Rahail Parvaiz, M. *Bioresour. Technol.* **2010**, *101*, 8406.

17. Marsilla, K. I. K.; Verbeek, C. J. R. *Macromol. Mater. Eng.* **2014**, *299*, 885.

18. Marsilla, K. I. K.; Verbeek, C. J. R. *Macromol. Mater. Eng.* **2015**, *300*, 161.

19. Smith, M. J.; Verbeek, C. J. R.; Lay, M. C. *Ind. Eng. Chem. Res.* **2015**, *54*, 4717.

20. Verbeek, C. J. R.; Pickering, K. L.; Viljoen, C.; Van den Berg, L. E. (Novatein Limited). U.S. Pat. 2010/0234515 A1 (**2010**).

21. Sigma-Aldrich, Available at: http://www.sigmaaldrich.com (accessed February 2017).

22. Zhang, J.; Ravati, S.; Virgilio, N.; Favis, B. D. *Macromolecules.* **2007**, *40*, 8817.

23. Liu, B.; Jiang, L.; Liu, H.; Zhang, J. *Ind. Eng. Chem.* **2010**, *49*, 6399.

24. Zhang, J.; Jiang, L.; Zhu, L.; Jane, J. L.; Mungara, P. *Biomacromolecules.* **2006**, *7*, 1551.

25. Adams, N.; Schubert, U. S. *Adv. Drug Deliver. Rev.* **2007**, *59*, 1504.

26. Wang, H.; Sun, X.; Seib, P. *J. Appl. Polym. Sci.* **2001**, *82*, 1761.

27. Ham, Y. R.; Kim, S. H.; Shin, Y. J.; Lee, D. H.; Yang, M.; Min, J. H.; Shin, J. S. *J. Ind. Eng. Chem.* **2010**, *16*, 556.

28. Ooi, S. K.; Cook, W. D.; Simon, G. P.; Such, C. H. *Polymer.* **2000**, *41*, 3639.

29. Piazza, D.; Silveira, D. S.; Lorandi, N. P.; Birriel, E. J.; Scienza, L. C.; Zattera, A. J. *Prog. Org. Coat.* **2012**, *73*, 42.

30. Pire, M.; Norvez, S.; Iliopoulos, I.; Le Rossignol, B.; Leibler, L. *Polymer.* **2011**, *52*, 5243.

31. Schwach, E.; Averous, L. *Polym. Int.* **2004**, *53*, 2115.

8

Manipulating Morphology in Thermoplastic Protein-Polyester Blends for Improved Impact Strength

A paper published in

Advances in Polymer Technology

By

M. J. Smith & C. J. R. Verbeek

.

Manipulating Morphology in Thermoplastic Protein-Polyester Blends for Improved Impact Strength

Lastly, Chapter 8 looked into how morphology could be tailored in Novatein/PBAT blends by actively changing viscosity ratio, interfacial tension and chemical interaction. The compatibilizer system used was the epoxy functionalized chain extender with imidazole catalyst used in Chapter 7. This study incorporated the previous learning regarding the interplay between the various material and processing parameters to alter morphology and in turn impact strength.

As first author of this paper, I prepared the initial draft manuscript, which was refined and edited in consultation with my supervisor, who has been credited as co-author.

WILEY

Manipulating morphology in thermoplastic protein/polyester blends for improved impact strength

Matthew J. Smith [ID] | **Casparus J. R. Verbeek** [ID]

University of Waikato, Hamilton, New Zealand

Correspondence
Matthew J. Smith, University of Waikato, Hamilton, New Zealand.
Email: matthew.smith@waikato.ac.nz

Funding information
MBIE (New Zealand), Grant/Award Number: C04X1205

Abstract

Novatein thermoplastic protein was blended with 10 wt% poly(butylene adipate-co-terephthalate) (PBAT) compatibilized with Joncryl ADR-4368 and 2-methylimidazole (2MI). Morphology was tailored for favorable impact strength through changing viscosity ratio (λ) and interfacial tension (γ_{12}). For uncompatibilized blends, λ decreased and γ_{12} increased with increasing Novatein water content, whereas compatibilizers caused a decrease in both λ and γ_{12}. PBAT continuity was high when uncompatibilized, but dispersion improved with decreasing λ and increasing γ_{12}. The dispersed domain size decreased in all compatibilized blends; PBAT continuity was lowest in samples with the smallest λ. Compatibilized blends had higher impact strength than Novatein and uncompatibilized blends through improved interfacial adhesion, smaller domain size, and increased dispersion. By altering λ and γ_{12}, and with appropriate chemical interaction, a morphology can be created for improved impact strength. Increasing PBAT content showed further increases in impact strength; however, a cocontinuous morphology formed, demonstrating that composition can override the effect of λ and γ_{12}.

KEYWORDS

blends, impact resistance, morphology development, polyester, thermoplastic protein

1 | INTRODUCTION

Novatein thermoplastic protein is produced from bloodmeal, a waste product of the meat processing industry. It has low energy absorbing properties but can be improved to some extent through reactive polymer blending[1] or particulate reinforcement.[2]

Polymer blending is a solution for improving material properties; however, there is a fine balance between viscosity ratio, interfacial tension, and chemical reactivity to achieve the correct morphology. For binary blends of immiscible polymers, the breakup of the minor phase during processing is often governed by the ratio of shear stress to the interfacial stress, otherwise known as the capillary number (Ca).[3] Shear stress during processing is the driving force for the minor phase deformation, whereas interfacial tension resists the deformation. Hence, droplets will continue to break up during

mixing as long as the shear stress is greater than the interfacial stress, a point which is quantified by the critical capillary number (Ca_{crit}).[4] In contrast, viscosity ratio (λ) governs the breakup time, which is why droplet formation is favoured when λ is lower and close to unity.[5] This situation becomes more complicated in ternary blends, and morphology is governed by the spreading coefficients and wettability of phases toward one another as shown in detail experimentally by Le Corroller and Favis.[6] Complex morphologies such as core-shell structures[7] and triple percolated (cocontinuous) phase structures[8] can be produced in ternary blends depending on the balance of all the aforementioned properties. It has also been stated that viscosity ratio plays less of a role in morphology development in ternary blends than interfacial tension.[9]

A large focus has been placed on the impact modification of biopolymers, such as polylactic acid (PLA), polyhydroxyalkanoates, and thermoplastic starch (TPS), due

to their substandard energy absorbing properties, similar to Novatein.[10] For instance, the impact strength and other mechanical properties of PLA/polybutylene adipate-co-terephthalate (PBAT) blends were shown to increase drastically when compatibilized with functionalities such as epoxides[11] and anhydrides,[12] attributed to strong interfacial adhesion and formation of a dispersed droplet morphology. Other biopolymers have been shown to be effectively impact modified. For example, the impact strength and elongation of polyhydroxybutyrate-co-valerate (PHBV) could be enhanced by up to 120% when plasticized with epoxidized soybean oil.[13] Similarly, increased glycerol plasticizer content in TPS increased the impact resistance of TPS/polycaprolactone blends, albeit that the mechanism of modification is different to when relying on morphology.[14]

Polybutylene adipate-co-terephthalate is a synthetic rubbery biodegradable aliphatic-aromatic copolyester which has received considerable attention for its potential to modify the impact properties of polymers it is blended with.[15] For example, the inclusion of 20–30 wt% PBAT in a PLA matrix caused the impact strength to double compared to neat PLA, and triple when epoxy functionalized compatibilizer was added.[11,16,17] With good interfacial adhesion and dispersed droplet morphology, PBAT is a good candidate for impact modification in other biopolymer systems such as poly(trimethylene terephthalate).[18]

Novatein has previously been blended with biodegradable polyesters.[19–21] Blending with PBS, compatibilized with a dual system of poly-2-ethyl-2-oxazoline (PEOX), polymeric diphenyl methane diisocyanate (pMDI), brought about an increase in tensile energy-to-break,[19] while blends of Novatein and 10 wt% PBAT compatibilized with a GMA-modified styrene-acrylic copolymer (Joncryl) caused an increase in impact strength while tensile strength and elongation at break were maintained.[21] It was found that the Novatein/PBAT/Joncryl blend was the most promising, but improvements to mechanical properties were dependent on PBAT being present above a critical concentration, similar to particulate reinforced polymers. In a previous study,[2] using core-shell reinforced Novatein, the critical matrix ligament thickness was achieved at a particle content of 20 wt%, after which significant improvements were observed.

The previous study[21] examined compatibilization and compositional effects on morphology development in Novatein/PBAT blends. However, this investigation specifically examines the effect of changing viscosity ratio and interfacial tension on morphology development, while keeping the compatibilizer type and amount constant. The aim of this was to improve the energy absorbing properties of Novatein purely by tailoring the phase behavior of the minor component. This was carried out by altering the water content in Novatein (which is included as a processing aid with a plasticizing effect), which modifies both the viscosity and the interfacial tension.

2 | EXPERIMENTAL

2.1 | Materials

Novatein thermoplastic protein, comprising mainly of blood-meal and a proprietary mixture of plasticizers and additives, was procured from Aduro Biopolymers LP, New Zealand. PBAT is an aliphatic-aromatic biodegradable polyester produced from 1,4-butanediol, adipic acid, and terephthalic acid. The grade used was BASF Ecoflex C1200 (MFI at 190°C, 2.16 kg = 2.7–4.9 g/10 min). Joncryl ADR-4368 is a multifunctional reactive coupling agent containing glycidyl methacrylate functionalities. Joncryl has an epoxy equivalent weight of 285 g/mol, molecular weight of 6,800 g/mol, and a functionality of 9.[22] Ecoflex and Joncryl were both sourced from Clariant, New Zealand. To catalyze epoxy ring opening, 2-methylimidazole (2MI) was acquired from Sigma-Aldrich, New Zealand.

2.2 | Processing

As received, Novatein granules (containing 36 pph$_{Bloodmeal}$ H$_2$O as a processing aid) was further hydrated over 7 days to produce Novatein containing 40, 60, and 80 pph$_{Bloodmeal}$ water to form Novatein 4020, 6020, and 8020, respectively. For compatibilized blends, the appropriate mass of 2-methylimidazole was dissolved in the water used for Novatein hydration, and upon the completion of rehydration, the Novatein/2MI granules were compounded with Joncryl in a LabTech corotating twin screw extruder (L/D 44:1) to form modified Novatein (m-4020, m-6020, m-8020). Previous studies determined that the optimal compatibilizer content for Joncryl/2MI systems was 70% of the PBAT phase but was limited to 5 wt% Joncryl and 2 wt% 2MI.

The relevant compositions of Novatein, m-Novatein, and PBAT (Table 1) were tumble mixed in ziplock bags prior to extrusion in the same corotating twin screw extruder. The extruder parameters were kept constant for processing modified Novatein and the subsequent blends. Temperature profile of the extruder was 70°C at the feed throat, 100–120°C along the main barrel section, increasing to 140°C at the die. Screw speed was 300 rpm.

A BOY 35A injection molding machine was used to produce test specimens. A barrel temperature profile of 100°C at the feed throat increasing to 150°C at the nozzle was used, and a temperature controlled mold was kept constant at 50°C. Conditioning of samples at 23°C and 50% RH for 7 days was carried out before testing.

TABLE 1 Blend compositions

Material/blend	Novatein (wt.%)	PBAT (wt.%)	Joncryl ADR-4368 (wt.%)	2-methylimidazole (wt.%)
4020	100	—	—	—
6020	100	—	—	—
8020	100	—	—	—
4020/PBAT-U	90	10	—	—
6020/PBAT-U	90	10	—	—
8020/PBAT-U	90	10	—	—
4020/PBAT-C	83	10	5	2
6020/PBAT-C	83	10	5	2
8020/PBAT-C	83	10	5	2
6020/PBAT30-C	63	30	5	2

2.3 | Analysis

Surface energy parameters of each material were determined using dynamic contact angle measurements of three solvents. Droplets of water, ethylene glycol (both polar), and diiodomethane (nonpolar) were placed onto a sample using an FTA1000B instrument (First Ten Angstroms, USA), and contact angle values were calculated from an average of six drops. The Young–Dupré equation[23] was used for surface energy calculations, and subsequently, the harmonic mean equation[24] was used to calculate blend interfacial tension.

Scanning electron microscopy was used to assess morphology. Impact fractured samples were mounted onto aluminum studs and placed into a Hitachi E-1030 ion sputter coater for platinum coating. The microscope used was a Hitachi S-4700 instrument, and the accelerating voltage used for imaging was 5 kV.

Dynamic mechanical analysis was carried out in single cantilever mode, from −80 to 150°C at a frequency of 1 Hz. A Perkin Elmer DMA 8000 instrument was used, and data were analyzed in Perkin Elmer's Pyris software. Injection molded impact bars were used for testing (thickness ~ 4 mm, width ~ 9 mm, free length ~ 13 mm) at a dynamic displacement of 0.05 mm. The conventional span-to-width ratio ~ 3.5 was not considered in this study for the convenience of using already prepared samples. This caused the storage modulus obtained to become closer to a shear modulus than a Young's modulus.

Viscosity ratio (λ) of blends was approximated as the ratio of the blend components complex viscosity (η*), from data obtained through unconditioned DMA testing of Novatein, modified Novatein and PBAT, with the same procedure described above. With the sample dimensions used, and by testing at a frequency of 1 Hz, complex modulus (E*) approximates to complex shear modulus (G*), from which η* (Equation 1) and λ (Equation 2) were calculated.

$$\eta^* = G/\omega \tag{1}$$

$$\lambda = \eta^*_{Novatein}/\eta^*_{PBAT} \tag{2}$$

Soxhlet extractions were conducted to remove PBAT from the blends using chloroform. Extractions were 18 hr long and performed in triplicate on samples (approximately 250 mg) sealed in 74-μm wire mesh. After the solvent extraction, samples were air-dried for 24 hr and oven-dried for a further 24 hr at 105°C. The final sample weight after extraction was corrected for the mass loss of pure Novatein and the mass fraction of Novatein in the blend (Equation 3); Novatein contains processing aids and plasticizers lost during drying and chloroform may also partially remove some additives in Novatein.

$$m_c = m_f + (m_i \times m_N) \times w_N \tag{3}$$

where m_c is corrected final sample mass, m_f is sample weight after extraction and drying, m_i is initial sample weight, m_N is the average percentage mass loss for pure Novatein after extraction and drying, and w_N is mass fraction of Novatein in the blend. Subsequently, mass loss (phase continuity) of PBAT in the blend could be calculated (Equation 4).

$$\text{Mass Loss} = (m_i - m_c)/m_i \times 100 \tag{4}$$

Moisture absorption of Novatein, PBAT, and blends was conducted on unconditioned, injection molded samples. These were submerged in a water bath (40°C) for 10 min. Before testing, and at each 1-min interval, samples were weighed and then placed back into the water bath. Testing was done in triplicate.

Injection molded samples were tensile tested using an Instron 33R4204 (ASTM D368) at a crosshead speed of 5 mm/min. A Ray-Ran Pendulum Impact System was used for Charpy impact testing, with a hammer weight of 0.952 kg and a speed of 2.9 m/s equating to an impact

Material	γ^{TOT}	γ^{LW}	γ^{AB}	γ^+	γ^-	γ_{12}	λ
4020	37.81	30.99	6.81	0.39	30.62	3.93	1.44
6020	32.80	31.95	0.86	0.01	37.51	6.47	0.87
8020	30.59	30.42	0.18	0.00	26.05	8.78	0.58
m-4020	30.77	28.52	2.25	0.05	30.21	6.26	0.96
m-6020	36.33	35.09	1.24	0.02	37.07	4.56	0.79
m-8020	30.28	28.30	1.98	0.02	54.68	6.66	0.53
PBAT	53.46	48.19	5.27	1.05	6.64		—
Joncryl	50.74	48.30	2.43	0.27	5.50		—

TABLE 2 Surface energy parameters (mN/m), blend interfacial tension (mN/m), and viscosity ratio (Novatein/PBAT) for Novatein, modified Novatein, and PBAT

energy of 4 J. Samples were tested in an edgewise orientation. For notched samples, an in-house built notch cutter was used (ISO 179).

3 | RESULTS AND DISCUSSION

3.1 | Surface energy, interfacial tension, and viscosity ratio

The harmonic mean equation was applied to calculate the blend interfacial tension (γ_{12}) using the measured solid surface energy of each blend component (Table 2). In blends containing reactive functionalities, the eventual composition of the interface is unknown, making the harmonic mean equation less accurate. However, it can be approximated as being inversely proportional to the interfacial thickness L (although it has been shown that $\gamma_{12} = 7.6L^{-0.86}$).[5]

For the unreactive systems, γ_{12} showed an increase in γ_{12} with increasing water content, brought about due to the decrease in polarity of Novatein. The dispersive component (γ^{LW}) for all Novatein formulations was relatively unaffected by changing water content or the inclusion of compatibilizer, meaning that the changes in interfacial tension are dictated by the polar component (γ^{AB}). It is known that the greater the polarity difference between blend components, the higher the interfacial tension will be.[5] Water, which is polar, interacts heavily with hydrophilic groups present along the protein backbone, which in turn causes aggregation of these groups. This exposes more apolar hydrophobic groups, leading to the decrease in polarity. This is supported by a decrease in both γ^+ and γ^- signifying less electron acceptor/donor sites and less hydrogen bonding sites[25] due to the greater interaction of water with the protein.

The interfacial thickness of the compatibilized blends could not be measured, but based on using the harmonic mean equation it showed that γ_{12} fluctuated compared to uncompatibilized blends (Table 2); however, the exact composition of the interface is unknown. With m-4020, processing difficulties required high temperature and pressure for the material to be molded. This means that there are two possible reasons for the fluctuation; either the

inclusion of Joncryl causes γ_{12} of all the blends to become similar (within reason) or the processing difficulties faced with m-4020 caused γ_{12} to be inaccurate. Furthermore, when incorporating compatibilizers into a blend, the interfacial tension is expected to drop, hence the latter situation is more likely. A decrease in γ_{12} tends to bring about a better dispersion of the minor phase, which occurs in this case, and is explained later.

The viscosity ratio decreased with increasing water content, as the increased water allowed for improved chain mobility, thereby producing a viscosity closer to PBAT. The values for λ are probably underestimated, as PBAT's viscosity drops more rapidly than Novatein's. Viscosity ratio was measured at 100°C and would be much higher at higher temperatures. However, the order of λ in the blends was 4020 > 6020 > 8020 and would remain in that order at higher temperature. What the results revealed was that blends with higher water content, that is 8020, will have a better dispersion of PBAT, and λ will likely be closer to unity.

The introduction of Joncryl/2MI compatibilizer reduced λ in all systems, likely due to the plasticization effect of the compatibilizer system. The most prominent change was seen in the m-4020 blend, whereas m-6020 and m-8020 systems only showed small decreases in λ, as these were already highly plasticized. These results suggest that the compatibilizer brings λ closer to unity during processing and would lead to a better dispersion of the minor phase.

3.2 | Morphology development

Scanning electron microscopy was used to assess the changes in morphology between Novatein, uncompatibilized, and compatibilized blends. It is known that Novatein fracture surfaces are featureless, with little plastic deformation. This observation is true regardless of water content (Figure 1). In contrast, the addition of 10 wt.% PBAT to Novatein brings about a heavily phase separated blend, with little to no interfacial interaction. With PBAT being hydrophobic and Novatein being hydrophilic, a lack of adhesion between phases is expected without compatibilizers present.
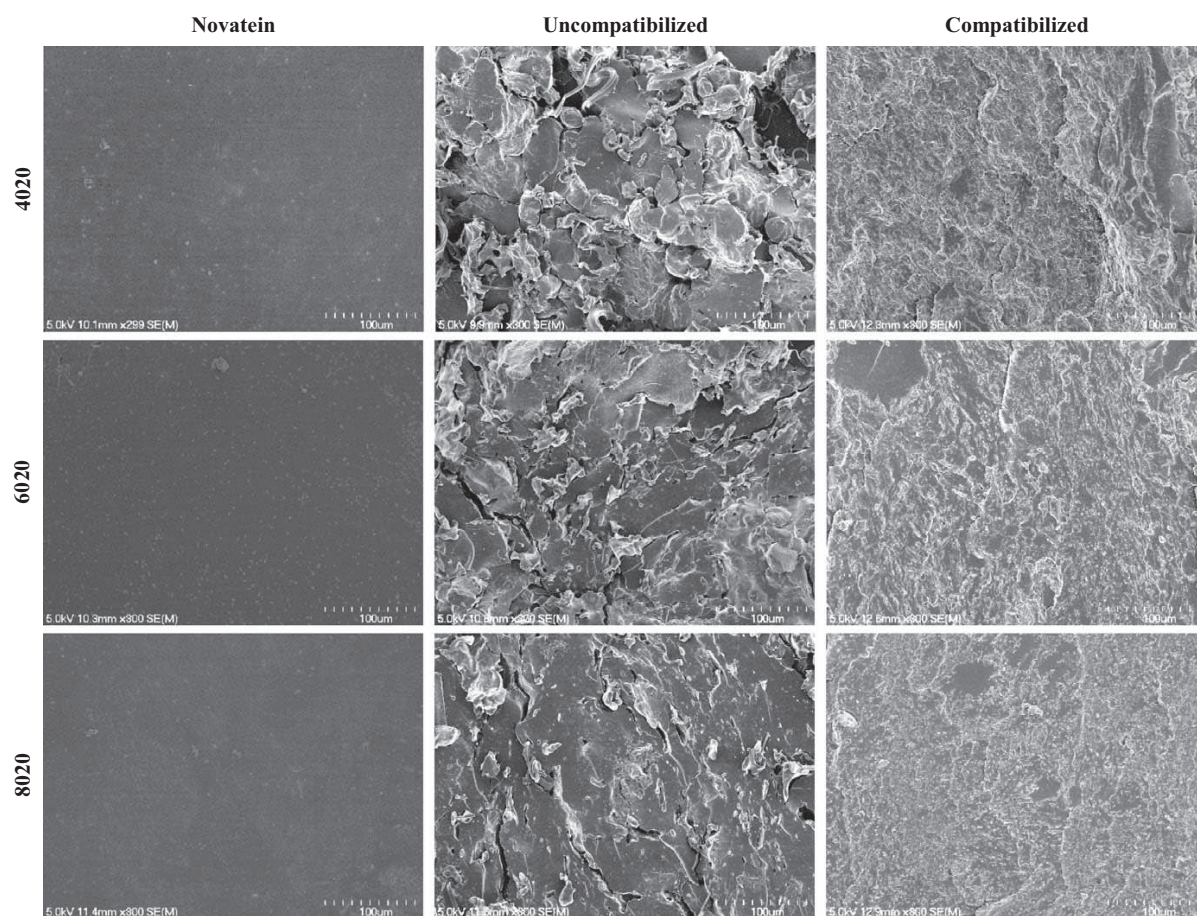
FIGURE 1 Scanning electron micrographs (×300 mag.) of notched impact fracture surfaces for Novatein, uncompatibilized, and compatibilized blends with varying water content

For uncompatibilized blends, the water content influenced the blend morphology strongly. In 4020/PBAT-U, and to some extent 6020/PBAT-U, PBAT encapsulated discrete regions of Novatein suggesting a percolated network of PBAT. It is known that the onset of percolation is less than 10 wt.% in Novatein when uncompatibilized.[21] On the other hand, PBAT appeared far better dispersed in 8020/PBAT-U; a result that was anticipated based on the high interfacial tension and lower viscosity ratio.

The inclusion of Joncryl and 2-methylimidazole changed the morphology of the blend drastically. The PBAT phase became better distributed and although there were some large domains of discrete Novatein (ranging up to 100 μm), the dispersion of PBAT was also greatly improved. On a macro-scale, it appeared that water content did not play a significant role in terms of the morphology developed during processing.

However, on a micro-scale, significant differences in morphology were present as water increased (Figure 2). At low water content, it was challenging to tell the two phases apart, although this is reminiscent of the Novatein/PBAT system

presented previously.[21] For that system, it was established that a very fine cocontinuous network of PBAT had percolated throughout a Novatein matrix despite the appearance of a mostly homogeneous surface. In contrast, 6020/PBAT-C and 8020/PBAT-C showed discrete regions of PBAT dispersed through a Novatein matrix. These regions range from submicron to micron size. Some domains appeared to be connected to one another, suggesting that some percolation may have occurred in these samples, but on the whole a finely dispersed second phase was observed.

To further understand the morphology of the blends, soxhlet extraction was conducted with chloroform to remove any accessible PBAT while leaving the Novatein phase intact (Table 3). In the case of solvent extraction in polymer blends, the terms mass loss and continuity can often be used interchangeably. This is because with selective phase removal, the greater the mass that is lost directly correlates to the interconnectedness of the minor phase. With percolation often comes encapsulation of the major phase at some level, meaning it is feasible to lose greater mass than the wt% of the minor phase
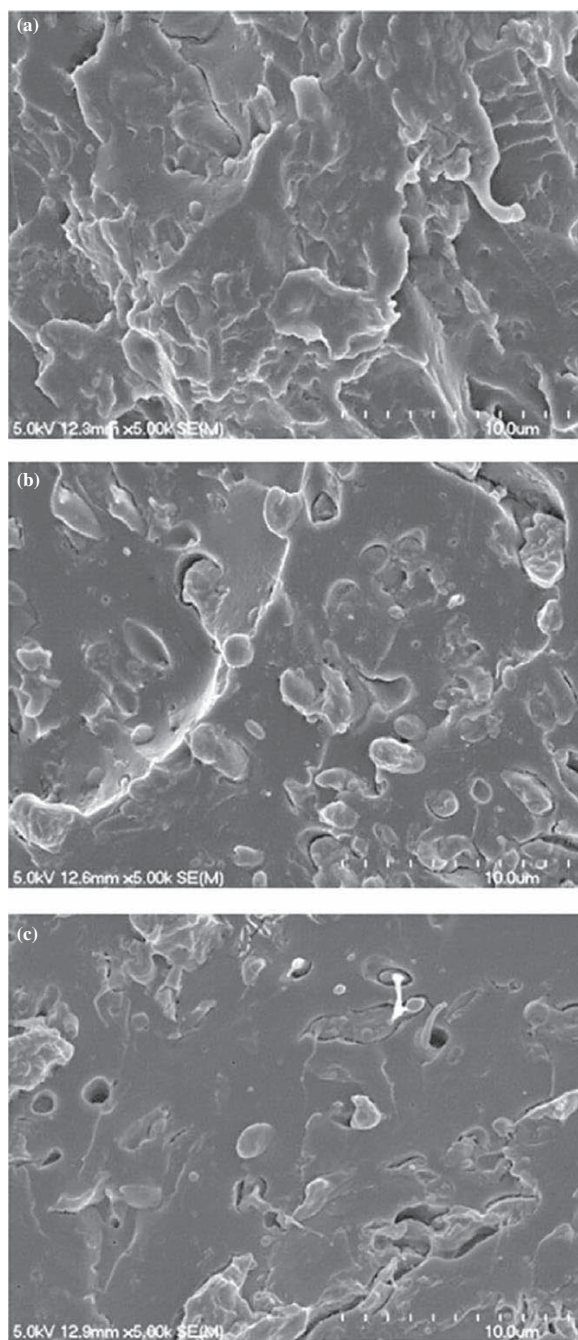
FIGURE 2 High magnification scanning electron micrographs (×5,000 mag.) of notched impact fracture surfaces. (a) 4020/PBAT-C; (b) 6020/PBAT-C; (c) 8020/PBAT-C

TABLE 3 Mass loss data from Novatein, uncompatibilized, and compatibilized blends after soxhlet extraction

Material/blend	Average mass loss (%)
4020	3.1 ± 0.3
4020/PBAT-U	27.9 ± 0.4
4020/PBAT-C	30.3 ± 1.3
6020	12.3 ± 0.2
6020/PBAT-U	25.1 ± 0.2
6020/PBAT-C	17.1 ± 0.2
8020	18.3 ± 0.5
8020/PBAT-U	23.4 ± 0.5
8020/PBAT-C	14.3 ± 1.0

added, as the discrete particles of the major phase are also washed away.

In pure Novatein, mass loss increased with increasing water content, attributed to the greater starting amount of moisture that is lost in the drying phase after extraction. In uncompatibilized blends, mass loss increased dramatically compared with Novatein; however, the greatest mass loss (or PBAT continuity) was seen in 4020/PBAT-U, and the least in 8020/PBAT-U. This is in agreement with the SEM analysis, whereby it was determined that increasing water content caused the PBAT phase to become better dispersed, as a result of more favorable interfacial tension and viscosity ratio. However, a significant level of coalescence of the minor phase was present in all blends, despite the well-dispersed appearance in the SEM images. This highlights the need for multiple analysis techniques, as SEM only focusses on the sample in two dimensions.

With the inclusion of Joncryl/2MI, continuity of PBAT decreased greatly with increasing water content, supporting the theory that PBAT becomes much better dispersed. In 8020/PBAT-C, the mass loss dropped below that of pure Novatein, suggesting a substantial chemical change in the sample, attributed to the strong interfacial adhesion brought about by the Joncryl/2MI compatibilizer. In contrast though, the mass loss for 4020/PBAT-C showed a small increase. This tells us that although the PBAT appeared well dispersed on a macroscale, there was actually a substantial level of percolation of the PBAT phase throughout the Novatein matrix. At higher temperature, the increased λ of 4020/PBAT-C compared with 8020/PBAT-C facilitated coalescence, while the decrease in γ_{12} facilitated dispersion and a fine phase structure, hence the fine percolated phase structure of the lower water content sample.

The predicted morphology was confirmed through electron microscopy of the samples after soxhlet extraction. It was clear to see that the Novatein phase appeared less granular with increasing water content (Figure 3), highlighting the decreased percolation and better dispersion of PBAT. Similarly, the comparison of uncompatibilized blends with the relevant compatibilized samples showed that the minor phase became very finely dispersed with the inclusion of the compatibilizer (Figure 3). Phase size decreased from hundreds of microns
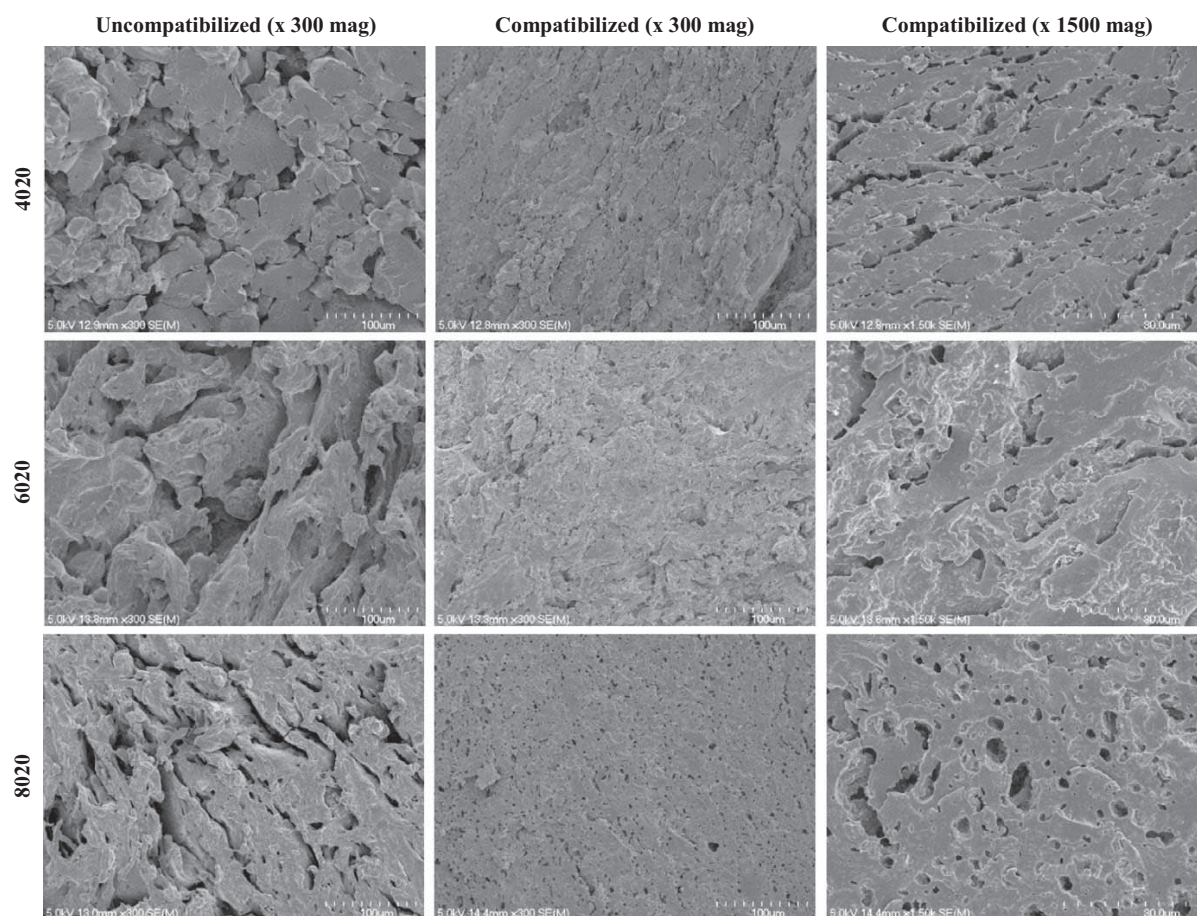
Uncompatibilized (x 300 mag)	Compatibilized (x 300 mag)	Compatibilized (x 1500 mag)

FIGURE 3 Scanning electron micrographs (×300 mag. and ×1,500 mag.) of the Novatein phase of uncompatibilized and compatibilized blends with varying water content, after soxhlet extraction of poly(butylene adipate-co-terephthalate)

in some cases, down to <5 μm; however, it appeared that the extracted domains in 8020/PBAT-C were more spherical than those in 6020/PBAT-C and 4020/PBAT-C, highlighting that viscosity ratio and interfacial tension are not completely overwhelmed by chemical interaction when forming morphologies in thermoplastic protein blends.

When looking more closely at the compatibilized samples, micro-domains remained after extraction (Figure 4), with some appearing as small as 500 nm in size. These domains were thought to be Joncryl, as PBAT would have been removed via the chloroform wash. These domains were found predominantly at what would have been the interface between Novatein and PBAT, although there was Joncryl seen in the Novatein phase as well, in both 6020/PBAT-C and 8020/PBAT-C. This suggests that a ternary blend had been produced, whereby the third component (Joncryl) compatibilizes the other two components.

Spreading coefficients can be calculated for ternary blends to predict the morphology based on the interfacial tension between blend components. Using the surface energy values for Novatein, PBAT, and Joncryl, and the method extensively described by Le Corroller and Favis,[6] the morphology predicted for Novatein/PBAT/Joncryl blends was as follows: in 4020/PBAT-C, the Joncryl phase would show complete wetting, locating exclusively in the PBAT phase, while in 6020/PBAT-C and 8020/PBAT-C, Joncryl would spread between the Novatein and PBAT phases evenly. In reality, Joncryl exhibits partial wetting, forming micro-domains whereby a line of contact is likely between all phases, due to the complex balance of viscosity ratio, interfacial tension, and the influence of chemical functionalities present on Joncryl. Polypropylene/polyethylene/polystyrene ternary blends fit the model exceptionally well[6]; however, the Novatein blends presented here did not appear to follow the same trend, suggesting that the influence of chemical functionality plays a significant role in morphology development, rather than just γ_{12} and λ.

Water absorption testing can also be used to establish morphology in the case of Novatein blends (Figure 5). Pure Novatein 4020 and 6020 both increased in mass ~16% after
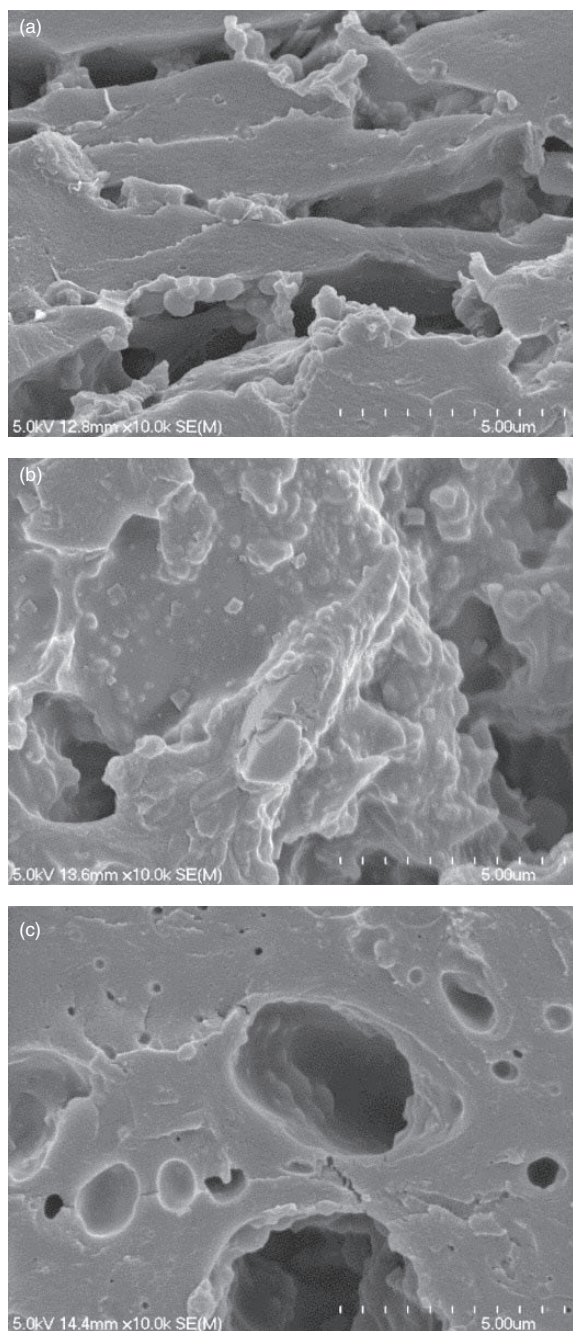
FIGURE 4 High magnification scanning electron micrographs (x 10000 mag.) of samples after soxhlet extraction. (a) 4020/PBAT-C; (b) 6020/PBAT-C; (c) 8020/PBAT-C

10 min in the water bath. This decreased to ~12% in Novatein 8020, attributed to the higher starting moisture content and increased hydrophobicity as described earlier. In comparison, PBAT's moisture absorption was negligible, with a mass increase of 0.3% after 10 min.
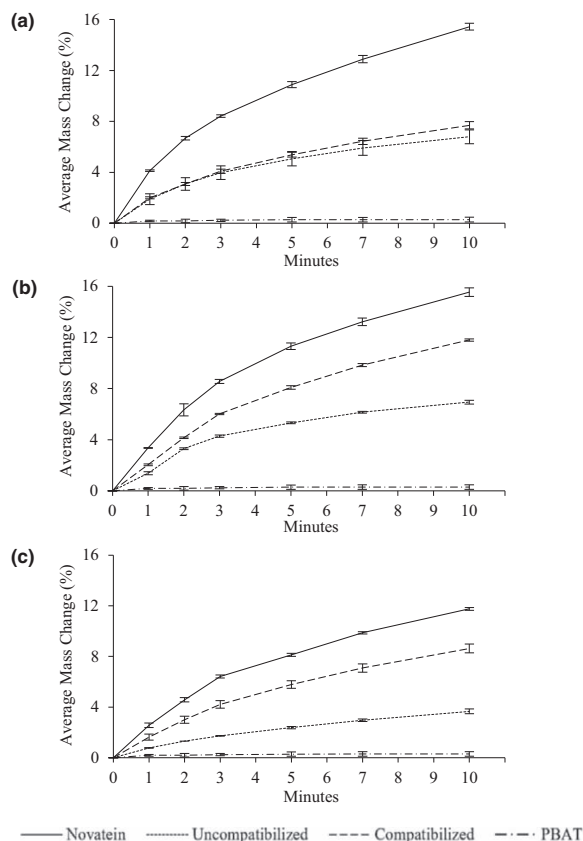

FIGURE 5 Moisture absorption data for (a) 4020 and blends; (b) 6020 and blends; (c) 8020 and blends

Interestingly, for all water contents, the compatibilized blends showed an increased change in mass compared to the uncompatibilized samples. The encapsulation of Novatein by PBAT in the uncompatibilized blends protected the protein phase, meaning less Novatein was available for the uptake of water. On the other hand, the greater dispersion of PBAT in compatibilized blends allowed Novatein to become more accessible to water, leading to greater moisture uptake. It should be noted that the mass change values for compatibilized blends were still far below pure Novatein, highlighting both the fact that there was some degree of percolation and protection from the PBAT phase and also that the chemical change in the blend at the interface between Novatein, Joncryl/2MI, and PBAT occurred at reactive functionalities that otherwise would have been involved in interactions with water.

Dynamic mechanical analysis, in particular storage modulus (E'), is helpful when determining morphology of blends. The modulus values will tend to mimic the matrix in a blend with a dispersed second phase; however, upon percolation of the minor phase, E' becomes an intermediate of the two. This is useful for determining whether the minor phase is
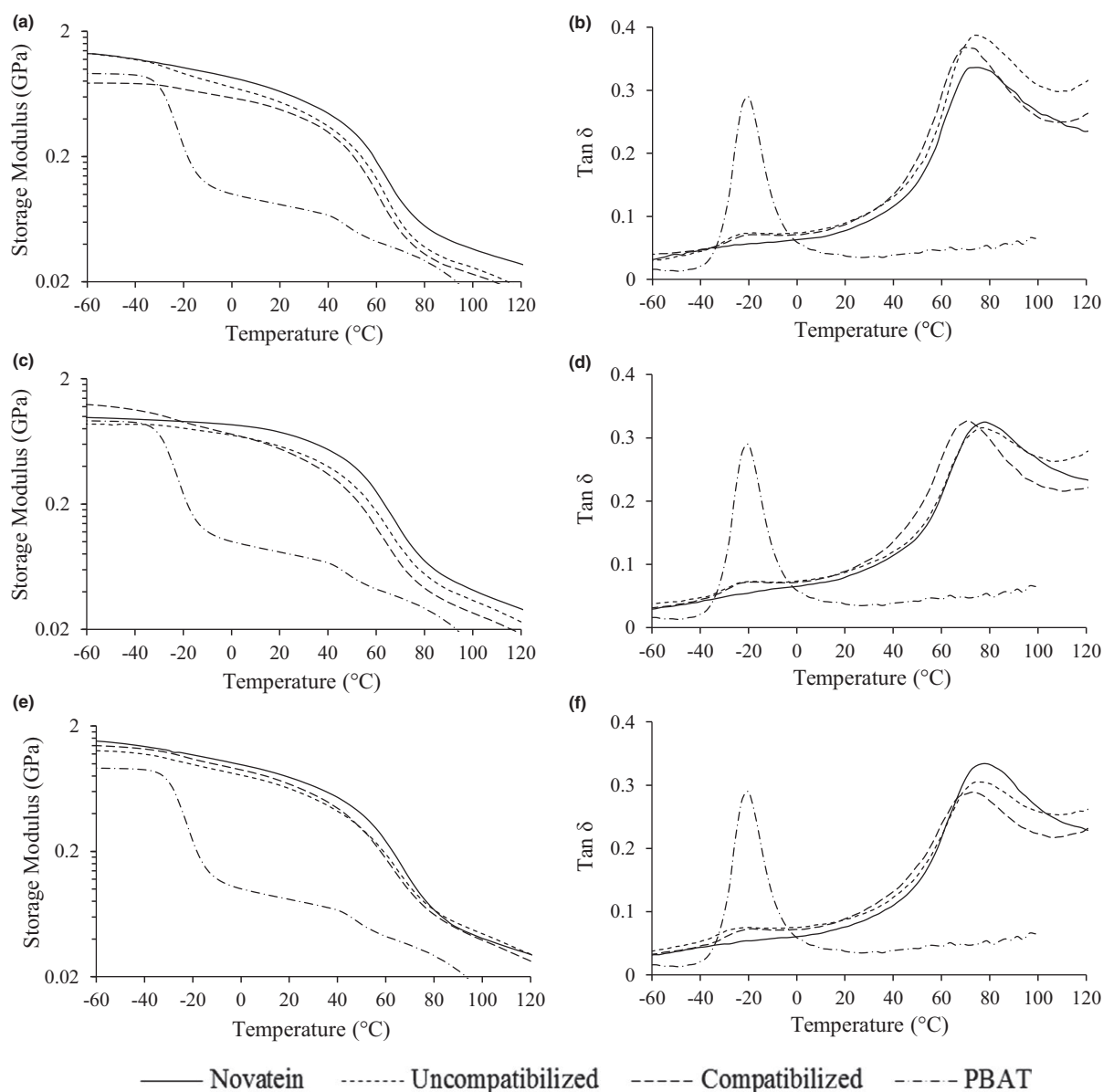
142

FIGURE 6 DMA plots for Novatein, poly(butylene adipate-co-terephthalate), and blends showing storage modulus (E') and tan δ of; (a and b) 4020; (c and d) 6020; (e and f) 8020

truly dispersed or whether a cocontinuous phase structure is formed.[26]

The E' plots for Novatein, PBAT, and blends (Figure 6) confirm the conclusion that with increasing water, a better dispersion of the minor phase was achieved. For 4020 and 6020 blends (Figure 6a,c), E' decreased compared to Novatein due to the effect of the onset of PBAT coalescence, whereas in comparison, the 8020 blends (Figure 6e) are very similar to the neat Novatein as the PBAT phase is well dispersed.

In the tan δ plots, PBAT showed a strong peak at −20°C, while Novatein had a major transition at ~80°C. Both of

these peaks are attributed to the materials respective T_g's. With regard to all blends, the small PBAT T_g peak was visible at ~20°C and did not shift as a result of blending with Novatein or with the inclusion of Joncryl/2MI. Similarly, the Novatein T_g peak did not shift in the uncompatibilized blends, but the inclusion of compatibilizer caused a decrease in the Novatein T_g by 5–10°C. Also of interest was the decrease in magnitude of the Novatein peak in compatibilized blends with increasing water content attributed to increased energy absorption of the minor PBAT phase.

TABLE 4 Mechanical properties of Novatein, uncompatibilized, and compatibilized blends

Blend	Tensile strength (MPa)	Strain-at-break (%)	Secant modulus (MPa)	Energy-to-break (kPa)	Impact strength (kJ/m^2)	
					Notched	Unnotched
4020	15.1 ± 2.1	2.2 ± 0.6	948 ± 104	201.6 ± 92.4	0.56 ± 0.20	1.54 ± 0.49
4020/PBAT-U	5.2 ± 0.2	0.9 ± 0.1	765 ± 67	31.4 ± 4.3	1.07 ± 0.13	1.28 ± 0.15
4020/PBAT-C	8.8 ± 0.9	1.8 ± 1.2	709 ± 44	95.6 ± 27.4	1.07 ± 0.27	2.99 ± 0.48
6020	15.3 ± 1.5	14.1 ± 8.6	815 ± 115	1792.6 ± 1159.4	0.68 ± 0.27	1.71 ± 0.53
6020/PBAT-U	7.3 ± 0.4	2.2 ± 0.2	584 ± 34	109.1 ± 19.2	1.09 ± 0.18	1.30 ± 0.14
6020/PBAT-C	10.2 ± 0.6	3.9 ± 0.7	576 ± 68	265.5 ± 72.8	0.93 ± 0.19	3.84 ± 1.22
6020/PBAT30-C	9.9 ± 0.1	12.5 ± 1.1	391 ± 24	1031.9 ± 110.5	3.4 ± 0.3	15.6 ± 2.7
8020	15.0 ± 1.3	19.1 ± 15.2	791 ± 112	2386.3 ± 1996.4	0.82 ± 0.37	1.40 ± 0.34
8020/PBAT-U	8.3 ± 0.7	2.4 ± 0.4	612 ± 35	134.3 ± 34.8	1.02 ± 0.46	1.64 ± 0.40
8020/PBAT-C	9.0 ± 0.4	3.5 ± 0.8	577 ± 66	171.9 ± 77.6	0.99 ± 0.22	4.64 ± 1.64

3.3 | Mechanical properties

After conditioning to equilibrium moisture content, the tensile strength of Novatein was ~15 MPa regardless of water content (Table 4). However, with increasing water, strain-at-break increased drastically from ~2% in 4020 to ~20% in 8020, attributed to increased water before processing, which was found to have a significant effect on Novatein's mechanical properties after conditioning.[27] However, the deviation seen in strain-at-break for Novatein 6020 and 8020 was extremely large, and the calculated standard error for both groups (6.19 and 3.86 for 6020 and 8020, respectively) suggests that these mean values do not truly represent the sample group. Novatein has poor impact resistance, with notched impact strength falling between 0.5 and 1 kJ/m^2 for all Novatein formulations, while unnotched impact strength does not exceed 2 kJ/m^2.

The addition of PBAT to the blends caused a decrease in all tensile properties attributed to the poor interfacial adhesion between Novatein and PBAT. In contrast, there was an increase in notched impact strength and a maintenance of unnotched impact strength. It has been previously stated that a cocontinuous morphology is conducive to improved impact resistance, and in this case, it is likely that the PBAT phase was able to absorb much of the energy during fracture due to its continuous nature, despite the lack of adhesion between phases.

With the addition of Joncryl/2MI compatibilizer to the Novatein/PBAT system, there was increased tensile strength in all blends, but no significant change to strain-at-break, hence little change was seen in energy-to-break also. Secant modulus decreased slightly, potentially due to the low molecular weight of the Joncryl and 2MI (6,800 and 82 g/mol, respectively). Notched impact strength was maintained compared with uncompatibilized blends, while unnotched impact strength was doubled in 4020/PBAT-C and tripled in 8020/PBAT-C, with 6020/PBAT-C being intermediate of the two.

The mechanical properties presented from the compatibilized blends are underwhelming, considering that the morphology achieved appeared conducive to improved energy absorption. However, it is known that for Novatein reinforced with elastomeric core-shell particles, the critical reinforcement level needed for improvement in energy absorption was ~15–20 wt%,[2] while in reactive Novatein/polyethylene blends, this point was >20 wt% for some blends.[1] Furthermore, it has been shown that optimal properties of Novatein/polybutylene succinate (PBS) blends have a PBS content of >30 wt%.[19] This suggests that the 10 wt% PBAT included in blends in this study falls below the critical composition, hence a sample with 30 wt% PBAT (aiming to be above the composition threshold) was tested in Novatein 6020 as comparison.

3.4 | Effect of composition

Composition has a large influence on morphology development and subsequently mechanical properties; with increasing minor phase content, the likelihood of percolation is greater, hence a larger contribution of the minor phase is made to the material properties. Table 4 shows that 6020/PBAT30-C (30 wt% PBAT) showed substantial increases to both notched and unnotched impact strength compared with 6020/PBAT-C, as well as a maintenance of tensile strength and comparable strain-at-break to neat Novatein. There was also very little spread of values for 6020/PBAT30-C, as shown by the small standard deviations, suggesting good reproducibility. Of the 30 wt% PBAT samples, only the secant modulus was significantly less than the 10 wt% blend, but this is to be expected as neat PBAT has a much lower secant modulus (64 MPa) than Novatein. From this analysis, it was concluded that the critical composition was above 10 wt%
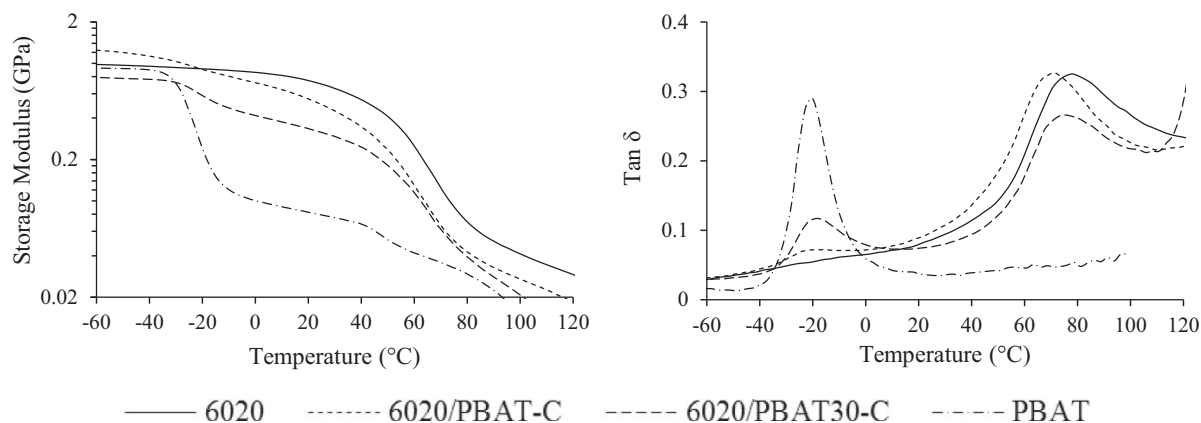
FIGURE 7 DMA plots for Novatein 6020, poly(butylene adipate-co-terephthalate), and 6020 blends showing storage modulus (E') and tan δ

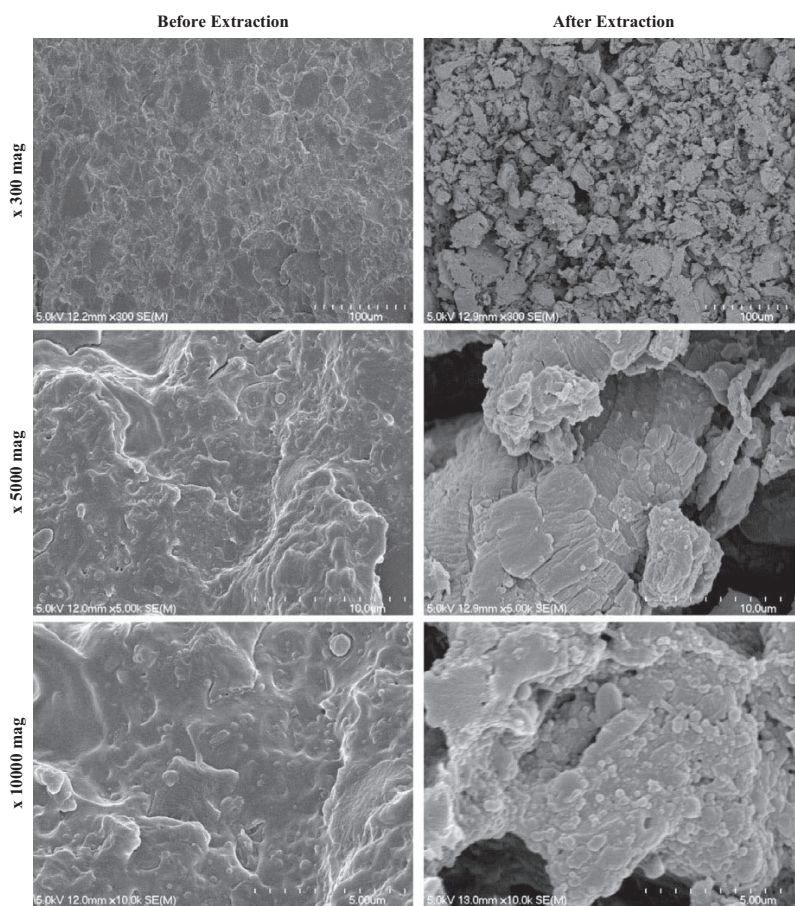

FIGURE 8 Scanning electron micrographs (×300 mag., ×5,000 mag., ×10,000 mag.) of 6020/PBAT30-C, before and after soxhlet extraction of PBAT

PBAT and that the 30 wt% sample was above this compositional threshold for improved energy absorption.

The comparison of DMA data for samples containing 10 and 30 wt% PBAT (Figure 7) shed light on the change in morphology with increasing minor phase. Storage modulus clearly showed a decrease in 6020/PBAT30-C, compared with the 10 wt% sample, highlighting the percolation of PBAT and the formation of a cocontinuous phase structure. Similarly, the increase in the PBAT peak in tan δ and corresponding decrease in magnitude of the Novatein T_g peak showed that the
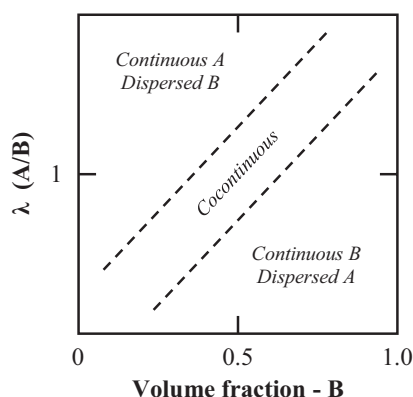
FIGURE 9 Relationship between composition and viscosity ratio with reference to morphology development[26]

PBAT phase had a bigger contribution in the absorption of energy. Similarly, the solvent extraction data of 6020/PBAT30-C showed a large increase in PBAT continuity compared to 6020/PBAT-C (10 wt% PBAT) (51.8 % and 17.1 % mass loss, respectively). This confirms the DMA findings that the PBAT phase is highly percolated throughout Novatein.

On a macro-scale, there appeared to be a homogeneous phase structure with high levels of plastic deformation as a result of the notched impact fracture (Figure 8), which brings about the improvement in impact strength. There were noticeable regions of Novatein, likely due to encapsulation by percolated PBAT. When magnified (Figure 8), it is apparent that there are phase separated micro-domains (some <0.5 μm in diameter). It is suggested that the micro-domains seen are Joncryl, as described previously, while the PBAT phase is highly continuous and cannot be distinguished from the Novatein phase. This is in agreement with the DMA and soxhlet analysis, which suggests a fully cocontinuous structure.

When examining 6020/PBAT30-C samples after soxhlet extraction, the cocontinuity becomes apparent. The mass loss was particularly high for the 30 wt% sample, losing ~52% mass, compared to ~17% mass for the corresponding 10 wt% sample. The macro-scale SEM image (Figure 8b) showed a somewhat granular structure to the Novatein phase after PBAT extraction. This may suggest that a phase inversion is likely to take place at compositions close to 30 wt% PBAT. Higher magnification images (Figure 8d,f) show that the Joncryl micro-domains seen in the notched impact fracture surface of the same sample are still present after extraction, again situating at what would be a three-way phase interface.

There is a well-known relationship between viscosity ratio and blend composition, whereby increasing minor phase content causes the onset of percolation before a phase inversion occurs (Figure 9).[26] The results from this study showed that composition had an overriding effect

on morphology in Novatein/PBAT blends. The amount of PBAT was above the critical level for impact modification of Novatein and this was accompanied by a significant change in morphology. Both the Novatein phase and the PBAT phase were highly continuous, indicated by the high mass loss during soxhlet extraction, and the remaining Novatein phase being intact after extraction. It was concluded that the increase in PBAT wt% pushed the blend from being mostly dispersed PBAT in a Novatein matrix (albeit with some degree of interconnectedness) into the cocontinuous region displayed in Figure 9. This is in spite of the favorable viscosity ratio, interfacial tension, and chemical interaction demonstrated earlier.

The morphology developed in Novatein/PBAT blends can be tailored by altering viscosity ratio and interfacial tension through varying water content. The introduction of chemical functionalities in the form of Joncryl caused the influence of these parameters to become less, although not entirely unimportant. The development of phase structure in Novatein blends, at lower minor phase content, is a fine balance between viscosity ratio, interfacial tension, and chemical reactivity, and predictions must include all three parameters, although the latter appeared to play a greater role at lower minor phase content. As demonstrated here, however, composition can have an overriding effect of these parameters. Further study of this system must be concerned with establishing whether Novatein can be sufficiently impact modified, while the PBAT phase remains well dispersed, or if the onset of cocontinuity is the driving force behind high impact strength in Novatein blends.

4 | CONCLUSIONS

The morphology of Novatein/PBAT blends was successfully manipulated by altering interfacial tension (γ_{12}), viscosity ratio (λ), and chemical interaction, thereby producing an impact modified material. For uncompatibilized systems, increasing water content in Novatein caused an increase in γ_{12} and a decrease in λ, leading to better dispersion of PBAT. Coalescence was still high in all uncompatibilized blends, while the inclusion of Joncryl/2MI caused a decrease in both γ_{12} and λ which brought about a drastic reduction in phase size and coalescence of PBAT. This level of coalescence followed the same trend as uncompatibilized blends (4020 > 6020 > 8020); however, the relative change in continuity was much larger with Joncryl included. Moisture uptake of compatibilized samples was higher than uncompatibilized samples due to the protection that the continuous PBAT phase offered Novatein in the absence of Joncryl. DMA offered similar conclusions, whereby E' for the low water content blends tended more toward neat PBAT than compatibilized blends or higher water content blends, signifying

greater continuity of the minor phase. The mechanical properties of compatibilized blends were far improved over those without Joncryl, attributed to the fine phase structure and good interfacial adhesion. Impact strength of compatibilized blends was greater than pure Novatein, regardless of water content, with unnotched impact strength increasing at least double, and threefold in the case of 8020/PBAT-C.

When PBAT content was increased to 30 wt%, it was highly continuous and indistinguishable from the Novatein phase. This was in agreement with the DMA and solvent extraction data, which suggested a fully cocontinuous structure. This blend (6020/PBAT30-C) showed substantial increases to both notched and unnotched impact strength compared with the 10 wt% blend, as well as a maintenance of tensile strength and strain-at-break. The amount of PBAT was above the critical level for impact modification of Novatein and this was accompanied by a significant change in morphology. It was concluded that the development of phase structure in Novatein blends, at low minor phase content, is a fine balance between viscosity ratio, interfacial tension, and chemical reactivity; however, composition can have an overriding effect.

ACKNOWLEDGMENTS

ORCID

Matthew J. Smith http://orcid.org/0000-0003-0826-6842
Casparus J. R. Verbeek
http://orcid.org/0000-0002-5171-9053

REFERENCES

[1] M. J. Smith, C. J. R. Verbeek, *Adv. Polym. Technol.* **2017**. https://doi.org/10.1002/adv.21847
[2] M. J. Smith, C. J. R. Verbeek, *Macromol. Mater. Eng.* **2016**, *301*, 992.
[3] M. A. Emin, H. P. Schuchmann, *J. Food Eng.* **2013**, *116*, 118.
[4] F. Chen, J. Zhang, *ACS Appl. Mater. Interfaces* **2010**, *2*, 3324.
[5] S. Wu, *Polym. Eng. Sci.* **1986**, *27*, 335.
[6] P. Le Corroller, B. D. Favis, *Polymer* **2011**, *52*, 3827.
[7] H. Ohishi, *J. Appl. Polym. Sci.* **2004**, *93*, 1567.
[8] J. Zhang, S. Ravati, N. Virgilio, B. D. Favis, *Macromolecules* **2007**, *40*, 8817.
[9] S. Shokoohi, A. Arefazar, *Polym. Adv. Technol.* **2009**, *20*, 433.
[10] B. Imre, B. Pukánszky, *Eur. Polym. J.* **2013**, *49*, 1215.
[11] N. Wu, H. Zhang, *Mater. Lett.* **2017**, *192*, 17.
[12] T. R. Rigolin, L. C. Costa, M. A. Chinelatto, P. A. R. Muñoz, S. H. P. Bettini, *Polym. Test.* **2017**, *63*, 542.
[13] M. O. Seydibeyoglu, M. Misra, A. Mohanty, *Int. J. Plast. Technol.* **2010**, *14*, 1.
[14] L. Averous, L. Moro, P. Dole, C. Fringant, *Polymer* **2000**, *41*, 4157.
[15] G. Guo, C. Zhang, Z. Du, W. Zou, H. Tian, A. Xiang, H. Li, *Ind. Crop Prod.* **2015**, *74*, 731.
[16] M. Kumar, S. Mohanty, S. K. Nayak, M. Rahail Parvaiz, *Bioresour. Technol.* **2010**, *101*, 8406.
[17] Z. Naiwen, W. Qinfeng, R. Jie, W. Liang, *J. Mater. Sci.* **2009**, *44*, 250.
[18] S. Dhandapani, S. K. Nayak, S. Mohanty, *Polym. Adv. Technol.* **2016**, *27*, 7.
[19] K. I. K. Marsilla, C. J. R. Verbeek, *Macromol. Mater. Eng.* **2014**, *299*, 885.
[20] K. I. K. Marsilla, C. J. R. Verbeek, *Macromol. Mater. Eng.* **2015**, *300*, 161.
[21] M. J. Smith, C. J. R. Verbeek, *J. Appl. Polym. Sci.* **2017**. https://doi.org/10.1002/app.45808
[22] R. Al-Itry, K. Lamnawar, A. Maazouz, *Polym. Degrad. Stabil.* **2012**, *97*, 1898.
[23] B. Mesic, M. Lestelius, G. Engström, *Packag. Technol. Sci.* **2006**, *19*, 61.
[24] R. N. Shimizu, N. R. Demarquette, *J. Appl. Polym. Sci.* **2000**, *76*, 1831.
[25] G. Biresaw, C. J. Carriere, *J. Polym. Sci., Part B: Polym. Phys.* **2001**, *39*, 920.
[26] P. Pötschke, D. R. Paul, *J. Macromol. Sci., Polym. Rev.* **2003**, *43*, 87.
[27] C. J. R. Verbeek, L. E. van den Berg, *J. Polym. Environ.* **2011**, *19*, 1.

9

Concluding Discussion

Concluding Discussion

Novatein® thermoplastic protein is typically brittle in nature, exhibiting low impact resistance and energy absorption during fracture. The aim of this thesis was to improve its impact strength through polymer blending and reactive extrusion, without excessively compromising other mechanical properties. A number of polymeric materials were blended with Novatein; elastomeric core-shell particles, functionalized polyethylene and biodegradable polybutylene adipate-co-terephthalate (PBAT) were all incorporated into a Novatein matrix through extrusion and injection moulding. The resulting blends were studied using an array of techniques characterizing mechanical, thermal and morphological properties.

Novatein is not a typical polymer, and while theories and ideas regarding conventional polymer blending and toughening can be applied to Novatein, a number of other considerations must be made during blending for impact strength modification. Firstly, morphology development in Novatein blends was highly dependent on viscosity ratio (λ), interfacial tension (γ_{12}), chemical interaction and composition, which in combination, form a complex scenario where each has a significant influence on the phase structure. Secondly, these factors also affect impact resistance. Increased energy absorption is typically brought about when the minor phase is well dispersed droplets, well adhered to the matrix and elastomeric in nature. If these factors are not balanced correctly, this morphology is unlikely, if not impossible to produce.

The incorporation of elastomeric core-shell particles into Novatein ensured that the minor phase was spherical in shape. Particles functionalized with epoxy groups in the form of glycidyl methacrylate (GMA) produced a better dispersion of particles than unmodified ones, due to a likely decrease in γ_{12} and the emulsifying effect of

the reactive group. These well dispersed, functionalized particles brought about large increases in impact strength, elongation and tensile energy-to-break above a particle weight fraction of ~ 15 wt. %. This improvement in energy absorption with increasing minor phase was linked to the critical matrix ligament thickness (τ_c), otherwise known as the surface-to-surface interparticle distance. When the distance between particles, τ, was < τ_c the matrix was able to freely elongate due to the transition from plane strain to plane stress. The mechanism of fracture was also related to τ_c; when particle content was high (and hence τ was small) extensive matrix yielding was observed, whilst when τ was high (low particle content), fracture was brittle and extensive crazing occurred with little energy absorption.

FT-IR mapping of the samples with high particle content showed that the protein secondary structures in the highly yielded areas were much more ordered compared to the bulk matrix. This was attributed to the orientation of randomly aligned structures during fracture. The transformation of secondary structures requires energy and it was suggested that in the case of core-shell particle reinforced Novatein, the transformation of secondary structures contributed to energy absorption during fracture. The correlation was drawn between the ability of the matrix to freely elongate and structural transformations, for example the low particle content blends (with high τ) exhibited little to no yielding and hence little change to secondary structure during fracture.

The idea of toughening Novatein through a dispersed second phase used in the core-shell particle reinforced blends was then applied to Novatein/polyethylene blends, where the aim was to produce a dispersed droplet morphology *in-situ*. Reactive functionalities present on PE negated the need for additional compatibilizers. Unmodified PE was highly incompatible with Novatein, as expected, forming a

highly continuous phase at very low compositions. Interestingly, similar results were displayed for blends of Novatein and GMA modified PE (Lotader). This was surprising after the success of GMA modified core-shell particles. However, the influence of λ and γ_{12} was not a factor when blending with particles, whilst these played a significant role in Novatein/PE blends. Despite the incompatibility of both unmodified PE and Lotader blends, at low composition one may expect a dispersed phase to have formed due to the favorable λ. But the high γ_{12} and lack of chemical reactivity (due to the onset of epoxy-protein reactions being $\sim$ 180 °C) promoted coalescence in these blends. The introduction of maleic anhydride grafted PE to the unmodified blend presented an interesting scenario whereby λ (not conducive to good dispersion) and γ_{12} (favoring coalescence at high minor phase content) were contradicting. In this case, chemical interaction was the driving force for morphology development, and as such a finely dispersed PE phase was developed. Lastly, the Novatein/PE blend containing methacrylic acid neutralised by zinc ions to form an ionomer produced the most stable and dispersed morphology as well as the best energy absorbing properties (albeit at least 20 wt. % was required for significant improvement). This study concluded that manipulation of morphology in Novatein blends is a complex balance of λ, γ_{12} and chemical interactions and that for any prediction to be made on the morphology formed, all three factors must be considered. The FT-IR mapping of these samples showed no change to protein secondary structure as a result of blending or fracture, hence the improvements in mechanical properties observed were due to morphological effects rather than structural transformations.

One of the desirable traits of Novatein is its biodegradability and compostability. The incorporation of synthetic core-shell particles and polyethylene obviously compromise these characteristics, hence the focus shifted to producing impact

strength modified blends of Novatein with biodegradable PBAT. PBAT is a rubbery polymer, and it was postulated that blending it with Novatein could bring about properties similar to that of core-shell particle reinforced Novatein. The key factors of the study up to this point, i.e. the relationship between λ, γ_{12} and chemical interaction and their influence upon morphology and subsequently impact properties, were applied to the new Novatein/PBAT blends in an effort to drive the morphology to dispersed PBAT droplets.

Uncompatibilized blends behaved in a similar fashion to uncompatibilized Novatein/PE blends, which was to be expected. Dual compatibilizer systems were used for the study. Firstly a combination of poly-2-ethyl-2-oxazoline (PEOX) and polymeric diphenyl methane diisocyanate (pMDI) was used, as it was found to be successful for compatibilizing blends of Novatein/polybutylene succinate. However this compatibilizer system caused embrittlement in the blend and a phase structure which included a well dispersed PBAT phase but also large Novatein rich domains which acted as severe stress concentrations, hence reducing energy absorption during fracture. In contrast, the second compatibilizer system included a multifunctional chain extender with glycidyl methacrylate functionalities (Joncryl) combined with an imidazole catalyst (2MI), to promote epoxy-protein reactions at lower temperatures than highlighted previously. PBAT was well dispersed in this blend and distribution of the minor phase was much improved over the PEOX/pMDI compatibilized blend. A threefold improvement in impact strength and no decrease in tensile strength and elongation was observed for Joncryl/2MI compatibilized blends. Interestingly, the onset of PBAT coalescence was observed at very low compositions (~ 2 - 7 wt. %), although this was not detrimental to mechanical properties.

Based on the knowledge that PBAT began to coalesce at very low compositions, an attempt was made to investigate how manipulating the λ and γ_{12} of Joncryl/2MI blends would influence the phase structure. Water is used as a processing aid in Novatein, and due to its polar nature and the plasticizing effect it has on Novatein, increasing water content prior to processing changed λ and γ_{12} in Novatein/PBAT blends. For uncompatibilized blends, increasing water content in Novatein caused an increase in γ_{12} and a decrease in λ, leading to better dispersion of PBAT, although coalescence was still high in all blends. Compatibilizer decreased both γ_{12} and λ which caused a reduction in both phase size and coalescence of PBAT. DMA offered the same conclusions, whereby storage modulus suggested that increasing Novatein water content correlated to a less continuous PBAT phase. The mechanical properties of compatibilized blends were far improved over uncompatibilized, attributed to the fine phase structure and good interfacial adhesion, whilst impact strength of compatibilized blends was greater than pure Novatein, regardless of water content. Unnotched impact strength increased at least double, and the improvement was threefold in the compatibilized blend with the highest water content. When PBAT content was increased (30 wt. %) it was highly continuous and indistinguishable from the Novatein phase. This blend showed substantial increases to both notched and unnotched impact strength compared with the 10 wt. % blend, as well as a maintenance of tensile strength and strain-at-break.

This final study showed that the morphology of Novatein/PBAT blends can be successfully altered through changing λ, γ_{12} and chemical reactivity. However, when the amount of PBAT was increased so as to be above the critical level for impact strength modification of Novatein, there was a significant change in phase structure. It was concluded that the development of morphology in Novatein blends,

at low minor phase content, is a fine balance between λ, γ_{12} and chemical reactivity, however composition can have an overriding effect.

With regards to recommendations for future work, there is a large amount of knowledge around Novatein blends that remains unknown. In this thesis, the principles of reactive extrusion relating to processing parameters were not explored. It is known that variables such as residence time, screw speed and screw design can all have a significant impact on the morphology development in polymer blends, which in turn has a knock on effect to impact properties. The investigation of these parameters on Novatein blends can answer a number of questions such as, the effect of size, length and stagger angle of kneading blocks in extruder mixing zones, the effect of residence time on reaction conversions and the relationship with morphology development when shear rate is altered. This knowledge will allow for the accurate customisation of morphology in Novatein blends.

Fiber reinforcement is another technique known to improve impact strength and the incorporation of fibers into Novatein has shown promise in early scoping work. The use of natural fibers does not compromise the biodegradability of Novatein and these fibers have shown to have a good mechanical property-availability-cost relationship, particularly for plant fiber native to New Zealand.

Lastly, the examination of rheological properties of Novatein blends can also shed light on the degree of interaction between phases and is applicable for the processing of blends into profiles such as sheets, and when moulding intricate part geometries. The use of capillary rheometry for the characterization of Novatein rheology is in its infancy and a better grasp of properties such as elongational flow in Novatein and blends will allow for improved processing and a wider variety of applications.

10

Appendix

Co-Authorship Form

THE UNIVERSITY OF
WAIKATO
Te Whare Wānanga o Waikato

This form is to accompany the submission of any PhD that contains research reported in published or unpublished co-authored work. **Please include one copy of this form for each co-authored work**. Completed forms should be included in your appendices for all the copies of your thesis submitted for examination and library deposit (including digital deposit).

Please indicate the chapter/section/pages of this thesis that are extracted from a co-authored work and give the title and publication details or details of submission of the co-authored work. Chapter 3 'Nonisothermal Curing of DGEBA with Bloodmeal-based Proteins' – Pages 64-75 Published in *Industrial & Engineering Chemistry Research*, DOI: 10.1021/acs.iecr.5b00580	
Nature of contribution by PhD candidate	As first author of this paper, the PhD candidate conducted all experimental work under the guidance of the supervisors, and prepared the initial draft manuscript, which was refined and edited with consultation with the supervisors, who have been credited as co-authors
Extent of contribution by PhD candidate (%)	85

CO-AUTHORS

Name	Nature of Contribution
Johan Verbeek	Guidance with experimental work and editing of manuscript
Mark Lay	Guidance with experimental work and editing of manuscript

Certification by Co-Authors

The undersigned hereby certify that:

❖ the above statement correctly reflects the nature and extent of the PhD candidate's contribution to this work, and the nature of the contribution of each of the co-authors; and

Name	Signature	Date
Johan Verbeek		23/02/2018
Mark Lay		23/02/2018

156

July 2015

THE UNIVERSITY OF
WAIKATO
Te Whare Wānanga o Waikato

This form is to accompany the submission of any PhD that contains research reported in published or unpublished co-authored work. **Please include one copy of this form for each co-authored work**. Completed forms should be included in your appendices for all the copies of your thesis submitted for examination and library deposit (including digital deposit).

Please indicate the chapter/section/pages of this thesis that are extracted from a co-authored work and give the title and publication details or details of submission of the co-authored work.   - Chapter 4 'Impact Modification and Fracture Mechanisms of Core–Shell Particle Reinforced Thermoplastic Protein' – Pages 76-93   Published in *Macromolecular Materials & Engineering*, DOI: 10.1002/mame.201600043

Nature of contribution by PhD candidate	As first author of this paper, the PhD candidate conducted all experimental work under the guidance of the supervisor, and prepared the initial draft manuscript, which was refined and edited with consultation with the supervisor, who has been credited as co-author
Extent of contribution by PhD candidate (%)	90

CO-AUTHORS

Name	Nature of Contribution
Johan Verbeek	Guidance with experimental work and editing of manuscript

Certification by Co-Authors

The undersigned hereby certify that:
❖ the above statement correctly reflects the nature and extent of the PhD candidate's contribution to this work, and the nature of the contribution of each of the co-authors; and

Name	Signature	Date
Johan Verbeek		23/02/2018

157

Co-Authorship Form

THE UNIVERSITY OF
WAIKATO
Te Whare Wānanga o Waikato

This form is to accompany the submission of any PhD that contains research reported in published or unpublished co-authored work. **Please include one copy of this form for each co-authored work**. Completed forms should be included in your appendices for all the copies of your thesis submitted for examination and library deposit (including digital deposit).

Please indicate the chapter/section/pages of this thesis that are extracted from a co-authored work and give the title and publication details or details of submission of the co-authored work.

- Chapter 5 'The relationship between morphology development and mechanical properties in thermoplastic protein blends' – Pages 94-106 Published in *Advances in Polymer Technology*, DOI 10.1002/adv.21847

Nature of contribution by PhD candidate	As first author of this paper, the PhD candidate conducted all experimental work under the guidance of the supervisor, and prepared the initial draft manuscript, which was refined and edited with consultation with the supervisor, who has been credited as co-author
Extent of contribution by PhD candidate (%)	90

CO-AUTHORS

Name	Nature of Contribution
Johan Verbeek	Guidance with experimental work and editing of manuscript

Certification by Co-Authors

The undersigned hereby certify that:
- ❖ the above statement correctly reflects the nature and extent of the PhD candidate's contribution to this work, and the nature of the contribution of each of the co-authors; and

Name	Signature	Date
Johan Verbeek		23/02/2018

158

July 2015

Co-Authorship Form

This form is to accompany the submission of any PhD that contains research reported in published or unpublished co-authored work. **Please include one copy of this form for each co-authored work**. Completed forms should be included in your appendices for all the copies of your thesis submitted for examination and library deposit (including digital deposit).

Please indicate the chapter/section/pages of this thesis that are extracted from a co-authored work and give the title and publication details or details of submission of the co-authored work.
- Chapter 6 'Structural Changes and Energy Absorption Mechanisms during Fracture of Thermoplastic Protein Blends Using Synchrotron FTIR' – Pages 107-120 Published in *Polymer Engineering & Science*, DOI 10.1002/pen.24734

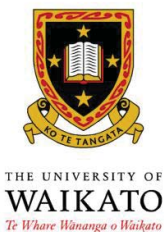| Nature of contribution by PhD candidate	As first author of this paper, the PhD candidate conducted all experimental work under the guidance of the supervisor, and prepared the initial draft manuscript, which was refined and edited with consultation with the supervisor, who has been credited as co-author
Extent of contribution by PhD candidate (%)	90

CO-AUTHORS

Name	Nature of Contribution
Johan Verbeek	Guidance with experimental work and editing of manuscript

Certification by Co-Authors

The undersigned hereby certify that:
❖ the above statement correctly reflects the nature and extent of the PhD candidate's contribution to this work, and the nature of the contribution of each of the co-authors; and

Name	Signature	Date
Johan Verbeek		23/02/2018

159

Co-Authorship Form

This form is to accompany the submission of any PhD that contains research reported in published or unpublished co-authored work. **Please include one copy of this form for each co-authored work.** Completed forms should be included in your appendices for all the copies of your thesis submitted for examination and library deposit (including digital deposit).

Please indicate the chapter/section/pages of this thesis that are extracted from a co-authored work and give the title and publication details or details of submission of the co-authored work.

- Chapter 7 'Compatibilization Effects in Thermoplastic Protein/Polyester Blends' – Pages 121-132 Published in *Journal of Applied Polymer Science*, DOI 10.1002/app.45808

Nature of contribution by PhD candidate	As first author of this paper, the PhD candidate conducted all experimental work under the guidance of the supervisor, and prepared the initial draft manuscript, which was refined and edited with consultation with the supervisor, who has been credited as co-author
Extent of contribution by PhD candidate (%)	90

CO-AUTHORS

Name	Nature of Contribution
Johan Verbeek	Guidance with experimental work and editing of manuscript

Certification by Co-Authors

The undersigned hereby certify that:
- ❖ the above statement correctly reflects the nature and extent of the PhD candidate's contribution to this work, and the nature of the contribution of each of the co-authors; and

Name	Signature	Date
Johan Verbeek	*C/W.*	23/02/2018

160

Postgraduate Studies Office
Student and Academic Services Division
Wahanga Ratonga Matauranga Akonga
The University of Waikato
Private Bag 3105
Hamilton 3240, New Zealand
Phone +64 7 838 4439
Website: http://www.waikato.ac.nz/sasd/postgraduate/

Co-Authorship Form

THE UNIVERSITY OF
WAIKATO
Te Whare Wānanga o Waikato

This form is to accompany the submission of any PhD that contains research reported in published or unpublished co-authored work. **Please include one copy of this form for each co-authored work**. Completed forms should be included in your appendices for all the copies of your thesis submitted for examination and library deposit (including digital deposit).

Please indicate the chapter/section/pages of this thesis that are extracted from a co-authored work and give the title and publication details or details of submission of the co-authored work. - Chapter 8 'Manipulating Morphology in Thermoplastic Protein-Polyester Blends for Improved Impact Strength' – Pages 133-147 Published in *Advances in Polymer Technology*, DOI 10.1002/adv.21911	
Nature of contribution by PhD candidate	As first author of this paper, the PhD candidate conducted all experimental work under the guidance of the supervisor, and prepared the initial draft manuscript, which was refined and edited with consultation with the supervisor, who has been credited as co-author
Extent of contribution by PhD candidate (%)	90

CO-AUTHORS

Name	Nature of Contribution
Johan Verbeek	Guidance with experimental work and editing of manuscript

Certification by Co-Authors

The undersigned hereby certify that:
❖ the above statement correctly reflects the nature and extent of the PhD candidate's contribution to this work, and the nature of the contribution of each of the co-authors; and

Name	Signature	Date
Johan Verbeek		23/02/2018

156

161

July 2015